IBEREO15

Challenges in rheology and product development

FCT/UC, Coimbra, Portugal

September 7–9, 2015

Full Papers

· U C ·

UNIVERSIDADE DE COIMBRA

ISBN Digital: 978-989-26-1056-6

Table of Contents

Welcome Message	**I**
Committees	**II**
Oral Communications	**1**
Poster Presentations	**94**
Author Index	**267**

IBEREO'15 IBERIAN RHEOLOGY CONFERENCE, 2015

Coimbra, Portugal

September 7th – 9th 2015

IBEREO'15, the Iberian Rheology Conference 2015, was the 5th in the series of conferences organized jointly by the Portuguese Society of Rheology (SPR) and the Spanish Group of Rheology (GER), which started in 2004 in Beja, Portugal. IBEREO presently takes place every two years, either in Portugal or in Spain, and this time took place in Coimbra, Portugal, hosted by the University of Coimbra, well known by its history of over 700 years, in its engineering campus. This year's conference was subjected to the topic "*Challenges in Rheology and Product Development*", having addressed the most recent trends in rheology, including: Experimental Methods; Modelling and Simulation in Rheology; Multiphase Systems and Composites; Product Formulation; Interface Rheology; Microrheology and Micro Fluidics and Applications, with special emphasis on food, polymers and biopolymers and cosmetics.

The Conference, which took place from the 7th to the 9th of September, joined together around 100 participants from eleven different countries, and was an opportunity to bring together experts in the field of rheology to discuss and learn about different and important topics in this field, exchanging experiences and creating the opportunity for networking and establishment of future collaborations. A selection of papers is being published in the on-line journal e-Rheo.Iba (Ibero_American Journal of Rheology).

On behalf of IBEREO'15 Organizing Committee
Maria Graça Rasteiro (IBEREO'15 Chair)
University of Coimbra, Coimbra, Portugal

IBERREC15
Coimbra 2015

COMMITTEES

ORGANIZING COMMITTEE

Abel Ferreira (University of Coimbra and CIEPQPF-UC)

Fátima Barreiros (Polytechnic Institute of Leiria and CEMUC-UC)

Filipe Antunes (University of Coimbra, Portugal)

Hermínio Sousa (University of Coimbra and CIEPQPF-UC)

Maria Graça Rasteiro (Chair) (University of Coimbra and CIEPQPF-UC)

Maria Teresa Cidade (Vice-chair) (New University of Lisbon and President of SPR)

SCIENTIFIC COMMITTEE

Antxon Santamaria (University of the Basque Country, Spain)

Bob Powell (Davis University, USA)

David Harbottle (Leeds University, UK)

Francisco Rubio Hernandez (University of Malaga, Spain)

Isabel Sousa (University of Lisbon, Portugal)

José Covas (University of Minho, Portugal)

José Maria Franco (University of Huelva, Spain)

José Muñoz Garcia (University of Seville, Spain)

Juha Salmela (VTT, Finland)

Maria Graça Rasteiro (Chair) (University of Coimbra and CIEPQPF-UC)

Maria Teresa Cidade (New University of Lisbon and President of SPR, Portugal)

Miguel Nóbrega (University of Minho, Portugal)

Oral Communications

Applications (Food)

O1

Mechanical characteristics of acorn starch gels

María Dolores Torres Pérez[1]

[1]Department of Chemical Engineering, University of Santiago de Compostela, Lope Gómez de Marzoa St., Santiago de Compostela E-15782, Spain

Correspondence to: M.D. Torres (E-mail: *mariadolores.torres.perez@usc.es*)

ABSTRACT

Some underexploited renewable sources of biopolymers are found in the northwest of the Iberia Peninsula, in abundance and at low cost. One of them is the acorn from cork oak (*Quercus suber L.*), a non-conventional source of starch. The purpose of this study was to investigate the thermo-mechanical characteristics of acorn starch samples at different concentrations. Rheological testing at small amplitude oscillatory shear was made using a stress-controlled rheometer to follow the evolution of the structure of acorn systems. Texture characteristics of the final gels were determined from the texture profile analysis. Preliminary physicochemical properties of the starch were also studied. Mechanical properties of studied gels were notably dependent on acorn starch concentration, given a set of gels with suite gelling properties for a wide range of applications.

KEYWORDS acorn starch, gluten-free, gels, rheology, texture

INTRODUCTION

A non-conventional source of starch founded in the Iberian Peninsula is the acorn from cork oak (*Quercus suber L.*). Acorn starch is an unexploited ingredient which could have attractive characteristics to be used in gluten-free diets. This could be also a strategy to add value to the acorn industry by-products. Naturally, acorns show a high content of tannins, which must be removed in the process of producing starch for food applications[1]. Despite its promising properties, this source of starch has had very little research into its structural and thermo-rheological features.

The development of alternative gluten-free products based on gelled systems from starches involves the understanding of how these carbohydrates behave under food processing conditions. The final structure and textural properties of these systems are strongly dependent on processing temperature/time, cooling rates, polysaccharide content or pH conditions since they can affect the dynamic process of competition between phase separation and gel formation. In this context, the main objective of this work is to carry out a systematic investigation of the mechanical properties of acorn starch samples at different experimental conditions. The evolution of the structure of these systems was monitored by rheological testing at small amplitude oscillatory shear (SAOS) using a stress-controlled rheometer. Texture characteristics of the final gels were determined from the texture profile analysis. Preliminary physicochemical characteristics of the starch were also studied.

MATERIAL AND METHODS

Raw materials

Acorns from cork oak (*Quercus suber L.*) were collected in the northwest of the Iberian Peninsula. Acorns of uniform size were selected for the extraction of starch. Selected samples were peeled and cut into small pieces. Representative samples of 500 g were ground in a blender with 1 L of water. After filtration of the slurry, the residue was ground again with the same proportion of water (1:2) and filtered. Both filtrates were let to settle over 24 h. Settled solids were separated from the supernatant and, then washed with distilled water several times until the acorn starch was free of colour; the acorn starch was then dried in a ventilated oven at 40ºC.

Acorn gels were prepared at several concentrations (from 15 to 85% w/w). The starch was dispersed in demineralised water by stirring at 800 rpm for 10 min at room temperature. Acorn starch suspensions were heated up to 90ºC and kept at this temperature for 30 min in order to prepare the gels. After, samples were placed in a fridge to allow full maturation of gels, which were kept at 5ºC for 24h before performing texture measurements.

Methods

Initial moisture, carbohydrates and starch content were determined according to standard methods. The measurements were made in triplicate.

Gels firmness (N) was determined in triplicate from the texture profile analysis (TPA) using a TA-XT2i (Stable Micro Systems, UK) texturometer (load cell of 5 kg). Before performing any measurements, gels were allowed to equilibrate at 20 ºC for around 1 h in a temperature-controlled room.

Thermo-rheological measurements were performed at least in duplicate on a controlled-stress rheometer using serrated parallel plates (35 mm diameter and 0.5 mm gap). Suspensions of starch were held at 20ºC between the plates for 10 min before testing. After, samples were heated to 90ºC at 2ºC/min. Then, time sweeps were conducted at 90ºC for 60 min at 0.1 Hz. After, samples were cooled down to 5ºC at 1 ºC/min. Temperature sweeps were performed at 0.1 Hz. A constant stress (2 Pa) within the linear viscoelastic region (LVR) was used in above tests. After cooling, time sweep tests were conducted at 5 ºC, during 60 min at 1 Hz. Without disturbing the gel, frequency sweep measurements were made at 20ºC, with oscillation frequencies over the range 0.01 to 100 rad/s. A constant stress (30 Pa) within the LVR of gels was used in the two latter tests.

Experimental data were analysed by one-factor analysis of variance followed by Scheffe test to differentiate means with 95% confidence ($p < 0.05$) using PASW Statistics (v.18, NY, USA).

RESULTS AND DISCUSSION

Acorn samples contained (% w/w, dry weight) 82% of carbohydrates, of which 64% was starch. The extracted starch from cork oak's acorn presented an average moisture content of 11.2%. These values are consistent with those previously reported for different gluten-free starches with similar starch content[2].

Thermo-rheological outcomes gathered that the interval of gelatinization temperature range of acorn starch extracted experimentally (from intitial gelatinization temperature, T_0, around 61ºC to final gelatinization temperature, T_1, around 76ºC) is similar to starches from other commercial sources[2] (Figure 1).

Rheological and texture measurements were notably dependent on acorn starch concentration. These results are in harmony with those reported for other gluten-free starches such as chestnut

starch[2]. Overall, this study delivered a set of acorn starch gels showing a suite of gelling properties for a wide range of applications.

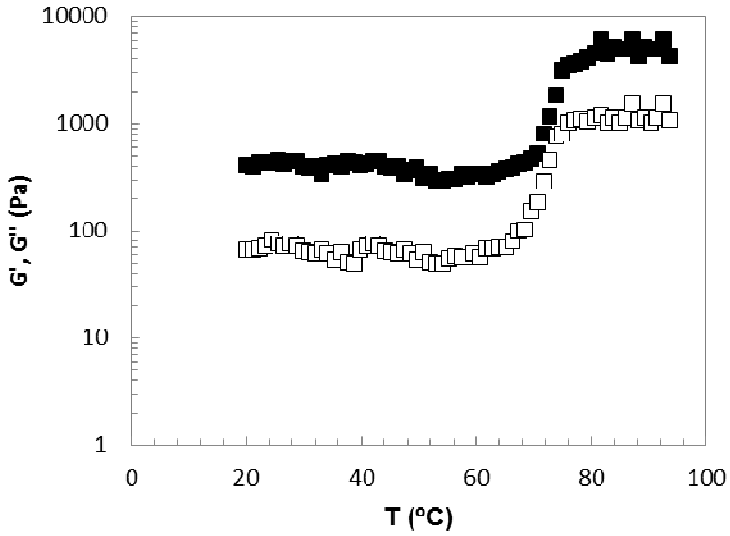

FIGURE 1 Representative temperature sweep profile of acorn starch gels prepared at concentration of 85%. Symbols: closed squares – storage (G') open squares– loss (G") moduli.

CONCLUSIONS

This study showed that extracted acorn starch samples at different concentrations induces different degrees of gel structure that could be applied in the production of a large variety of food products. This knowledge allows to create a new markets, add value and new applications to underexploited renewable sources of the northwest of the Iberia Peninsula, acorn starch extracted from cork oak.

ACKNOWLEDGEMENTS

The authors acknowledge the financial support (POS-A/2012/116) from Xunta de Galicia of Spain and the European Union's European Social Fund. The authors also wish to thank Professor D. Pérez and Professor G. Torres for his help with the experiments and for useful discussions.

REFERENCES AND NOTES

1. Stevenson, D.G.; Jane, J.; Inglett, G.E., *Starch,* **2006**, 58, 553-560.

2. Moreira, R.; Chenlo, F.; Torres, M.D., Glazer, J., *Journal of Food Engineering*, **2012**, 112, 94-99.

Evaluation by DMTA of Gelatinization Temperatures of Starch in Maize and Chestnut Flour Doughs

Ramón Moreira, Francisco Chenlo, Santiago Arufe

Departamento de Enxeñaría Química, ETSE, Universidade de Santiago de Compostela, Rúa Lope Gómez de Marzoa, s/n, 15782 Santiago de Compostela (Spain)

Correspondence to: Ramón Moreira (E-mail: ramon.moreira@usc.es)

ABSTRACT

Gluten-free flour doughs (three from different maize varieties and one from chestnut fruit) processed at the same consistency level (1.10 ± 0.07 Nm) with different water absorption were used to determine the starch gelatinization by means of two different experimental techniques, differential scanning calorimetry (DSC) and dynamic thermal mechanical analysis (DMTA). The ranges of temperatures of gelatinization (G) and amylopectin melting (M1) for all tested flour doughs were determined by both experimental techniques and results showed good agreement between them. In DMTA, G and M1 were determined by means of the elastic modulus or damping factor evolution with temperature. The temperatures of the transitions determined by DSC depended on water content, the nature and characteristics of the starch and the presence of other compounds (mainly lipid and sugars) in the flour doughs.

KEYWORDS amylopectin melting, DSC, gluten-free flour, water absorption

INTRODUCTION

Gelatinization of different starches is well studied in the bibliography by its importance in starch processing for food and non-food purposes. At high water content, using DSC technique, one broad endothermic peak, G, by the swelling of the amorphous region and subsequent melting of crystallites is observed, but at intermediate water content, this transition is partially postponed to higher temperatures resulting M1 transition[1]. Nevertheless, some endothermic peaks associated to the thermal transitions are very weak and consequently their determination and evaluation is troublesome and other techniques are necessary. The study of the starch transitions in cereal flour doughs is more complex than the study of isolated starch from different sources. The

presence of other biopolymers like proteins and lipids, together with the particle size of the flour, affect significantly the water absorption of the samples to achieve a determined consistency. Dynamic Mechanical Thermal Analysis (DMTA) consists on the application of a sinusoidal force to the sample at fixed angular frequency measuring the stress and strain inside the LVR at constant heating/cooling rate. DMTA was employed to evaluate the starch gelatinization due to strong structural changes take place during the plasticizing process promoted by water[2].

The aim of this work is to determine the G and M1 transitions of gluten-free flour doughs processed at the same consistency level with different water absorption by DSC and DMTA. Starch transitions are discussed regarding to physicochemical properties of flours and doughs.

EXPERIMENTAL

Maize (*Zea mais*) flours obtained from 3 different varieties of Spanish maize kernels, white (WM, *Rebordanes*), yellow (YM, *Sarreaus*) and purple (PM, *Meiro*) and chestnut (CH, *Castanea sativa Mill.*) flour were used. Flours were placed in a desiccator at 25ºC and RH 54%, until flours equilibration with constant moisture content (8-10 %, d.b.). Flours were stored at 4ºC in vacuum sealed bags until use. Doughs for DMTA experiments were prepared by using Mixolab® apparatus (Chopin Technologies, France)[3]. At the consistency of 1.10 Nm, water absorption (WA, % d.b.) was determined. In the case of DSC studies, samples, at the same WA of doughs studied by DMTA, were prepared by other protocol. The flour (~1g) was put in a glass vial and water was added to obtain the desired WA. The vial was sealed and sample was equilibrated for 24 h at room temperature. A portion of the sample (< 18 mg) was introduced in a steel pan and sealed. Thermal properties were determined with a calorimeter (Q200, TA Instruments, USA). An empty steel pan was used as reference. Sample was heated from 40ºC up to 110ºC at 4ºC/min.

Flour doughs at the target consistency were tested in a controlled stress rheometer (MCR 301, Anton Paar, Austria) equipped with a chamber (CTD 450, Anton Paar, Austria) using parallel plates (50 mm diameter, 2 mm gap) by DMTA. The assays were performed in the LVR of the doughs (0.1 % of strain, 1 Hz). Temperature increased from 30 to 110ºC at 4ºC/min. G´ and tan δ values were used to determine the temperatures associated with starch transitions. All assays were performed at least in duplicate. Differences among means were identified by one-factor analysis of variance with Scheffe test and significant P-values ≤ 0.05 (IBM SPSS Statistics 22).

RESULTS AND DISCUSSION

In DSC experiments, all samples showed gelatinization endotherm, G, which appeared at low temperature (66.7-69.1ºC, see Table). This endotherm at high WA corresponds to the gelatinization of amylopectin[4]. When water is restricted, gelatinization can be partly postponed to higher temperatures due to the melting of the remaining amylopectin crystallites giving as result M1 peak. At intermediate WA, M1 peak appears as a shoulder overlapped with the G peak giving as result a broad temperature range of gelatinization. At lower WA, M1 is separated from G and shifted to higher temperatures. In maize doughs, YM dough (low WA) showed separately G and M1 peaks and WM and PM doughs only one peak (G + M1). CH dough also showed a peak with shoulder (G + M1), in spite of it is the sample with the lowest WA. This result reveals that the nature of starch and its interactions with other hydrophilic components (carbohydrates and proteins) modify the available water for starch gelatinization. Samples with peaks overlap showed a broad temperature range for the glass transition (from 66.7 to 93.3 ºC, Table).

TABLE. Onset (T_o), peak (T_p) and final (T_1) temperatures of thermal starch transitions determined by DSC and DMTA for tested maize and chestnut flour doughs♣

			YM	WM	PM	CH
WA (%, d.b.)			63.0±1.0b	90.0±2.0d	81.1±1.4c	52.9±0.5a
T (ºC)				DSC		
G	To		66.7a	66.7a	68.2b	69.1b
	Tp		74.0a	76.7b	78.8c	77.5b
	T1		82.6a	90.6b	93.3c	90.2b
M1	To		83.0	-	-	-
	Tp		91.7	-	-	-
	T1		100.7	-	-	-
				DMTA		
G	To´	G´	53.6±0.1a	50.0±1.3a	56.1±0.2a	56.9±2.5a
		tan δ	-	-	-	-
	To	G´	-	-	-	-
		tan δ	66.9±0.1a	68.6±1.9a	71.5±0.6a	71.0±0.7a
	Tp	G´	74.4±0.1a	74.5±0.3a	77.3±0.5b	76.9±0.2b
		tan δ	77.0±0.2a	75.8±2.0a	79.0±0.6a	78.9±0.6a
	T1	G´	-	86.8±0.2a	85.0±0.4a	86.5±0.3a
		tan δ	-	83.0±0.2a	87.5±1.5a	84.5±0.1a
M1	T1	G´	102.5±2.1	-	-	-

♣Standard deviations of temperature data for DSC were ±0.2ºC. Data with different letters in rows are significantly different, P ≤ 0.05.

Figure shows the G´ peaks during DMTA of YM and WM dough samples, as example of two behaviours observed. At low temperatures G´ values decreased slightly with increasing temperature up to achieve a minimum. This point, labeled like To´, determines the beginning of the physical phenomena of gelatinization, corresponding to the swelling of the starch granules. G´ increased due to the growing turgor of starch granules. G´ values sharply increase from 50-

57ºC. This point was not detected by DSC, because thermal properties of dough were not modified. Starch gelatinization continues at higher temperatures with the disintegration of the granules and starchy polymers melting with a generation of a continuous matrix of leached amylose molecules that increases the viscous character. In fact, tan δ increased above To, measured by DSC, up to a maximum value, Tp. This peak temperature coincides with Tp given by relative maximum of G´, Table. To and Tp measured by DSC and DMTA showed deviations < 2ºC. Final temperature, T1, can be evaluated through the minimum value of tan δ and also by the point in which the slope (straight line in Figure) of G´ changes after Tp. This peak is the sum of G and M1 transitions for WM, PM and CH doughs while YM sample showed separated peaks. In DMTA both peaks of YM dough were not observed, but a broader temperature interval with constant slope was found. Consequently, structural changes and phase transitions promoted during G and M1 endotherms measured by DSC are jointly observed by DMTA.

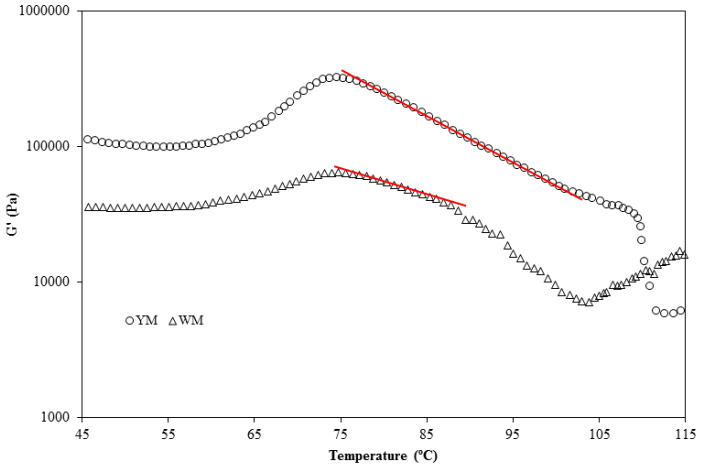

FIGURE. DMTA rheograms for yellow (YM) and white (WM) maize flour doughs.

ACKNOWLEDGEMENTS

The authors acknowledge the financial support to Ministerio de Economía y Competitividad of Spain and FEDER (CTQ 2013-43616/P).

REFERENCES AND NOTES

1. Jang, J.K.; Pyun, Y.R. *Starch/Stärke*, **1996**, 48, 48-51.
2. Chanvrier, H.; Appelqvist, I.; Li, Z. *Food Research International*, **2013**, 53, 73-80.
3. ICC. Standard Methods. International Association for Cereal Chemistry, Vienna 337, **1996**.
4. Liu, H.; Yu, L.; Xie, F.; Chen, L. *Carbohydrate Polymers*, **2006**, 65, 357-363.

O20

Rheology and texture of liquid whey protein concentrates (LWPC) based gels: influence of the acidification process

Marta Helena Fernandes Henriques[1,2], David Manuel Gama Simões Gomes[1,2], Carlos José Dias Pereira[1,2]

[1]Polytechnic Institute of Coimbra - College of Agriculture, Department of Food Science and Technology, Bencanta, 3040-316 Coimbra, Portugal

[2]CERNAS – Research Center for Natural Resources, Environment and Society, Bencanta, 3040-316 Coimbra, Portugal

Correspondence to: Marta Helena Fernandes Henriques (E-mail: *mhenriques@esac.pt*)

ABSTRACT

The aim of this work was to study the gelation properties of liquid whey protein concentrate (LWPC) as raw material for dairy food applications. The gelation was promoted by acidification. Acid-induced gels were produced with non-defatted LWPC by bacterial fermentation (yogurt type) and glucono-δ-lactone (GDL) acidification (dessert type) with or without fortification with skimmed milk powder (SMP). All the produced gels showed viscoelastic behaviour. The fermented systems formed weaker gel structures than the equivalent chemically acidified gels. The acidification process and the sequence in which protein denaturation is performed may be responsible for these differences. It was also observed that molecular rearrangement continues during cold storage, and that fortification with SMP favoured gelation improving the rheological properties and the viscosity of the LWPC gels.

KEYWORDS Liquid whey proteins, acid gelation, rheology, viscosity, texture

INTRODUCTION

Whey proteins are pointed out as carriers for ligands and trace elements as well as for their biological functions [1]. In food products, dry whey protein concentrates (WPC) are widely used in bakery and confectionary products [2], salads [3], beverages [4], meat and dairy products [5,6]. The application of WPC in food, in order to increase nutritional and functional properties (e.g. emulsifying and gelling) is not random, and depends on the origin, production process and chemical composition of the whey protein concentrates. Among the functional properties of whey proteins, gelation is cited as one of the most interesting hydration-related properties.

Membrane technologies, namely ultrafiltration (UF) enable the extraction and concentration of whey proteins from whey. Despite WPC are largely used as ingredients the direct use of liquid whey protein concentrates (LWPC), being a less expensive alternative [7] avoiding drying processes, is rarely applied and no attention has been paid to its functionality.

MATERIAL AND METHODS

Bovine cheese whey used in the production of non-defatted (ND) LWPC was supplied by Queijaria Serqueijos SA (Portugal). GDL was supplied by Enzilab and the mixed culture of *Streptococcus thermophilus* and *Lactobacillus bulgaricus* was supplied by Ezal YO-MIX 601.

Manufacture of LWPC and gel preparation

No defatted LWPC was produced according to Henriques [7], whose chemical composition was 20.5% of total solids, 7.1% of fat, 9.6% of protein and 0.85% of ash. Titratable acidity (TA) was 0.52% lactic acid.

Acid gels of ND LWPC, used as food model for yogurt and dessert, were produced by lactic fermentation or acidification by GDL respectively, with or without SMP. For yogurt type acid gel production, the LWPC was first pasteurized at 90 ºC/5 min and cooled down to 60 ºC. The product was divided into two parts and SMP was added to one part to obtain 5% incorporation in the final formulation. After that, both products were homogenized at 100 bar. The fermentation, performed by a commercial mixed culture of bacteria, took place at 44 ºC until pH reached 4.6. In the case of the acid gel desserts, 5% sucrose was added to the ND LWPC and two separate formulations were produced (0% and 5% SMP). Both mixtures were heated to 60 ºC and homogenized at 100 bar. GDL was then added to a level of 1.5% (w/w, protein basis) and the mixture was gently stirred and distributed into glass cups. Acidification by GDL hydrolysis to gluconic acid was performed also at 44 ºC until pH 4.6. Finally, acid gel desserts were heat treated at 90 ºC/30 min. All the samples were then refrigerated and stored at 5 ºC.

Gel composition and physicochemical analyses

Acid gels were analysed in triplicate and characterised in terms of dry matter, fat, total proteins, ash, carbohydrates, titratable acidity (TA) and pH. Gel water retention capacity (WRC) was determined according to the method of Gauche [7]. The texture profile analysis (TPA) was run in a Stable Micro Systems Texture analyser (TA.XT Express Enhanced model) with a penetration distance of 5 mm at 1 mm/s test speed, using an acrylic cylindrical probe with a diameter of 0.6 mm and a height of 3.5 mm. The rheological properties, elastic modulus (G') and viscous modulus (G") were evaluated at 15ºC in the range of 0.05 - 1.5 Hz at 3 Pa, using a controlled stress rheometer (Rheostress 1, ThermoHaake) in oscillatory mode. The measuring system consisted of a cone and plate geometry, C60/Ti - 0.052 mm (60 mm Ø and of 1º angle).

RESULTS AND DISCUSSION

As expected, the products with SMP had significantly higher total solids than the unfortified products. The fat content did not vary in each product type ($p > 0.05$) with the addition of SMP. Although the protein content increased in products with 5% SMP, due to the incorporation of caseins, no significant differences ($p > 0.05$) were observed between formulations or product types. Lactic desserts had significantly higher levels of other solids (mainly carbohydrates) due to the addition of sucrose in the formulation (5%, wet basis). Solvent evaporation due to the longer heat treatment (30 min) and the

fermentation process in the case of yogurts, which converted lactose into lactic acid, may also have contributed to this difference.

The titratable acidity (Table 1) achieved for LWPC yogurt type acid gels (1.30-1.88%) was higher than for the dessert gels (1.05-1.58%). This may indicate that acidification by bacterial fermentation is more effective than by GDL hydrolysis to gluconic acid. A significant decrease in pH was also observed during storage for yogurts, which may point out that fermentation continues during storage. A distinctive type of behaviour was found in desserts. This divergence in the pH between products may be due to the period at which the heat treatment was performed during gel production. In the case of yogurts, whey protein denaturation occurs during the pasteurisation (90 ºC, 5 min) of LWPC, prior to the addition of SMP and fermentation whereas in the case of desserts, acid-induced gelation occurs when the whey proteins are still in their native form. Specific WRC behaviour (Table 1) can be observed in the LWPC acid gels according to their nature (yogurt or dessert), SMP incorporation and storage time. The desserts showed a higher WRC (64.12-100%) than yogurts (53.11-65.74%), which can be attributed firstly to their higher total solids content and also to the heat treatment after acidification. With regard to hardness, it was observed that desserts presented higher values than yogurts, and the incorporation of SMP in the formulation also contributes to this. These results concur with the higher WRC observed for desserts with 5% SMP, indicating that harder gel structures have the ability to prevent syneresis more efficiently.

TABLE 1 TA, WRC and hardness of ND LWPC yogurts and desserts (0% and 5% of SMP) during storage

Gel type		Yogurt		Dessert	
Parameter	Time (days)	0%	5%	0%	5%
Titratable acidity TA (% lactic acid)	1	1.38±0.17 ^{aA}	1.46±0.18 ^{aA}	1.05±0.01 ^{aA}	1.58±0.02 ^{bA}
	21	1.30±0.08 ^{aA}	1.88±0.11 ^{bB}	1.19±0.08 ^{aB}	1.21±0.14 ^{aB}
Water retention capacity WRC (%)	1	65.74±1.62 ^{bA}	53.11±1.16 ^{aA}	70.49±4.58 ^{aB}	99.52±0.58 ^{bA}
	21	64.04±1.03 ^{bA}	56.59±2.94 ^{aB}	64.12±4.87 ^{aA}	100.00±0.00 ^{bA}
Hardness (N)	1	0.10±0.00 ^{aA}	0.09±0.01 ^{aA}	0.11±0.02 ^{aA}	0.59±0.12 ^{bA}
	21	0.11±0.00 ^{aA}	0.15±0.01 ^{bB}	0.18±0.02 ^{aA}	0.44±0.16 ^{bA}

Means without the same letter differ statistically at $p < 0.05$. ^{a,b} Lowercase letters represent differences between products (0 and 5% of SMP). ^{A,B} Uppercase letters represent differences over time (1st and 21st days).

In Fig. 1 it can be observed that in all cases G' is higher than G'' demonstrating the gel structure and the viscoelastic behaviour of both products. An increase in G' and G'' was observed over time, indicating that protein polymerization and molecular structure rearrangements continue during refrigeration, thus making the gels stronger. In yogurts no significant differences were observed between products one day after production, with or without SMP fortification. However, at the end of the storage time the yogurts with SMP presented lower G' and G'' values than the ones with no SMP addition. The presence of casein micelles that were not denatured may increase protein heterogeneity and disturb the protein network by producing weaker gels. In the case of desserts, a very stable product was obtained using SMP (Fig. 1). These results corroborate the higher hardness values and WRC (Table 1) achieved for these acid gels.

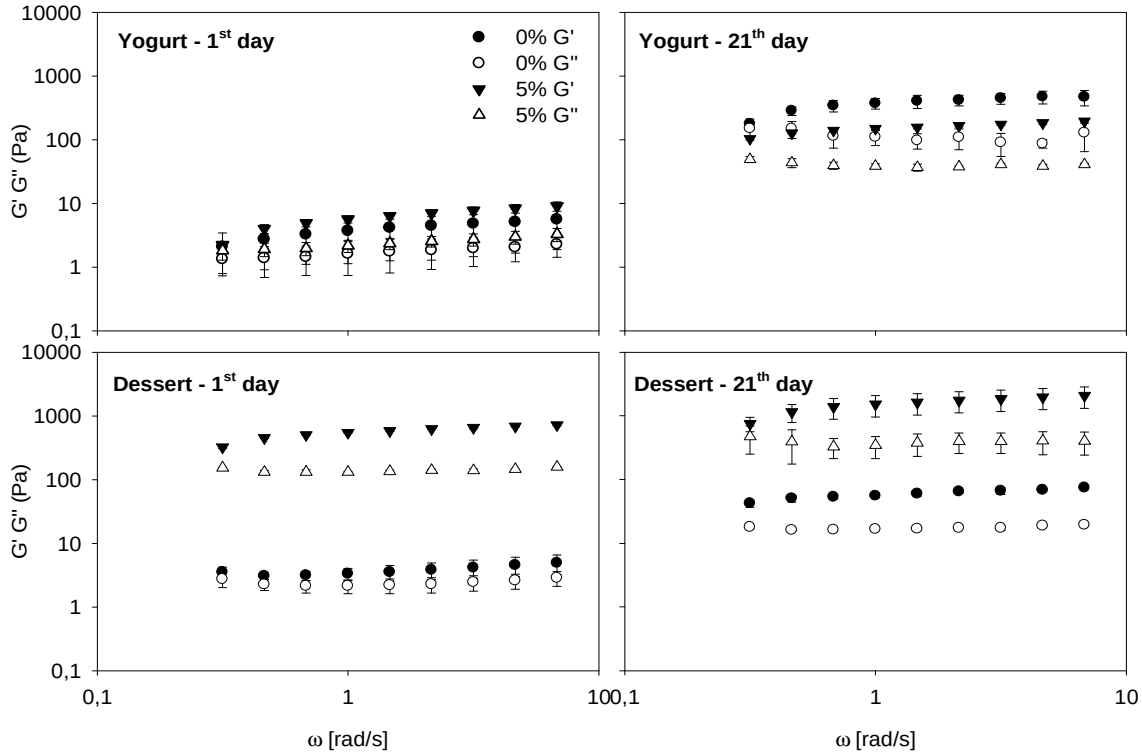

FIGURE 1 G' of ND LWPC yogurts and desserts with 0% (●) and 5% (▼) SMP; G" of ND LWPC yogurts and desserts with 0% (○) and 5% (Δ) SMP, during storage.

CONCLUSIONS

Due to the process simplicity and the easiness of adjusting the production parameters to target specific industrial requirements, the use of LWPC allows for the production of high value and highly nutritional dairy products as a direct and low cost alternative to the use of powdered products.

REFERENCES

1. de Wit, J.N., *Journal Dairy Science*, **1998**,*81*, 597-608.
2. Strouts, B. In Reference manual for U.S. whey and lactose products; Page, J.; Meyer, D.; Haines, B.; Lagrange, V.; Kenney, A., Eds., U.S. Dairy Export Council, **2004**; Chapter 10, pp. 98-99.
3. Christiansen, K.F.; Vegarud, G.; Langsrud, T.; Ellekjaer, M.R.; Egelandsdal, B., *Food Hydrocolloids*, **2004**,*18*, 757-767.
4. de Wit, J.N. In Encyclopedia of dairy sciences; Roginski, H.; Fuquay, J. W.; Fox, P. F., Eds., Academic Press, London, **2003**; Volume 2; pp. 718-727.
5. Remeuf, F.; Mohammed, S.; Sodini, I., Tissier, J.P., *International Dairy Journal*, **2003**,*13*, 773-782.
6. Henriques, M.; Gomes, D.; Pereira, C.; Gil, M, *Food and Bioprocess Technology*, **2013**,*6(4)*, 952-963.
7. Henriques, M.H.F., Recovery and applications of whey proteins in conventional and nonconventional food systems, PhD thesis, Department of Chemical Engineering, University of Coimbra, Coimbra, **2013**

O21

Soybean proteins as basis on the formation of superabsorbent materials

Lucia Fernández-Espada, Carlos Bengoechea, Felipe Cordobés, Antonio Guerrero

Departamento de ingeniería química, Universidad de Sevilla, España

Correspondence to: Carlos Bengoechea (E-mail: *cbengoechea@us.es*)

ABSTRACT

Superabsorbent materials (SAMs) can absorb large volumes of aqueous fluids, retaining absorbed water even under heating or some pressure. The environmentally friendly characteristics of materials have become an essential index to evaluate their applicability in practice. Currently, the biodegradable SAMs are mainly focused on the natural polysaccharide family (e.g. starch) having been applied in many fields, prominently in agriculture, horticulture, and hygiene products.

Due to its hygroscopic character, a soy protein isolate (SPI) was selected to produce materials through injection molding with the goal of evaluate their water uptake capacity

In order to obtain a material with a higher water uptake capacity, sodium bicarbonate was introduced in the formulation, along glycerol as plasticiser. Depending on the composition used and on the processing conditions selected, water uptake values as higher as 900.02 ± 21% (2.5% bicarbonate) were reached.

Moreover, it was clear how a higher content of bicarbonate produced materials with a lower Young modulus and higher maximum strain. These materials show a remarkable capacity to absorb water, explained by the hygroscopic character of both the protein and plasticizer and presumably by the high porosity produced due to the bicarbonate decomposition, which may be of special interest for future applications.

KEYWORDS soy protein, bioplastic, injection moulding, superabsorbent, water uptake

INTRODUCTION

Petroleum-based plastics are well extended, though many drawbacks result from their use. A great concern goes to the generation of important wastes that are difficult to degrade. Those negative attributes have led to an increasing interest on environmentally friendly plastics from alternative sources[1].

Even if environmentally friendly bioplastics have been produced from proteins, lipids or polysaccharides[2,3,4], there is still a lot of work ahead in order to improve mechanical and physical

properties of protein-based bioplastics. Depending on their future applications, possible inconveniences may be found, as good hygroscopic properties normally are paired with lower elastic properties.

Soybean proteins may be transformed into biodegradable plastics when mixed with a plasticizer[5,6]. However, these soybean bioplastics have showed low mechanical strength and high moisture absorption. Thus, they may have potential applications in the field of Superabsorbent Materials (SAMs).

The objective of the present work is to study how composition and processing conditions may produce soybean protein-based bioplastic materials with a higher water uptake capacity and proper mechanical properties with potential application as SAMs.

RESULTS AND DISCUSSION

Soybean protein is known for its high higroscopicity, which may be an asset when the aim is a material with a high water uptake capacity, which eventually would have a potential application as SAM. Among the several methods available to produce protein-based bioplastic materials, injection moulding was selected.

Processing condiitions		Water uptake (%)	E' (Pa) $\cdot 10^{-8}$	E'' (Pa) $\cdot 10^{-8}$	tanδ
$T_{cylinder}$	80ºC	243 ± 21	1.33 ± 0.06	0.44 ± 0.03	0.33 ± 0.01
	100ºC	213 ± 43	1.33 ± 0.06	0.44 ± 0.01	0.33 ± 0.03
	120ºC	125 ± 48	1.46 ± 0.03	0.45 ± 0.04	0.31 ± 0.02
T_{mould}	80ºC	523 ± 19	1.23 ± 0.20	0.36 ± 0.34	0.29 ± 0.01
	100ºC	429 ± 14	1.74 ± 0.13	0.50 ± 0.12	0.29 ± 0.00
	120'ºC	243 ± 21	1.46 ± 0.03	0.45 ± 0.04	0.31 ± 0.02
	140ºC	218 ± 5	1.29 ± 0.36	0.41 ± 0.11	0.32 ± 0.01
$P_{injection}$	250 bars	233 ± 6	1.38 ± 0.05	0.38 ± 0.00	0.28 ± 0.01
	500 bars	224 ± 27	4.25 ± 0.26	1.20 ± 0.11	0.28 ± 0.01
	1000 bars	260 ± 13	7.68 ± 0.78	2.19 ± 0.24	0.28 ± 0.00

TABLE 1 Flexural parameters (1Hz, 25ºC) for SPI/Gly (50/50) bioplastics processed through injection moulding. When not indicated: $T_{cylinder}$: 80ºC; T_{mould}: 120ºC; $P_{injection}$: 500 bars. No bicarbonate included.

The first stage of this research focused on the optimization of the processing parameters. Thus, different 50/50 SPI/Gly bioplastic materials were obtained at different cylinder temperature ($T_{cylinder}$), mould temperature (T_{mould}) and injection pressure ($P_{injection}$) values.

The best capacity to absorb water when immersed is observed at lower cylinder and mould temperature values (e.g. 80ºC), being the impact of pressure on water uptake seemingly less important (Table 1). When observing the influence on flexural properties (elastic and viscous moduli, E' and E'' respectively), T_{mould} and especially $P_{injection}$ show the greater effect: an increase in T_{mould} over 100ºC produces a lowering in E' and E'', while an increase in $P_{injection}$ results in a strengthening of the structure (higher E', E'').

Once those processing conditions have been studied, the effect of the addition of sodium bicarbonate on the water uptake capacity is studied. The decomposition of sodium bicarbonate on the injection-moulding device leads to the formation of a porous structure that may enhance the water absorption. Milder processing conditions ($T_{cylinder}$: 40ºC; T_{mould}; 70ºC) were used in order to avoid a major decomposition of bicarbonate in the injection-moulding device. Moreover, it has been proved how lower temperature values promote a higher water uptake.

As observed in Figure 1, the addition of bicarbonate in the formulation in a concentration within 1 to 5% results in higher water uptake capacities, and also in a decrease in their Young moduli and an increase in their maximum strength.

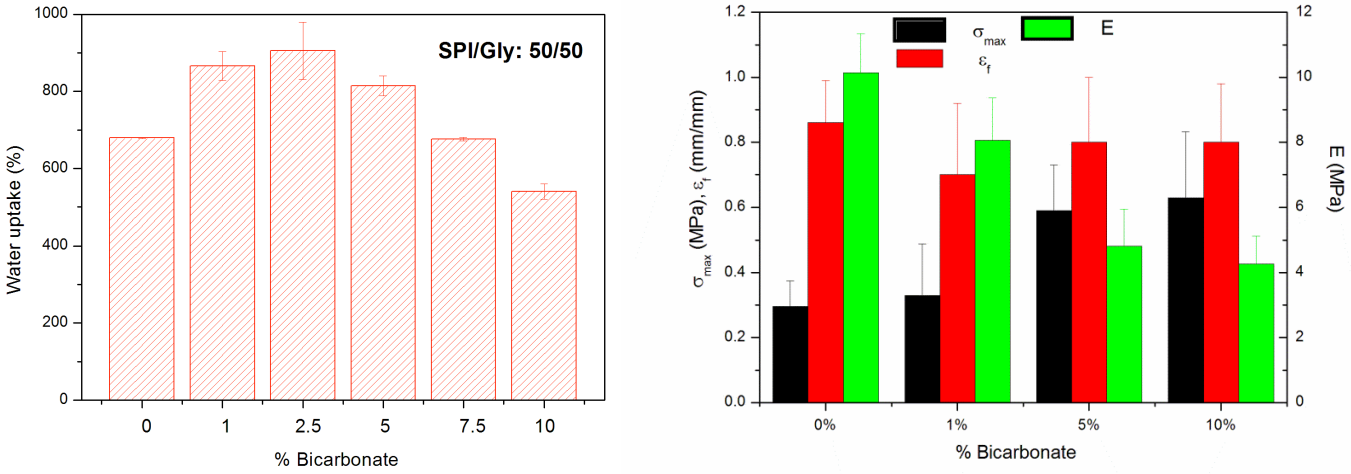

FIGURE 1. Water uptake capacity (*left*); and tensile parameters (maximum strength (σ_{max}), strain at fracture (ε_f), Young modulus (E)) (*right*) for SPI/Gly (50/50) bioplastics processed through injection moulding ($T_{cylinder}$: 40ºC; T_{mould}: 70ºC; $P_{injection}$: 500 bars) and different sodium bicarbonate concentrations

CONCLUSIONS

When a high water uptake capacity is pursued for 50/50 SPI/Gly bioplastic materials through injection moulding, low mould temperatures and medium to high pressures are required.

At those processing conditions, a higher water uptake capacity is obtained when bicarbonate is present in the formulation of 50/50 SPI/Gly bioplastic materials, especially at concentrations ranging from 1 to 2.5%, obtaining water uptake values around 900%. These high values may be used in the production of SAMs, though further research in this direction is needed.

ACKNOWLEDGEMENTS

The authors would like to kindly acknowledge the financial support from MCI (MAT2011-29275-C02-02).

REFERENCES

1. Jones, A., Ashton Zeller, M., Sharma, S., *Progress in Biomaterials*. **2013**, 2:12
2. Avérous, L., *Macromolecular Science -Polymer Reviews*., **2004**, C4(3): 231-274.
3. Hernández-Izquierdo, V.M., Krochta, J.M., *Journal of Food Science*, **2008** (73): 30–39.
4. Siracusa, V., Rocculi, P., Romani, S., Dalla Rosa, M., *Trends in Food Science & Technology*, **2008**, (19): 634–643.
5. Liu, W., Mohanty, AK., Askeland, P., Drzal, LT., Mirsa, M., *Polymer*, **2004**, 45: 7589-7596
6. Liu, W., Mohanty, AK., Askeland, P., Drzal, LT., Mirsa, M., *Polymer,* **2005**, 46: 2710-2721

Rheology of healthy bonbons with functional characteristics

Vanessa Batista, Margarida Faísca, Patrícia Fradinho, Anabela Raymundo, Isabel de Sousa
LEAF- Instituto Superior de Agronomia/Universidade de Lisboa, Edifício Ferreira Lapa-Tapada da Ajuda 1349-017 Lisboa, Portugal

Correspondence to: Isabel de Sousa (E-mail: isabelsousa@isa.ulisboa.pt)

ABSTRACT

The present work is part of a joint project with a traditional confectionery company. The aim of the project was to develop gourmet fillings for bonbons, based on gelled matrices of Portuguese products of unquestioned quality and international recognition including port wine, olive oil, olives and fruits. The gelling system was obtained by adding rice flour and *Psyllium fiber*. The objective was to reduce the calories of the product and enrich the fillings in i) functional ingredients: chicory fiber (inulin) and *Psyllium fiber* and ii) spices as natural antimicrobials (cinnamon, ginger, clove and nutmeg).
Characterization of fillings included chemical composition and nutritional content, rheology behaviour and water activity (a_w of quick Rotronic, Hygrolab).

The rheology behaviour of the new fillings was compared with the traditional/commercial fillings. The results show that the fillings under study have a similar viscoelastic behavior to the commercial fillings, the latter showing higher values in the viscoelastic functions.

KEYWORDS

Healthy bonbons, functional ingredients, spices, chicory fiber, *psyllium* fiber, rheology behavior.

INTRODUCTION

Currently, there is an increased awareness of consumers towards the consumption of healthy products with functional characteristics. Bonbons are products of high demand and due to high calorie intakes their consumption is limited by dietary issues. Therefore, some studies on low calorie bonbons can be seen on literature[1].

Fat has multiple effects on food products, e.g., thermal stability, mouthfeel lubrication and smoothness. When fat is to be replaced for nutritional/dietary reasons, it is often necessary the use of combinations of hydrocolloids to reach the expected sensory properties of the low fat food product [2].

The incorporation of *Psyllium* and inulin fibers in bonbons fillings was an important innovation in this project and the spices were used to improve the sensory characteristics of the fillings and extend the shelf-life of the products.

The *Psyllium* husk has about 80% of soluble fiber and is an excellent source of soluble and insoluble fiber[3, 4]. This fiber has been reported as an important health promoter in the prevention of several diseases[5].

The *Psyllium*, besides being a functional ingredient, is also important for the gelling capacity and for this reason is a good alternative to replace fat, keeping the texture and smooth mouthfeel.

The Inulin is a dietetic fiber extracted from chicory, whose extensive use in food industry is based on the nutritional and technological properties of inulin. Other important properties of inulin are the positive effect on bowel habit, but also the prebiotic effect[6].

METHODS

Preparation of the filling

In the technological diagram below (FIGURE 1), the steps for the fillings production are presented.

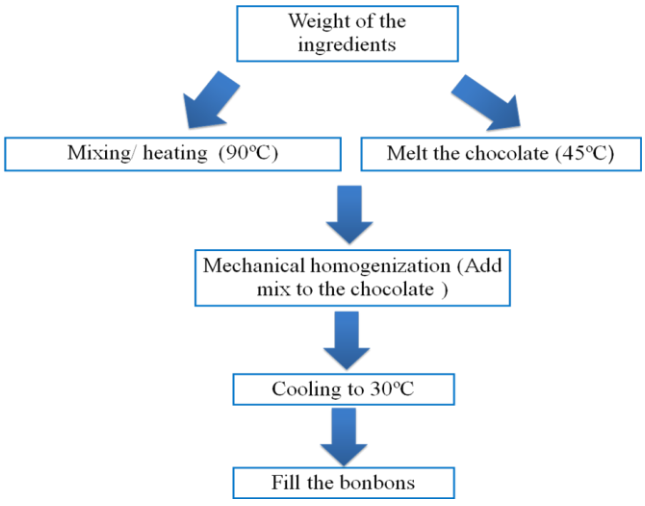

FIGURE 1. Technological diagram of the developed fillings

Characterization of filling

Rheology measurements

The internal structure of the filling matrices was evaluated by small amplitude oscillatory shear (SAOS) with a controlled stress MARS III (Haake) rheometer coupled with a Peltier system, to control temperature. The texture properties were analyzed in texturometer TA XTplus through TPA-Texture Profile Analysis.

Analysis of the chemical filling composition

The chemical composition and nutritional content of the developed and the commercial fillings was evaluated by determining protein (Kjeldahl), fat (Soxhlet), total sugars (NP 1420:1987) and fibers (methods AOAC).

Determination of water activity

The water activity (a_w) was evaluated using a Rotronic device (20ºC ± 1ºC).

RESULTS AND CONCLUSIONS

The results from the rheology behaviour of the new fillings and traditional/commercial fillings are presented in FIGURE 2.

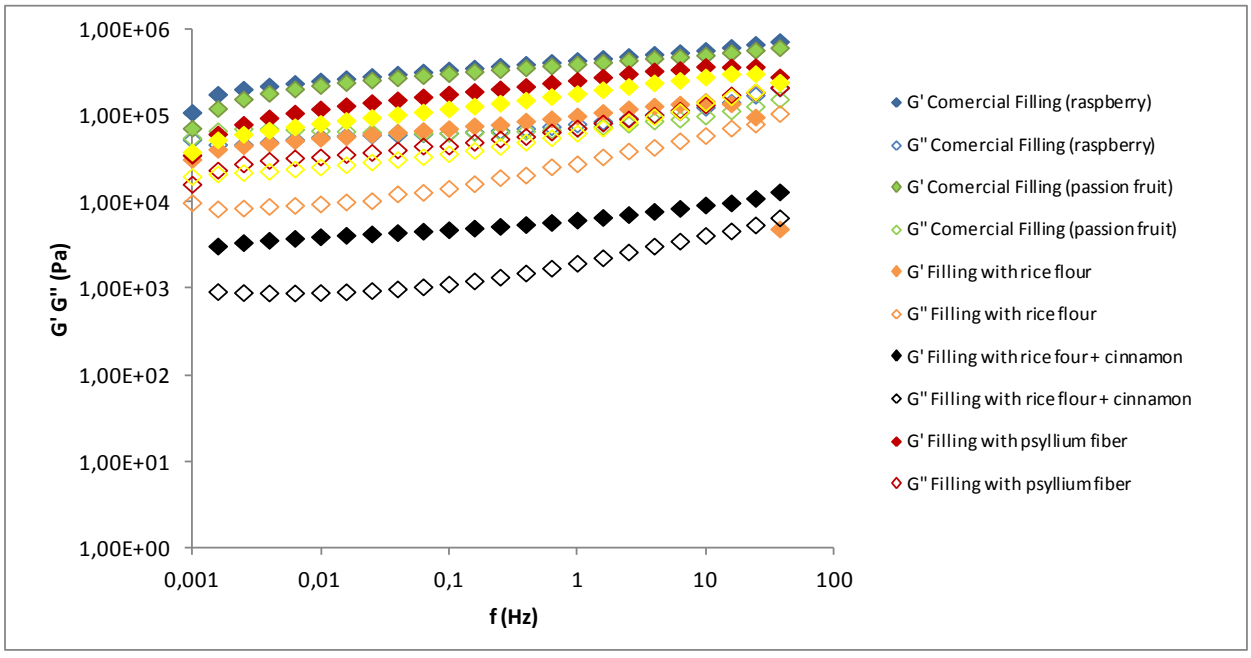

FIGURE 2. Mechanical spectra of the fillings

The new fillings have a viscoelastic behavior similar to the commercial fillings, with the later showing higher values in the viscoelastic functions, therefore being more structured.

It was verified that the storage modulus G' is always higher than the loss modulus G'' and both the moduli increase with the increase of frequency, which reflects a predominance of the elastic component over the viscous component, in all the samples, typical for the weak gel model. It is highlighted that the new filling with rice flour and cinnamon is the one that shows the lower level of structure, with lower values for the viscoelastic functions.

The developed fillings presented a high potential to scale up into the market. These products follow the present consumption trends, in markets with well-informed consumers that look for products with high quality differentiating features.

ACKNOWLEDGEMENTS

This work was supported by COMPETE program: QREN- " Healthybonbons" project 33880 in collaboration with AJM pastelarias, Lda .

REFERENCES

1. Dias, J.; Sousa, I., Accepted for publication on the Journal of Food Science and Technology **2004,** JFST-D-14-00666.
2. McClements, J.; Demetriedes, K., Crit.Rev. Food Sci. Nutr., Philadelphia, **1998**, 38, 6, 511-536.
3. Yu, L.; Perret, J., Journal of Agricultural and Food Chemistry, **2003**, 51, 492-495.
4. Raymundo, A.; Fradinho, P.; Nunes., M., Bioactive Carbohyrates and Dietary Fibre, **2014**, 3, 96-105.
5. Bijkerk, C. J.; Muris, J. W. M.; Knottnerus, J. A.; Hoes, A. W.; Wit, N. J., Alimentary Pharmacology & Therapeutics, **2004**, 19, 245-251.
6. Tungland, B. C.; Meyer, D., Comprehensive Reviews in Food Science and Food Safety, **2002**, 3, 73 and 92.

O33

Rheological assessment of *carolino* rice flour gels for pasta making

Patrícia Fradinho, Ana Filipa Rocha, Isabel de Sousa, Anabela Raymundo

LEAF – Instituto Superior de Agronomia/Universidade de Lisboa, Tapada da Ajuda-Edifício Ferreira Lapa, 1349-017 Lisboa, Portugal

Correspondence to: Anabela Raymundo (anabraymundo@isa.ulisboa.pt)

ABSTRACT

Rice is a largely consumed cereal, with high nutritional value. However, during dehusking and polishing steps, high quantities of by-products are originated, of which about 15% is broken rice. This by-product can be ground and the resulting flour used to develop added-value gluten free food products.

This study aims the development of gluten-free gel based on *carolino* rice flour from broken rice to future incorporation in a pasta formulation. Aqueous suspensions with 5% to 60% (w/w) flour were prepared, and the viscoelastic behaviour was evaluated using SAOS measurements.

The critical gelation concentration of rice flour was 7% (w/w). The gel with 40% rice flour was selected for pasta incorporation.

KEYWORDS rice flour, viscoelasticity, gel, gelatinization, gluten-free pasta

INTRODUCTION

Carolino rice is a traditional Portuguese variety, much used due to its gastronomic singularities. Understanding how this flour behaves under processing conditions could be the key factor in producing a viscoelastic dough for gluten-free pasta production.

Since rice protein lacks the functionality of gluten to produce a viscoelastic dough structure, several authors suggested starch gelatinization as an essential step to improve the properties of rice dough and produce pasta with good quality[1].

In order to optimize the gelatinization process, *carolino* rice flour suspensions in water, with concentrations between 5% and 60% (w/w) were prepared, and its thermorheological behaviour was assessed.

EXPERIMENTAL

Carolino broken rice was milled into flour by a rice company and used for gel preparations. *Carolino* rice flour solutions were prepared, ranging from 5% to 60% (w/w). Flour was dispersed in water, under mechanical stirring (Eurostar Digital, IKA-WERKE) at 350 rpm and heated at 90ºC during 30 min, in a water bath[2]. The mixtures between 5 and 20% were poured into a glass container and left for 24h at 4ºC to ensure full gel maturation. Rice flour suspensions between 30 and 60% were transferred to the bottom plate of a 35 mm serrated parallel plate sensor (PP35) on the rheometer (MARS III, Haake), to promote the gelation *in situ*.

Viscoelastic behaviour was investigated using SAOS measurements, performed in a controlled stress rheometer coupled with an UTC-Peltier system, using the PP35. Stress sweep tests were conducted on suspensions and gels in order to identify the linear viscoelastic region. Temperature, time and frequency sweeps tests were performed inside this region at 1Hz.

The suspensions were heated from 20 to 90ºC at 1ºC/min, maintained at this temperature for 30 min, and cooled down to 5 ºC. The gel maturation was performed at this temperature, during 30 min, followed by the mechanical spectra. After maturation, flow curves were obtained, using the same sensor system. Each formulation was tested at least in duplicate.

RESULTS AND DISCUSSION

In Figure 1 the evolution of viscoelastic parameters G' and G'' is depicted.

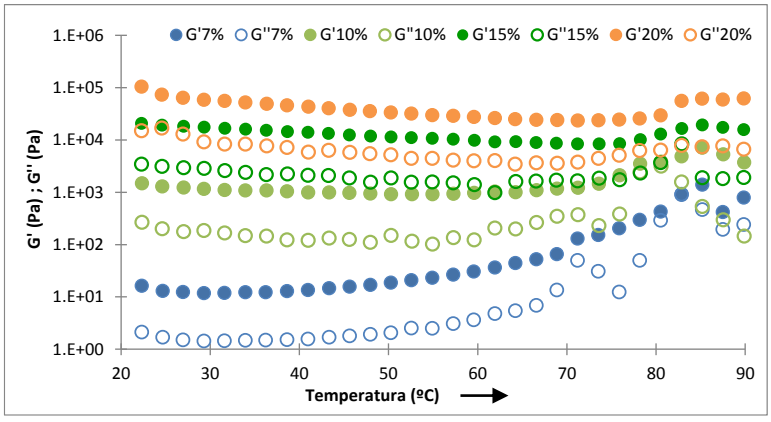

FIGURE 1. Thermorheological measurements from 20 to 90ºC at 1ºC/min of aqueous suspensions with rice flour: ● 7%; ● 10%; ● 15%; ● 20% (closed symbols-G'; open symbols–G'').

During the initial heating, systems with 10 to 20% rice flour show a practically constant viscoelastic parameters, with G' larger than G''. Around 75ºC both modulli increase about half a decade until 82ºC, corresponding to the starch gelatinization temperature. 7% rice flour gel

shows a different heating behaviour, since viscoelastic modulli are strongly temperature dependent. The variations observed for G'' value of 7% and 10% curves could result from the low rice concentration close to critical gelling concentration.

During the cooling cycle (data not shown), the gel structure was slightly reinforced, especially in 7% rice gel. Both modulli increased, achieving larger values at the lowest temperatures.

The maturation kinetics at 5ºC of studied gels are presented in Figure 2.

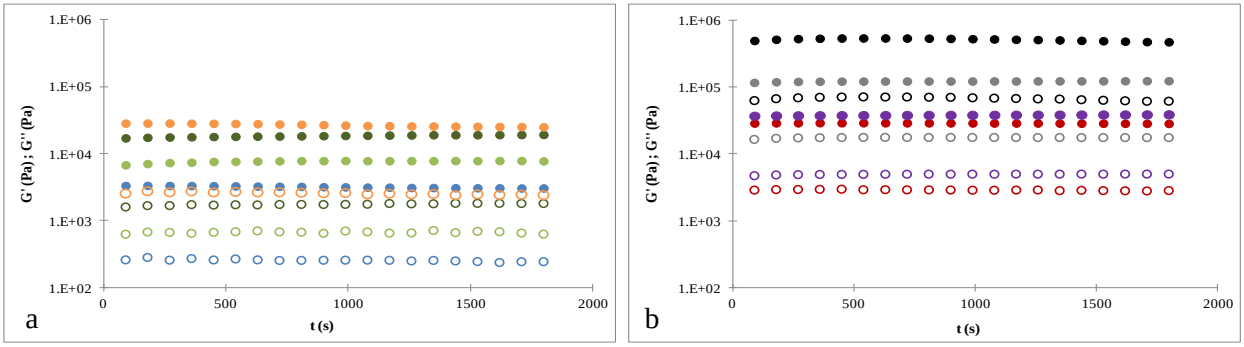

FIGURE 2. Maturation kinetics of rice flour gels: a) ● 7%; ● 10%; ● 15%; ● 20%; b) ● 30%; ● 40%; ● 50%; ● 60% (closed symbols-G'; open symbols–G'').

All gels show rapid maturation, since both modulli remained stable after 30 min maturation. This may be considered an important advantage from an industrial point of view.

The mechanical spectra of rice flour gels ranging from 7 to 60% (w/w) obtained after the heating/cooling cycle previously described are resumed in Figure 3.

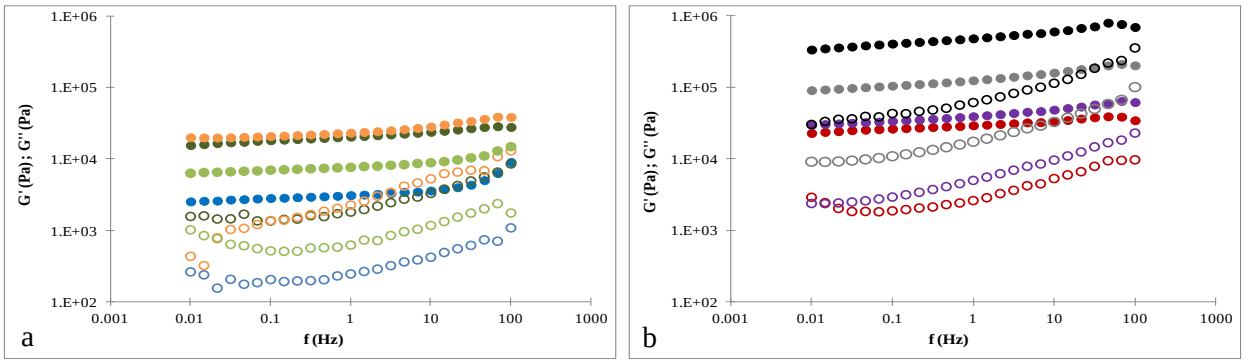

FIGURE 3. Mechanical spectra of rice flour gels ranging from: a) 7 to 20% (w/w); b) 30 to 60% (w/w). (● 7%; ● 10%; ● 15%; ● 20%; ● 30%; ● 40%; ● 50%; ● 60%; closed symbols-G'; open symbols–G'').

From the mechanical spectra, weak gel-like structures are observed, as G' is always higher than G'', but both modulli show a frequency dependence. For all concentrations it is observed an increase in the linear viscoelastic functions with rice flour content, which reflects an increase in

gel structure level. According to Cham, et al (2010)[3] a soft gel is more suitable for making making fresh pasta, whereas a stronger one is preferable for dry pasta production.

The critical concentration for rice flour gelation was 7%. The mechanical spectrum of 5% mixture (data not presented) show an overlap of the viscoelastic functions, meaning that for this concentration a gel structure is not formed.

The flow curves of the developed rice flour mixtures are presented in Figure 4.

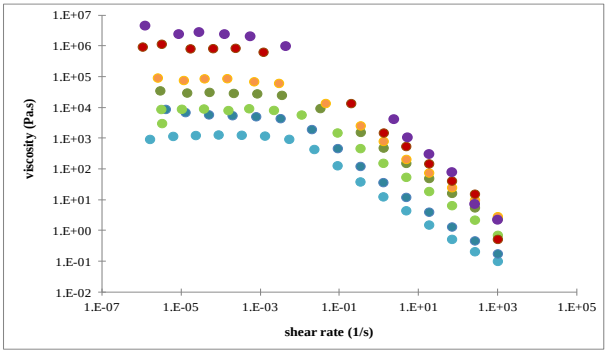

FIGURE 4. Flow curves of *carolino* rice flour mixtures from 5 to 40% (w/w).
(● 5% (w/w); ● 7% (w/w); ● 10% (w/w); ● 15% (w/w); ● 20% (w/w); ● 30% (w/w); ● 40% (w/w))

Above 40% rice flour, the gel becomes very hard and brittle, making impossible to proceed with the rheological assessment of viscosity of 50% and 60% rice flour gels.

All flow curves present the same pattern, with a newtonian plateau region at lower shear rates, followed by a shear-thinning region. Viscosity increases with the rice flour concentration.

CONCLUSIONS

The optimum rice gel concentration for pasta making was established at 40% (w/w), due to its high viscosity. The study of different proportions of gelled rice flour with raw rice flour and other gluten free flours, will be the next step for the optimization of pasta specially designed for celiac population.

ACKNOWLEDGEMENTS

This work was supported by COMPETE program: QREN - "Arroz +" project n.38749.

REFERENCES AND NOTES

1. Marti, A.; Seetharaman, K.; Pagani, M.A., *Journal of Cereal Science*, **2010**, 52, 404-409.
2. Torres, M.D.; Fradinho, P.; Raymundo, A; Sousa, I., *Food & Bioprocess Tech*, **2014**, 7, 1171-1182.
3. Cham, S. & Suwannaporn, P., *Journal of Cereal Science*. **2010**, 51(1), 284-291.

O34

Formulation and processing of egg white protein-based nanobiocomposites

Isabel Diañez, Inmaculada Martínez, Pedro Partal

Dpto. Ingeniería Química, Centro de Investigación en Tecnología de Productos y Procesos Químicos (Pro^{2}TecS), Universidad de Huelva-Campus Excelencia CeiA3, Campus El Carmen, 21071, Huelva, Spain

Correspondence to: Isabel Diañez (E-mail: *Isabel.dianez@diq.uhu.es*)

ABSTRACT

Egg white protein/montmorillonite clay nanobiocomposites have been obtained by thermomechanical processing. The influence of plasticizer composition on thermal and mechanical behaviour were analysed. Thus, it could be noticed that a change in the plasticizer used, as well as the reduction of mixing time and temperature can lead to a significant improvement of tensile properties of resulting protein-based nanobiocomposites.

KEYWORDS Nanobiocomposite, protein, clay, plasticizer, thermomechanical behaviour, water uptake.

INTRODUCTION

In the last few years, it has been spreading the use of different types of nanoparticles for reinforcing of all sorts of materials, specially plastics and bioplastics, in order to enhance their properties (mechanical performance [1], thermal stability [2], barrier effect against gases and vapours [3], etc.). However, to observe these effects it is necessary to achieve a proper dispersion of nanoparticles in the polymer matrix, which is critical for food packaging applications.

Both formulation and processing have been demonstrated to be essential factors when trying to develop nanobiocomposites with suitable properties for use in packaging and other purposes.

EXPERIMENTAL

The spray-dried egg white albumen (EW) was purchased from PROANDA, S.L. (Spain). Glycerol from Guinama (Spain), polyethylene glycol 300 (PEG) from Manuel Riesgo, S.A. (Spain) and distilled water were used as protein plasticizers. A natural sodium montmorillonite nanoclay, Cloisite® Na^+ (MMT-Na), provided by Southern Clay Products, Inc. (USA) was selected for this study.

In every formulation prepared, a constant plasticizer/protein ratio of 0.4 was always maintained. The influence of the addition of glycerol as plasticizer was studied over the neat matrix. With regard to the mixing time effect, a formulation at 3 wt.% nanoclay was used, plasticized with a blend of PEG, glycerol and distilled water. The overall compositions are included in Table 1.

TABLE 1 Final compositions of the samples studied

Sample	Composition (wt. %)				
	PEG	W	G	EW	Clay
PEG/W [a]	30	30	0	40	0
PEG/W/G [a]	30	15	15	40	0
MMT-Na-10 [a]	29.1	14.6	14.6	38.8	3
MMT-Na-6 [b]	29.1	14.6	14.6	38.8	3

[a] 10 min. mixing time, [b] 6 min. mixing time

The thermomechanical processing includes two steps: thermoplastic processing and compression-moulding. Mixing of the ingredients was carried out, for 10 or 6 min starting at room temperature, in the kneading tool (Rheomix 3000p) of a torque-rheometer (Polylab, Thermo Haake GmbH, Germany) equipped with two counter-rotating rollers turning at 50 rpm under adiabatic conditions. Specific mechanical energy (SME) was calculated as follows [4]:

$$SME = \frac{\omega}{m}\int_0^{t_{mix}} M(t)\partial(t) \quad (1)$$

where ω (rad/s) is the mixing speed, m (g) is the sample mass, M(t) (N·m) the torque and t_{mix} (s) the mixing time.

Compression-moulding of the resulting dough-like material (100 bar, 120 ^{0}C, 10 min) into ASTM D638 "Type IV" dogbone specimens, for tensile tests, and 50x10x3 mm^3 rectangular specimens were performanced.

Dynamic mechanical thermal analysis (DMTA) tests were conducted in a controlled-stress rheometer Physica MCR-301 (Anton Paar, Austria), in torsion mode, at 400 Pa (within the linear voscoeslastic region) and a constant frequency of 1 Hz, using a heating rate of 2 ºC/min, between 25 and 180 ºC.

Tensile tests were carried out with a Shimadzu AG-IS (Shimadzu, Japan) testing machine at a single cycle of 50 mm/min, meeting the ASTM D638-10 Standard.

RESULTS AND DISCUSSION

Thermoplastic processing

Table 2 shows the SME transferred and the temperature increase undergone by the blend during this process.

TABLE 2 SME values and temperature increment during thermoplastic processing of bioplastics

Sample	SME (kJ/kg)	ΔT (ºC)
PEG/W	15.5	28.4
PEG/W/G	1.2	5.0
MMT-Na-10	8.6	30.6
MMT-Na-6	1.0	6.5

It can be seen how the addition of only a 15 wt. % of glycerol radically decreases the value of SME and, consequently, the temperature increment. Apart from energy saving, this effect is very beneficial, since high temperatures adversely affect the protein performance. Thus, the PEG/W/G blend seems to be the best option for plasticizing EW nanobiocomposites, inasmuch as the friction due to presence of solid particles leads to a greater heat generation.

Thermomechanical behaviour

Figure 1 shows the evolution with temperature of storage and loss moduli, which continuously decay as temperature increases, as well as corresponding tanδ curves.

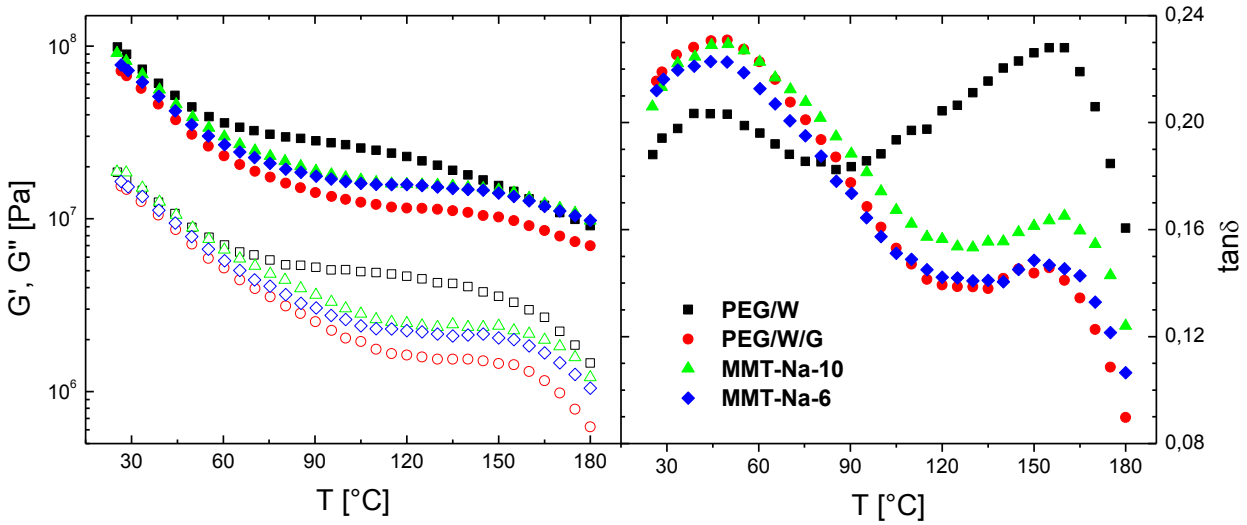

FIGURE 1 DMTA tests performed on bioplastics and nanobiocomposites, in torsion mode

PEG/W/G samples present higher values of tanδ at lowest temperatures if compared to the sample without glycerol as a plasticizer. But, around 85 ºC, this trend is reversed and these samples present a more elastic behaviour. Moreover, the addition of nanoparticles causes an increase in both storage and loss moduli, if compared with their non-nanoreinforced counterparts. However, the shortest mixing time leads to higher tanδ values within the whole range of temperatures studied.

Tensile properties

The use of glycerol as plasticizer provides a significant increase in elongation capacity (Table 3), while tensile strength and elastic modulus values remain very similar to those obtained for PEG/W samples.

TABLE 3 Tensile properties of bioplastics and nanobiocomposites

Sample	Tensile strength [MPa]	Strain at break [%]	Elastic modulus [MPa]
PEG/W	5.51±0.33	69.92±15.77	53.75±7.56
PEG/W/G	5.22±0.36	125.37±23.37	41.15±1.52
MMT-Na-10	3.29±0.45	17.93±7.45	38.41±1.93
MMT-Na-6	4.11±0.27	91.94±16.45	26.38±2.72

With regard to the nanobiocomposites, the enhancement of elongation capacity is even greater when reducing mixing time. Tensile strength is also increased in this case and only the elastic modulus is slightly reduced.

CONCLUSIONS

The most significant change that can be observed in thermomechanical behavior and processability of nanobiocomposites is that caused by the addition of glycerol as a plasticizer. However, both addition of glycerol and reduction in mixing time improved nanobiocomposites performance, especially regarding tensile properties.

REFERENCES AND NOTES

1. Lee, J.; Kim, K.M., *Journal of Applied Polymer Science,* **2010,** 118, 2257-2263.
2. Mohanty, S.; Nayak, S.K., *Journal of Polymers and the Environment,* **2012,** 20, 195-207.
3. Sanchez-Garcia, M.D.; Lopez-Rubio, A.; Lagaron, J.M., *Trends in Food Science & Technology,* **2010,** 21, 528-536.
4. Redl, A.; Morel, M.; Bonicel, J.; Guilbert, S.; Vergnes, B., *Rheologica Acta,* **1999,** 38, 311-320.

Multiphase Systems

O4

Rheological changes induced by the functionalization of the carbon nanotubes in a CNT/polymer nanocomposite

Maite Landa, Mercedes Fernández, María Eugenia Muñoz, Antxon Santamaría

Polymer Science and Technology Department and POLYMAT, Faculty of Quemistry, University of the Basque CountryUPV/EHU.20080 San Sebastián,Spain

Correspondence to: Maite Landa (E-mail: *maite.landa@ehu.es*)

ABSTRACT

The rheological changes induced by the functionalization of the carbon nanotubes in a CNT/polymer nanocomposite are investigated in this study. Non functionalized multiwalled carbon nanotubes (MWCNT) and functionalized ones (MWCNTOH) are dispersed, respectively, by melt mixing method in a polyurethane matrix. Composites based on MWCNTOH exhibit lower percolation threshold and a fastening of the crystallization process below the percolation threshold. Elongational flow measurements show that there is not strain hardening behaviour, indicating that the interfacial interactions between carbon nanotubes and polyurethane chains are not strong enough to produce an anchorage effect.

KEYWORDS (Carbon nanotubes, polyurethane, crystallization, elongational measurements)

INTRODUCTION

The performance of a carbon nanotube/polymer nanocomposite depends on the dispersion of the carbon nanotubes in the matrix and on the interfacial interactions between these and the polymer. Thus, a significant challenge in developing high performance polymer/CNTs composites is to achieve better dispersion and strong interfacial interactions, to improve the load transfer across the CNT-polymer matrix interface. In this study a polyurethane (PUR) matrix is loaded with multiwalled carbon nanotubes (MWCNT). In an effort to improve the interactions between the carbon nanotubes and the matrix, hydroxyl multiwalled carbon nanotubes (MWCNTOH) are also considered, with the final aim of obtaining electrically conductive hot melt adhesives. Within this context, we demonstrate that rheology is a powerful tool to evaluate the degree of success reached in the dispersion of nanoparticles in a polymer matrix.

EXPERIMENTAL PART

The matrix of the studied nanocomposites is a semicrystalline thermoplastic polyurethane produced by Merquinsa (Spain) and used as a Hot Melt adhesive. Multiwall carbon nanotubes (MWCNT) and hydroxyl multiwalled carbon nanotubes (MWCNTOH) were supplied by Cheap Tubes Inc. with the following characteristics: Diameter D=30-50 nm, length L=10-20 μm and purity greater than 95%. MWCNTOH carbon nanotubes contain 1 % of OH groups.

The dynamic viscoelastic behaviour in the molten state was analysed at T=100 ºC in a TA Instruments ARES viscoelastometer with parallel-plate shear geometry. The isothermal crystallization process was investigated using the same equipment; the variation of the elastic modulus with time was monitorised at a frequency of 1 Hz, at T = 50 ºC, at the lowest strain. The extensional properties were measured with an Anton Paar Rheometer MCR equipped with a SER device.

RESULTS AND DISCUSSION

It is well known that above percolation a significant alteration of the viscoelastic terminal zone takes place, owed to the formation of a polymer/nanoparticles network. As frequency tends to zero the storage modulus, G', prevails over the loss modulus, G'', and both moduli become independent of the frequency in percolated systems. Figure 1a shows the frequency dependence of the storage modulus (G'). On the other hand, it is expected that adding chemically functionalized nanotubes to the PUR matrix enhances G' at low frequencies (terminal flow zone), because of the interactions between MWCNTOH and PUR. In fact, only for the 1 wt. % MWCNTOH based nanocomposite a higher modulus and a weaker frequency dependence of G' at low frequencies is observed, as compared with MWCNT based nanocomposites.

On the other hand, the analysis of the thermal properties of hot melt adhesives is particularly interesting, because a crystallization process takes place during cooling, to give rise to a permanent weld[1]. Therefore, the study of the crystallization of the selected nanocomposites has a basic and applied purpose. In Figure 1b an analysis of the variation of the storage modulus, G' with time is presented. The modulus increases sharply after a certain induction time, revealing rheology as a sound tool to analyze crystallization. It can be seen that below the percolation

threshold MWCNTOH based nanocomposites exhibit a sharper slope than the non functionalized MWCNT based nanocomposites. Below percolation threshold, better dispersions are obtained with hydroxyl functionalized nanotubes, as indicated by the fastening of the crystallization and the higher storage modulus obtained from oscillatory results.

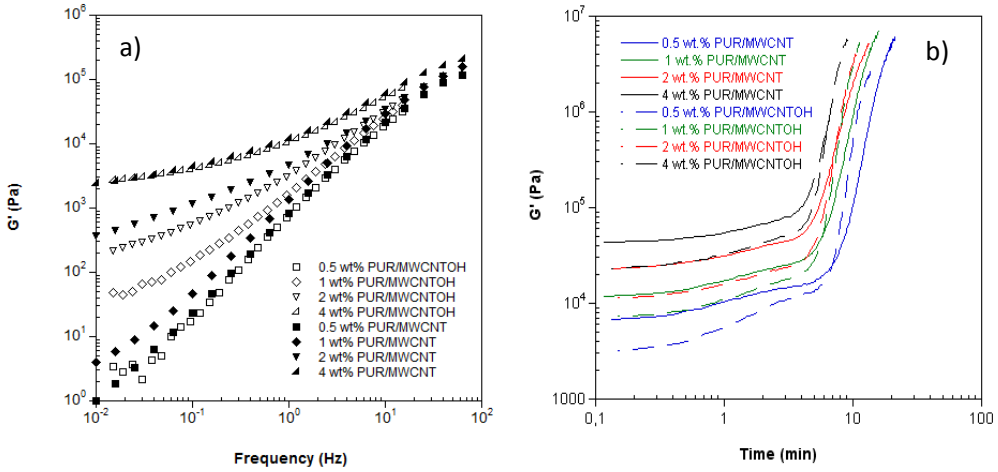

FIGURE 1. a) Storage modulus as a function of frequency at T = 100 ºC, for the PUR/MWCNTOH (empty symbols) and the PUR/MWCNT (full symbols) nanocomposites. b) Evolution of storage modulus with time at 50 º C for the PUR/MWCNTOH (empty symbols) and the PUR/MWCNT (full symbols).

In attempt to study interactions between the functionalized nanotubes and the PUR chains, elongational measurements were carried out. The elongational viscosity results are shown in Figure 2. As can be seen, the increase of viscosity due to the presence of the MWCNTs diminishes, when the Hencky rate is increased. These results lead to conclude that the MWCNT/polymer network is not able to produce a strain hardening response, because the structure does not stand the applied elongational flow[2]. Hydroxyl functionalized nanotubes were expected to bring about enhanced interfacial MWCNTOH/polymer interactions, which would produce strain hardening, but the observed behaviour is similar to that of non functionalized MWCNTs. This suggests that interactions between carbon nanotubes and polyurethane chains are not strong enough to produce an anchorage effect.

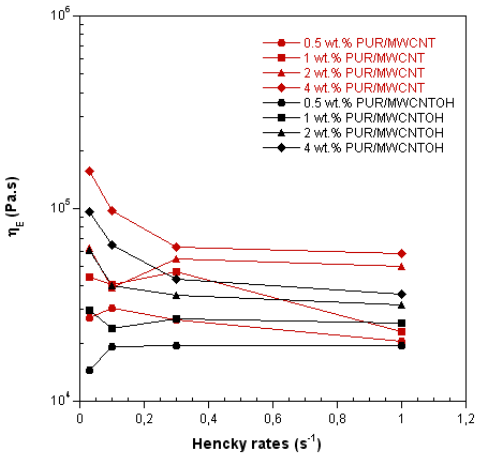

FIGURE 2. Uniaxial elongational viscosity versus time at different Hencky rates ($\dot{\varepsilon}_H$) at 70 ºC for the functionalized (black dots) and non-functionalized (red dots) nanotubes based nanocomposites.

CONCLUSIONS

The effect of the MWCNTs is clearly observed in the viscoelastic terminal zone, reflecting the obstruction caused to the motion of the polymer chains as a whole. The use of MWCNTOH functionalized nanotubes, leads to a decrease of the percolation threshold concentration, but above this concentration there are no noticeable differences in the storage modulus, as compared with non functionalized MWCNTs. The crystallization process, monitored by dynamic measurements, is fastened with the addition of MWCNTs. For MWCNTOHs below the percolation threshold, the slope of the storage modulus is sharpened, indicator of a fastening of the crystallization, due to a better dispersion of the MWCNTOHs in the matrix. The results obtained from elongational flow measurements show that there is not strain hardening behavior, as the interfacial interactions are not strong enough to give rise to an anchorage effect.

ACKNOWLEDGEMENTS

M.L. acknowledges the financial support of the University of the Basque Country by “Contratación de Doctores Recientes hasta su Integración en Programas de Formación Postdoctoral del Vicerrectorado de Investigación de la UPV/EHU” program. Financial support trough UPV/EHU (UFI 11/56) and GICIT-586-13 (Basque Government) projects is acknowledged.

REFERENCES AND NOTES

1. Landa, M.; Canales, J.; Fernández, M.; Muñoz, M.E.; Santamaría, A., *Polymer Testing*, **2014**, *35*,101-108.
2. Fernández, M.; Landa, M.; Muñoz, M.E.; Santamaría, A., *Int J Adhes Adhes,* **2010,** *30,* 609–614.

O5

Electrorheological Behavior of Suspensions of Camphorsulfonic acid (CSA) doped polyaniline nanofibers in silicone oil

Sumita Goswami, Paulo Gonçalves, Maria Teresa Cidade

Departamento de Ciência dos Materiais, CENIMAT/I3N, Faculdade de Ciências e Tecnologia, Universidade Nova de Lisboa, 2829-516 Caparica, Portugal

Correspondence to: Maria Teresa Cidade (E-mail: *mtc@fct.unl.pt*)

ABSTRACT

The electrorheological (ER) effect is known as the enhancement of the apparent viscosity upon application of an external electric field applied perpendicular to the flow direction. Suspensions of polarizable particles in non-conducting solvents are the most studied electrorheological fluids. The increase in viscosity observed in the suspensions is due to the formation of columns that align with the electric field.

This work presents the electrorheological (ER) behavior of suspensions, in silicone oil, of camphorsulfonic acid (CSA) doped polyaniline (PANI) nanofibers. The ER properties of the suspensions were investigated with a rotational rheometer, to which an ER cell was coupled, in steady shear, and electrical field strengths up to 2 kV/mm. The effects of the electric field strength, content of nanostructures and viscosity of the continuum phase, in the shear viscosity and yield stress, were investigated at room temperature.

As expected, the ER effect increases with the increase of the electric field as well as with the increase of content of nanofibers and it decreases with the increase of the oil viscosity. The suspensions present giant ER effects (higher than 2 decades increase in viscosity for low shear rates and high electric fields), showing their potential application as ER smart materials.

KEYWORDS: Electrorheological effect, suspensions, camphorsulfonic acid doped polyaniline, nanofibers, ER smart material

INTRODUCTION

The electrorheological (ER) effect can be considered as the change of the fluid apparent viscosity in the presence of an external electric field[1], sometimes having dramatic consequences, inducing fluid solidification[1,2]. The ER effect is an important phenomenon that brings new technological applications which may be used in a wide spectrum of domains, spanning from the electro-optical devices to automobile industries and robotics. The first observation of the ER effect was reported by Winslow[3], for a suspension of polarizable micro particles adsorbed in water. The variation of the apparent viscosity was due to the micro particles alignment in chains or

columnar structures oriented in the direction of the electric field, increasing the solution's viscosity in one order of magnitude.

In the past two decades, several experimental and theoretical studies of the ER effect in different systems have been reported, some of them presenting giant ER effects, with 2 or 3 decades increase in viscosity[4]. Liquid crystalline materials[5] and suspensions of polarizable particles in a non-conducting continuum phase[6] are two of the major kind of systems being studied in this framework.

EXPERIMENTAL

Materials

The synthesis of camphorsulfonic acid doped polyaniline nanofibers (PANICSA) is shown in figure 1, along with the FESEM image of the fibers. Analytical grade aniline (Merck) was purified by distillation under reduced pressure prior to use. All other reagents like, camphorsulphonic acid (CSA, Sigma Aldrich), ammonium persulphate or APS $(NH_4)_2S_2O_8$, Sigma Aldrich), were received as analytical grade and were used without further purification. Aniline monomer was polymerized in an ice bath (0˚C) to form polyaniline nanofibers using APS as the oxidant and CSA as the dopant as well as structure directing agent. During the reaction procedure, firstly the aqueous solution of CSA with aniline monomer was prepared (molar ratio, CSA: monomer 0.25:1) to form a colorless mixture of the two having aniline-CSA complex in micelle form. Then the APS aqueous solution (molar ratio, APS: monomer 1:1) was prepared. Both the solutions were kept at 0˚C for 15 minutes and then mixed slowly to each other. The reaction was maintained to stay undisturbed for 1 hour in the ice bath. Finally, the precipitate was collected after filtration and washing several times with distilled water and methanol. The sample was ready after the vacuum drying for 24 hours at 60˚C in oven.

The fibers were mixed with silicone oil to form a suspension. Silicone oil of two different viscosities were used (approximately 19 and 48 mPa.s), both purchased from Clearco Products Co., Inc (commercialized as silicone oils of 20 and 50 cSt). For each oil 1 and 2 wt% of PANICSA nanofibers were introduced. The suspensions were stirred and sonicated during 10min before subjected to rheological characterization.

Characterization

The ER properties of the suspensions were studied using a rotational rheometer, Bohlin Gemini HR^{nano} (Malvern, Worcestershire, UK), to which a ER cell of high-voltage supply (5kV) was coupled. The measurements were performed under a constant temperature of 25°C. The measuring system used was parallel plates of 40 mm diameter with the upper plate isolated and a gap of 500μm.

Before starting the measurements, the suspensions were subjected to a pre-shear stage of $1s^{-1}$ applied during 60s followed by an equilibrium time (the time elapsed after stopping the pre-shear and starting the measurements) of 180s.

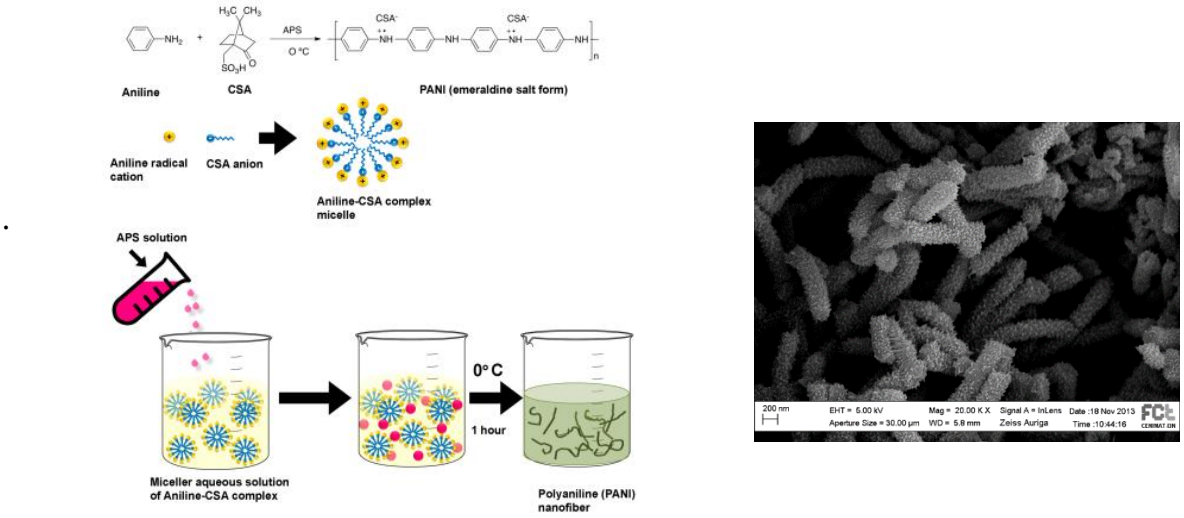

(a) (b)

Figure 1. Schematic representation of the synthesis (a) and FESEM image (b) of PANICSA nanofibers.

RESULTS AND DISCUSSION

Figures 2a and 2b present the apparent viscosity as a function of the shear rate for 2 wt% PANICSA in oils of two different viscosities. Comparing these two figures we conclude that the higher the viscosity of the oil the lower the ER effect, which may be explained in terms of an easier formation of the columns in the oil of lower viscosity. Figures 2c compares the increase in apparent viscosity for 2 different contents of nanofibers, showing, as expected, that the ER effect increases with the increase of the content of semi-conducting particles. The ER effect also increases, as expected with the electric field strength.

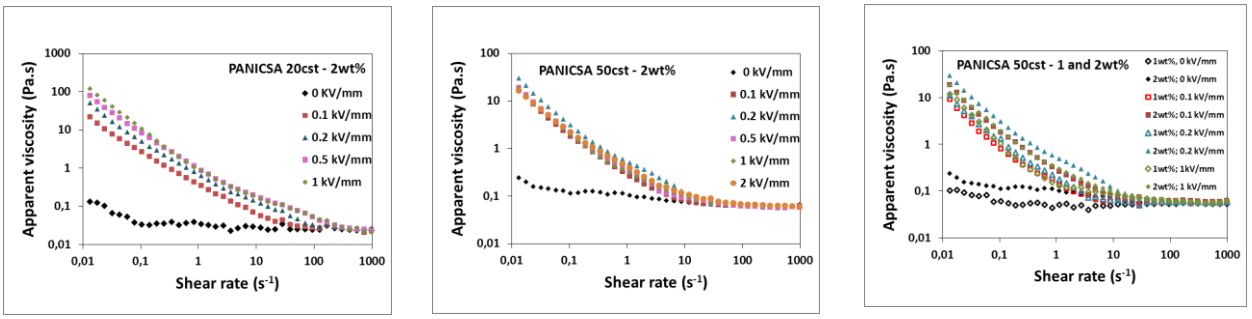

(a) (b) (c)

Figure 2. Apparent viscosity of 2 wt% PANICSA in a silicone oil of 19 mPa.s (a) and 48 mPa.s (b) and 1 and 2 wt% PANICSA in a silicone oil of 48 mPa.s cSt.

Figure 3 presents the flow curve of 2 wt% PANICSA/19 mPa.s silicone oil, as an example. During the absence of electric field the shear stress presents a small yield stress that increases abruptly when a DC electric field is applied, increasing with the electrical field from then on.

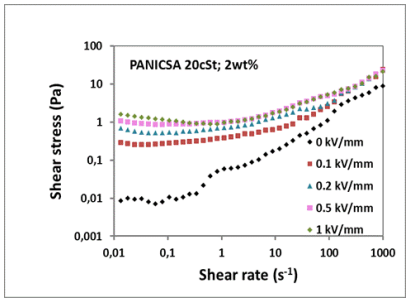

Figure 3. Flow curve of 2 wt% PANICSA/19 mPa.s silicone oil

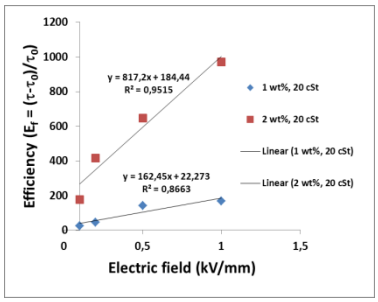

Figure 4. ER efficiency of PANICSA in oil of 19 mPa.s, at a shear rate of 0.0134 s^{-1}

Figure 4 presents the ER efficiency of the PANICSA/19 mPa.s silicone oil suspensions (similar results are presented for the oil of 48 mPa.s), measured from the increase of shear stress to the situation where no current is applied, at the smallest shear rate, the one for which the effect is more pronounced. The efficiency increases linearly with the electric filed strength and the increase is more pronounced for the higher PANICSA content.

CONCLUSIONS

Camphorsulfonic acid doped polyaniline nanofibers/silicone oil suspensions present an important ER effect, showing its potential as ER smart materials. The higher viscosities attained with the oil of smaller viscosity may be interpreted in terms of an easier formation of the columns. The increase of nanofibers content, as expected, increases the efficiency of the ER fluid, the same happening with the electric field strength.

ACKNOWLEDGEMENTS

This work is funded by FEDER funds through the COMPETE 2020 Programme and National Funds through FCT - Portuguese Foundation for Science and Technology under the project UID/CTM/50025/2013.

References

1. Wen, W, Huang, ., X., Sheng, P., *Soft Matter*, **2008**, 4, 200-210.
2. Larson. R.G., The Structure and Rheology of Complex Fluids; Keith E. Gubbins, Ed.; Oxford University Press: New York, Oxford, **1999**
3. Winslow, W.M., *J. Appl. Phys.*, **1949**, 20, 1137-1149.
4. Goswami, S. Brehm, T. Filonovitch, S., Cidade M.T., *Smart Mater. Struct*., **2014**, 23, paper no.105012.
5. Patrício, P., Leal, C.R., Pinto, L.F.V., Boto, A., Cidade, M.T., *Liquid Crystals*, **2012**,39, 25-37.
6. Brehm, T., Pereira, G., Leal, C.R., Gonçalves, C, Borges, J.P., Cidade, M.T., *Physica Scripta* , **2015**, 90, paper 035802.

Rheological behaviour of new nanoclay/MDI/bitumen composites

F.J. Ortega, F.J. Navarro, M. García-Morales, P. Partal

Departamento de Ingeniería Química, Centro de Investigación en Tecnología de Productos y Procesos Químicos (Pro^{2}TecS), Campus de 'El Carmen', Universidad de Huelva, 21071, Huelva (Spain)

Correspondence to: F.J. Ortega (E-mail: *francisco.ortega@diq.uhu.es*)

ABSTRACT

Bitumen, residue from crude oil distillation, is commonly utilized to provide waterproofing and protective coating, as well as for paving applications. However, problems related to temperature susceptibility and aging may change its properties leading to premature failure[1]. Lately, layered silicates have increasingly been used to improve bitumen performance[2]. In this sense, bitumen with penetration grade of 162 dmm was modified with polymeric MDI (4,4'-diphenylmethane diisocyanate) and the nanoclay Cloisite 20A® (OMMT). Chemical modification of bitumen with 2 wt.% MDI provoked a notable increase in the viscoelastic moduli, especially after 24 h curing. Physical modification with 10 wt.% OMMT dramatically improved the viscoelastic performance, what is attributed to the structural reinforcing effect of the intercalated/exfoliated clay tactoids[2]. However, further addition of 2 wt.% MDI to this previous formulation lowered its overall viscoelastic response at temperatures at which the bituminous matrix softens, especially after 24 h curing. This result might stem from the disruption of the clay-based reinforcing network, as a consequence of clay tactoid re-aggregation during blending[3], promoted by chemical interactions with MDI.

KEYWORDS

Bitumen, nanoclay, composite, isocyanate, intercalation, exfoliation

INTRODUCTION

Bitumen is a complex mixture of different organic molecules, predominantly hydrocarbons with a small amount of structurally analogous heterocyclic species, along with functional groups

containing sulphur, nitrogen and oxygen atoms[1]. Because of its good viscoelastic and waterproofing properties, it is widely used in road and building construction.

However, the combination of loads, extreme temperatures and environmental factors (oxygen diffusion, UV radiation, etc.) may affect its properties during in-life service, leading to problems related to thermal susceptibility and ageing, like high temperature rutting or low temperature cracking[1,4]. In order to improve its performance, bitumen has traditionally been modified by addition of polymers (EVA, SBS, etc.)[1]. Recently, a growing interest has arisen in the physical modification of bitumen using layered silicates (nanoclays), due to their nanoscale characteristics[2]; as well as in its chemical modification. Both have shown to improve its performance and resistance against the previously mentioned factors, extending its in-life service. With this aim, the viscoelastic behaviour of the binary blends bitumen/nanoclay and bitumen/MDI, and the corresponding ternary composite bitumen/nanoclay/MDI has been investigated in this work.

MATERIALS AND METHODS

Bitumen with penetration grade of 162 dmm (EN 1426) and softening point of 32ºC (EN 1427) was used as the base bitumen for the modification. Polymeric MDI (4,4'-diphenylmethane diisocyanate) was chosen as a modifier given it has shown to greatly enhance bitumen properties [1,5], its easy availability, and lower price and toxicity, if compared to other isocyanates sources. Cloisite® 20A nanoclay ("C20A" hereafter), a natural montmorillonite modified with N,N-dimethyl di-hydrogenated tallow (C_{14}-C_{18}) quaternary ammonium chloride, with a cation exchange capacity of 92.6 meq/100 g clay, was also employed as a bitumen modifier.

Formulations were prepared by melt blending. In ternary blends, bitumen was first heated at 150ºC and 10 wt.% C20A was added and low-shear blended for 10 min. Afterwards, an Ultraturrax™ high-shear mixer was used for 20 minutes to ensure the adequate dispersion of the nanoclay (a sample of this bitumen/nanoclay blend was taken for testing at this point). Thereafter, 2 wt.% polymeric MDI was added and low-shear blended for 24h. In MDI/bitumen binary blends, bitumen was first heated at 150ºC and 2 wt.% polymeric MDI was added and low-shear blended for 24h. In both procedures, samples were also taken 1h after MDI addition.

Oscillatory shear temperature sweep tests within LVE, at 10 rad/s, were conducted at a heating rate of 1 K/min, on a Physica MCR-301 rheometer (Anton Paar, Austria).

RESULTS AND DISCUSSION

As depicted in Fig. 1A, neat bitumen exhibits terminal-flow-shaped curves, typical of materials with prevailing viscous behaviour. The addition of MDI to neat bitumen leads to the same viscous behaviour, greatly influenced by the curing time. Hence, 1 h curing provokes a marked increase in both dynamic moduli, mainly attributed to the reactive interaction between isocyanate groups in MDI and pendant active hydrogen groups present in bitumen[5]. Extending curing time up to 24 h seems to promote the mentioned reactive interaction to a greater extent.

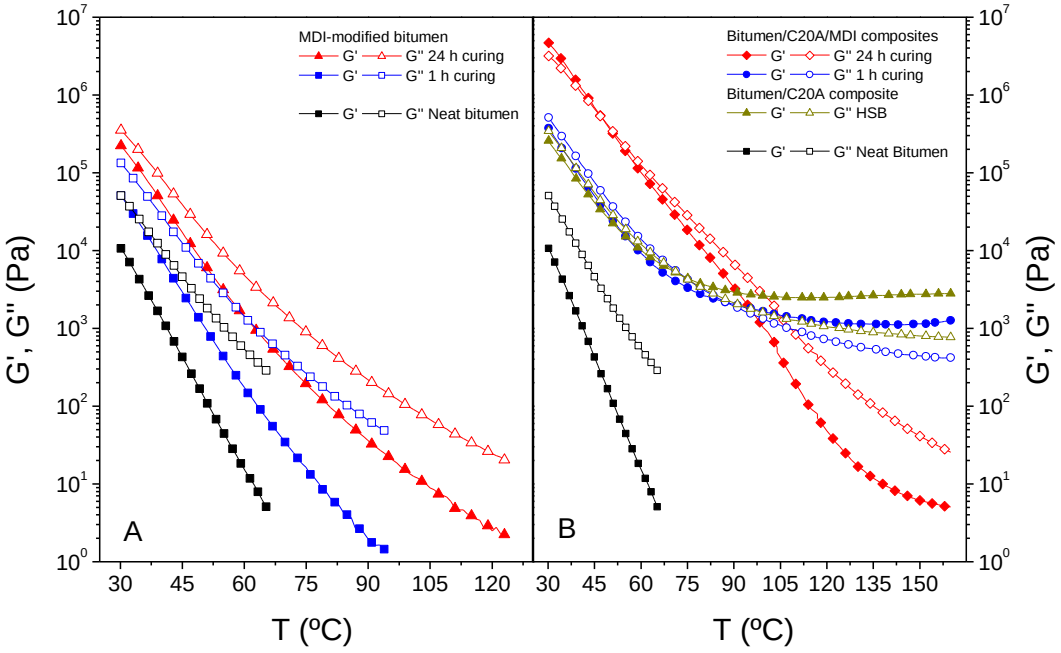

Fig. 1. (A) Temperature sweep tests in oscillatory shear, at 10 rad/s, for (A) neat and MDI-modified bitumen; and (B) bitumen/C20A and bitumen/C20A/MDI composites.

On the other hand, the modification of neat bitumen with 10 wt.% C20A gives rise to quite a different viscoelastic behaviour, as depicted in Fig. 1B, with nearly coincident values of G' and G'' (which increase significantly if compared to neat bitumen) in the low-to-medium temperature range, and a plateau zone (prevailing elastic response) at the highest temperatures studied. The LVE behaviour observed hints at the formation of a clay-based network which reinforces the system structure via inter-particle interaction, involving the assembly of individual silicate platelets, as similarly reported for composites forming a percolated network[2].

As portrayed in Fig. 1B, further addition of 2 wt.% MDI to the C20A-bitumen binary blend and curing for 1 h barely affects the above viscoelastic response, with G'' slightly higher than G' in the low-to-medium temperature range, and a plateau zone (with lower G' and G'' values than

before) at higher temperatures. A longer curing time of 24 h provokes, at low-to-medium temperatures, a major increase in both moduli, which continuously decay with increasing temperature, and fall well below the other two systems at temperatures higher than 100ºC approximately. This seemingly results from the promotion of the interaction between neighbour clay tactoids/platelets, leading to their agglomeration/re-aggregation[3], which significantly affects the composite overall viscoelastic response when the modified bitumen phase softens.

CONCLUSIONS

The single addition of 2 wt.% MDI to bitumen yields an improvement in the viscoelastic response, favoured by long curing times, with prevalence of the viscous response. This is mainly due to the development of a new and more complex microstructure, which stems from the formation of new urethane and urea bonds. By contrast, the bitumen/C20A composite exhibits a well-defined plateau zone, at high temperatures, which indicates the formation of a clay-based network. If MDI is further added and let react for 24 h, the ternary composite stiffness is improved at temperatures below that at which the modified bitumen phase softens. However, a worsening in the viscoelastic behaviour (with a predominant viscous response) is clearly noticed as temperature is raised, which is attributed to the agglomeration of neighbour clay tactoids, promoted by chemical interactions, with MDI acting as linking points.

ACKNOWLEDGEMENTS

This work is part of a research project sponsored by "Junta de Andalucia" (TEP-6689). The authors gratefully acknowledge their financial support.

REFERENCES AND NOTES

1. Read, J., Whiteoak, D., The shell bitumen handbook; Thomas Telford: London, **2003**.
2. Ray, S. S.; Okamoto, M., *Progress in Polymer Science*, **2003**, *28*(11), 1539-1641.
3. Rajasekar, R.; Pal, K.; Heinrich, G.; Das, A.; Das, C.K., *Materials & Design*, **2009**, *30*, 3839-3845.
4. Navarro, F. J.; Partal, P.; Martínez-Boza, F.; Valencia, C.; Gallegos, C., *Chemical Engineering Journal*, **2002**, *89*(1–3), 53-61.
5. Navarro, F. J.; Partal, P.; Martinez-Boza, F.; Gallegos, C.; Bordado, J. C. M.; Diogo, A. C., *Mechanics of Time-Dependent Materials*, **2006**, *10*(4), 347-359.

A study of the effect of pressure on the viscosity of PS filled with conductive nanoparticles of different morphologies

Mercedes Fernández[1], Estibaliz Rodriguez[1], Maria Eugenia Muñoz[1], Antxon Santamaria[1]

[1] Institute of Polymer Materials (POLYMAT) and Polymer Science and Technology Department, Faculty of Chemistry, University of the Basque Country (UPV/EHU), Paseo Manuel de Lardizabal 3, 20018 Donostia-San Sebastián, Spain

e-mail of the presenter: mercedes.fernandez@ehu.es

ABSTRACT

Notwithstanding the number of papers dealing with polymer nanocomposites has increased exponentially, the transfer of the generated knowledge towards industrial application is poor. There are two crucial factors that bring about this shortcoming: a) Difficulties on getting good dispersions using conventional mixing methods b) Lack of rheological studies related to the behaviour of the nanocomposites during processing. In this work we focus on the second issue.

We have investigated the viscosity of nanocomposites based on a polystyrene matrix, PS, that contains mutiwall carbon nanotubes (MWCNTs) and graphene platelets, respectively. Besides of studying the viscosity as a function of shear rate and temperature, we have analysed the effect of pressure. To our knowledge, values of the pressure-viscosity coefficient at different shear rates have never been reported for polymers filled with MWCNTs or graphene sheets, so far.

KEYWORDS Graphene, Multiwall Carbon Nanotubes, Pressure dependence of viscosity

INTRODUCTION

Previous studies on the pressure dependence of viscosity of polymer melts revealed that pressure effects are more important for those polymers with bulkier backbones in their molecular structure: the reduced amount of free volume available to molecules results in an increase in intermolecular interactions and, thus, a viscosity enhancement is observed experimentally.[1-2] The relationship between viscosity and free volume has been considered by several authors in terms of the free volume fraction determined by fitting Pressure-Volume-Temperature (PVT) data to the Simha–Somcinsky equation of state following the procedure developed by Utracki[3] and Sedlacek[4]. An alternative procedure using PVT data and activation energy of flow has also proved to be useful to evaluate the pressure sensitivity of several polymers. [5]

The addition of small amount of nanofillers to polymer matrix leads to the creation of composites materials where reinforcing particles can be distributed at the nanometer level. Although carbon nanotubes and graphene are both useful to elaborate electrically conductive polymers, their morphology is unlike. In the wide range of shear rates contemplated in our work, the arrangement and orientation of cylinder-like and platelet-like nanoparticles is different. The effects of the developed differents morphologies on the pressure-viscosity coefficient are investigated from both, direct experiment - using high pressure extrusion and indirect procedure-correlation with free volume property, in terms of PVT data.

EXPERIMENTAL

The Polystyrene considered in this work (STYRON) was kindly supplied by Dow (Germany). Commercial graphene, avanGRAPHENE-2 was purchased from Avanzare, (Spain) and Multiwall Carbon Nanotubes (MWCNT), which have specified diameters of D=30-50 nm, length between 10 and 20 μm and purity greater than 95% were supplied by Cheap Tubes Inc. (Brattleboro, VT, USA). The dispersion of the filler was carried out by melt mixing method in a co-rotating twin screw-mixer (Collin ZK-25) at T=200ºC. The screw speed was 300 rpm and the obtained extrudates were cooled down in a water bath and then pelletized.

The dynamic viscoelastic behavior in the molten state was investigated in an ARG2 rheometer (TA Instruments, USA), using parallel plates geometry. Small amplitude oscillatory experiments were carried out in the linear viscoelastic regime at temperatures in the range from 180-210ºC.

Extrusion flow experiments were performed in a Göttfert Rheograph 25 rheometer. The standard equipment was modified by an additional unit called the counter pressure chamber (CPC). The CPC is mounted below the rheometer barrel and capillary die. The pressure level in the chamber can be adjusted with a conical valve bolt mounted inside the CPC body. During the measurements, the pressure was monitored at two locations by pressure transducers: in the barrel just above the capillary and in the pressure chamber right below the capillary. The estimation of the viscosity is explained in detail elsewhere.[2]

Pressure-Volume-Temperature measurements were carried out in a PVT apparatus of the piston-die type (PVT 100 Haake, Germany) data were obtained using an isobaric cooling mode procedure in the pressure range from 200 to 1600 bar with a cooling rate of 5ºC.

RESULTS AND DISCUSSION

Dynamic viscoelastic results

Figure 1a, shows the complex viscosity for the neat PS and blends. Considering the applied scope of our work, compositions above percolation threshold were studied: 9 wt% Graphene/PS and 5 wt%MWCNT/PS nanocomposites. The similar yield stress behaviour found in both nanocomposites accounts for the percolated nanostructure.

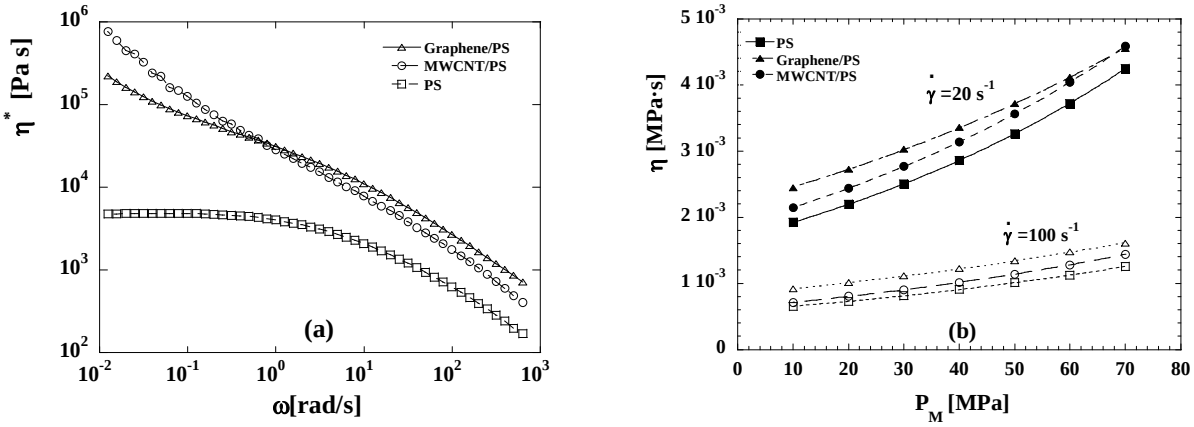

Figure 1. Melt viscosity at T=200ºC. a) Complex viscosity in the linear viscoelastic regime. b) Effect of pressure obtained in high pressure extrusion experiments

High pressure extrusion results

The dependence of viscosity on pressure (p) is usually accounted for by appropriate shift factors (a_p). For the pressure, an exponential function is commonly used, that is,

$$a_p = \exp[b(p - p_0)] \quad (1)$$

where b is a material-dependent pressure coefficient and p_0 is the reference pressure.

Based on the present viscosity measurements, the pressure coefficients were determined at different shear rates. The obtained PS pressure coefficients agreed well with the values reported in literature[2], clearly decreasing with shear, as expected. Figure 1b and Table 1, reveal different trends for the two nanocomposites. Graphene/PS coefficients were lower than that of the pure PS. In contrast, the pressure sensitivity of MWCNT/PS was found to be slightly higher.

Pressure-Volume-Temperature results

Glass Transition temperature, Tg, was found to increase with the nanoparticle addition. MWCNT and Graphene restrict the segmental motion of the polymer chain, resulting in a higher Tg. On

the other hand, compressibility parameters: $(\beta V)_{T=200^{o}C}$, $(\beta V)_{Tg}$ and pressure effect on Tg, $\frac{dTg}{dP}$, were slightly affected. The application of the procedure described in reference 5 allowed us to calculate the pressure coefficient (b2) using the PVT parameters together with the activation energy of flow calculated from extrusion experiments. The comparison between the pressure coefficients b1 and b2 is established in Table 1.

TABLE 1. Pressure coefficients: b1 (high pressure extrusion experiments) and b2 (procedure described in reference 5) together with PVT parameters and activation energy of flow, Ea.

Material	$b1(\dot{\gamma}$=20 $s^{-1})$ (1/MPa)	$b1(\dot{\gamma}$=100 $s^{-1})$ (1/MPa)	Tg (ºC)	$(\beta V)_{T=200^{o}C}$ (cm^3/g MPa)	$(\beta V)_{Tg}$ (cm^3/gMPa)	dTg/dP (°Pa^{-1})	Ea (Kcal/mol)	*b2* (1/MPa)
PS	0.0126	0.0109	87	$6.99\ 10^{-4}$	$3.78\ 10^{-4}$	0.21	29	0.025
MWCNT/PS	0.0132	0.0117	88	$6.36\ 10^{-4}$	$3.34\ 10^{-4}$	0.22	31	0.029
Graphene/PS	0.0103	0.0094	93	$6.53\ 10^{-4}$	$3.47\ 10^{-4}$	0.23	19	0.018

CONCLUSIONS

The pressure-viscosity coefficients of nanocomposites obtained dispersing commercial graphene and MWCNT in polystyrene matrix have been evaluated using high pressure extrusion rheometry and an indirect method based in PVT parameters[5]. Good agreement was observed between the two methods: both percolated structures were found to follow different trend depending on the nanoparticles investigated: MWCNT/PS (cylinder-like) resulted in higher values, whereas graphene (platelet-like) presented lower coefficient values than the polymer matrix.

ACKNOWLEDGEMENTS

Acknowledgements: UPV/EHU (UFI 11/56), GIC IT-586-13 (Basque Government) and CTQ 2013-41113-R (Spanish Government)

REFERENCES AND NOTES

1. Binding, D.M.; Couch, M.A. ; Walters K., *J-Non Newtonian Fluid Mech*., **1998** 79, 137-155.
2. Aho, J.; Syrjälä, S., in Annual Transactions of the Nordic Rheology Society, Vol 13, **2005**, pp55-60.
3. Utracki, L.A., *Polym. Eng. Sci*., **1985**, 25, 655-668.
4. Sedlácek, T.; Zatloukal, M. Filip, P. Boldizar, A. Sáha, P., *Polym. Eng. Sci.,* **2004**, 44, 1328-1337.
5. Fernández, M., Muñoz, M.E., Santamaría A., Syrjälä, S., Aho, J., *Polymer Testing***, 2009**, 28, 109-113.

Flowability of type II cement pastes in the presence of polymeric additives

Maria Graça G. Rasteiro[1] Fernando Branco[2]

[1]Chemical Eng. Dep., University of Coimbra, Rua Sílvio Lima, 3030-790 Coimbra, Portugal
[2]Civil Eng. Dep., University of Coimbra, Rua Sílvio Lima, 3030-790 Coimbra, Portugal

Correspondence to: Maria Graça G. Rasteiro (E-mail: *mgr@eq.uc.pt*)

ABSTRACT

Concrete preparation in hot environment often raises workability issues. A solution for this problem is the addition of admixtures. Most admixtures are surfactants, modified polycarboxylates being the most recent superplasticizers. In this study, cement properties (specific surface, particle size distribution, rheology, setting time, mechanical strengths and porosity) were analyzed for Type I and II cements and the workability of cement pastes was quantified through rheological tests. Several temperatures, that represent the in-situ application conditions of cement were tested. Tests were carried out to check if the inclusion of superplasticizers in cement pastes would contribute to reduce de rate of flowability decay.

KEYWORDS: flowability; cement; admixtures; Bingham fluid

INTRODUCTION

Cement's workability is closely related with the rate of cement hydration. A faster hydration process leads to quicker loss of workability. Concrete casting in hot environment, often raises workability issues[1]. This property significantly influences fundamental parameters related with the effectiveness of concrete use. A solution for this problem is the manipulation of the mixing process by the addition of admixtures. These substances are commonly used to improve the workability of cement, to reduce the need of mixing water or to increase the initial or final mechanical strength. During the mixing process, particles of cement tend to flocculate, water is consumed and the ability of cement to flow is reduced. The addition of high efficiency superplasticizers leads to a mechanism of steric impediment, resulting in deflocculation and dispersion of cement. However, high amounts of superplasticizer incorporated in a concrete with a low water/cement ratio, may lead to premature hardening and false workability, due to segregation and flow blocking[2]. As mentioned, the evaporation rate is a problem inherent during hot weather. The use of superplasticizers may reduce the amount of free water and increase the flow ability, i.e., reduce viscosity, keeping the workability of cement paste[2]. After mixing, flow

ability of cement pastes and mortars tends to decrease with time. This effect is especially noticeable at higher temperatures. Superplasticizers can counteract this tendency.

Cement behaves like a non-Newtonian fluid, in other words, at fixed temperature the viscosity varies depending on the flow conditions. Some authors classify cement as a Bingham plastic, therefore, cement flow and resistance to flow may be expressed by two fundamental rheological properties: yield stress (τ_y) and plastic viscosity (η). The rheological behavior is influenced by the cement particles concentration in the paste and by their fineness.

The aim of this study was to analyze the workability of type II Portland cement (CEM II/A-L 42.5R) at several temperatures, that represent the in-situ application conditions of cement mortars. The evolution of flow ability loss with time was evaluated using rheological tests. The performance of cement pastes when high-performance superplasticizers were used was analyzed.

EXPERIMENTAL

In this study, two types of Portland cement were used, CEM I/42.5R and CEM II/A-L 42.5R, both produced according the European standard EN 197-1 (2000) and supplied by CIMPOR (Portugal). Besides cement, two admixtures were also used: Sika® ViscoCrete® 3005 and the Sika® ViscoCrete® 3002 HE. These two products, are high-performance superplasticizers, constituted by anionic surfactants (modified polycarboxylates - polycarboxylate ethers). Using these materials, different series of cement pastes were prepared (Table 1). Series 2A was produced using ViscoCrete® 3005 and Series 2B used ViscoCrete® 3002. The tests were carried out in two stages: initially (Series 2A and 2B) the water content was kept equal to the one in paste 2; in a second stage, the water content was reduced about 16% (series 2A' and 2B').

TABLE 1 Summary of the cement pastes produced with and without superplasticizers

Paste	Constitution	Cement mass (g)	Water mass (g)	Superplasticizer volume (ml)
1	CEM I - Water: normal amount	500	145	-
2	CEM II - Water: normal amount	500	143	-
2A	CEM II - Water: normal amount SIKA 3005: 0.5% of cement mass	500	143	2.4
2A'	CEM II - Water: 84% of normal amount SIKA 3005: 0.5% of cement mass	500	120	2.4
2B	CEM II - Water: normal amount SIKA 3002 HE: 0.5% of cement mass	500	143	2.4
2B'	CEM II - Water: 84% of normal amount SIKA 3002 HE: 0.5% of cement mass	500	120	2.4

2AA	CEM II - Water: normal amount SIKA 3005: 0.7% of cement mass	500	143	3.3
2AA'	CEM II - Water: 84% of normal amount SIKA 3005: 0.7% of cement mass	500	120	3.3

Laboratory tests for physical and mechanical characterization of the cements and of the cement pastes produced were carried out. Several properties of cement (specific surface and particle size distribution) and of the cement pastes (rheology, setting time, mechanical strengths and porosity) were quantified. The cement pastes were analyzed in a rheometer (*Haake-Rheostress 1*) with the parallel plates (PP20Ti) configuration. Tests were carried out at temperatures of 10, 23 and 40°C. Cement pastes were kept in a bath at constant temperature prior to testing. Tests were performed from 1.5 till 66 minutes after paste preparation.

RESULTS AND DISCUSSION

The analysis of the rheological tests of the cement series pastes produced without superplasticizers allows concluding that higher shear stresses result from the increase of temperature, for both types of cement and for all ages of the cement paste. This fact is explained because as temperature increases, evaporation rate also increases and the resistance of mortar to flow increases, leading to a faster decrease of flow ability. Keeping the same type of cement, for the same temperature, it is possible to conclude, as expected, that higher shear stresses result when the age of the cement paste increases. At the same temperature and age, mortars produced with CEM II exhibit higher shear stresses than those produced with CEM I. This is quite obvious for the 40 ºC temperature, the behaviour of the two cements being similar for the other temperatures. This may be explained because CEM II has finer particles, which offer more resistance to shear and, simultaneously, lead to quicker flow ability drop, since the hydration reaction for this cement is quicker. CEM II specific surface is higher than that of CEM I.

Figure 1 presents the results of the flow tests carried out on a cement paste that was kept in a bath at 40°C. Results show that both superplasticizers increase the workability of the cement paste when water content is kept at the regular level (series 2A and 2B). Superplasticizer 3005 did not provide satisfactory results of workability if the amount of water is reduced (series 2A'). This cement paste loses flow ability at a higher rate than when superplasticizers are not present (series 2). On the other hand, for the same reduced amount of water, the presence of superplaticizer 3002 HE (series 2B') leads to a significantly better performance, since the cement paste keeps its workability for a longer period of time. The results obtained with a concentration

of superplasticizer 3005 of 0.5% of cement mass showed that a reduction of the water amount around 16% (series 2A') led to a significant loss of workability when compared with the situation where the amount of water was kept at the regular level (series 2A).

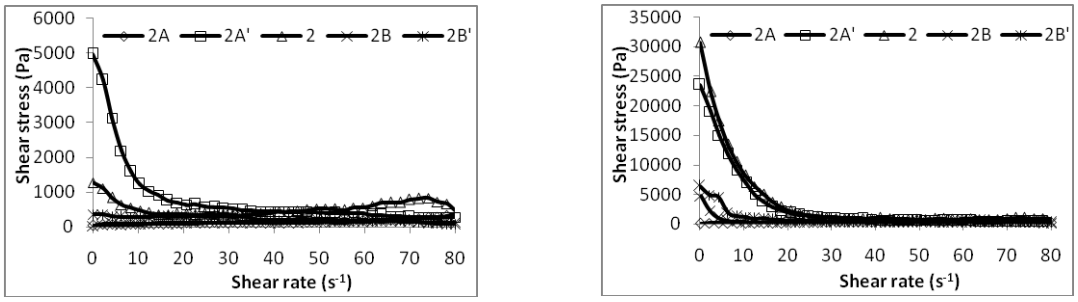

FIGURE 1 Shear stress/shear rate relationship at 40°C for several pastes: 1.5 minutes after preparation – (a) and 26.5 minutes after preparation – (b).

The use of superplasticizer 3002 HE improves the performance of the cement paste by extending both the initial and the final setting time as well as the mechanical strength. This effect was achieved when keeping the water content and also when reducing the water amount.

CONCLUSIONS

The workability of cement pastes tends to decrease with time. In the present work, the workability of cement pastes was quantified through rheological tests. When ambient temperature increases, the rate of decay of the cement paste flow ability increases. Tests were carried out to check if the inclusion of superplasticizers in cement pastes would contribute to reduce de rate of flow ability decay. Results using two different superplasticizers showed that the presence of this additive significantly increased the workability of the cement paste, for all temperatures tested, when the water amount was kept at the regular value. Some tests were also performed to check if the workability improvement was still visible if a 16% reduction on the water amount was implemented. At 40°C, the addition of either superplasticizer 3002 HE or 3005 showed remarkable improvements on CEM II paste workability.

REFERENCES

1. Ortiz, J.; Aguado, A.; Agulló, L.; García, T.; Zermeño, M., *Construction and Building Materials*, **2009**, *23*, 1808–1814.
2. Seabra, M.P.; Paiva, H.; Labrincha, J.A.; V.M. Ferreira, J. A., *Construction and Building Materials*, **2009**, *23*, 1147-1153.

O25

Study of rheological behaviour of stainless steel feedstock taking into account the thermal effects

Christian Kukla[1], Ivica Duretek[2], Stephan Schuschnigg[2], Joamin Gonzalez-Gutierrez[2], Ali Gooneie[2], Clemens Holzer[2]

[1] *Montanuniversitaet Leoben, Industrial Liaison Department, Peter Tunner Str. 27, 8700 Leoben, Austria*

[2] *Montanuniversitaet Leoben, Department of Polymer Engineering and Science, Chair of Polymer Processing, Otto Gloeckel-Str. 2, 8700 Leoben, Austria*

Correspondence to: Christian Kukla (E-mail: *Christian.Kukla@unileoben.ac.at*)

ABSTRACT

Powder injection moulding (PIM) process is well established for production of small precision components with both metal and ceramic powders. In comparison to unfilled polymers, the PIM-feedstocks are highly filled multiphase systems, whose flow behaviour is very sensitive to composition of binder and powder loading. Furthermore, the rheology of highly filled multiphase systems is characterized by strain and temperature dependence and influenced by flow instabilities and yield stress. In this study, the rheological behaviour of 316L feedstocks with a polypropylene/wax binder system and different powder loadings was investigated. The experimental work was performed with a rotational and a high pressure capillary rheometer. The aim of this work was to evaluate mixing rules predicting the viscosity of the feedstock out of its composition taking into account the melt temperature rise due to dissipative heating. Hence, measured data were corrected with respect to temperature. Thus the influence of the temperature onto the viscosity and the related model was evaluated.

KEYWORDS: rheology, powder injection moulding, highly filled polymer, heat dissipation, modelling

INTRODUCTION

PIM is a complex, multi-step process with a significant technological and economic potential. The binder system plays one big role in the production of PIM parts; even though as it is completely removed in the final part. One of the main functions of the binder system is to provide mouldability to the metal or ceramic powder. Thus the main property is viscosity. Knowledge of the dependence of viscosities of binder constituents and powder characteristics on the final composition is required for the solution of many engineering problems[1, 2].

In a previous work we calculated the final feedstock viscosity starting with the viscosities of the binder constituents[2]. We found that existing models mainly describe the viscosity increase by a certain powder loading but do not take into account further effects like the shift of the transition region from Newtonian to shear thinning behaviour. For the shift of the transition region we employed the model by Geisbüsch[3] and found good agreement with our measurements. In Fig. 1-left one can see that the transition region is described properly. Additional effects like the increase of viscosity in the region of low shear rates, due to Herschel-Bulkley behaviour, or the change of the slope in the shear thinning region as a function of powder loading cannot be described with this model.

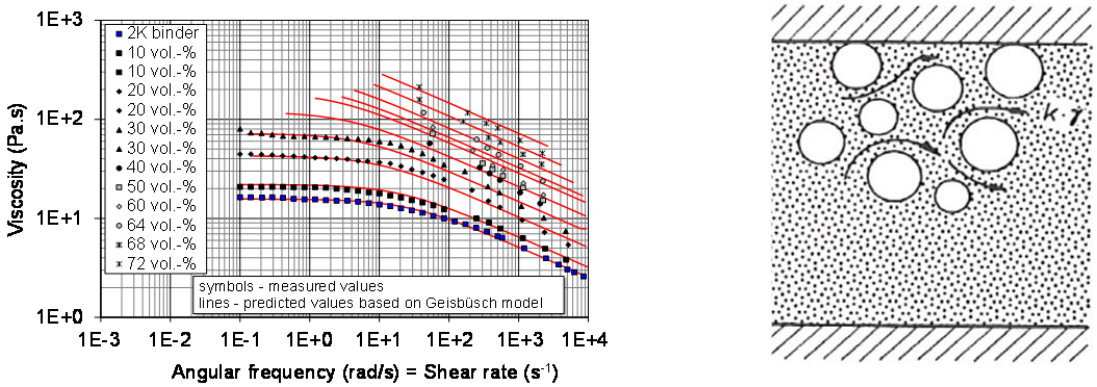

FIGURE 1 Left: Measured and according to Geisbüsch calculated viscosities for the feedstocks with polypropylene/wax binder system[2]; Right: Increased shear in highly filled polymers, where k is the factor to describe the increase in shear[3]

Here we look at the difference of the slope in the shear thinning region, whether it is due to an higher temperature increase caused by an increased shear rate in the binder system or not. As shown in Fig. 1-right in a highly filled polymer all the shear has to be taken by the polymer. When you look at this feedstock as a one phase system you get a certain value for the shear rate. In reality it is a two phase system with a stiff second phase. Thus the shear in the fluid has to be higher than the one calculated by the one phase approach. With this higher shear a higher temperature increase in the polymer due to dissipation should occur especially at higher shear rates.

Increased temperature in a polymer highly filled with stiff powders

To evaluate the amount of the increased temperature due to shear and its influence onto the viscosity measurements we followed three approaches. First, we evaluated the contribution of

viscous dissipation over the heat conduction normal to the direction of flow, by calculating the Griffith number (Gr). The Griffith number for a power law fluid can be calculated using Eq. (1):

$$Gr = \frac{k\dot{\gamma}^{n+1}\beta h^2}{\lambda} = \frac{\text{viscous dissipation}}{\text{heat conduction}} \qquad (1)$$

Where k is the binder's consistency index, $\dot{\gamma}$ is the shear rate, n is the binder's flow index, β is the temperature coefficient, h is the distance between particles estimated, and λ is the thermal conductivity of the binder. Calculation of Gr was done to show that at high shear rates the heat generated in the binder due to viscous dissipation is larger than the heat transmitted by conduction to the metal particles (i.e. Gr > 1), and thus the binder will have higher temperature than the filler particles (see Fig.2 left).

Second, finite element simulations (Polyflow-ANSYS) were performed assuming that feedstock material was a one-phase material with physical properties that are arising from the feedstock as a whole. Thus we got the lower limit for the temperature rise due to feedstock flow (Fig.2-right).

Third, finite element simulations (Polyflow-ANSYS) were performed assuming that the binder in the system was flowing through fixed spheres of steel. Thus we got the upper limit for the temperature raise due to binder flow (Fig. 2-right).

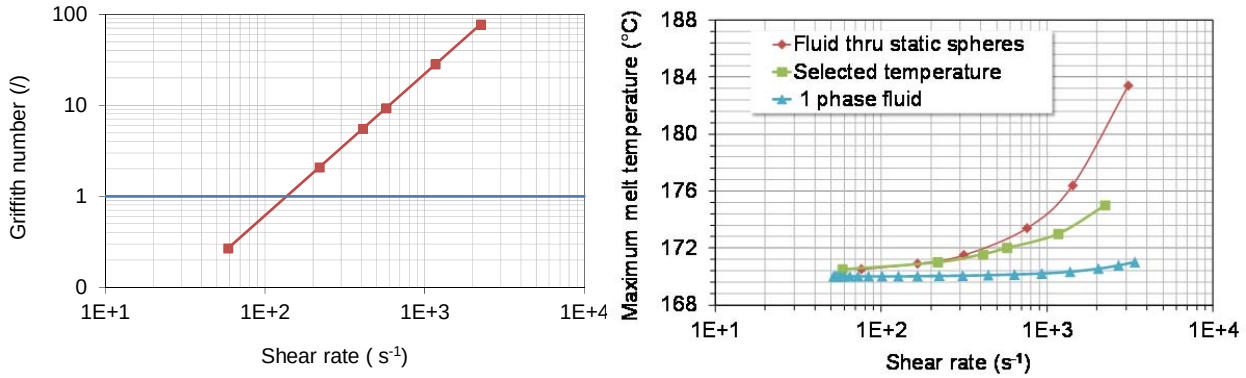

FIGURE 2 Left: Griffith number as function of shear rate for 60 vol.-% feedstock; Right: Increase in temperature as a function of shear rate for 60 vol.-% feedstock by simulations; selected temperature is estimation between the extremes of the flow of a fluid through static spheres and a 1 phase fluid.

It can be seen in Fig. 2-right that at shear rates lower than 100 s^{-1} the rise in temperature is very small. This is in agreement with the calculated Griffith number. In reality, the binder is not a one-phase system flowing through the die and it is not a fluid flowing through static spheres, but it is a two phase system with a fluid moving along with the filler particles, therefore the temperature raise should be between the two extremes calculated in the simulations (Fig. 2-right).

To undertake a first improvement of our Geisbüsch fitting of the viscosity curve we estimated deliberately a temperature between these two extremes by taking 97% of the maximum melt temperature of a fluid through static spheres (Fig. 3).

Viscosity corrections due to increased temperature in polymer

Using the estimated temperature rise, one can correct the viscosity at high shear rates and use the model proposed by Geisbüsch to predict the measured data. This is shown in Fig. 3 for the particular example of 60%vol feedstock. The viscosity values were shifted by using the Arrhenius equation, and it can be seen that the prediction from the model has improved at the higher shear rates; however some further corrections are needed.

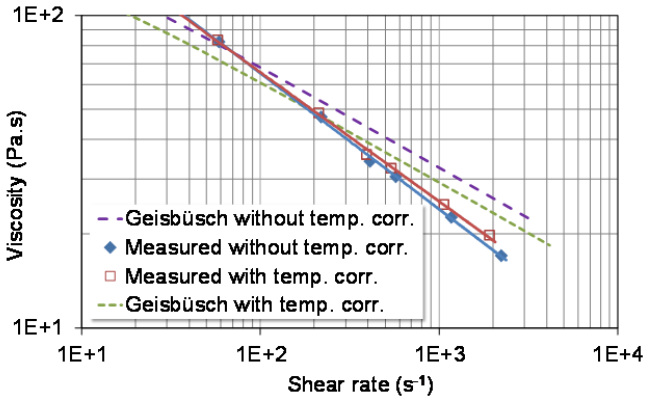

FIGURE 3: Viscosity corrections due to temperature increase at high shear rates and predictions by the Geisbüsch model for 60 vol.-% feedstock.

CONCLUSIONS

Increase in temperature due to viscous heating is certainly a factor that influences the viscosity behaviour of feedstock at high shear rates ($\dot{\gamma}$>100 s^{-1}), but it may not be the only one. Other important factor may be the particle-particle interactions, which the current model doesn't take into account. In the future, two-phase flow simulations will be implemented to obtain a more accurate estimate of the changes in temperature due to increased shear rates in the binder.

REFERENCES AND NOTES

1. C. Kukla, I. Duretek, C. Holzer: Rheological behaviour of binder systems for PIM and mixing rules for calculation of viscosity, EURO PM2013 Congress and Exhibition, Gothenburg, 2013.
2. C. Kukla, I. Duretek, C. Holzer: Modelling of rheological behaviour of 316L feedstocks with different powder loadings and binder compositions, EURO PM2014 Congress and Exhibition, Salzburg, 2014.
3. Geisbüsch, P.: Ansätze zur Schwindungsberechnung ungefüllter und mineralisch gefüllter Thermoplaste, Dissertation an der RWTH Aachen, 1980

Product Formulation

O7

Development of ecofriendly emulsions based on product engineering principles.

Nuria Calero[1], Jenifer Santos[1], José Muñoz[1].

[1]Reología Aplicada. Tecnología de Coloides. Departamento de Ingeniería Química. Facultad de Química. Universidad de Sevilla c/ P. García González, 1, E41012, Sevilla España.

Correspondence to: Nuria Calero (E-mail: *nuriacalero@us.es*)

ABSTRACT

The chemistry and technology of agrochemical products has undergone extensive changes over the last 20 years. New formulations and ingredients must meet the needs of the agrochemical industry for products exhibiting greater safety to users, much lower environmental impact and better performance. N,N-Dimethyldecanamide (AMD-10^{TM}) and D-limonene are solvents that fulfil the requirements to be considered green solvents. This contribution deals with the study of emulsions formulated with a mixture of these solvents and an eco-friendly emulsifier. All studied emulsions showed shear thinning behaviour which fitted fairly well the Cross model. The influence of aging time on zero shear viscosity was demonstrated to be a powerful tool to assist in predicting the destabilization process of emulsions.

KEYWORDS: eco-friendly emulsions, rheology, laser diffraction, product engineering, physical stability.

INTRODUCTION

Satisfying the needs of consumers is one of the basic principles of product engineering. Consequently, traditional organic solvents are being replaced by new eco-friendly solvents in agrochemical products in order to avoid contamination and reduce the risk for farmers[1]. N,N-Dimethyldecanamide (AMD-10) and D-Limonene are solvents that fulfill the requirements of a sustainable society. In addition, polyoxyethylene glycerol esters are also eco-friendly and nontoxic, hence they are considered as green surfactants.

Rheology is a useful tool to provide early information on destabilization mechanisms in emulsions. In order to detect the onset of creaming or coalescence, it is necessary to determine the viscosity at very low stresses.[2]

The main target of this work was to study the influence of AMD-10/D-limonene ratio on flow curves and droplet size distributions of stable O/W emulsions formulated with these eco-friendly solvents and a polyoxyethylene glycerol ester as emulsifier.

MATERIALS AND METHODS

Materials

N,N-Dimethyldecanamide (Agnique AMD-10^{TM}, BASF), D-Limonene (Sigma Aldrich) and Glycereth-17 Cocoate (Levenol C-201^{TM}, KAO) as emulsifier with HLB 13, were used. Some RD antifoam agent (DOW CORNING®) and deionized water were for the preparation of emulsions.

Methods

Preparation of emulsions

Emulsions containing 3 wt % Levenol C-201^{TM} as emulsifier, 0.1 wt % RD antifoam agent and 30 wt% solvent(s) were prepared. The ratio of solvents studied were 100/0, 85/15, 80/20, 75/25, 70/30, 65/35, 50/50, 25/75, and 0/100 of AMD-10/D-limonene. These O/W emulsions were prepared using a Silverson L5M at 6000 rpm during 60 s.

Laser diffraction measurements

Size distribution of oil droplets were determined by laser diffraction using a Mastersizer X (Malvern, Worcestershire, UK). The mean droplet diameter was expressed as Sauter´s diameter ($D_{3,2}$):

$$D[M,N] = \left[\frac{\int D^M\, n(D)dD}{\int D^N n\,(D)dD}\right]^{\frac{1}{M-N}} \quad (1)$$

Rheological measurements

Flow curve tests were conducted with a Haake MARS controlled-stress rheometer (Thermo-Scientific, Germany), equipped with a sand-blasted coaxial cylinder Z-20 to avoid slip effects. Flow curves were carried out from 0.05 to 1 Pa at 20ºC.

RESULTS AND DISCUSSION

Figure 1 shows $D_{3,2}$ as a function of the ratio of solvents for emulsions prepared at 6000 rpm. All emulsions formulated with the mixture of solvents yielded lower $D_{3,2}$ values than their counterparts with only one solvent. This is probably due to the combination of different properties of the solvents used. The addition of AMD-10 provokes a certain

decrease in the interfacial tension, whereas D-Limonene confers more apolar character[3]. The combination of both solvents led to emulsions with submicron mean diameters. In fact, it was possible to obtain emulsions with $D_{3,2}$ as low as 290 nm, using just a rotor stator device. This demonstrates that the choice of an optimum formulation made possible to use a relatively low-energy homogenizer to get fine emulsions, which fits one of the basic principles of product engineering.

Figure 2A shows flow curves of 1-day-aged stable emulsions studied as a function of the ratio of solvents. Only the most stable emulsions were measured. All emulsions exhibited a trend to reach a Newtonian region at low-shear rates, which allowed the zero-shear viscosity, (η_o) to be estimated. This range was followed by a slight decrease in viscosity (shear-thinning behaviour) above a critical shear rate. Figure 2A also illustrates the fitting quality to the Cross model (R^2>0.999).

$$\eta = \frac{\eta_0}{1+\left(\frac{\dot{\gamma}}{\dot{\gamma}_C}\right)^{1-n}} \qquad (2)$$

Two levels in zero shear viscosity values were observed. Emulsions with higher D-Limonene content (65/35, 70/30 and 75/25) showed higher η_0 than 80/20 and 85/15 emulsions, which is consistent with laser diffraction results and different flocculation degree.

Figure 2B shows the relative increase in zero-shear viscosity from day 1 to day 40, calculated as the ratio of the difference of the zero shear viscosities on day 40 and day 1 to the zero-shear viscosity on day 1. A negative value means that a decrease in η_o took place. Conversely, an increase in η_o yields a positive value. Two different trends were observed. There is a decrease in zero shear viscosity for 65/35 and 70/30 emulsions, which is consistent with an increase in the droplet sizes. The higher viscosity values of these emulsions at 1-day aging time may not be only attributed to a droplet size effect, but also to a flocculation process, which in turn led to coalescence upon aging due to the disruption of the O/W interface under compression. On the contrary, the increase in zero shear viscosity for 75/25, 80/20 and 85/15 emulsions may indicate the onset of creaming.

CONCLUSIONS

Submicron emulsions were obtained using an optimised mixture of eco-friendly solvents. All emulsions exhibited shear-thinning behaviour. Monitoring calculated

values of zero shear viscosity with aging allowed us to detect the onset of two different destabilization processes. 85/15, 80/20 and 75/25 emulsions underwent incipient creaming, whereas 65/35 and 70/30 emulsions shows coalescence. Hence, this work has demonstrated that the use of mixture of solvents is a powerful tool to reduce the energy input to prepare emulsions with submicron mean diameters.

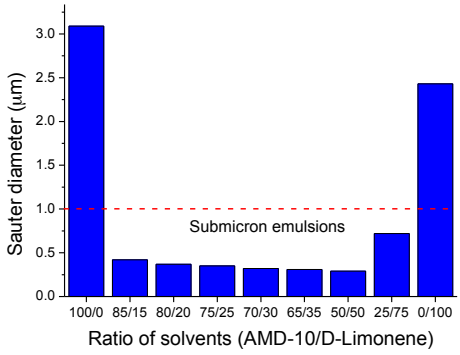

FIGURE 1. Sauter´s diameter as a function of ratio of solvents for the emulsions studied.

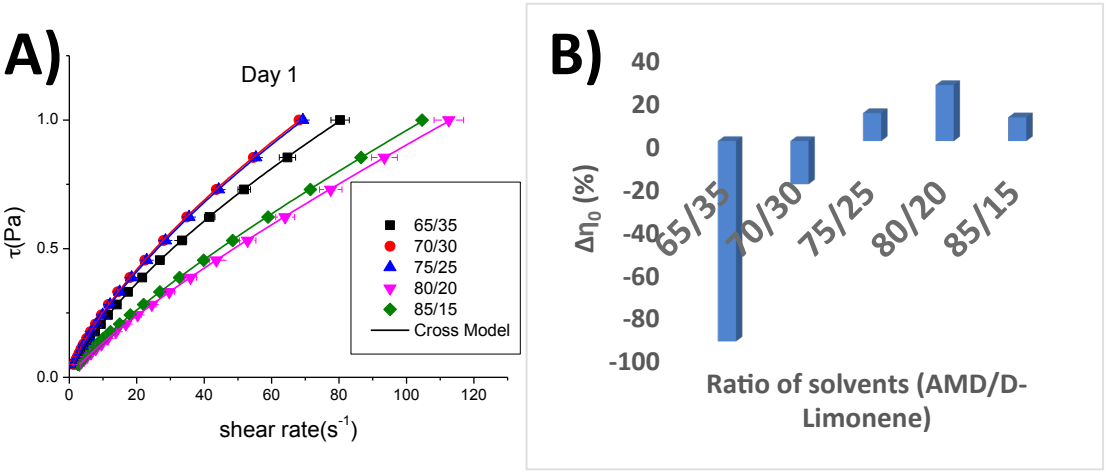

FIGURE 2.A) Flow curves for studied emulsions as a function of ratio of solvents at 20°C. B) Normalized increase of the zero shear viscosity from day 1 to day 40.

ACKNOWLEDGEMENTS

The financial support received (Project CTQ2011-27371) from MINECO (Spain), the European Commission (FEDER Programme) and from the V Plan Propio Universidad de Sevilla is kindly acknowledged.

REFERENCES

1. Hofer, R.; Bigorra, J., *Green Chemistry*, **2007**,9,203–212.
2. Tadros, T. F., Rheology of dispersions: principles and applications. John Wiley & Sons, **2011**.
3. Santos, J.; Trujillo-Cayado, L. A.; Calero, N.; & Muñoz, J,*AIChE Journal*, **2014**, 60, 2644-2653.

O8

Rheological development and characterization of a bio sourced feedstock of superalloy in metal injection molding process

Alexandre Royer[1], Thierry Barrière[1], Jean-Claude Gelin[1]

[1] Institut Femto-ST département de mécanique appliquée, UMR 6174 CNRS, ENSMM, 24 rue de l'épitaphe, 25030 Besançon cedex, France

Thierry Barrière (E-mail: *thierry.barriere@femto-st.fr*)

ABSTRACT

In the Metal Injection Molding (MIM) process the binder play the most important role. It provides fluidity of the feedstock mixture for injection molding and adhesion of the powder to keep the molded shape. The binder must provide strength and cohesion for the molded part and must be easy to be removed from the molded part. Moreover it must be recyclable, environmentally friendly and economical. The goal of this study is to develop a feedstock of Inconel 718 environmentally friendly. For this, a study of a new binder formulation based on polyethylene glycol, because of is water debinding properties, and bio sourced polymer was made. Polylactic acid and polyhydroxyalkanoates were investigated as bio sourced polymers. The results are compared to a standard formulation. The chemical and rheological behavior of the binder formulation during mixing, injection and debinding process were investigated. The miscibility between polymers affects the homogeneity and was studied by differential scanning calorimetry and microscopy. Moreover, a powder of Inconel 718 was chosen to produce a feedstock. The feedstock was characterized like the binder. The results show the well adapted formulation of polymer binder to produce a superalloy Inconel 718 feedstock

KEYWORDS Metal injection molding, poly(ethylene glycol), Polylactic acid, Inconel, polyhydroxyalkanoates.

INTRODUCTION

The binder is the most important part in the MIM process as it contributes fully to multitask like to be able to support a load rate by importing powder, typically 60%, and to direct the powder in the mold [1]. Enneti [1] show the binder must give strength and cohesion to the molded part and be easily removed from the molded part and be recyclable, environmentally friendly and economical. Enneti [1] also explains the importance of a low viscosity, good adhesion to the powder, no chemical interactions with the powder and a low coefficient of thermal expansion for binders. Thavanayagan [2] shows the influence of the binder on the homogeneity of the feedstock.

He explains that the binder and the powder have to be miscible and have desired rheological properties. In this study, a micro powder of Inconel 718 was investigated to an application in the MIM process. A micro powder was chosen because Quinard [3] demonstrated that a micro powder is well adapted for μPIM experiments, including injection, debinding and sintering stages. The use of Inconel on MIM process had been study by Özgün et al [4] and a formulation was developed. Özgün et al [4] explains Inconel superalloy are used in aviation, aerospace and nuclear power for its high resistance to corrosion and oxidation but also for its excellent mechanical strength at high temperature. Superalloys most often used are currently Inconel 718 and 625. Here an Inconel 718 powder is chosen as final material of the piece. The binders developed by Özgün [4] for superalloys are composed of PP, CW, PW and SA but this formulation is not water debinding. The goal of this study is to develop new binder formulation water soluble formulation for Inconel 718 powder with ecological polymers. The formulation studied was compared to a usual water soluble binder.

MATERIALS AND METHODS

The polymers used for this study are polypropylene (PP), polyethylene glycol (PEG), polylactic acid (PLA) and polyhydroxyalkanoates (PHA) and stearic acid (SA). Two grades of PLA are used, namely PLA003 and PLA005. The polymer blends are made in a Brabender twin screw mixer which has a volume capacity of 50 cm^3, a speed of 50 rpm and at a temperature of 180°C except for the PLA005 and PHA which are mixed at 200°C. The powder used is an Inconel 718 atomized by argon with an average size of 32μm. The binders are composed in volume of 55% of PEG, 5% of SA and 40% of primary binder. Four different primary binders were used: PP, PLA005, PLA003 and PHA. The rheological tests were performed on a Haake Mars supplied by ThermoFisher. The tests are realized with a cone/plate geometry at 180°C, the temperature of injection.

RESULTS

1) Polymers analysis

The viscous behavior of polymer was studied in a cone/plate rheometer at the temperature of injection, 180°C. The results are shown figure 1. The results show Newtonian behavior with different flow threshold and different shear viscosity. The viscous behavior of the different PLA and the PHA are similar. The PP is different with a flow threshold which appears at 1 s^{-1} and has a higher shear viscosity at low shear rate but a lower share viscosity at high shear rate than the other polymers.

2) Binders study

The viscous behavior of binders was characterized by the same way and the results are shown figure 2. The results show lower shear viscosity due to the addition of the PEG which have a very low shear viscosity (approximatively 1 Pa.s). The results also show a modification of the viscous behavior with the addition of the PEG. The PLAs and PHA have now a pseudo Newtonian behavior. This Newtonian behavior is the same that the viscous behavior of the PEG. These results may be explained by the miscibility between the different polymers indeed the miscibility between the PLA and the PEG is well known and studied [5]. The miscibility between PHA and PEG was not studied but can be deduced from the results shown in figure 2A contrary to the behavior of the PP-PEG mixture which shows possible immiscibility. These results are confirmed by the optical microscopy as shown in figure 3. The image of the PP-PEG mixture shows inhomogeneity with parts of pure PP (in white) and parts of pure PEG (transparent).

3) Feedstocks analysis

The feedstocks are realized in the same time that the binders with a rate load in volume of 60%. First the binder is mixed in the mixer and then after stabilization of the mixing torque the powder is added. The viscous behavior of the different feedstock was studied in a cone/plate rheometer. These results are shown in figure 2B. These results show higher shear viscosity due to the addition of powder and a modification of the viscous behavior of all formulations. At high shear rates, the shear viscosity values are very similar for all formulations, it means that the inject ability are similar.

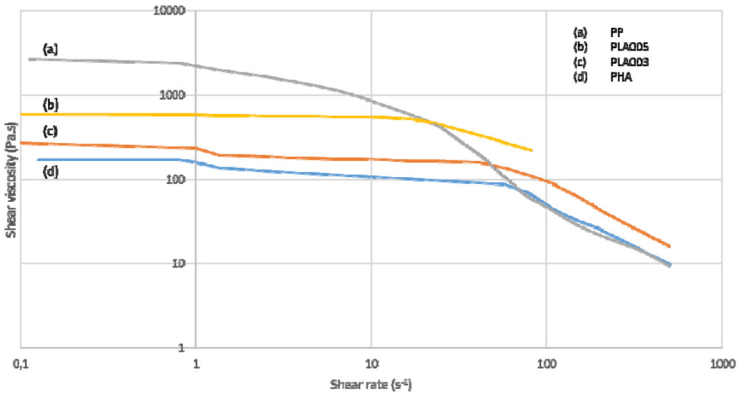

FIGURE 1 Shear viscosity versus shear rate of the polypropylene (a), polylactic acid 005 (b), polylactic acid 003 (c) and polyhydroxyalkanoates (d) at 180°C.

CONCLUSION

The present study has shown that the bio sourced polymers PLA and PHA are well adapted in MIM binder formulation based on PEG. It is also shown that, contrary to the polypropylene, these polymers are miscible with the PEG and this produce better homogeneity of the injected piece. It is also shown that this miscibility affect the viscous behavior of the mixture. Moreover the shear viscosity is lower for the bio sourced polymer which is better for the injection and the rate load volume of powder which can be used.

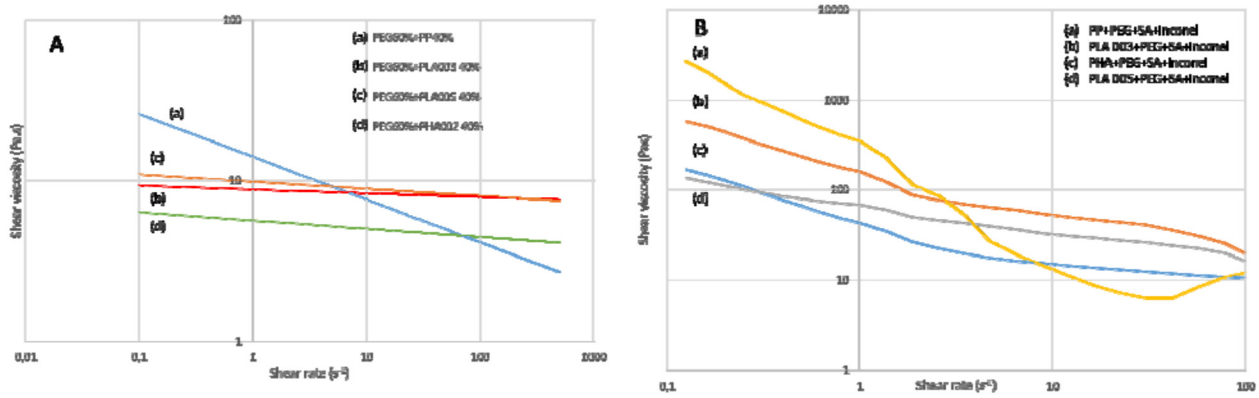

FIGURE 2A Shear viscosity versus shear rate of PP-PEG (a), PLA003-PEG (b), PLA005-PEG (c) and PHA-PEG (d) mixtures at 180°C, 2B Shear viscosity versus shear rate of the different formulations of feedstock at 180°C.

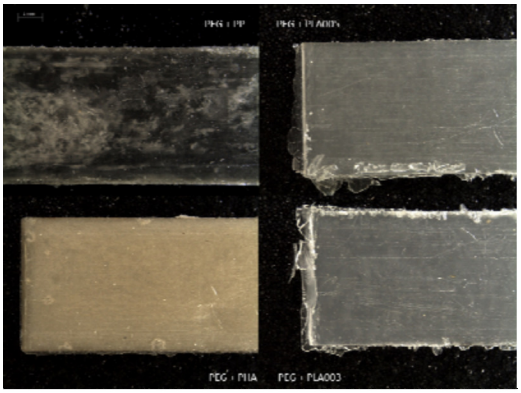

FIGURE 3 Optical microscopy of injected parts of the different binders.

ACKNOWLEDGEMENTS

The authors wish to thanks the Fui PROPIM project for the financial support.

REFERENCES AND NOTES

1. Enneti RK, Powder binder formulation and compound manufacture in metal injection molding (MIM), *Handbook of metal injection molding*, **2012**, 64-92.
2. Thavanayagan G, Pickering KL, Swan JE, Cao P, Analysis of rheological behaviour of titanium feedstocks formulated with a water-soluble binder system for powder injection moulding, *Powder Technology*, **2015**, 269, 227-232.
3. Quinard C, Barriere T, Gelin JC, Development and property identification of 316L stainless steel feedstock for PIM and µPIM, *Powder Technology*, **2009**, 190, 123-128.
4. Özgün Ö, ÖzkanGülsoy H, Yilmaz R, Findik F, Injection moulding of nickel based 625 superalloy : sintering, heat treatment, microstructure and mechanical properties, *Journal of alloys and compounds*, **2013**, 5476, 192-207.
5. Laia WC, Liaua WB, Lin TT, The effect of end groups of PEG on the crystallization behaviors of binary crystalline polymer blends PEG/PLLA, *Polymer*, **2004**, 45, 3073-3080.

Rheological properties of biopolymer-stabilized emulsions formulated with a nonionic eco-friendly surfactant

Luis A. Trujillo-Cayado[1*], Mª Carmen Alfaro[1], José Muñoz[1], A. Raymundo[2], I. Sousa[2]

[1] Reología Aplicada. Tecnología de Coloides. Departamento de Ingeniería Química. Facultad de Química. Universidad de Sevilla. C/ P. García González, 1, 41012, Sevilla, Spain.

[2] LEAF – Linking Landscape Environment Agriculture and Food. Instituto Superior de Agronomia, University of Lisbon, Tapada da Ajuda, 1349-017 Lisboa, Portugal

Correspondence to: Luis Alfonso Trujillo Cayado (E-mail: *ltrujillo@us.es*)

ABSTRACT

The influence of surfactant and gum concentrations, as well as rhamsan/welan gum ratio on rheological properties, droplet size distribution and physical stability of eco-friendly O/W emulsions stabilized by an ecological surfactant were studied in the present work. The gum concentrations in the aqueous solutions of rhamsan, welan and blends of both gums were selected to ensure the formation of weak gel matrices. Flow curves at steady shear demonstrated the lack of synergism between rhamsan and welan gums, whose ratio controlled the shear thinning properties of these emulsions. Mechanical spectra exhibited G´ values higher than those of G´´ in the whole frequency range studied, indicating the formation of a network supported by the cooperative contribution of the biopolymer continuous phase and the packing effect due to the great number of α-pinene droplets.

KEYWORDS: Eco-friendly, Emulsion, Rhamsan gum, Rheology, Welan gum

INTRODUCTION

Polysaccharides are frequently employed to stabilize oil-in-water emulsions for their biocompatibility, biodegradability and nontoxicity[1]. The efficiency depends on the concentration of hydrocolloids in the aqueous phase and on the characteristics of the structure formed by the biopolymer. Microbial polysaccharides can be manufactured under controlled conditions, resulting in commercial batches with outstanding reproducibility of their functional properties.

Welan gum and rhamsan gum are exopolysaccharides that act as thickening and stabilizer agents. They have a wide range of commercial applications in food, ink, petroleum and other industries. The role of surfactants is also essential to provide long-term stability to emulsions, since they adsorb at the oil/water interface preventing droplet coalescence. Interactions between surfactants and polysaccharides can affect the macroscopic properties of emulsions. Polyoxyethylene glycerol esters derived from cocoa oil are ecological surfactants with good emulsifying properties[2]. This study focuses on the rheological properties of emulsions formulated with a biosolvent (α-pinene) as oil phase, an eco-friendly surfactant as emulsifier and two exopolysaccharides (welan and rhamsan gums) as thickeners.

MATERIALS AND METHODS

Oil-in-water emulsions using α-pinene (30 wt%) as dispersed phase was prepared using a rotor-stator device (Ultraturrax T25) at 9500 rpm for 120 s. Seven emulsions were prepared using different surfactant concentrations (0.0, 3.5 and 7.0 wt%), gum concentrations (0.33, 0.56 and 0.80 wt%) and rhamsan/welan gum ratios (100/0, 50/50 and 0/100) as can be seen in table 1.

TABLE 1. Values of surfactant concentration, gum concentration and rhamsan/welan gum ratio for all studied emulsions.

Emulsion name	Surfactant concentration (wt%)	Gum concentration (wt%)	Rhamsan/Welan gum ratio
0.0 - 0.56 - 50R/50W	0.0	0.56	50/50
7.0 - 0.56 - 50R/50W	7.0	0.56	50/50
3.5 - 0.33 - 50R/50W	3.5	0.33	50/50
3.5 - 0.80 - 50R/50W	3.5	0.80	50/50
3.5 - 0.56 - 100R/0W	3.5	0.56	100/0
3.5 - 0.56 - 0R/100W	3.5	0.56	0/100
3.5 - 0.56 - 50R/50W	3.5	0.56	50/50

The rheological characterization involved stress and frequency sweeps in small amplitude oscillatory shear experiments (SAOS) and steady shear flow tests at 20ºC. Rheological experiments were conducted for emulsions aged for 24 hours with a Haake MARS III controlled-stress rheometer (Thermo-Scientific), using a serrated plate-plate sensor (60 mm diameter, gap: 1 mm) to prevent wall slip effect.

RESULTS AND DISCUSSION

Figure 1A shows the frequency dependence of the linear viscoelastic functions of all emulsions to illustrate the influence of the studied variables. First, it should be noted that there are no results for the emulsion with 0.0 wt% surfactant because it could not be prepared due to the lack of surface-active ingredients. All samples display clear viscoelastic properties with a predominance of the elastic over the viscous component in the frequency range studied. The emulsion with central values of all variables, which contains 3.5 wt% surfactant, shows higher values of the storage modulus than the emulsion that contains 7 wt% surfactant for all the frequency range studied. This supports the decrease of the viscoelastic properties with increasing surfactant concentration; probably due to the higher mean diameters (coalescence) induced by depletion flocculation. Furthermore, the addition of gum yielded the formation of a much stronger and more elastic structure, demonstrating the high influence of gum concentration on viscoelastic properties. It should be also noted that the slope of G´ with frequency for the emulsion containing only rhamsan gum as thickener is lower than that of welan gum. The use of rhamsan and welan in identical percentages does not lead to a positive synergistic effect on the mechanical spectrum. This means that the resulting dispersion does not show higher elastic properties. The results obtained are consistent with the occurrence of enhanced solid-like viscoelastic properties in emulsions containing rhamsan gum. Furthermore, this fact may suggest that rhamsan gum predominates over welan gum when both gums are used.

All samples exhibited shear thinning behavior and a trend to reach a Newtonian region at low shear rate enabling the estimation of a zero-shear viscosity (η_0). The shear rate dependence of viscosity fitted fairly well the Cross model. Figure 1B displays flow curves for all samples. The increase of η_0 with gum concentration may be explained by the fact that polysaccharides exert a thickening effect on the continuous phase. The emulsions formulated with rhamsan gum show higher zero-shear viscosity values than those shown by emulsions with welan gum. Furthermore, the mixture of both gums gives rise to intermediate values of zero-shear viscosity and power law index. Finally, it should be noted that the zero shear viscosity is not affected significantly by surfactant concentration

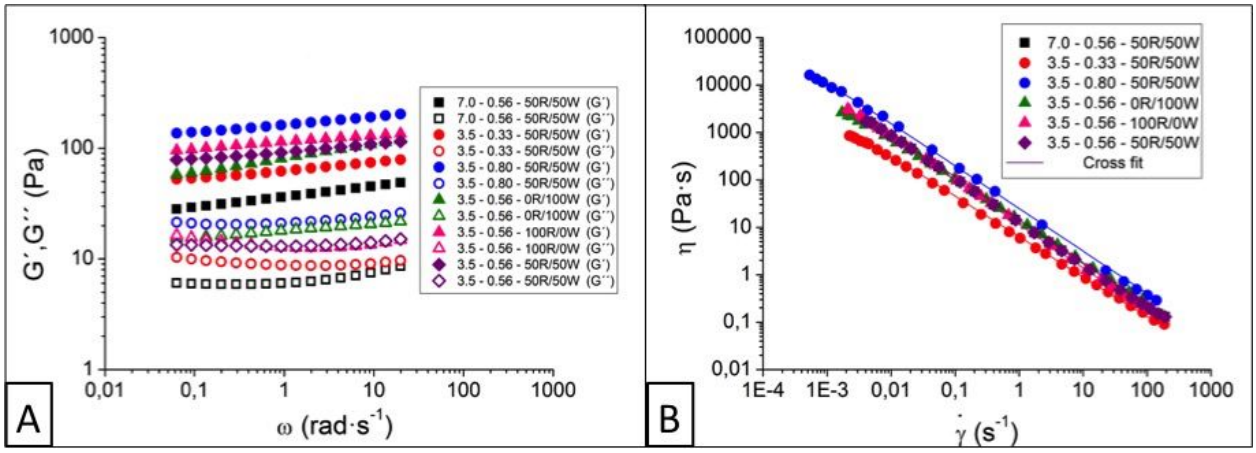

FIGURE 1. (A) Mechanical spectra and (B) flow curves of emulsions aged for one day, at 20°C, as a function of all studied variables.

CONCLUSIONS

Linear viscoelastic properties of emulsions formulated with rhamsan and/or welan gum and a non-ionic emulsifier strongly depend on all studied variables. The elastic component dominates over the viscous one in all samples. The use of rhamsan and welan gums in identical percentages does not yield a positive synergistic effect on the mechanical spectrum. Mechanical spectra suggest that the rheological properties of emulsions formulated with both gums as thickeners are essentially controlled by rhamsan better than welan gum. All samples showed shear thinning behavior above a critical shear rate. Zero-shear viscosity values strongly depend on the gum concentration and rhamsan/welan gum ratio.

ACKNOWLEDGEMENTS

The financial support received (Project CTQ2011-27371) from the Spanish Ministerio de Economía y Competitividad (MINECO) and from the European Commission (FEDER Programme) is kindly acknowledged.

REFERENCES

1. Phillips, G.O., Williams, P.A., Handbook of hydrocolloids; Elsevier, Amsterdam, **2009**.
2. Trujillo-Cayado, L. A.; Ramírez, P.; Alfaro, M. C.; Ruíz, M.; Muñoz, J., Adsorption at the biocompatible α-pinene–water interface and emulsifying properties of two eco-friendly surfactants. *Colloids and Surfaces B: Biointerfaces*, **2014**, *122*, 623-629.

On the yield stress of Ca(2+)-induced gellan fluid gels under torsional shear flow

M.C. García[1], M.C. Alfaro[1], J. Muñoz[1]

[1] Reología Aplicada. Tecnología de Coloides. Departamento de Ingeniería Química. Facultad de Química. Universidad de Sevilla. C/ P. García González, 1, 41012, Sevilla, Spain.

Correspondence to: J.Muñoz (E-mail: jmunoz@us.es)

ABSTRACT

The goal of this work was to check the efficiency of creep-recovery-creep tests to accurately determine the yield stress of very shear thinning materials free of previous memory effects. This method is assessed with a fluid gel prepared with low-acyl gellan gum. The rheological response at shear stresses around the yield stress turned out to be rather unstable. Yet, solid-like or fluid-like behaviours were observed by just changing the stress by 0.25 Pa or by conducting a second creep test. The lack of reproducibility observed at 2.25 Pa was attributed to shear banding effects promoted by the use of a serrated plate & plate measuring system. Nominal shear stresses and viscosities provided by the rheometer were corrected using standard equations.

KEYWORDS: yield stress, torsional flow, fluid gel, gellan gum, very shear thinning

INTRODUCTION

Gellan gum is among the biopolymers capable of forming fluid gels from very low gum concentrations. Fluid gels are interesting materials insofar as they exhibit fluid-like consistency, i.e. they are “flowable” materials, but they simultaneously possess significant elastic properties. Confocal laser scanning microscopy reveals that the microstructure of gellan fluid gels consists of a dispersion of gel-like domains in an aqueous continuous phase [1]. Therefore, they are prone to undergo wall-depletion (slip) phenomena under shear. For this reason, the parallel plate geometry with serrated surfaces is one of the measuring systems of choice when dealing with the characterization of fluid gels under shear flow. However, torsional flow poses the problem that neither shear stress nor shear rate are constant along the plate radius, such that stress corrections must be made. Determining a practical yield stress is quite important for the onset of flow

calculations. This study was carried out by checking that samples were free of thermo-mechanical history effects. Therefore, standard flow curves were not run but independent tests at constant shear stress. Series of creep-recovery-creep tests allowed the viscosity recovery to be estimated.

MATERIALS AND METHODS

Fluid gels were prepared with deionised water at 0.2 wt% with low-acyl gellan gum (Kelcogel F^{TM}) kindly provided by CP Kelco and 0.2 wt % calcium chloride (Panreac) as reported elsewhere [2]. The effects of sample loading and those associated to reach the measuring gap (1mm) were counterbalanced by an equilibration time above 1200 s, as determined by SAOS/time tests. Creep-recovery-creep tests were carried out at 20ºC in the (2 – 6) Pa range. Stress and viscosity corrections were made using standard methods [2].

RESULTS AND DISCUSSION

Imposing a shear stress of 2 Pa for about 45 s resulted in a very low shear rate which is by far below the minimum shear rate guaranteeing observable flow (Figure 1).

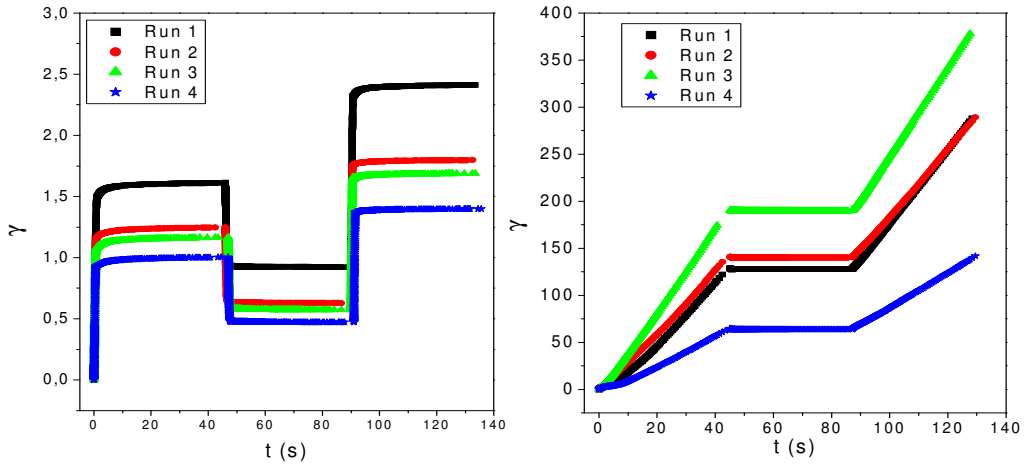

FIGURE 1. Creep-recovery-creep results at 2 Pa (figure a) and 2.5 Pa (figure b) (strain versus shear time) for a fluid gel containing 0.2 wt % LA-gellan gum 0.2 wt % CaCl2 and 0.1 wt % sodium azide. T = 20º C. Runs 1, 2, 3 and 4.

In fact, the response is controlled by the viscoelasticity of gellan fluid gel as supported by the great recovery and the similar response after the second creep test. Figure 2 illustrates that

chaotic results were obtained at 2.25 Pa. While some results were closer to those typical of linear creep flow, others supported the onset of clear shear flow. The variability of results also influenced the recovery step and the resulting strain range.

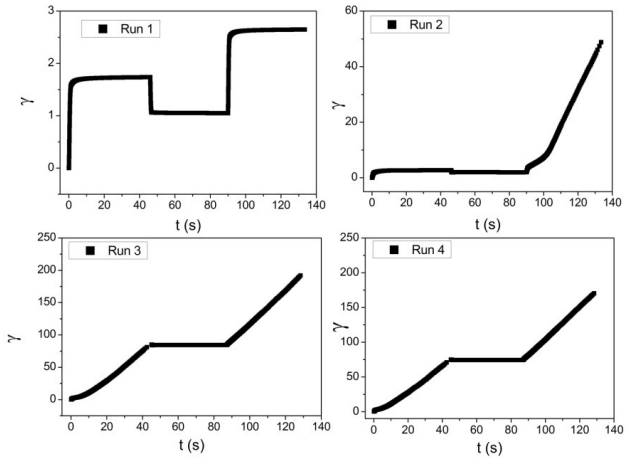

FIGURE 2. Creep-recovery-creep test at 2.25 Pa (strain versus shear time) for a fluid gel containing 0.2 wt % LA-gellan gum 0.2 wt % CaCl2 and 0.1 wt % sodium azide. T = 20º C. Runs 1, 2, 3 and 4.

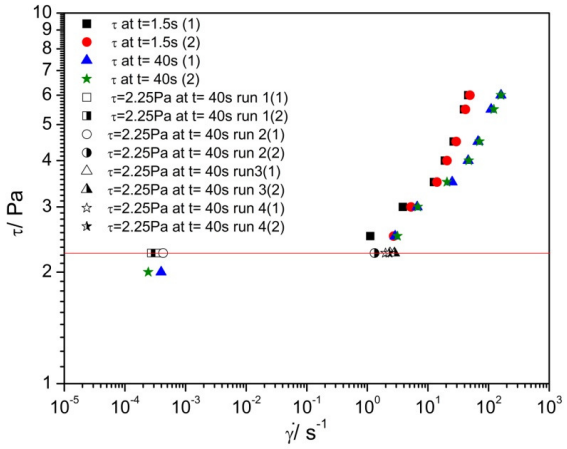

FIGURE 3. Shear stress versus shear rate for a fluid gel containing 0.2 wt% gellan gum, 0.2 wt% CaCl2 and 0.1 wt% sodium azide. Note: all data derive from creep-recovery-creep tests. T=20ºC. (1): data derived from the first creep test. (2): data derived from the creep test conducted after the recovery step.

Results obtained at 2.50 Pa were clearly consistent with the development of a significant shear flow since straight lines were quickly obtained and the recovery degree was null. Figure 3

illustrates that the practical yield stress was 2.25Pa and above this value, the longer the shear time at constant shear stress, the higher the shear rate, i.e. the lower the viscosity.

CONCLUSIONS

Series of independent creep-recovery-creep tests carried out at several shear stresses on samples free of thermo-mechanical history effects allowed a practical yield stress to be accurately determined. This yield stress located the onset of the so-called very shear thinning behaviour more accurately than flow curves and resulted in rather unstable results in the case of gellan fluid gels. This indicated the occurrence of shear banding, which was promoted by the use of torsional flow. A serrated-surface parallel plate measuring geometry was used since fluid gels are prone to show slip effects. A slight decrease by 0.25 Pa below the yield stress gives rise to quite reproducible and extremely low shear rates. Conversely, a slight increase by just 0.25 Pa above the yield stress resulted in clear fluid-like behaviour as demonstrated by the 4-decade rise of shear rate.

ACKNOWLEDGEMENTS

The financial support received (Project CTQ2011-27371) from the Spanish Ministerio de Economía y Competitividad (MINECO) and from the European Commission (FEDER Programme) is kindly acknowledged.

REFERENCES

1. García, M.C; Alfaro, M.C; Calero, N.; Muñoz, J., Influence of gellan gum concentration on the dynamic viscoelasticity and transient flow of fluid gels, *Biochemical Engineering Journal*, **2011**, 55, 73-81.
2. García, M.C; Alfaro, M.C; Muñoz, J., Yield stress and onset of nonlinear time-dependent rheological behaviour of gellan fluid gums. *Journal of Food Engineering*, **2015**, 42-47.

O18

Utilisation of Optical Coherence Tomography in Rheological Characterisation of Montmorillonite Dispersions

Martina Lille[1], Ari Jäsberg[1], Sanna Haavisto[2], Seppo Kasa[2], and Antti Koponen[1]

[1]VTT Technical Research Centre of Finland Ltd., P.O. Box 1000, FI-02044 VTT, Finland; [2]Spinnova Ltd., Kankitie 3, FI-40320 Jyväskylä, Finland; [1]Posiva Oy, Olkiluoto, FI-27160 Eurajoki, Finland

Correspondence to: Antti Koponen (E-mail: antti.koponen@vtt.fi)

ABSTRACT

In this work the flow behaviour of aqueous sodium montmorillonite dispersions (0.1 – 4.0 vol%) was investigated in a parallel plate geometry with a rheometer. During the rheometer measurements, true velocity profiles in the whole gap (1000 µm) were determined with Optical Coherence Tomography (OCT), which revealed that wall slip and deviations from laminar flow gave rise to artefacts in the flow profiles measured with the rheometer.

KEYWORDS montmorillonite, rheology, flow, wall slip, optical coherence tomography, OCT

INTRODUCTION

Dispersions of clay particles, such as bentonite, are widely applied as rheology modifiers[1] and underground sealing agents[1,2]. The rheological characterisation of clay dispersions is not always straightforward as they (like many multiphase materials) may behave non-ideally in the measuring geometry. The flow may manifest, e.g., apparent wall slip and wall depletion[3] or deviations from laminar flow and radial migration especially at high shear rates[4]. In this work we studied the flow behaviour of bentonite dispersions in parallel plate geometry. Optical Coherence Tomography (OCT)[5,6] was used to measure the true velocity profiles in the geometry gap and thus to identify possible challenges in the used measurement method.

MATERIALS AND METHODS

Aqueous sodium montmorillonite (NaMt) dispersions with solids contents ranging from 0.1 to 4.0 vol% were used in the experiments. The dispersions were prepared in the presence of 17 mM NaCl according to the procedure described by Eriksson and Schatz[2]. Shear flow measurements were carried out in a parallel plate geometry with a Discovery Hybrid rheometer (DHR-2)

from TA Instruments. An optics plate accessory (OPA) with a transparent glass plate as lower plate was used in the experiments; this enabled OCT scanning (Telesto Spectral Domain, Thorlabs) of the velocity profiles in the gap. A hard anodised aluminium plate with a diameter of 20 mm (for 1.5 to 4.0 vol% NaMt samples) or 40 mm (for water and 0.1 to 1.0 vol% NaMt samples) was used as upper plate. The gap between the plates was set to 1000 µm. In the shear sweep experiments, a logarithmic flow sweep was carried out at room temperature with shear rate increasing from 1 to 1500 s^{-1}. Each shear rate was applied for a total of 35 s and the result was calculated as the average of the last 30 s. Velocity profiles were measured at one radial position close to the outer rim of the parallel plate geometry, at each single shear rate of the flow sweep, just after the initial conditioning time of 5 s.

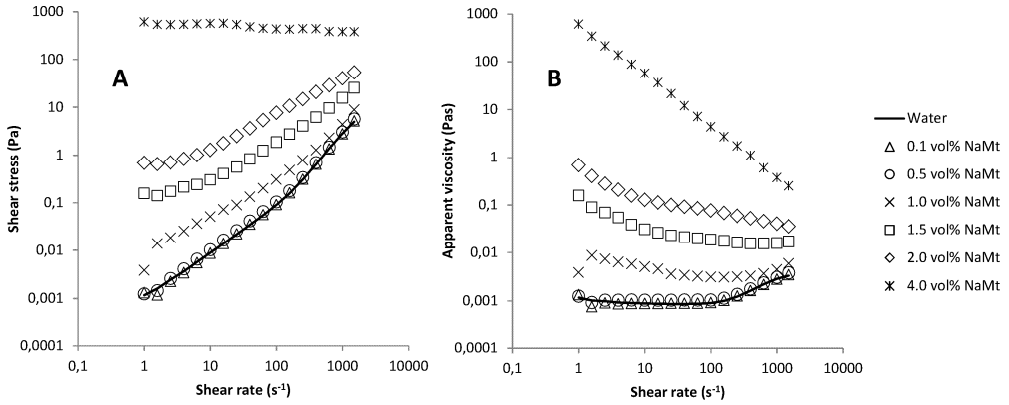

FIGURE 1 The impact of NaMt concentration (vol%) on flow properties of NaMt dispersions: A) shear stress versus shear rate and B) apparent viscosity versus shear rate.

RESULTS

The results of the shear flow measurements carried out in the rheometer are shown in Figure 1. The flow behaviour of the most dilute NaMt dispersions, up to a volume fraction of 0.5%, was comparable to that of pure water. The apparent viscosity was constant (Newtonian) up to a critical shear rate of about 100 s^{-1}, after which an increase in the viscosity curve was detected. The 1.0 vol% NaMt dispersion showed a clearly higher apparent viscosity than water and the viscosity increased gradually with further increase in NaMt concentration. The 1.0-2.0 vol% NaMt dispersions showed slightly shear-thinning. The dispersions were liquid-like (pourable) up to a volume fraction of 2.0%. At a volume fraction of 4.0%, NaMt formed a gel, which resulted

in a great increase in apparent viscosity and shear-thinning behaviour. Interestingly the shear stress slightly decreased with increasing shear rate for the 4.0 vol% sample (Figure 1A).

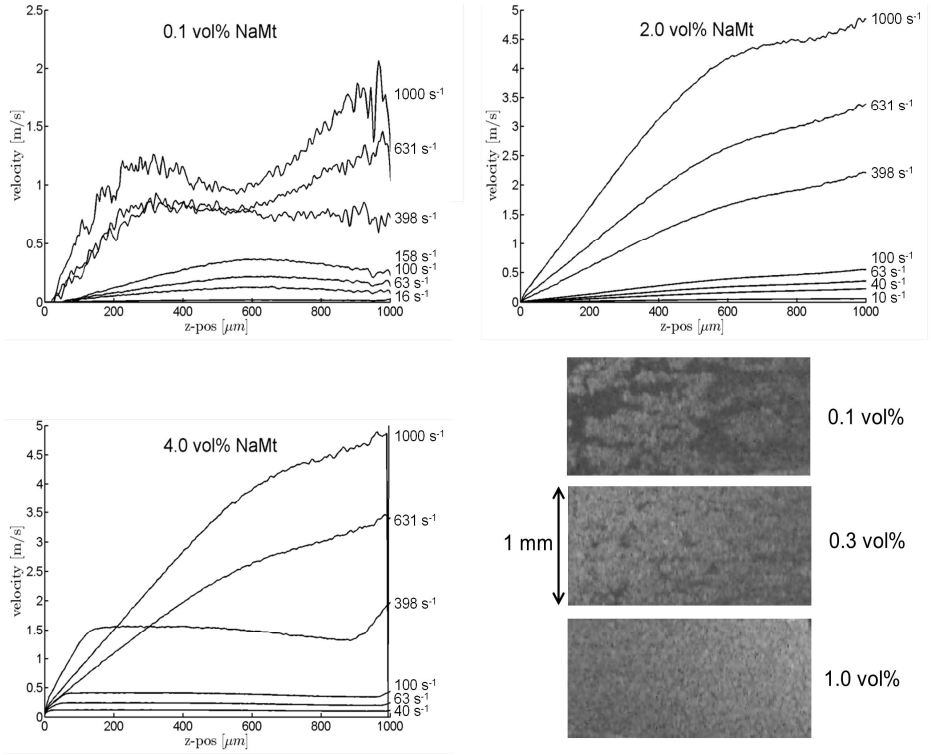

FIGURE 2 Velocity profiles measured with OCT inside the rheometer gap (1 mm) for 0.1, 2.0 and 4.0 vol% NaMt dispersions. The shear rates applied on the rheometer are shown on the right in the velocity graphs. The stationary plate was at z=0 μm and the rotating plate at z=1000 μm. Structural OCT- images (cross sections from sample edge) are shown for three different solids contents. Notice that the bending of the velocity profiles is not likely to be caused by shear banding effects – it is probably due to the decrease of the quality of the OCT beam as the distance from the OCT-probe increases.

Some examples of velocity profiles measured with OCT are shown in Figure 2. No slippage was found to take place at the plates for NaMt dispersions having a concentration of 2.0 vol% or lower. All the samples were sheared throughout the rheometer gap even at the lowest shear rate of 1 s^{-1}. The velocity profile of the 4.0 vol% NaMt sample (Figure 2) differed from that of the more dilute samples. No flow was detected at a shear rate of 10 s^{-1} or below, but the sample showed slippage at the rotating plate. At a shear rate of 40 s^{-1} the sample was sheared in narrow layers next to each plate. Increasing the shear rate widened these shearing layers until

they met inside the gap. At a shear rates of 631 s^{-1} and above, shearing took place throughout the sample. The non-ideal velocity profiles of the 4.0 vol% NaMt dispersion indicate that its flow profiles presented in Figure 1 do not reflect the true flow behaviour of the whole dispersion but are affected by wall slip and local deviations from ideal flow, which may partly originate from the elastic, gel-like nature of the material. With the most dilute NaMt dispersions (0.1 and 0.5 vol%), a sudden transition in the shape of the velocity profile was found as the shear rate was increased above 200 s^{-1}. Above this threshold, the velocity profiles exhibited fluctuations in various length scales, which were most probably caused by secondary flow vortices and/or by temporal flow instabilities. These flow instabilities may have been the cause for the increase in apparent viscosity seen in Figure 1 for the most dilute NaMt samples at highest shear rates. All liquid-like NaMt dispersions (up to 2 vol-%) showed sedimentation over time, which may have introduced some additional error to the shear flow measurements, especially for the most dilute dispersions (0.1-0.5 vol-%) which sedimented very fast. Sedimentation was markedly slower in the 1.5 and 2.0 vol-% samples.

CONCLUSIONS

Acquiring rheological data with multiphase materials, such as clay dispersions, is not always straightforward due to possible non-ideal behavior of the material in the measuring geometry. By combining the rheometer with OCT one can often overcome this problem, as direct information is then obtained both on the velocity profile and the structure of the analyzed material.

ACKNOWLEDGEMENTS

B+Tech Oy, Posiva Oy, The Academy of Finland (project ReCoF), and Euratom (BELBaR project) are acknowledged for financially supporting this work. Rasmus Eriksson and Timothy Schatz (B+Tech Oy) are acknowledged for providing the montmorillonite samples and for planning of the test matrix.

REFERENCES

1. Abend, S.; Lagaly, G., *Applied Clay Science*, 2000, *16*, 201-227
2. Eriksson, R.; Schatz, T., *Applied Clay Science*, 2015, *108*, 12-18
3. Barnes, H.A., *Journal of Non-Newtonian Fluid Mechanics*, 1995, *56*, 221-251
4. Dakhil, H.; Wierschem, A., *Applied Rheology*, 2014, *24*, 63795: 1-6
5. Haavisto, S.; Koponen, A.I.; Salmela, J., *Frontiers in Chemistry*, 2014, *2*, 27: 1-6
6. Haavisto, S.; Salmela, J.; Koponen, A., *Experiments in Fluids*, 2015, *56*, 96: 1-6

O17

Linear viscoelasticity and microstructure of bioactive gels made from crayfish protein concentrate and hydrolysates

Manuel Felix[1], Alberto Romero[1], Turid Rustad[2], Antonio Guerrero[1]

[1]Departamento de Ingeniería Química. Facultad de Química. U de Sevilla. Sevilla. Spain
[2]Department of Biotechnology, Norwegian university of science and technology (NTNU), Trondheim.
Correspondence to: Antonio Guerrero (E-mail: aguerrero@*us.es*)

ABSTRACT

The freshwater red-swamp crayfish (Procambarus Clarkii) has undergone a fast increase in population over the last decades due to favourable weather conditions, abundant food and the lack of predators. Obtaining a protein concentrate from the crayfish meat may be a useful method to benefit from the crayfish surpluses through applications such as gels with bioactive properties. The main objective of this work is to evaluate the potentials of crayfish protein concentrate (CF2L) as well as two hydrolysates obtained from this concentrate ($CF2LH_1$, $CF2LH_2$) in gel products and evaluate their bioactivity by means of their antioxidant activity.

KEYWORDS Bioactive Properties, Crayfish, Protein Gelation, SAOS, Thermal Enhancement.

INTRODUCTION

In the last few years, there has been an increasing interest in both the functional and nutritional value of by-products from the food industry that might be used in the development of food products showing benefits in the human health[2]. Antioxidant activity is regarded as one of the primary functional properties contributing to increase the quality of these by-products.

The overall objective of this is to evaluate the gelling properties and bioactive potentials of gels made from non-denatured crayfish protein concentrate and hydrolisate at two different pH values (2 and 8). To achieve these objectives, rheological measurements of aqueous protein dispersions were performed in order to follow the gelation process by means of temperature ramp tests. Protein interactions were characterized in different buffers. Finally, antioxidant activity of the gels were evaluated and expressed as Propyl Gallate (PG) equivalent units.

EXPERIMENTAL SECTION

Materials

Crayfish (CF) meat was separated from the shell by grinding and sieving. CF pulp was homogenized and subjected to centrifugation at 15,000 x g for 15 minutes, obtaining three different phases: CF1, CF2 which consists of mainly water soluble proteins, and CF3. Finally, the intermediate phase CF2 was freeze-dried, obtaining the protein concentrate CF2L.

Characterization of gelation process

Small amplitude oscillatory shear (SAOS) measurements

Dynamic viscoelasticity measurements were performed in a controlled-stress rheometer (Kinexus Ultra + from Malvern, UK). The gelation process was simulated through heating in situ in the rheometer with three different stages: (i) a temperature ramp carried out at constant heating rate (5 °C/min) from 20 °C to 90 °C; (ii) an isothermal stage, performed at 90ºC for 30 min; (iii) a cooling stage carried out at constant rate (5 °C/min) from 90 °C to 20 °C.

Protein interactions

Solubility of CF2L gels in selected solutions was measured to determine electrostatic, hydrophobic, hydrogen and disulfide interactions according to the method of Gomez-Guillen[3].

Antioxidant activity

DPPH, ABTS and Folin-Ciocalteu (FC) assays were carried out according to the procedures of Brand-Williams[4], Nenadis[4] and Singleton[5], respectively. Results were expressed as equivalent activity of the gel compared to the reference (PG).

RESULTS

Small amplitude oscillatory shear (SAOS)

Figure 1 shows the evolution of the elastic modulus (G') of the samples over the thermal cycle applied at constant protein concentration (12 wt. %) for two different pH values (2 and 8). Different thermal responses can be observed. For CF2LH1 and CF2LH2 at pH 8, three different regions can be described, basically corresponding to the three heating stages carried out. Initially (T < 45º C), a smooth decrease in G' takes place that is associated to an increase in mobility of the protein chains with increasing temperature[3]. Subsequently, all systems show a strong increase in G' as the temperature increases above 60ºC. This effect may be related to structural changes of the helical rod segments of myosin proteins. During the isothermal stage, an increase in the elastic modulus can be observed, which suggests that disulphide bonds increase during this stage. Finally, during the cooling stage, an increase in G' occurs associated to the recovery of physical interactions.

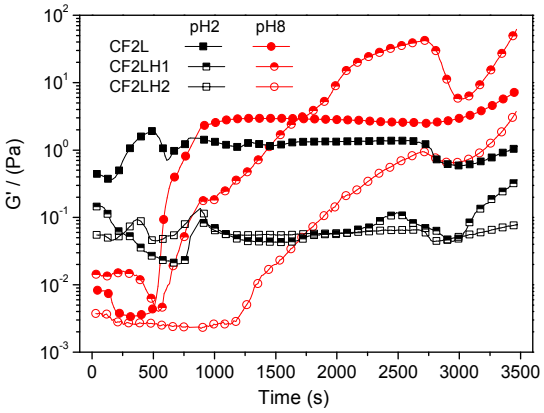

Figure 1: Storage modulus over thermal cycle of protein concentrate (CF2L) and hydrolysates (CF2LH1 and CF2LH2) dispersions at 12 wt. % at two different pH values (2 and 8).

CF2L dispersion at pH 8 does not exhibit thermal-enhancement potential during the second stage. This result indicates that all possible sulphide-bonds have been formed during the first stage.

Finally, systems at pH 2 do not show any remarkable increase in elastic modulus, neither for protein concentrate nor hydrolysates. At this pH value, proteins form a weak gel-like network.

The gel structure has been evaluated by quantifying the interactions between different protein chains present in gels at pH 2 (Figure 2A) and pH 8 (Figure 2B).

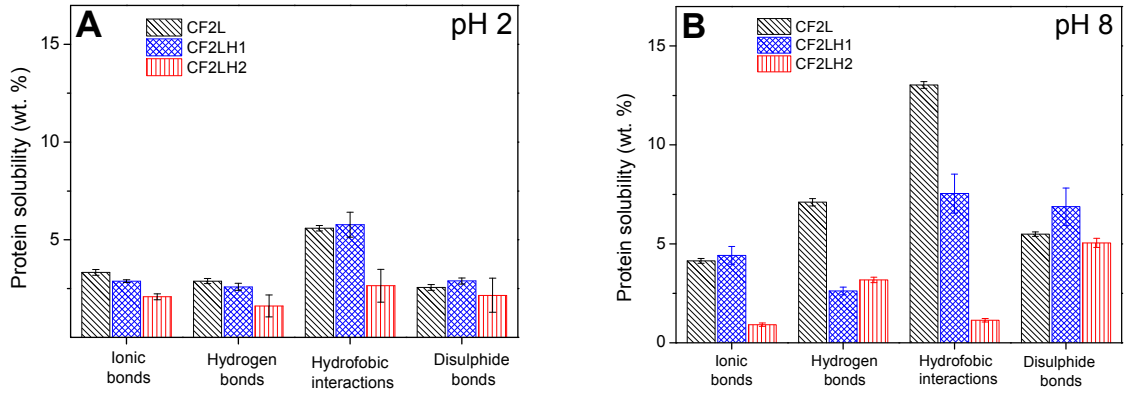

Figure 2: Physical interactions for all the systems studied A) at pH 8; B) at pH 2

Interactions depend strongly on the pH value. At acidic pH, interactions are small such that gel structures are weak, which is consistent with the moderate values obtained for G'. At alkaline pH, hydrophobic forces become the most important interactions, in spite of the fact that disulphide bonds are also noticeable, compared to pH 2. As a general rule, hydrolysis tends to reduce physical interactions, excepting for disulphide bonds that become larger for CF2LH1.

Table 1 shows the antioxidant activity of the gels formed at different pH values compared to the reference (PG), measured with three different methods: DPPH, FC and ABTS. It can be observed that the antioxidant activity is present in any case. DPPH activity is constant for all the systems. FC activity is also quite constant (with a slight increase in hydrolysates systems at pH 2), whereas the activity behind ABTS is quite pH-dependent. Thus, the ABTS activity is higher at pH 8 than at pH 2. This fact is probably related to the different effect that pH exerts on protein denaturation that seems to be more remarkable at pH2.

		DPPH (PPG mEq)	Folin (PPG mEq)	ABTS (PPG mEq)
pH 8	**CF2L pH 8**	302.1 ± 0.8	16.2 ± 0.1	5504.3 ± 17.1
	CF2LH1 pH 8	292.7 ± 0.7	16.9 ± 0.7	7504.7 ± 29.6
	CF2LH2 pH 8	302.1 ± 0.8	15.1 ± 0.3	5514.3 ± 22.1
pH 2	**CF2L pH 2**	310.8 ± 0.8	12.4 ± 0.1	466.9 ± 15.1
	CF2LH1 pH 2	314.4 ± 3.8	18.8 ± 0.1	696.3 ± 16.1
	CF2LH2 pH 2	313.9 ± 0.8	19.9 ± 0.2	547.3 ± 22.7

Table 1: Antioxidant activity by using DPPH, Folin reagent and ABTS for all studied systems.

CONCLUSIONS

Systems at pH 2 do not show any remarkable increase in elastic modulus during the gelation process, neither for the protein concentrate nor for any of the hydrolysates. As a result, a rather weak gel is formed. CF2LH1 at pH 8 is the system showing the best ability for gel formation, which is consistent with the protein interactions found from the solubility of gels in different buffers. Finally, as regards to the antioxidant activity, all systems exhibit antioxidant activity, where the most remarkable effect is the increase in antioxidant activity for ABTS at pH 8.

ACKNOWLEDGEMENTS

Authors were sponsored by Andalousian Government, (Spain) (project TEP-6134). The authors also were supported by a grant from Iceland, Liechtenstein and Norway through the EEA Financial Mechanism. Operated by Universidad Complutense de Madrid

REFERENCES AND NOTES

1- Geiger, W.; Alcorlo, P.; Baltanas, A.; Montes, C., *Biological Invasions*, **2005**, 7, 49-73.

2- Glew, R.H.; Glew, R.S.; Chuang, L.T., *Plant Foods for Human Nutrition*, **2006**, 61**,** 51-56.

3- Gomez-Guillen, M.C., Borderias, A.J.;Montero, P., *F. Scic. and Tech*, **1997**, 30, 602-608.

4- Singleton, V.L.; Orthofer, R, *Oxidants and Antioxidants*, 1999, 299, 152-178.

5- Nenadis, N., Lazaridou, O., *J. of Agr. and Food Chemistry*, **2007**, **55,**: 5452-5460.

Rheological properties and microstructure of a bitumen modified by phosphogypsum waste

Antonio Abad Cuadri, F. Javier Navarro, Moisés García-Morales, Pedro Partal

Departamento de Ingeniería Química, Centro de Investigación en Tecnología de Productos y Procesos Químicos (Pro2TecS), Campus de 'El Carmen', Universidad de Huelva, 21071, Huelva (Spain)

Correspondence to: F. Javier Navarro (frando@uhu.es)

ABSTRACT

Nowadays, a widely accepted and environmentally friendly option of reusing many waste materials is its incorporation to asphaltic pavements as a bitumen modifier[1]. Here we consider phosphogypsum that is a waste/by-product of the wet-acid process for producing phosphoric acid from phosphate rock. In this sense, the potential utilization of phosphogypsum, as a bitumen modifier for paving industry was evaluated and compared with natural gypsum. It was found that, when activated with a small quantity of sulfuric acid (0.5 wt.%), the addition of 10 wt.% phosphogypsum leads to a notable improvement in the rheological response of the resulting material, especially at high in-service temperatures[2]. Instead, poor level of modification was noticed when in such a formulation, phosphogypsum was substituted by the same concentration of commercial gypsum. This result is mainly attributed to de development of a more complex microstructure in the resulting binder as a consequence of chemical reactions involving phosphorus compounds[3].

KEYWORDS (Bitumen, waste, phosphogypsum, reactive modification, FTIR)

INTRODUCTION

Phosphogypsum (PG) is the by-product of the wet manufacturing process of phosphoric acid. PG consists mainly of calcium sulphate dehydrated ($CaSO_4 \cdot 2H_2O$ or gypsum) but also contains a high levels of impurities including fluorides, sulphates, natural radionuclides, metals, and other trace elements

PG is usually stored in huge open piles exposed to various weathering conditions in which contaminants may be carried away from the waste by rainwater, leading to serious environmental

problems. Unfortunately, the presence of impurities can negatively affect the valorization of phosphogypsum in some applications except for road construction. In this context, the aim of the present study was to evaluate the feasibility of using a phosphogypsum waste from a fertilizers factory as a modifier of bitumen for the paving industry.

EXPERIMENTAL

Bitumen (Construcciones Morales), with a penetration of 40dmm and R&B softening temperature of 52 ºC was mixed, in a low shear device, with different additives at concentrations and processing conditions shown in Table 1. Phosphogypsum (PG) sample was supplied by the Fertiberia Huelva factory (Spain), and H_2SO_4 and commercial gypsum, $CaSO_4 \cdot 2H_2O$ (CG), were supplied by Panreac, S.A. (Spain). For the sake of comparison, a reference bituminous sample containing 3 wt.% commercial SBS Kraton D1101 ("SBS-reference" sample) was also prepared.

Table 1. Nomenclature, additive concentration and processing conditions of the samples studied.

Name	Additive	[wt.%]	Proces. T (ºC)	Proces. time (min)
SBS	SBS	3	150	120
PG-150	PG	10	150	60
CG-150	CG	10	150	60
PG- H_2SO_4-150	PG H_2SO_4	10 0.5	150	60
CG- H_2SO_4-150	CG H_2SO_4	10 0.5	150	60
H_2SO_4-150	H_2SO_4	0.5	150	60

RESULTS AND DISCUSSION

The viscous flow curves, at 60 ºC (maximum expectable temperature reached in a pavement), for the binders are presented in Figure 1. All the samples present a Newtonian region, at low shear rates, followed by a shear-thinning drop beyond a threshold value of shear rate.

As shown in Figure 1, the addition of 10 wt.% PG ("PG-150") or CG ("CG-150") results in a poor viscosity increase which suggests that PG and CG act merely as a "filler" and does not interact with the bituminous matrix. However, a very remarkable increase in viscosity is noticed if 0.5 wt.% sulfuric acid is added to the PG sample ("PG-H_2SO_4-150" sample).

In order to explore the cause behind the high level of modification observed after addition of sulfuric acid to the phosphogypsum sample, the viscous flow behavior of a binder containing commercial gypsum (major component of phosphogypsum) and sulfuric acid, mixed at 150 ºC,

was also evaluated ("CG- H_2SO_4-150" sample). As can be deduced from Figure 1, the viscous response shown for this binder is similar to that of a sample of bitumen to which only 0.5 wt.% sulfuric acid was added ("H_2SO_4-150" sample). From this result, it can be deduced that some of the compounds contained in the PG fraction (not $CaSO_4$ which is about 8 wt.%) are the responsible for the viscosity increase observed, if compared to the increase due to the mere addition of sulfuric acid ("H_2SO_4-150" sample). In addition, this modification is probably due to the activation of those "modifying" compounds present in the phosphogypsum by means of sulfuric acid. This provokes a viscosity enhancement, at 60 ºC, of more than one order of magnitude if compared to the "SBS-reference" sample. This result represents by far a larger degree of modification than that corresponding to the "SBS-reference" sample.

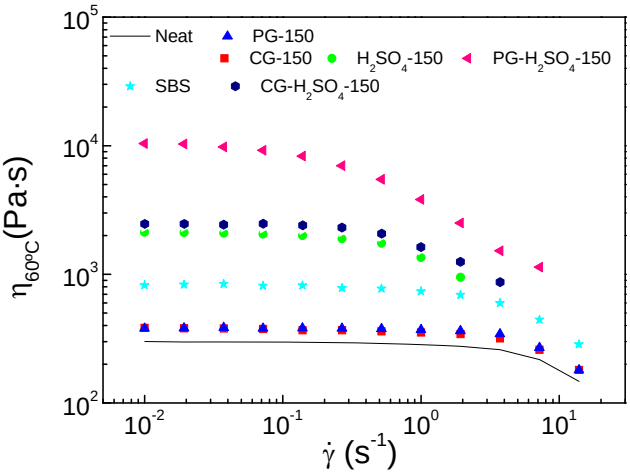

Figure 1. Viscous flow curves, at 60 ºC, for the neat bitumen and the different modified binders studied.

Moreover, FTIR spectroscopy carried out on selected samples (Figure 2) points out that only the "PG- H_2SO_4-150" sample displays a new absorption band, from 1060 to 1180 cm^{-1}, related to C−O−P vibrations [2-3], providing evidences of chemical reactions between phosphorus contained in the PG fraction and some bitumen compounds (only with the presence of small amount of sulfuric acid). This fact would explain the enhancement in the rheological behavior [2-3].

CONCLUSIONS

The addition of 10 wt.% phosphogypsum to a bitumen (activated with a small quantity of sulfuric acid) leads to a notable improvement in the rheological response of the resulting material

at high temperatures. This result is related to the existence of chemical reactions involving phosphorus and bitumen compounds.

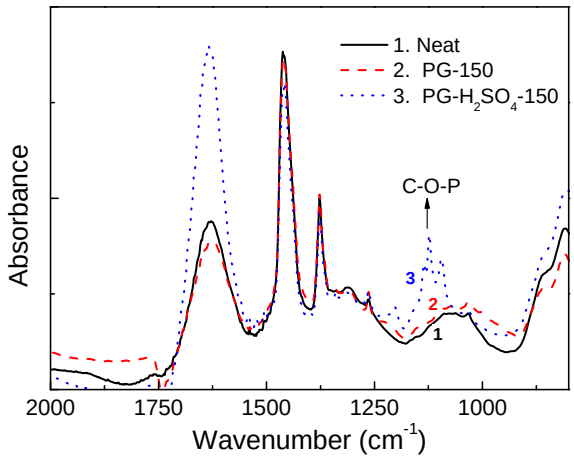

Figure 2.FTIR spectra for the neat bitumen and selected modified binders.

ACKNOWLEDGEMENTS

This work is part of a research project sponsored by a Junta de Andalucía Programme (TEP 6689). The authors gratefully acknowledge their financial support. A.A. Cuadri thanks "University of Huelva" for the concession of a postdoc research grant "*Programa de Fortalecimiento de las Capacidades en I+D+i de la Universidad de Huelva*" (2014/215).

REFERENCES AND NOTES

1. García-Morales M., Partal P., Navarro F.J., Martínez-Boza F., Gallegos C., González, N. González O., Muñoz M.E., *Fuel*, **2004**, 83, 31 – 38.

2. Cuadri A.A., Navarro F.J., García-Morales M., Bolívar J.P., *Journal of Hazardous Materials,* **2014,** 279, 11–16.

3. Masson J. F., *Energy and Fuels* 22, **2008,** 2637-2640.

O27

Evaluation of the stability of a novel w/o emulsion for topical administration using a rheological approach

Joana Marto[1], Sérgio M. C. Silva[1,2], Filipe E. Antunes[2], Luís Filipe Gouveia[1], Alberto Canelas Pais [2], Eduardo Oliveira[3], António José Almeida[1], Helena Margarida Ribeiro[1]

[1] iMed.ULisboa, Faculty of Pharmacy, University of Lisbon, Av. Professor Gama Pinto, 1649-003 Lisboa, Portugal
[2] Chemistry Department, University of Coimbra, Coimbra, Portugal
[3] Laboratórios Atral S.A., Rua da Estação 42, Vala do Carregado, 2600 – 726 Castanheira do Ribatejo, Portugal
E-mail: *jmmarto@ff.ulisboa.pt*

ABSTRACT

Pickering emulsions differ from classical emulsions because they are stabilized by solid particles. These emulsions has been widely investigated in pharmaceutical and cosmetic fields since they present less adverse effects than the classical emulsions. In this work, the rheological and mechanical behaviour was evaluated on three innovative w/o emulsions, differing only in concentration of starch (ASt) (2.5%, 5% and 7.5%). Rotational viscosity was determined using a C35 mm cone geometry, with an angle of 1º. Dynamic viscosity measurements were carried out between 1 and 1000 Pa and oscillation frequency sweep tests were performed at frequencies ranging between 0.01 and 1 Hz. A Texture Analyzer TA.XT Plus was used to examine the texture properties of the emulsions, using an analytical probe (P/10, 10 mm Delrin). It was observed that, for each formulation tested, G' increases with ASt content. This indicates that the structure of the emulsions become more robust with higher content of ASt, which assured stability during the stress tests and exhibited long-term storage stability. The hardness, compressibility and adhesiveness increased markedly for higher amounts of ASt, what contributes to increase the formulation shelf-life and skin adhesiveness. The results obtained suggest that ASt-stabilized emulsions are therefore an attractive, robust and a novel template for the production of pharmaceutical and cosmetics vehicles.

KEYWORDS Pickering emulsions; Starch; Stability; Skin application; texture analysis; rheology

INTRODUCTION

Concerning conventional topical drug delivery systems, pharmaceutical emulsions emerge as a good solution for skin drug deposition. Current pharmaceutical emulsions are mostly stabilized by synthetic surfactants, which can be intrinsically toxic or may alter the distribution and elimination of drugs [1]. Consequently, solid-stabilized emulsions, i.e. the Pickering emulsions, constitute an interesting strategy for encapsulating drugs in pharmaceutical formulations. Many types of solid particles, either organic or inorganic can be used for stabilizing Pickering

emulsions [2]. The use of starch to stabilize emulsions has been attracting substantial research interest due to their distinctive characteristics and promising technological applications. These solid-stabilized emulsions show improved stability, especially at high internal phase ratio, allowing easy fabrication of stable large droplets up to millimeter size, when compared to classical surfactant-based emulsions [3]. Additionally, Pickering emulsions can be considered either as a new dosage form for topical drug delivery or as a new targeting system in pharmaceutical and cosmetic products.

METHODS

Preparation of emulsions

A w/o emulsion stabilized by aluminium starch octenylsuccinate (ASt) was prepared using purified water as disperse phase. The continuous phase consisted of liquid paraffin (LP) and the solid particles were ASt granules at different concentrations (2.5%, 5.0% and 7.5%, w/w). The oil and aqueous phases of the emulsion were then mixed together with an UltraTurrax® T25 homogeniser (20 krpm for 5 minutes).

Dynamic viscosity - Flow curves

Shear rate vs shear stress measurements were performed at 25°C using a HAAKE MARS III Rotational Rheometer, equipped with automatic gap setting. Rotational viscosity was determined using a C35 mm cone geometry, with an angle of 1º.

Oscillation measurements

Oscillation frequency sweep tests were performed at frequencies ranging between 0.01 and 1 Hz. Prior to the oscillation tests, stress sweep tests were performed to determine the values of shear stress for which the viscoelastic functions are independent from the magnitude of the applied stress.

Texture profile analysis (TPA)

A Texture Analyzer TA.XT Plus was used to examine textural characteristics (hardness, elasticity, compressibility, adhesiveness and cohesiveness) of the emulsions. TPA mode was carried out using an analytical probe (P/10, 10 mm Delrin). Data collection and calculation were performed using the Texture Exponent 3.0.5.0 software package of the instrument.

RESULTS AND DISCUSSION

Dynamic viscosity - Flow curves

The apparent viscosity values were determined at $1s^{-1}$ (Table 1). As expected, an increase in the concentration of ASt promotes the increase in viscosity of the formulations due to the interaction between ASt particles. Since the emulsions behave as a shear-thinning fluid, they are suitable for topical administration and the apparent viscosity values provide a good comparison between formulations regarding the resistance to structural collapse.

TABLE 1 - Apparent viscosity values were obtained at a shear rate of $1s^{-1}$(mean ± SD, n=2).

ST granules (%)	Apparent Viscosity (Pa.s)
2.5	54.18±0.38
5	78.33±0.11
7.5	86.61±0.20

Oscillation measurements

The results presented in Figure 1 show the variation of the G' and G'' with shear stress. For each formulation tested, G' increases with an increase in the amount of ST. This behavior is typical of a viscoelastic liquid and indicates that the structures of the ASt-stabilized emulsions with high concentration of ASt and LP as external phase are robust [4].

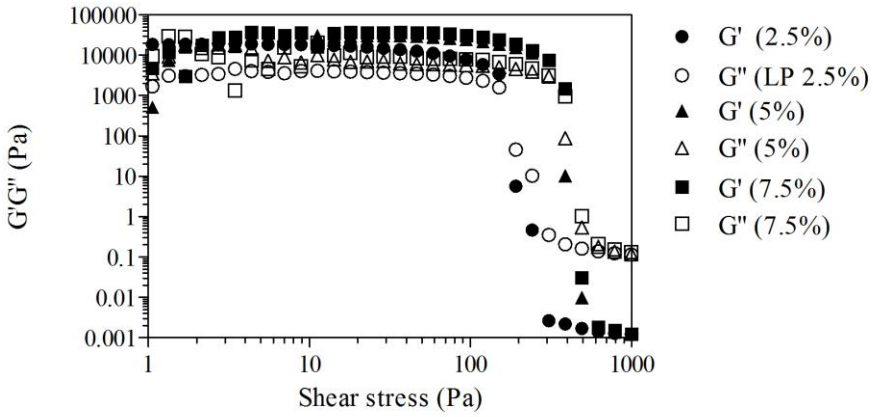

FIGURE 1 - Dependence of storage (G') and loss (G'') moduli with shear stress for ASt-stabilized emulsions.

TPA

The TPA technique is relevant and adequate for the mechanical characterization of pharmaceutical semisolid formulations, in order to determine interactions between formulation components, and a good complement the rheological information. The hardness, compressibility

and adhesiveness increased markedly for high amounts of ST, what contributes to increase the formulation shelf-life and skin adhesiveness (Table 2). Once more, the results reflect an easier application and a higher adhesion, which is suitable to the compliance and to retain the emulsions in contact with the skin.

TABLE 2 - Mechanical properties of the ASt-stabilized emulsions (mean ± SD, n=3).

ASt granules (%)	Compressibility (g.sec)	Hardness (g)	Adhesiveness (g.sec)	Elasticity	Cohesiveness
2.5	112.97±5.84	79.14±5.72	80.56±4.27	0.99±0.01	0.55±0.02
5	146.83±1.71	102.93±0.80	109.77±8.35	1.00±0.01	0.56±0.03
7.5	161.54±5.09	109.75±5.26	103.04±9.13	0.99±0.01	0.52±0.02

CONCLUSIONS

The results showed that the amount of ST influenced the rheological and mechanical properties of the Pickering emulsions, confirming a robust microstructure and suggesting that these emulsions are stable vehicles with a high potential for topical drug delivery. The selection of the ASt granules amount is an important aspect to consider in the development of this type of topical formulations.

ACKNOWLEDGEMENTS

This work was supported by FEDER, the Portuguese government (FCT; grant SFRH/BDE/51599/2011), strategic project Pest-OE/SAU/UI4013/2011 and Laboratórios Atral S.A., Portugal.

REFERENCES

1. Bouyer, E.; Mekhloufi, G.; Rosilio, V.; Grossiord, J. L.; Agnely, F., Proteins, polysaccharides, and their complexes used as stabilizers for emulsions: alternatives to synthetic surfactants in the pharmaceutical field? Int J Pharm, **2012**, 436(1-2), 359-378.

2. Chevalier, Y.; Bolzinger, M.A.; Emulsions stabilized with solid nanoparticles: Pickering emulsions. Colloids Surf., A, **2013**, 439(0), 23-34.

3. Frelichowska, J.; Bolzinger, M. A.; Pelletier, J.; Valour, J. P.; Chevalier, Y., Topical delivery of lipophilic drugs from o/w Pickering emulsions. Int J Pharm, **2009**, 371(1-2), 56-63.

4. Raposo, S., Salgado, A., Eccleston, G., Urbano, M., & Ribeiro, H. M. (2014). Cold processed oil-in-water emulsions for dermatological purpose: formulation design and structure analysis. Pharm Dev Technol, **2014**, 19(4), 417-429.

Activation energy in particle suspensions

F.J. Rubio-Hernández[1], S. Murillo-González[1], A.I. Gómez-Merino[1], N.M. Páez-Flor[2]

[1]Depto. de Física Aplicada II, Universidad de Málaga, C/Doctor Ortiz Ramos s/n, Málaga (Spain) CP 29071
[2]DECEM, Universidad de las Fuerzas Armadas, Avda. Gral. Rumiñaui s/n, Sangolquí (Ecuador) CP 170501

Correspondence to: F.J. Rubio-Hernández (E-mail: *fjrubio@uma.es*)

ABSTRACT

The viscosity of polypropylene glycol-based SiO_2 fluids at different solid concentration was studied in the temperature range 10-50°C. The viscosity increases with decreasing temperature and increasing particle concentration. Shear-thickening behaviour between two shear-thinning regions was observed. The onset of the shear-thickening displaces to higher shear rates when temperature increases and particle concentration decreases. The molar activation energy, interpreted as a measure of the potential energy barrier required for a fluid molecular movement, increases with solid concentration. Despite the presence of solid particles in a suspension improves the performance of the base liquid as heat exchange fluid, the higher viscosity temperature dependence of these fluids should be considered in technical applications.

KEYWORDS: Particle suspensions; Shear-thickening; Molar activation energy; Temperature dependence; Concentration dependence

INTRODUCTION

The mechanical and thermal properties of pure fluids can be modified by the addition of a solid phase, which must have the proper physical features to enhance appropriate characteristics or reduce undesirable behaviours[1]. The presence of solid particles in a suspension increases the distortion of the flow field when the system flows, therefore, as it is expected the viscosity of the suspension is higher than that of the pure solvent at a given temperature. For example, the dependence of the viscosity of water-based Al_2O_3 and TiO_2 suspensions with temperature and particle concentration has extensively been studied[2-11]. The main conclusion is the viscosity increases with decreasing temperature and increasing particle concentration. The presence of solid particles in a suspension improves the performance of the base liquid as heat exchange fluid[12-13]. This useful technical development for the thermal tasks in the industry has been related to the nature and size of the particles dispersed in the liquid phase[14]. However, to increase the possible technical applications of suspensions as heat transfer fluids, a more detailed study on the physical mechanisms that are in the basis of the phenomenon is necessary. In this study, the viscosity of polypropylene glycol-based SiO_2 fluids at different solid concentration was studied in the temperature range 10-50°C using a controlled stress rheometer (MARS III, Thermo-Haake).

MATERIALS AND METHODS

A commercially available hydrophobic fumed silica, Aerosil®R816 (Degussa A.G.), which is obtained from Aerosil®200 (Degussa A.G.) by means of replacing silanol (Si-OH) groups by alkyl groups ($C_{16}H_{33}$), was used as solid phase. Its specific surface area BET is ≈190±20m^2/g and its primary spherical particles size is 12nm. The continuous phase here considered is polypropylene glycol (HO-[CH_2-$CH(CH_3)$-O]*n*-H) with a molecular weight of 400g/mol (PPG400) on average (Sigma-Aldrich, Chemical GmbH, Düsseldorf, Germany). This is a low-viscosity Newtonian media having, under ambient conditions, a viscosity of 100mPa·s. The suspension with the higher solid content (20wt.%) was prepared by adding the

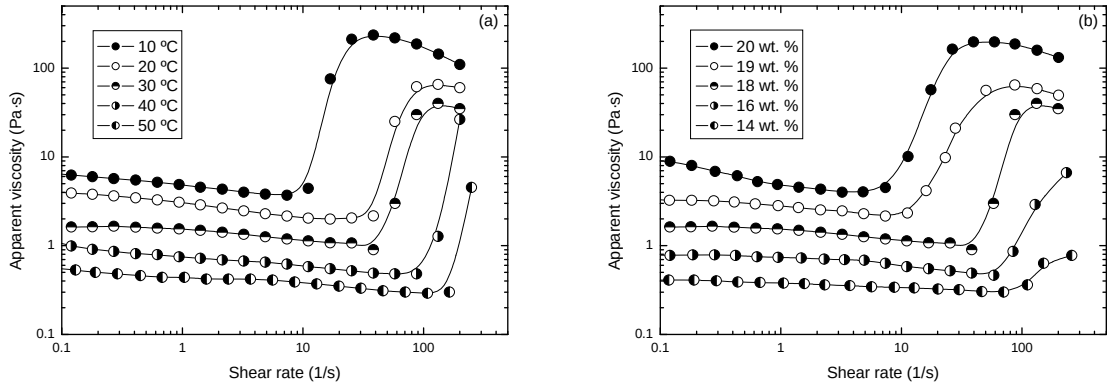

Figure 1. Influence of (a) temperature (18 wt.%) and (b) particle concentration (30 ºC) on the steady viscosity curve of R816/PPG400 suspensions.

liquid to the silica. Afterwards they were mixed in a stirrer for 10min at 796rpm. Samples were made in batches of 35cm^3 and placed under vacuum and sonication at room temperature for about 1h in order to remove air bubbles. The sample was allowed to rest for 12h in an airtight plastic bottle before starting measurements. The other suspensions (19, 18, 16 and 14 wt.%) were obtained by diluting the more concentrated suspension with the liquid phase (PPG400). Rheological experiments were carried out with a Peltier system for the control of the temperature, on a MARS III (Thermo-Haake, Germany) using a cone-plate sensor system with a cone angle of 1° and a diameter of 20mm. Experiments were conducted under steady shear.

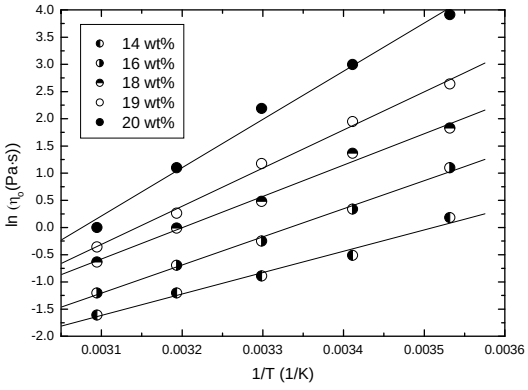

Figure 2. Temperature dependence of the zero shear viscosity of R816/PPG400 suspensions.

RESULTS AND DISCUSSION

The steady viscosity curve was obtained by applying discrete shear rates at increasing succession. Each point of the plot was obtained after shearing the sample at a certain shear rate until the equilibrium stress response was obtained. Around 60s of shear was necessary to accomplish with this condition at the lowest shear rate values. Fig. 1 shows suspensions of R816 in PPG400 exhibiting shear-thickening behaviour between two shear-thinning regions. A critical shear rate limits a weak shear-thinning region for shear rates relatively low, and a strong shear-thickening region for intermediate shear rates. This is a typical behaviour for non-flocculated suspensions[15]. Therefore, it is expected a Newtonian plateau in the limit of zero shear rate. The influence of temperature is shown in Fig. 1a. The dependence of this complex shear behaviour with the solid concentration is shown in Fig. 1b. It is confirmed the main conclusion obtained from the literature reviewed for this study, i.e. the viscosity increases with decreasing temperature and increasing particle concentration[16-17]. The other main observation is that the onset of the shear-thickening displaces to higher shear rates when temperature increases and particle concentration decreases. The increase of temperature leads to an increase of the system internal energy, resulting also in an increase in its free volume[18] and so, the intermolecular separation in solution increases and, therefore, higher shear rates are required to induce shear-thickening behaviour[19].

Table 1. Molar activation energy

Φ (wt.%)	E (kJ/mol)	r^2
14	33±3	0.9839
16	43±2	0.9949
18	48±3	0.9907
19	58±3	0.9955
20	72±4	0.9902

As it can be seen in Fig. 1a, the zero-shear rate viscosity (η_0) decreases when temperature increases. The temperature dependence of this viscosity parameter was fitted (Fig. 2) using Arrhenius equation, which is approximately valid in the temperature interval here considered,

$$\ln \eta_0 = \frac{E}{RT} - \ln C \qquad (1)$$

In this relationship C represents a system-dependent constant, E is the molar activation energy for viscous flow, T is the absolute temperature and R is the universal gas constant. The value for E is determined from the slope of the linear relationship between $\ln \eta_0$ and $1/T$, which was obtained by linear regression analysis. The molar activation energy increases with solid concentration (Table 1). This magnitude can be interpreted as a measure of the potential energy barrier required for a fluid molecular movement[18]. The viscosity of a fluid depends on the actual size of the molecules, since they may progress in the shear field as a whole. As it was shown, the presence of silica particles increases the dissipation of energy when the system flows at a given temperature. When temperature decreases the formation of larger particle aggregates in the suspension is favored due to the reduction of thermal agitation. This effect should be added to the increase of the number of links among the molecules of the liquid

phase. Therefore, a reduction of temperature must give place to two collaborative effects in the suspension viscosity. First, an increase of the viscosity because of the higher molecular links, and second, an increase of the viscosity owing to the formation of larger particle aggregates. As the solid concentration increases, the number of particles that take part in the formation of larger aggregates increases. This contribution to the temperature dependence of the viscosity is more and more dominant on the effect of the liquid phase when the solid concentration increases. The fact that the molar activation energy was larger with the increasing of solid concentration means the size of the particle aggregates must be more sensitive to temperature changes than to the number of molecule links. This is a reasonably result that can be assumed from the preliminary results of this research. However, deeper and extensive studies should be made to get conclusive statements.

CONCLUSION

Despite it has been claimed that the presence of solid particles in a suspension improves the performance of the base liquid as heat exchange fluid, the higher viscosity temperature dependence of these fluids should be considered in technical applications.

ACKNOWLEDGEMENT

NMPF expresses his gratitude to SENESCYT (Ecuador) for a pre-doctoral grant.

REFERENCES

1. SK Das, SU Choi, W Yu, T Pradeep. *Nanofluids: Science and Technology.* Wiley, New York, **2008**.
2. BC Pak, YI Cho. *Exp. Heat Transfer* **1998**, 11, 151-170.
3. Y He, Y Jin, H Chen, Y Ding, D Cang, H Lu. *Int. J. Heat Mass Transfer* **2007**, 50, 2272-2281.
4. W Duangthongsuk, S Wongwises. *Exp. Therm. Fluid. Sci.* **2009**, 33, 706-714.
5. M Silambarasan, S Manikandan, KS Rajan. **2012**, 55, 7991-8002.
6. L Fedele, L Colla, S Bobbo. *Int. J. Refrig.* **2012**, 35, 1359-1366.
7. S Bobbo, L Fedele, A Benetti, L Colla, M Fabrizio, C Pagura, S Barison. *Exp. Therm. Fluid. Sci.* **2012**, 36, 65-71.
8. T Teng, YH Hung, CS Jwo, CC Chen, LY Jeng. *Particuology* **2011**, 9, 486-491.
9. CT Nguyen, F Desgranges, G Roy, N Galanis, T Maré, S Boucher, HA Mintsa. *Int. J. Heat Mass Transfer* **2007**, 28, 1492-1506.
10. M Hosseini, S Ghader. *J. Mol. Liq.* **2010**, 153, 139-145.
11. M Jarahnejad, EB Haghighi, M Saleemi, N Nikkam, R Khodabandeh, B Palm, MS Toprak, M Muhammed. *Rheol. Acta* **2015**, 54, 411-422.
12. A Ijam, R Saidur. *Appl. Therm. Eng.* **2012**, 32, 76-82.
13. SUS Choi, ZG Zhang, W Yu, FE Lockwood, EA Grulke. *Appl. Phys. Lett.* **2001**, 79, 2252-2254.
14. M Chandrasekar, S Suresh, AC Bose. *Exp. Therm. Fluid. Sci.* **2010**, 34, 210-216.
15. SR Raghavan, HJ Walls, SA Khan. *Langmuir* **2000**, 16, 7920–7930.
16. T Tian, G Peng, W Li, J Ding, M Nakano. *Korea-Australia Rheol. J.* **2015**, 27, 17-24.
17. FJ Rubio-Hernández, AI Gómez-Merino, MH Spillman-Daniele, NM Páez-Flor. *J. Non-Newtonian Fluid Mech.* (under review).
18. B Briscoe, P Luckham, S Zhu. *J. Appl. Polym. Sci.* **1998**, 70, 419–429.
19. D Rivero, LM Gouveia, AJ Müller, AE Sáez. *Solutions* **2012**, 51, 13–20.

Miscellaneous

O31

Cell necklaces behave as a soft glassy material

José M. Franco[1], Pedro Patrício[2,3], Pedro Almeida[2,4], Raquel Portela[5], Rita G. Sobral[5] and Catarina R. Leal[2,6]

[1]*Dpt. Ingeniería Química, Facultad de Ciencias Experimentales, Universidad de Huelva, Spain*

[2]*ISEL – Instituto Superior de Engenharia de Lisboa, Instituto Politécnico de Lisboa, Portugal*

[3]*CEDOC, Faculdade de Ciências Médicas, Universidade Nova de Lisboa, Portugal*

[4]*CENIMAT/I3N, Faculdade Ciências e Tecnologia, Universidade Nova de Lisboa, Portugal*

[5]*UCIBIO@REQUIMTE, Faculdade de Ciências e Tecnologia, Universidade Nova de Lisboa, Portugal*

[6]*Centro de Investigação em Agronomia, Alimentos, Ambiente e Paisagem, LEAF, Instituto Superior de Agronomia, Universidade de Lisboa, Portugal*

Correspondence to: Catarina R. Leal (E-mail: cleal@adf.isel.pt)

ABSTRACT

Previously we have reported a complex and rich viscoelastic behavior observed during the planktonic growth of *S. aureus* strain COL[1]. In particular, in stationary shear flow, the viscosity keeps increasing during the *exponential phase* and returns close to its initial value for the *late phase* of growth, where the bacteria population stabilizes. In oscillatory flow, the elastic and viscous moduli exhibit power-law behaviors whose exponents are dependent on the bacteria growth stage. These power-law dependencies of G' and G'' match a Soft Glassy Material behavior. To describe this behavior, we have hypothesized a microscopic model considering the formation of a dynamic web-like structure, where percolation phenomena can occur, depending on growth stage and cell density. We describe the formation of these web-like structures, resembling cell necklaces at a specific time interval during bacterial growth. These findings were obtained by combining the previous data with new measurements performed in a rheometer with real-time image acquisition.

KEYWORDS Real-time image rheology, bacteria, SGM

INTRODUCTION

Complex and rich viscoelastic behavior was revealed in active bacterial *Staphylococcus aureus* cultures during growth[1]. These behaviors can be associated with cell density and aggregation patterns that are developed during culture growth, showing a collective behavior. At a given moment of the *exponential phase* of growth the shear viscosity increases steeply (~30x the initial value) and returns to close to the

initial value. This behavior has no counterpart in the bacterial growth curve obtained by optical density monitorization. In oscillatory flow, the elastic and viscous moduli exhibit power-law behaviors whose exponents are dependent on the bacteria growth stage. These power-law dependencies of G' and G'' can be described in the framework of the Soft Glassy Material[2] model. The microscopic model proposed to describe this behavior considers the formation of a dynamic web-like structure, where percolation phenomena can occur, depending on growth stage and cell density. Below we present new results obtained from rheological measurements in-line with real-time image acquisition that will show the formation of such structures during shear flow.

EXPERIMENTAL

The human pathogen *Staphylococcus aureus* was used as a study model due to its coccoid shape, regular morphology and clinical relevance: methicillin-resistant *Staphylococcus aureus* (MRSA) strain COL[3] was chosen. Bacterial growth and rheological measurements are described in detail elsewhere[1].

Real-time image acquisition was performed during steady-state shear flow measurements in a Haake RheoScope equipment, which combines the principles of a conventional controlled-stress rheometer with an optical microscope. A constant shear rate of 10 s^{-1} was imposed using a cone-plate geometry with 70mm diameter and 1° and a gap of 25μm, at 37 °C. The cone had a mirror surface and the plate a cover glass, to allow optical microscopic observations (20x) during shear (schematic details are enclosed in Fig. 2), at an intermediate radius plate fixed position. Video image acquisition was performed during 150 min. A photo image was selected from the video at each minute. In these tests, the growth of a *S. aureus* culture was followed starting measurements already at the *exponential phase* (approximately at an OD_{600nm}=2.5).

THEORY

Based on the Soft Glassy Material[2] (SGM) model, the elastic and the viscous moduli present the same weak power law dependence on the angular frequency, as given by eqs. (1) and (2).

$$G' \sim \omega^x \quad and \quad G'' \sim \omega^x \tag{1}$$

$$G''/G' \sim tan\ \pi x/2 \tag{2}$$

where the exponent x is an effective noise-temperature factor, taking values in the range $0<x<1$. When x=0 one obtains the ideal solid, perfect elastic body; when x=1 one obtains the ideal liquid, perfect viscous fluid system; when $0<x<1$ the system has an intermediate behavior.

RESULTS AND DISCUSSION

The viscosity growth curve and the oscillatory measurements were reported previously[1]. In Table 1, the angular frequency exponent values of G' and G'' are compared with the SGM model predictions. A good agreement between experimental measurements and theory is obtained.

In Figure 1 the steady-state shear viscosity growth curve of a *S. aureus* culture, measured at a constant shear rate of 10 s^{-1} is represented in relative values. An increase of ~40x the initial viscosity value was observed and the recovery to the initial one occurred in approximately 50 min. These results reproduce the essential features already observed[1] in a different experimental set-up (equipment and geometry).

TABLE 1 Growth-time dependency of the angular frequency exponent, x, experimental and theoretical SGM predictions

Growth stage	time (min)	x	$tan\ \pi x/2$	G''/G'
lag phase	250	~0.80	3.1	~2.4
exponential phase	350	~0.79	2.9	~2.2
	475	~0.23	0.4	~0.6
late phase	550	~0.39	0.8	~0.9

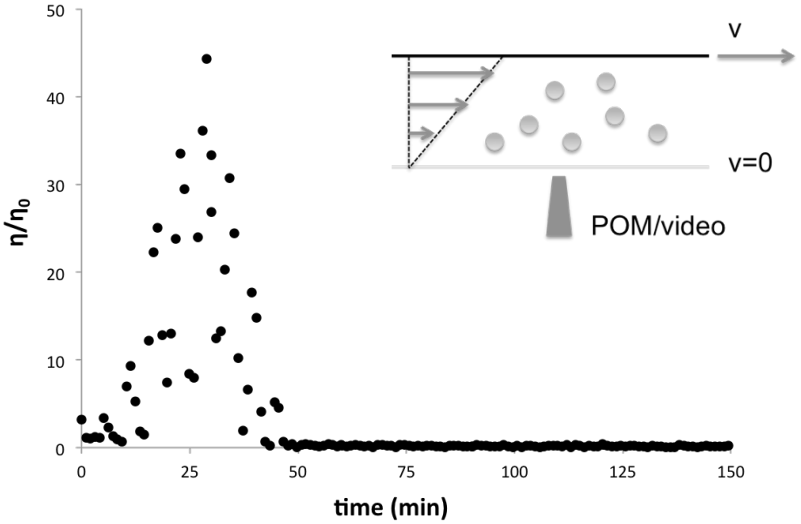

FIGURE 1 Relative steady-state shear viscosity growth curve of a *S. aureus* culture, measured at a constant shear rate of 10 s^{-1}; measurements were started with a culture already at the *exponential phase* of growth; inset: schematic details on the image acquisition set-up at an intermediate radius-plate position. Measurements were performed at 37°C.

During this measurement a video was recorded and images were taken at specific/representative times, which are included in Figure 2. It can be clearly observed the formation of a web-like structure in the time interval 17 – 28 min: the bacteria present a dynamic self-organization where wave rows are formed, with dozens of cells, resembling cell necklaces. This structure can only be maintained during the *exponential phase* and starts to collapse as the bacteria culture approaches the *lag phase*, see image for 38min. For longer times, a cell deposition process is initiated and small aggregates sediment, as dark regions in images at 75 min and 125 min (more and bigger aggregates formed). This explains the viscosity decrease in the *lag phase* of growth, although the number of cells present in the culture is high they are no longer suspended in the culture medium.

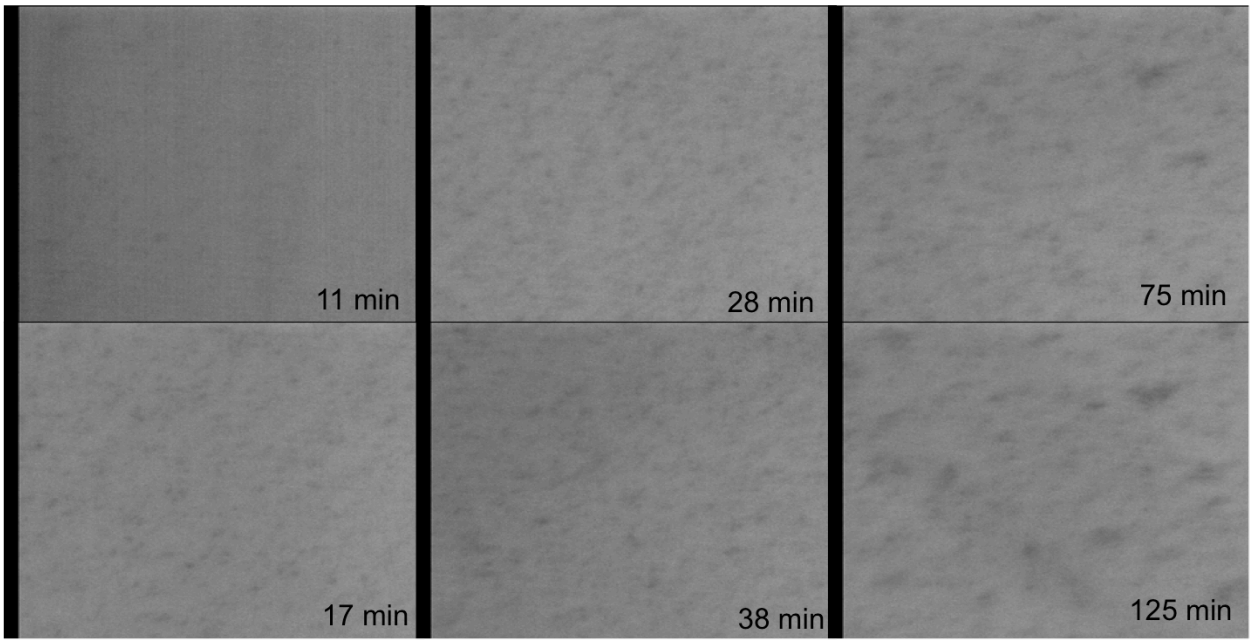

FIGURE 2 Real-time images obtained during steady-state viscosity growth curve measurements of a *S. aureus* culture, with correspondent times to η/η_o curve represented in Figure 1; in images collected at 11, 17 and 38 min, percolated structures can be observed; in images collected at 75 and 125 min cell aggregates are observed (dark areas), which correspond to cell deposition in the fixed bottom glass-plate of the RheoScope. Images width: 100 µm.

CONCLUSIONS

We have observed the formation of web-like structures, resembling cell necklaces at a specific time interval during the *exponential phase* of the bacteria growth, followed by, during the *stationary phase,* the sedimentation and subsequent enlargement of bacterial aggregates. These findings were essential to corroborate our microscopic model previously proposed[1].

ACKNOWLEDGEMENTS

Strain COL was a kind gift from H. de Lencastre. We acknowledge the support from FCT (Portugal) through Grant No. PEst-C/CTM/LA0025/2011 (CENIMAT/I3N), UID/Multi/04378/2013 (UCIBIO) and through Project PTDC/BIA/MIC/3195/2012 (awarded to RGS).

REFERENCES AND NOTES

1. R. Portela, P. L. Almeida, P. Patrício, T. Cidade, R. G. Sobral and C. R. Leal, Real-time rheology of actively growing bacteria, *Physical Review E*, **2013**, 87, 030701(R).
2. P. Sollich, F. Lequeux, P. Hebraud, and M. E. Cates, *Phys. Rev. Lett*., **1997**, 78, 2020.
3. S. R. Gill et. al., *J. Bacteriol*., **2005**, 187, 2426-38.

Poster Presentations

Applications: Food

P1

Effect of pressure treatment on the rheological properties of aqueous glucomannan dispersions at low deacetylation degree

Clara. A. Tovar[1],Verónica Bargiela[1], Beatriz Herranz[2], A.Javier Borderías[2]

1 Departamento de Física Aplicada, Facultad de Ciencias de Ourense. As Lagoas, 32004 Ourense, (Spain).

2 Departamento de Productos, Instituto de Ciencia y Tecnología de los Alimentos y Nutrición (CSIC), José Antonio Novais, 28040 Madrid, (Spain).

Clara A. Tovar (tovar@uvigo.es)

ABSTRACT

This study reports an analysis of the effect of different rates of high hydrostatic pressure (HHP) on the viscoelastic properties of a 3% aqueous glucomannan dispersion (AGD). Glucomannan (GM) was weakly deacetylated (pH=9.8). The samples analysed were: *A0* (0 MPa), *A1* (100 MPa), *A2* (200 MPa), *A4* (400MPa) and *A6* (600MPa). All samples were weak viscoelastic gels with storage (*G'*) and viscous (*G''*) moduli low and strongly frequency-dependent. There were significant differences in stress (σ_{max}) and strain (γ_{max}) amplitudes modulated by the oscillation frequency. The influence of HHP on σ_{max} and γ_{max} was also strongly frequency-dependent. Mechanical spectra showed the critical transition-point (gel-sol), whose crossover frequency increased slightly with HHP, suggesting that HHP partially weakened the physical cross-links in AGDs reducing the cross-link density in GM network. In summary, HHP weakened the gel network slightly as compared with control sample, particularly at 200-600 MPa. All measurements were made at 25°C.

KEYWORDS glucomannan high pressure viscoelastic properties

INTRODUCTION

Konjac glucomannan (GM), a polysaccharide derived from the tuber of Amorphophallus konjac C. Koch, can be used to improve food protein functionality, namely in surimi type products. Eliminating acetyl groups produces deacetylated GM after addition of 0.6N KOH as an alkaline agent[1]. The importance of GM gels lies in their ability to extensively modify the rheology of aqueous media to which they are added, even at fairly low concentrations, and that is the basis of their functional properties as thickening and gelling agents. Previous papers explored the influence of thermal conditions[2] on the rheological and structural characteristics of aqueous GM dispersions (AGD). It may therefore be useful to analyse how the pressure affects the dynamic

behaviour of GM molecules in AGD dispersions, since pressure has a broad range of applications in the food industry. Other previous research has analysed the influence of the deacetylation ratio on the structural and rheological properties of AGDs with a 3% GM concentration[3]. The physical networks behaved in either of two different ways depending on the pH, in terms of the phase transition (sol to gel) between pH ≤9 and pH≥10 when samples were true gels according to the deacetylation ratio. The aim of this work was thus to explore the influence of HP on viscoelastic properties of AGD dispersions with a 3% GM concentration at an intermediate pH (9.8) which produces a low deacetylation ratio near the point of gelation, to choose the most suitable pressure conditions for making restructured seafood products.

EXPERIMENTAL METHODS

AGD dispersions (3%) (w/v) from konjac GM were prepared as was reported by Herranz et al., 2012[1]. AGDs were subjected to 0 (lot control A0), 100 (lot A1), 200 (lot A2), 400 (lot A4) and 600MPa (lot A6), for 10 min at 25ºC. Small amplitude oscillatory shear (SAOS) were gathered as Herranz et al., 2012 reported. The temperature was kept at 25.0±0.1 ºC.

RESULTS AND DISCUSSION

Stress sweeps

An initial study showed that AGD with a 3% GM concentration and pH=9.8 had produced soft viscoelastic materials. For that reason the linear viscoelastic (LVE) range was reached at two frequencies, 0.05 and 1Hz, to determine the change in the limit magnitudes of the LVE range as stress (σ_{max}) and strain (γ_{max}) amplitudes, with frequency at several HP levels. At low frequency (0.05 Hz), σ_{max} significantly ($p<0.05$) increased with pressure in the lower HP range (100-200 MPa) and remained constant between 400 and 600 MPa comparing with control (Figure 1). Conversely, at the higher frequency (1Hz) σ_{max} increased strongly with increasing HP from 100 to 400-600 MPa, but σ_{max} at 100-200 MPa was significantly lower than in the control (Figure 1). These results showed the strong effect of frequency in the stress amplitude of AGDs, evidencing their transient nature[3]. The γ_{max} values were significantly ($p<0.05$) greater at low (0.05 Hz) than at high frequency (1 Hz), but there was no definite trend with increasing HP (data not shown).

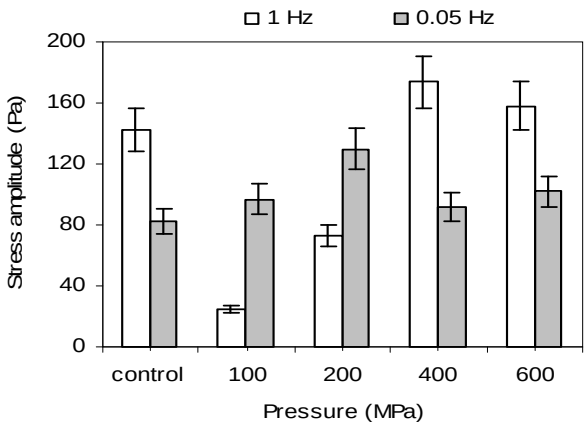

FIGURE 1 Effect of HP on the stress amplitudes of AGD dispersions in the LVE range at two frequencies. T= 25 °C.

These results were consistent with the higher phase angles (δ) at 0.05 Hz, in particular δ values at 0.05 Hz were greater than 45° irrespective of HP (Figure 2), indicating the behaviour of a viscoelastic fluid. Thus, AGD dispersions had a larger percentage of energy loss during oscillation at 0.05 Hz, so that at pH=9.8 and 3% GM concentration the deacetylation ratio was ~32%[3]. This could be important in that it may produce GM-chain disentanglements resulting in a fluid-like material[4].

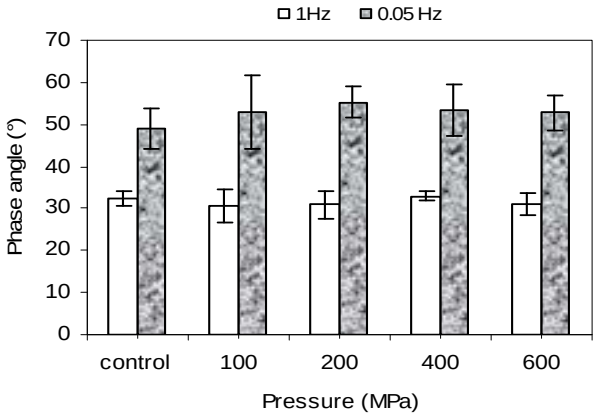

FIGURE 2 Effect of HP on the phase angle of AGDs in the LVE range at two frequencies. T= 25 °C.

Frequency sweeps

Mechanical spectra varied depending on the frequency range selected. In a higher frequency range (0.2-10 Hz), *G'* was somewhat greater than *G''* indicating solid-like behaviour (Figure 3). Conversely, at a lower frequency interval (0.01-0.1 Hz) *G''* was greater than *G'*, showing typical liquid-like behaviour. The gel-sol transition was registered between 0.06 and 0.1 Hz (crossover interval) where *G'*≈*G''*. Pressure (100-600MPa) slightly increased the crossover frequency as

compared with A0 (data not shown), suggesting that HP partially weakened the physical cross-links in AGDs. Thus, the viscoelastic response from frequency sweeps clearly showed the primacy of the temporal (frequency) over the mechanical (pressure) effect, indicating that at a GM deacetylation ratio of 32%[3], HP can induce new rearrangements in AGDs, producing a minor rupturing of hydrogen bonds, ionic and dipolar interactions and thus reducing the firmness of samples.

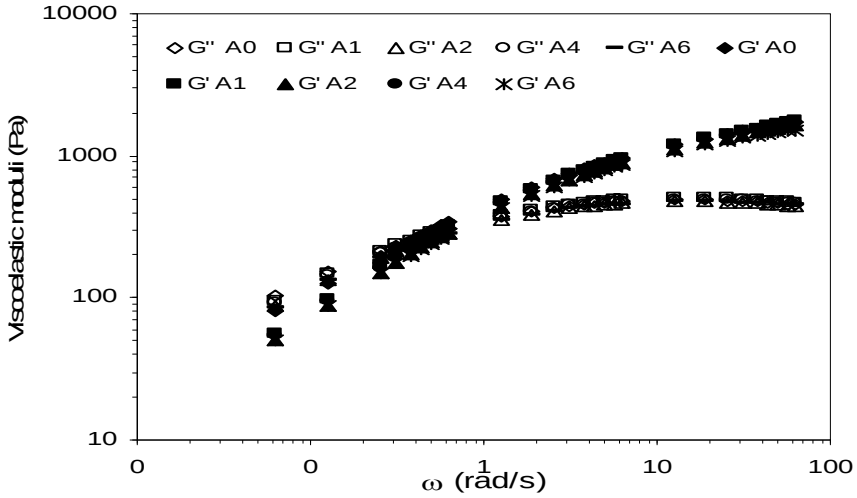

FIGURE 3 Influence of high pressure on mechanical spectra of the AGDs at T=25°C.

CONCLUSIONS

The effect of high-pressure treatment on the viscoelastic properties of 3% aqueous glucomannan dispersions at pH=9.8 was weak. Samples were strongly time-dependent. Mechanical spectra were practically pressure- independent, showing that at pH=9.8 there was phase transition from gel to sol when frequency diminished. The crossover frequency interval was near 0.1Hz and shifted slightly to higher frequencies at greater pressures**.**

REFERENCES

1. Herranz, B.; Tovar, C.A.; Solo-de-Zaldívar, B.; Borderias, A.J., Food Hydrocolloids, **2012a**, 27, 145-153.

2. Herranz, B.; Borderias, A.J.; Solo-de-Zaldívar, B.; Solas, M.T.; Tovar, C.A., Food Hydrocolloids, **2012 b**, 29, 85-92.

3. Solo-de-Zaldivar, B.; Tovar, C.A.; Borderías, A.J.; Herranz, B., Food Hydrocolloids, **2014**, 35, 59-68.

4. V dit, S. In Physical Networks Polymers and Gels. London Burchard, W.; Ross-Murphy,S.B., Eds.; Elsevier applied Science, **1990**; Chapter 10, pp 125-132.

P2

Influence of frozen storage on the viscoelasticity of suwari gels made with pressurized flying fish (Parexocoetus brachyterus) surimi

Verónica Bargiela,[1] Helena M. Moreno[2], Beatriz Herranz[2] , Javier Borderías[2], Clara A. Tovar[1]

1 Departamento de Física Aplicada, Facultad de Ciencias de Ourense. As Lagoas, 32004 Ourense, (Spain).

2 Departamento de Productos, Instituto de Ciencia y Tecnología de los Alimentos y Nutrición (CSIC), José Antonio Novais, 28040 Madrid, (Spain).

Clara A. Tovar (tovar@uvigo.es)

ABSTRACT

The effect of frozen storage on the viscoelastic properties of five lots of suwari gels (SG) made using flying fish surimi (FFS) has been analysed. FFS had been subjected to low-intensity pressures (0 control-*C*), 40 (*A*), 80 (*B*), 125 (*D*) and 200MPa (*E*) at -15°C/10min. Viscoelastic properties of SG (5°C/24h) were determined after 5 months of frozen storage at -20°C and compared with unfrozen gels. After frozen storage the trend of stress (σ_{max}) and strain (γ_{max}) amplitudes remained the same with pressure as with the unfrozen suwari gels, except in sample *D*; in this case σ_{max} was significantly larger after frozen storage, evidencing the increase of the structural stabilization. Mechanical spectra showed that frozen storage reduced the values of storage (*G'*) and viscous (*G''*) moduli, except in sample D, where *G'* and *G''* increased with respect to t=0. A new viscoelastic parameter was proposed based on *G'* and *G''* data: the fraction of ideal network (f_{in}). Naturally, in C sample f_{in} was lower after frozen storage, but in the pressurized gels, frozen storage produced some structural improvement (high f_{in}), particularly in samples *D* (125 MPa) and *E* (200 MPa).

KEYWORDS flying, fish, frozen, suwari, gel

INTRODUCTION

The surimi industry is constantly changing, so new resources have to be found for use as species with lower-quality protein such as flying fish (*Parexocoetus brachyterus*), to process surimi-based products with suitable gel properties. One possible alternative to improve the gel forming ability is hydrostatic high pressure (HHP)[1]. When surimi is subjected to low temperatures (0 to 40 °C), the resulting suwari gel (SG) is soft, elastic and deformable[2]. Moreno et al., 2015 reported that low-intensity HHP was more suitable for improving the gelling ability of proteins in frozen flying fish surimi (FFS). The aim of the present study was to analyse how the

application of HHP to frozen FFS preserves the protein functionality in suwari gels after 5 months of frozen storage at -20°C.

EXPERIMENTAL METHODS

SGs were made as Moreno et al., 2015 reported. The HHP treatments were: 0, 40, 80, 125 and 200MPa for 10 min at -15±3 ºC by Stansted Fluid Power CTD, FPG 7100:-2C. SGs were called: A (40MPa), B (80MPa), D (125MPa) and E (200MPa), along with a control sample (C) made with unpressurized frozen FFS. SGs were frozen at -20°C in a blast-freezer and stored for 5 months. Frozen gels were called FA (40), FB (80), FD (125) and FE (200). The viscoelastic parameters were obtained following the method reported by Moreno et al., 2015.

RESULTS AND DISCUSSION

Linear viscoelastic (LVE) range

Stress sweeps were used to determine the stress (σ_{max}) and strain (γ_{max}) amplitudes in the linear viscoelastic (LVE) range for SGs before[3] and after frozen storage. σ_{max} and γ_{max} maintained the same trend as in fresh gels with increasing HHP (data not shown). Gel stiffness (G^*) decreased slightly in FC comparing with C, the same trend was observed in FA vs A and FB vs B. However, in E gels G^* was significantly higher in FE vs E (Figure 1). Thus, frozen storage enhanced the rigidity of SGs with pressurized FFS at 200MPa, and consequently the loss of firmness undergone by fresh suwari gels with increasing HHP was reduced in FE (Figure 1).

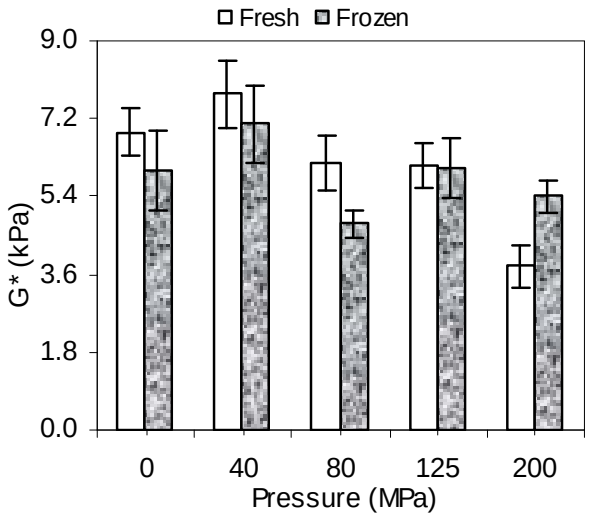

FIGURE 1 Complex modulus after 5 months of frozen storage for Suwari gels made with pressurized-frozen FFS ν=1Hz,T=25°C. G* of fresh suwari gels were reproduced from [3].

Frequency sweeps

A new viscoelastic parameter derived from mechanical spectra was proposed to determine whether a SG network was ideal and how it evolved with the oscillation frequency. A SG network is a soft structure stabilized by covalent (non-disulphide) bonds forming non-ideal structures[4]. It is possible to determine the ratio of stored energy (*G'*) to total (stored-*G'* and dissipated-*G''*) energy to derive the ideal-network fraction (f_{in}), by means of equation 1.

$$f_{in} = \frac{G'}{G'+G''} \quad (1)$$

Figure 2 compares mechanical spectra of fresh (A-E) with frozen (FA-FE) SGs in terms of f_{in} vs angular frequency (ω). The structural damage (frozen storage) was evidenced in FC gel as compared with C gel. Thus, f_{in} values decreased with decreasing frequency (Figure 2).

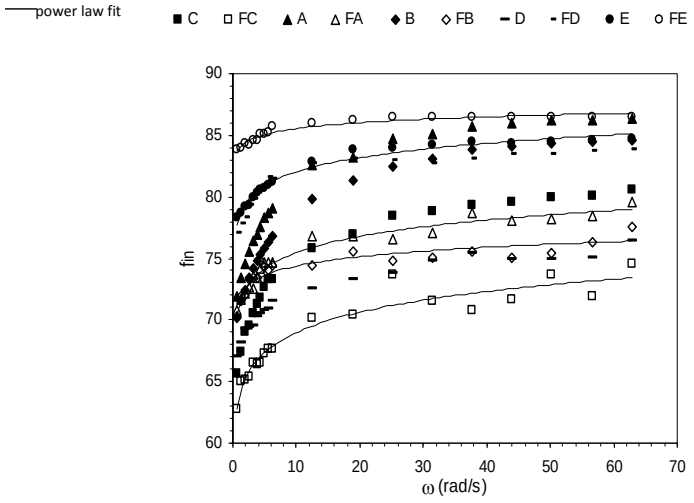

FIGURE 2 Influence on ideal-network fraction of 5 months of frozen storage of suwari gels made with pressurized-frozen FFS, T=25°C.

The same trend of f_{in} vs ω was observed in less pressurized samples (FA vs A and FB vs B) (Figure 2). However in D and E samples pressure produced some viscoelastic benefit, since after frozen storage FD and FE gels exhibited greater values of f_{in} with less frequency dependence than D and E respectively (Figure 2).

thermal gelation profiles of suwari gels

The thermal gelation profiles for control (C) and pressurized samples (A, B, D and E) are shown in terms of changes of f_{in} with T. The influence of the HHP treatment was evident in A and E, in which f_{in} was higher and lower respectively than C (Figure 3a). At 35<T<50°C, f_{in} rapidly

increased due to the unfolding of myofibrillar protein in the suwari gels, promoting intermolecular interaction among hydrophobic fragments[2] to form a three-dimensional gel network (end of first stage of gelation). The subsequent increase of f_{in} (T>50°C) is the second age of gelation, which involves actin denaturation as part of the gel strengthening stage[2]. The principal difference in thermal profiles of frozen gels was the practical disappearance of the second stage of thermal gelation. Thus, at T> 50°C, f_{in} remained practically constant up to 90 °C (Figure 3b). This could be a consequence of structural damage in the protein network caused by freezing and frozen storage, since myofibrillar proteins were partially denatured and aggregated, principally by non-covalent interactions[2]. The benefit produced by HHP was reflected by the fact that values of f_{in} were higher in pressurized samples than in the control at higher T (Figure 3b).

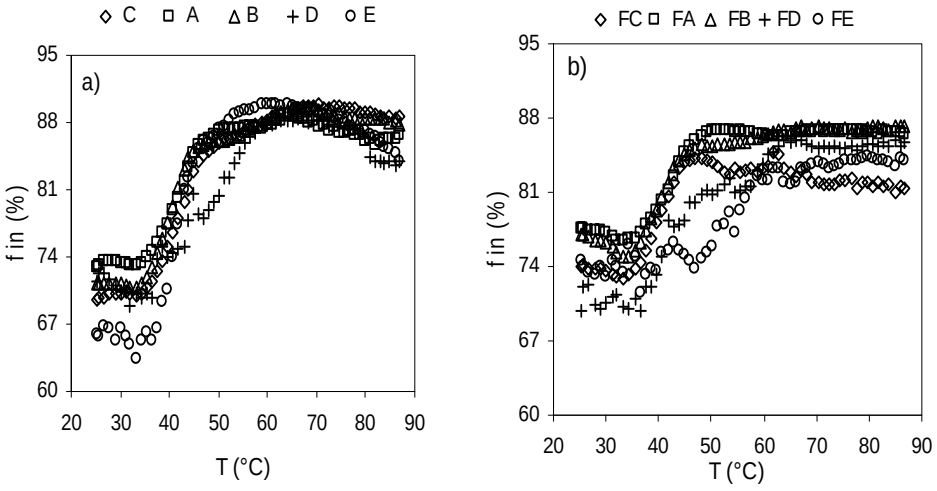

FIGURE 3 Influence of frozen storage of suwari gels on their thermal gelation profiles ν=0.1Hz, 1°C/min.

CONCLUSIONS

125 and 200MPa produced viscoelastic benefit in frozen suwari gels enhancing the fractions of ideal network and giving more time stable structures in gel networks.

REFERENCES

1. Herranz, B.; Tovar, C.A.; Borderias, A.J.; Moreno, H.M., *Innovative Food Science and Emerging Technologies,* **2012***,* 20, 24-33.
2. Park, J.W., Surimi and Surimi Seafood, Marcel Dekker, Inc. New York, **2005**.
3. Moreno, H.M.; Bargiela, V.; Tovar, C.A.; Cando, D.; Borderias A.J.; Herranz, B., *Food Hydrocolloids,* **2015,** 48, 127-134.
4. Nijenhuis, K., Thermoreversible Networks. Viscoelastic Properties and Structure of Gels, Advances in Polymer Sciences, Springer, Berlin, **1997.**

P3

Thermo-rheological properties of chickpea flour gels

María Dolores Torres Pérez[1]

[1]Department of Chemical Engineering, University of Santiago de Compostela, Lope Gómez de Marzoa St., Santiago de Compostela E-15782, Spain

Correspondence to: M.D. Torres (E-mail: *mariadolores.torres.perez@usc.es*)

ABSTRACT

Gels are well known as a basis for food puddings or sweet desserts in gluten-free products, an actual rising market at surprising rates. In this context, the subsequent gel research focuses on an alternative gluten-free flour. The main objective was to perform a systematic investigation of the thermo-mechanical characteristics of chickpea flour (CpF). A parallel objective was to determine the physicochemical properties of studied gluten-free flours. The evolution of the structure of these systems was monitored by rheological testing at small-amplitude-oscillatory-shear (SAOS) using a stress-controlled rheometer. Texture properties of the final gels were determined from the texture profile analysis. Relevant physicochemical characteristics of the flour were also determined using standard methods commonly employed in these flours. Rheological results indicated that thermal profiles on heating of CpF gels were similar to those reported for other gluten-free flours. Overall, all systems showed stable and strong gel characteristics, however gels from CpF at 40% present larger stability.

KEYWORDS chickpea flour, gluten-free, gels, viscoelasticity, texture

INTRODUCTION

As celiac disease is becoming more common nowadays the consumers' demand for gluten-free foodstuffs with high nutritional and taste quality is considerably increasing. However, the employed formulations available on the market show low technological and nutritional quality, particularly compared to their wheat counterparts[1]. One possibility with a great potential to improve the quality of available products could be the chickpea flour (CpF) and its starch[2].

Despite its healthy properties, there are scarce literature concerning the rheological properties of these systems. The challenge is to understand how the gluten-free flours behave under food processing conditions since the final structure and texture properties are strongly dependent on processing temperature/time, cooling rates, flour composition and its content. During gel formation, these factors affect the dynamic process of competition between phase separation and gel formation.

The main aim of this study is to perform a systematic investigation of the thermo-rheological and textural properties of chickpea flour. A parallel objective was to determine the physicochemical properties of studied gluten-free flours. The evolution of the structure of these systems was monitored by rheological testing at small-amplitude-oscillatory-shear (SAOS) using a stress-controlled rheometer. Texture properties of the final gels were determined from the texture profile analysis (TPA). Preliminary physicochemical properties of the CpF were also determined.

MATERIAL AND METHODS

Samples preparation

Chickpea (*Cicer arietinum*) materials were purchased in a local market (Galicia, Spain). These materials were grinded to obtain the corresponding chickpea flour, CpF. Gels were prepared using CpF at several concentrations (10, 20, 30, 40, 50, 60, 70, 80, 90% w/w). The flour was dispersed in demineralised water by stirring at 800 rpm for 10 min at room temperature. To prepare the gels, suspensions were heated up to 90ºC and kept at this temperature for 30 min. After, samples were placed in a fridge to allow full maturation of gels, which were kept at 5ºC for 24h before performing colour and texture tests.

Methods

Standard sieves (750, 350, 75 µm) of 200 mm diameter were employed to determine the average particle size (D_w) of tested flour. The sieving procedure was carried out according to ASAE Standards[3]. Initial moisture, fat, dietary fibre, protein and carbohydrate content were determined according to AOAC methods. The assays were made in triplicate.

Colour tests were performed using a Chroma Meter CR-400 (Minolta Co., Japan). Colour parameters (L*, a* and b*) were assessed by CIELAB, where L* is the lightness and a* and b* are chromaticity responsible parameters. At least ten measures were carried out for each sample.

Firmness (N) was determined from the texture profile analysis (TPA) using a TA-XT2i (Stable Micro Systems, UK) texturometer (load cell of 5 kg). Before performing any measurements, gels were allowed to equilibrate at 20 ºC for around 1 h in a temperature-controlled room.

Rheology was performed at least in duplicate on a controlled-stress rheometer using serrated parallel plates (35 mm diameter and 0.5 mm gap). Flour suspensions were held at 20ºC between the plates for 10 min before testing. After, samples were heated to 90ºC at 2ºC/min. Then, time sweeps were conducted at 90ºC for 60 min at 0.1 Hz. After, samples were cooled down to 5ºC at 1 ºC/min. Temperature sweeps were performed at 0.1 Hz. A constant stress (2 Pa) within the linear viscoelastic region (LVR) was used in above tests. After cooling, time sweeps were conducted at 5 ºC, during 60 min at 1 Hz. Without disturbing the gel, frequency sweeps were made at 20ºC, with oscillation frequencies over the range 0.01 to 100 rad/s. A constant stress (30 Pa) within the LVR of gels was used in the two latter tests.

All experimental data were analysed by one-factor analysis of variance followed by Scheffe test to differentiate means with 95% confidence ($p < 0.05$) using PASW Statistics (v.18, NY, USA).

RESULTS AND DISCUSSION

The studied chickpea flour presented an average composition (% w/w) of 8.3 moisture content, 16.3 protein, 4.1 lipids, 9.2 fibre and 62.1 carbohydrates, and of the total grain carbohydrates, 45.9 is starch. These values are consistent with those reported for other chickpea materials[2]. The average particle size determined for the studied flour was 71.5 μm.

Texture studies suggested that gels from chickpea flour at 40% gathered the right texture to develop new savoury gluten-free gelled products, with subsequent multiple advantages from the nutritional point of view. These results are in harmony with those reported for other gluten-free flours with similar chemical composition[1]. Rheological results indicated that the thermal profiles on heating of chickpea flour gels were similar to those obtained for other gluten-free flours. Although all systems showed stable and strong gel characteristics, rheological tests suggested

that gels from chickpea flour at 40% present an industrial advantage over the other concentrations, since the stability is larger (Fig. 1).

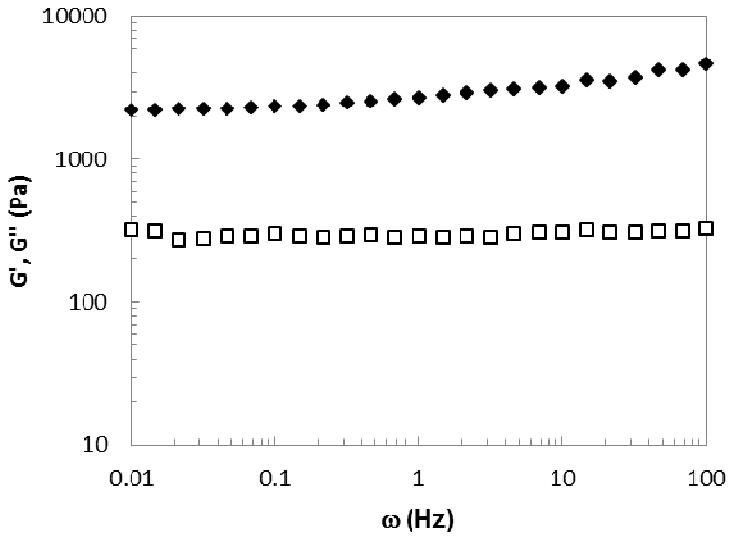

FIGURE 1 Frequency sweep of CpF gels (40%). Symbols: closed – storage (G') open – loss (G") moduli.

CONCLUSIONS

This work demonstrated that chickpea flour at different concentrations induces different degrees of gel structure that could be applied in the production of a large variety of food products. Even though all systems showed stable and strong gel characteristics, thermo-mechanical tests indicated that gels from chickpea flour at 40% present an industrial advantage over the other concentrations, since the stability is larger.

ACKNOWLEDGEMENTS

The authors acknowledge the financial support (POS-A/2012/116) from Xunta de Galicia of Spain and the European Union's European Social Fund. The authors also wish to thank Professor D. Pérez and Professor G. Torres for his help with the experiments and for useful discussions.

REFERENCES AND NOTES

1. Torres, M.D.; Fradinho, P.; Raymundo, A., Sousa, I., *Food and Bioprocess Technology*, **2014**, 7, 1171-1182.

2. Singh, N.; Sandhu, K.S.; Kaur, M., *Journal of Food Engineering*, **2004**, 63, 441-449.

3. ASAE Standards, S319.2: Methods for determining and expressing fineness of feed materials by sieving. ASAE, St. Joseph, Michigan, **1995**.

P4

Satiety of vegetable purees thickened with different hydrocolloids

Ana Salvador and Teresa Sanz

[1] Instituto de Agroquímica y Tecnología de Alimentos (IATA-CSIC).

Agustín Escardino, 7. 46980 Paterna (Valencia), Spain

e-mail of the presenter: asalvador@iata.csic.es

ABSTRACT

Four thickening agents (modified waxy corn starch, λ-carrageenan, guar gum and HPMC) were used to prepare vegetable purees. The effect of mouth and stomach in vitro digestion of the different purees on the viscoelastic properties was studied. After mouth digestion, starch puree suffered a complete breakdown of the structure whereas practically no changes in G' and G" were observed in the other purees. After stomach digestion, the lowest effect in the viscoelastic properties was found in the carrageenan pure. Consumer acceptability results showed that the acceptability of the carrageenan puree was similar to the traditional starch puree.

KEYWORDS (puree, rheology, in vitro digestion, hydrocolloid, acceptability)

INTRODUCTION

Satiety and satiation are part of a complex system of appetite control, including cognitive factors, sensory sensations and post-ingested feedback mechanisms (1). Satiety is defined as the inhibition of appetite and occurs as a consequence of eating. Satiety signals differ as the meal moves through the gut but include oral, gastric, and intestinal factors (2). Increasing the viscosity of nonnutrient meals delays gastric emptying, increases satiety and decreases hunger. Several human studies indicated that meals containing solids typically have a greater effect on satiety than liquid meals of equivalent size and energy content (3, 4). Part of this effect can be explained by the slower gastric emptying of solid meals but unfortunately, highly viscous beverages or beverages containing unchewed solids are unpalatable and cannot provide a feasible method for weight control. However, the relation between meal viscosity and satiety remain poorly understood. So, the aim of this work was to study the viscoelastic properties of vegetable purees prepared with four different thickening agents after mouth and stomach in vitro digestions as a

way to evaluate the structural changes during digestion. Consumers sensory acceptability of purees was also studied.

MATERIALS AND METHODS

Vegetable purees elaboration

The vegetable puree formulation consisted of zucchini (33.3% w/w), powdered skimmed milk (6% w/w), olive oil (5% w/w), waxy corn modified starch (3.5% w/w) or λ-carrageenan (1.7% w/w) or guar gum (0.9% w/w) or hidroxypropylmethyl celulose (1.6% w/w), salt (0.23% w/w) and water up to 100% w/w. Zuchinis were cutted into pieces mixing with the oil and heated to 90ºC at 100 rpm for 1min in a cooking device (Thermomix TM 31). After that, the rest of the ingredients were placed in the cooking device and heated to 90 °C at 600 rpm for 20 min. Finally, the mix was stirred to 2000 rpm for crushing. The resulting puree was cooled to 37 °C. For in vitro mouth incubation 25 g of puree were mixed with 0.5ml human stimulated saliva. Subsequently 6ml H_20+1.5ml pepsin solution were added and the pH was adjusted to 2.5 with HCl (6N) (stomach digestion). The stomach digestion was carried out inside the starch pasting cell of the rheomether.

Rheological measurements

The linear viscolastic properties of the purees were performed with a controlled stress rheometer (AR-G2, TA Instruments). A 60-mm diameter plate–plate geometry and a gap of 1 mm was employed in fresh and saliva samples and a starch pasting cell in stomach digested samples. The mechanical spectra in the linear region from 10 to 0.01 Hz at 37 °C were recorded in fresh purees and in purees after mouth and stomach digestion.

Sensorial analysis

Sensory analysis of purees was carried out by 80 untrained assessors in a sensory laboratory equipped with individual booths. A hedonic test was carried out using a 9-hedonic scale labelled on the bottom with “dislike extremely” and on the top “like extremely” and the assessors evaluated their liking of appearance, consistency, taste, and overall acceptability. Data acquisition and analysis was performed by Compusense five release 5.0.

RESULTS AND DISCUSSION

Viscoelastic properties

Before mouth digestion, the starch puree showed the highest viscoelasticity, followed by the carrageenan pure, the guar pure and the HPMC pure. The effect of frequency in the values of G' and G" of the guar, HPMC and carrageenan puress, before and after mixing with saliva is shown in Figure 1. After mixing with saliva, the starch puree showed, as expected, a complete structure breakdown, (G' and G" was not measured) indicating that in this type of puree no effect of satiety associated to a delay in gastric emptying could be expected. In the guar and HPMC puree only a very small decrease in the viscoelastic functions was found, and in the carragenan puree no effect of saliva was observed.

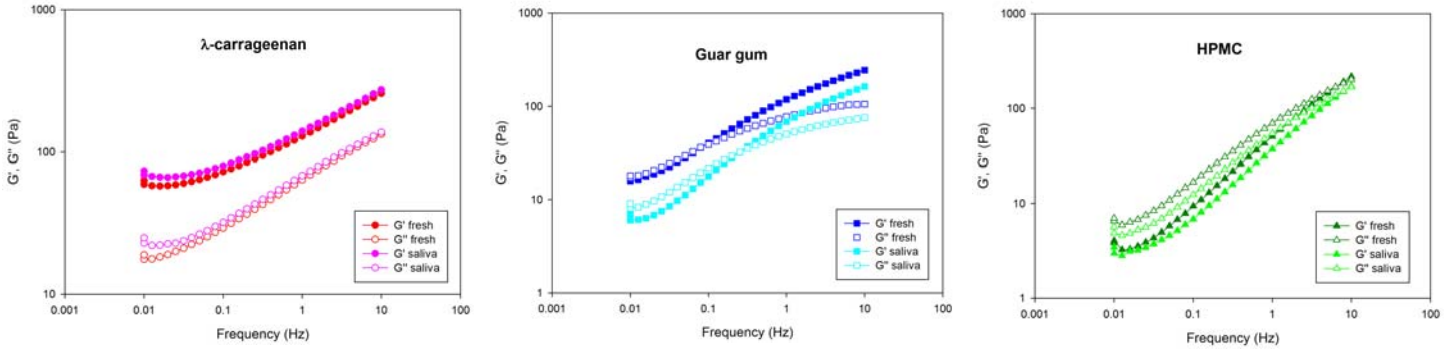

FIGURE 1. Mechanical spectra of purees of fresh samples and after mouth digestion.

After the stomach incubation, a significant decrease in G', G" and in viscoelasticy was observed, although the differences were more noticeable for the guar and HPMC puree than for the carrageenan puree (Figure 2). In conclusion the viscoelastic properties of the carragenan puree were the least affected after in vitro digestion.

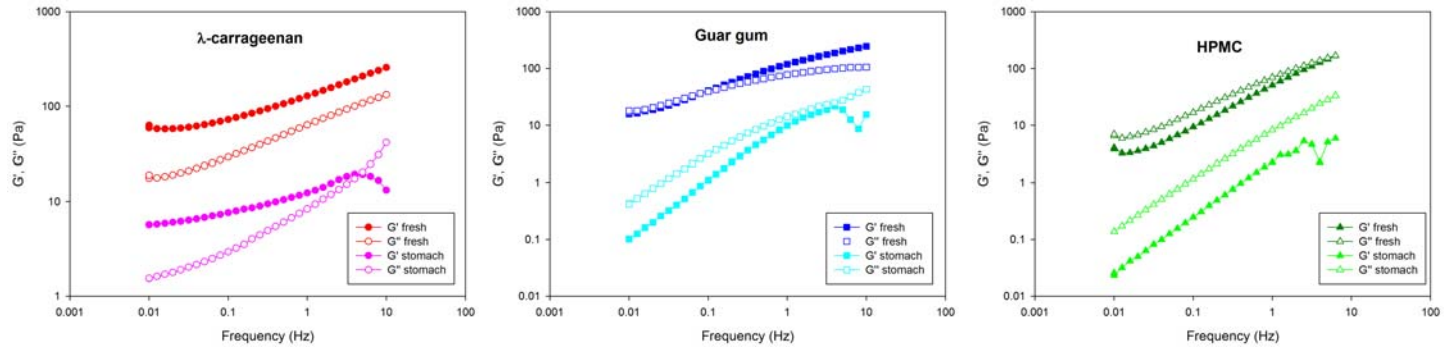

FIGURE 2. Mechanical spectra of purees of fresh samples and after stomach digestion.

Sensorial acceptability

The results of the acceptability of purees are shown in Figure 3. Starch puree was the most acceptable puree in taste, consistency and global acceptability presenting significant difference with the other purees. On the contrary, the HPMC puree was the worst scored puree. It can be noticed that carrageenan puree was the closest to the starch puree, showing little difference in the attributes studied. No differences in appearance were found among all the samples.

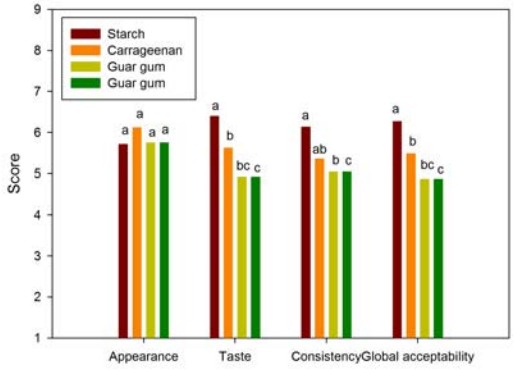

FIGURE 3. Acceptability scores of the different purees.

CONCLUSIONS

Viscoelastic properties of carrageenan puree were the less affected by in vitro digestion. This indicate that this puree has a more resistent structure than the others and could imply a more saciant effect with similar sensorial properties than traditional starch puree.

REFERENCES AND NOTES

1. Benelam, B. Satiation, satiety and their effects on eating behaviour. *Nutrition Bull*etin, **2009**, 34, 126–173.

2. Read, N., French, S., Cunningham, K. The role of the gut in regulating food- intake in man. *Nutrition Review*, **1994**, 52: 97-105.

3. Bolton, R. P., Heaton, K. W., Burroughs, L. F. The role of dietary fiber in satiety, glucose, and insulin—studies with fruit and fruit juice. *American Journal of Clinical Nutrition*, **1981**, 34, 211–217.

4. Himaya, A., Louis-Sylvestre, J. (1998) The effect of soup on satiation. *Appetite*, **1998**, 30, 199–210.

P5

Determination of Melting Points of Amylose-Lipid Complexes and Amylose in Gluten Free Flour Doughs by DMTA

Ramón Moreira, Francisco Chenlo, Santiago Arufe

Departamento de Enxeñaría Química, ETSE, Universidade de Santiago de Compostela, Rúa Lope Gómez de Marzoa, s/n, 15782 Santiago de Compostela (Spain)

Correspondence to: Ramón Moreira (E-mail: ramon.moreira@usc.es)

ABSTRACT

Gluten-free doughs made from white, yellow and purple maize flours and from chestnut flour were processed in a laboratory kneader (Mixolab®) at the same consistency level (1.10 Nm) and water content variable. Amylose-lipid complexes melting (M2) and amylose melting (M3) were studied by means DMTA employing a controlled stress rheometer using parallel plates. The rheological assays were performed in the LVR of the doughs. Temperature was increased from 90 to 180ºC at heating rate of 4ºC/min. Results showed that M2 (99-122ºC) can be determined by DMTA by means of thermal behaviour of G´ and M3 (121-146ºC) can be determined by the monitoring of tan δ. Transitions depended on water content, nature and characteristics of the starch and the presence of other compounds (mainly sugars) in the flour doughs. Results obtained by DMTA were also evaluated by comparison to endotherms determined by DSC.

KEYWORDS DMTA, DSC, gluten-free flour, starch, thermal transitions

INTRODUCTION

The use of traditional starch source like maize or alternative source like chestnut is necessary to increase the supply of gluten-free products with high quality to a growing market. The research on the transformations experienced by starchy food materials, particularly in flour dough, during thermal processes is essential to estimate and control the final product properties.

Gelatinization is the main starch transition but other thermal transitions, due to biopolymer interactions, can take place at higher temperatures as the reversible dissociation of amylose-lipid complexes, called M2, and also melting amylose, labelled M3.[1] Traditionally, DSC is the

employed technique to determine these endothermic transitions. Nevertheless, these phase transitions can give as result modifications of the mechanical properties of the doughs. At these conditions, DMTA can be a useful experimental technique to determine the corresponding thermal ranges by the viscoelastic moduli monitoring with temperature.

The aim of this work is to determine the temperatures of M2 and M3 transitions of several gluten-free flour doughs processed at the same consistency level with different water absorption by two different experimental techniques (DSC and DMTA) in order to establish comparisons between the results obtained.

EXPERIMENTAL

Maize (*Zea mays*) flours obtained from 3 different varieties of Spanish maize kernels, white (WM, *Rebordanes*), yellow (YM, *Sarreaus*) and purple (PM, *Meiro*) and chestnut (CH, *Castanea sativa Mill*) flour were employed as raw material. Flours were placed in a desiccator at 25ºC and relative humidity 54%, until flours equilibration with constant moisture content (8-10 %, d.b.). Flours were stored at 4ºC in vacuum sealed bags until use. Doughs for DMTA tests were prepared by using Mixolab® apparatus (Chopin Technologies, France)[2]. At the consistency of 1.10 Nm, water absorption (WA, % d.b.) was determined. Samples, at the same WA of doughs prepared for DMTA, were prepared for DSC studies. The flour (~1g) was put in a glass vial and water was added to obtain the desired WA. The vial was sealed and sample was equilibrated for 24 h at room temperature. A portion of the sample (< 18 mg) was introduced in a steel pan and sealed. Thermal properties were determined with a calorimeter (Q200, TA Instruments, USA). An empty steel pan was used as reference. Samples were heated from 90ºC up to 180ºC at 4ºC/min.

Flour doughs at the target consistency were tested in a controlled stress rheometer (MCR 301, Anton Paar, Austria) equipped with a chamber (CTD 450, Anton Paar, Austria) using parallel plates (50 mm diameter, 2 mm gap) by DMTA. The assays were performed in the LVR of the doughs (0.1 % of strain, 1 Hz). Temperature increased from 90 to 180ºC at 4ºC/min. G´ and tan δ values were used to determine the temperatures associated with starch transitions. All assays were performed at least in duplicate. Differences among means were identified by one-factor analysis of variance with Scheffe test and significant P-values ≤ 0.05 (IBM SPSS Statistics 22).

RESULTS AND DISCUSSION

Above 90ºC, the first transition, denominated M2 (94.6-122.2ºC), was observed in all flour doughs and it corresponds to the melting of amylose-lipid complexes using DSC. At higher temperatures appeared a new peak, M3, (129-147ºC) corresponding to the melting of amylose[3]. This endotherm sets in a narrow interval of temperatures (< 7ºC) and in maize doughs the Tp showed an inversely relationship with WA. This trend was observed in high amylose starches[4]. M3 peak of CH dough was shorter and at intermediate temperature (134.6-136.0ºC) in spite of its low hydration, indicating the importance of the amylose nature (molecular size, presence of polymorphs) on its thermal behaviour.

In DMTA, M2 and M3 peaks were observed by means of the evolution of G´ or tan δ with temperature. M2 peak was difficult to observe because coincides with the water evaporation from the dough. In these circumstances, simultaneous processes affecting to mechanical properties take place and G´ data show some dispersion. G´ showed a minimum value, Tp of M2 peak. To and T1 were determined by means of slope changes of G´ before and after Tp, respectively. The peaks took place in a narrow interval of temperatures, 99-111ºC for WM dough and 109-122ºC for CH doughs. T_o and T_p determined by DMTA of M2 peak shifted to higher temperatures than those measured by DSC. This result indicates that amylose-lipid complexes melting is retarded when moisture diminishes. Nevertheless, the end of M2 transition, T1, were the same by means of both methods, see Table.

Above M2 transition, G´ values increase sharply during baking by the complex phenomena related to the crust formation that give as result a more rigid and stiff material. Regarding to M3 peak, corresponding to the melting of amylose, it was monitored by tan δ. To corresponded to the slope increase of the tan δ curve, Tp was the temperature with the maximum value of tan δ and T_1 with a later change of the slope, see Figure (illustrated the peaks determination for PM dough). In the YM and CH doughs no M3 peak was observed in tan δ curve. This fact can be related to low hydration levels of both doughs. M3 peaks determined by DMTA are broader than those obtained by DSC due to the associated structural changes and re-arrangements of the transitions take place in an extensive range of temperatures. In spite of the acceptable agreement between DSC and DMTA peaks, more experimentation with simultaneous moisture measurement is needed to confirm these results.

TABLE. Onset (T_o), peak (T_p) and final (T_1) temperatures of M2 and M3 transitions determined by DSC and DMTA for tested maize and chestnut flour doughs♣

			YM	WM	PM	CH
WA (%, d.b.)			63.0±1.0b	90.0±2.0d	81.1±1.4c	52.9±0.5a
T (ºC)				DSC		
M2	T_o		100.7c	94.6a	97.8b	102.8d
	T_p		109.6c	102.1a	105.0b	114.0d
	T_1		117.6b	112.0a	112.4a	122.2c
M3	T_o		140.1c	130.2a	129.0a	134.6b
	T_p		140.2c	130.3a	129.1a	134.7b
	T_1		146.4d	137.9c	132.5a	136.0b
				DMTA		
M2	T_o	G´	106.9±0.5b,c	99.1±1.2a	102.8±0.1a,b	109.1±0.4c
		tan δ	-	-	-	-
	T_p	G´	113.7±0.1c	103.7±0.2a	108.5±0.5b	114.9±0.6c
		tan δ	-	-	-	-
	T_1	G´	118.9±0.8a	111.4±2.8a	111.7±2.4a	121.8±1.3a
		tan δ	-	-	-	-
M3	T_o	G´	-	-	-	-
		tan δ	-	121.9±2.5	126.4±1.5	-
	T_p	G´	-	-	-	-
		tan δ	-	131.2±2.7	136.8±1.2	-
	T_1	G´	-	-	-	-
		tan δ	-	138.2±2.7	146.2±0.1	-

♣Standard deviations of temperature data for DSC were ±0.2ºC. Data with different letters in rows are significantly different, P ≤ 0.05.

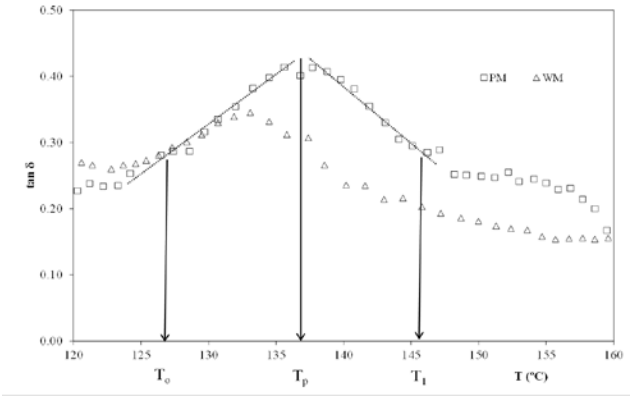

FIGURE. DTMA for purple (PM) and white (WM) maize doughs. Trend of tan δ from 120 to 160ºC.

ACKNOWLEDGEMENTS

The authors acknowledge the financial support to Ministerio de Economía y Competitividad of Spain and FEDER (CTQ 2013-43616/P).

REFERENCES AND NOTES

1. Torres, M.D.; Moreira, R.; Chenlo, F.; Morel, M.H. *Food Hydrocolloids*, **2013**, 33, 192-198.
2. ICC. Standard Methods. International Association for Cereal Chemistry, Vienna 337, **1996**.
3. Liu, H.; Yu, L.; Chen, L.; Li, L. *Carbohydrate Polymers*, **2007**, 69, 756-762.
4. Liu, H.; Xie, F.; Chen, L.; Yu, L.; Dean, K.; Bateman, S. *International Journal of Food Engineering*, **2005**, 1, 3-8.

P6

Rheological Properties of White, Yellow and Purple Maize Flour Doughs

Santiago Arufe, Silvia N. Rubinos, Francisco Chenlo, Ramón Moreira

Departamento de Enxeñaría Química, ETSE, Universidade de Santiago de Compostela, Rúa Lope Gómez de Marzoa, s/n, 15782 Santiago de Compostela (Spain)

Correspondence to: Santiago Arufe (E-mail: santiago.arufe@gmail.com)

ABSTRACT

Three different flours doughs of white (WM), yellow (YM) and purple (PM) maize were studied. Average particle diameter by mass (D_w) and damaged starch (DS) of flours were determined. Maize flour doughs were prepared at constant dough consistency with different water absorptions (WA) by mixing flour and water in a laboratory kneader. Rheological characterization was carried out at 30ºC by means of oscillatory frequency sweep and creep-recovery tests using a rheometer. At the same milling conditions, WM flour showed higher D_w than PM and YM flours. The presence of DS increased WA. The mechanical spectra showed that G was dominant over G´´ and tanδ varied slightly with angular frequency. From modelled creep-recovery data it was observed that WM and PM flour doughs showed the highest J_0, that varied with the same trend than G´, J_m increased linearly with WA, λ_c and λ_r with increasing DS and no significant differences in η_0.

KEYWORDS maize, flour, dough rheology, damaged starch, Mixolab®

INTRODUCTION

In the northwest of Spain maize is cultivated for self-consumption in small farms. Maize bread is traditionally made with whole grain of maize, following similar procedures as for manufacturing the common wheat bread[1]. Although most consumers prefer white maize (Rebordanes variety), other types are also used for making bread, like yellow (Sarreaus variety) and purple (Meiro variety) maize.

The main aim of this work is to characterize rheologically doughs from flours of three different types of Spanish maize manufactured at the same consistency using a laboratory kneader.

EXPERIMENTAL

Maize (*Zea mais*) kernels (0.40±0.05 kg water/kg dry solid, dry basis (d.b.) of white (WF, Rebordanes variety), yellow (YF, Sarreaus variety) and purple (PF, Meiro variety) Spanish maize were dried at 45ºC, 2 m/s of air velocity, 30% of relative humidity and 5 kg/m^2 of load density using a pilot-scale tray dryer (Angelantoni Challenge 250) until average maize moisture content of 11% d.b. was achieved. Flours were obtained from dried kernels by milling using an ultra-centrifugal mill (ZM200 Retsch GmbH) with an internal sieve of 200 μm. Mass fraction of flours particle sizes were obtained by sieving employing standard sieves from 40 up to 200 μm (Cisa Cedacería Industrial) to obtain the average particle diameter by mass ($D_w=x_i \cdot D_{pi}$, where D_{pi} (μm) is the average diameter of the fraction and x_i (%) the mass fraction).

Damaged starch (DS, % g damaged starch/g dry solid) of flours was determined as the starch fraction that is thermal or mechanically damaged, using a "Starch Damage Kit"[2]. Flour doughs preparation were performed in a laboratory kneader (Miloxab®, Chopin Technologies) following a standard protocol[3] until a target consistency of 1.10 ± 0.07 Nm was achieved.

The rheological characterization of doughs, at the target consistency, was carried out using a controlled stress rheometer (MCR 301, Anton Paar Physica) with parallel plates (50 mm diameter, 2 mm gap) at 30ºC (±0.1ºC). Two different tests were performed in triplicate: 1) Oscillatory frequency sweep (1–100 rad/s, 0.1% strain), 2) Creep and recovery (50 Pa/60 s (creep step), 0 Pa/180 s (recovery step). Experimental data of creep and recovery were analyzed by means of creep compliance rheological parameters (J(t) (Pa^{-1})) and modelling by Burgers model[4] using the Eqs. (1) and (2) for creep and recovery steps, respectively:

$$J(t) = J_0 + J_m\left(1 - \exp\left(\frac{-t}{\lambda_c}\right)\right) + \frac{t}{\eta_0} \quad (1)$$

$$J(t) = J_{max} + J_0 + J_m\left(1 - \exp\left(\frac{-(t-60)}{\lambda_r}\right)\right) \quad (2)$$

where J_0, J_m and $J_{máx}$ (Pa^{-1}) are the instantaneous, viscoelastic and maximum creep compliance, respectively, t (s) is the phase time, λ_c (s) and λ_r (s) are the mean retardation time of creep and recovery steps, respectively, η_o (Pa s) is the zero-shear viscosity and J_r (Pa^{-1}) the recovery compliance (J_0 + J_m). The $J_r/J_{máx}$ ratio gives information on relative elastic component of the maximum creep compliance.

RESULTS AND DISCUSSION

For flours obtained D_w varied in a narrow interval (90-113 μm), Table 1. Higher values for WM flours are probably due to the higher hardness of WM kernels regarding to YM and PM kernels. DS content showed significant differences, WM variety showed the highest (25.0 %) and YM the lowest (8.6 %). This fact is related to the different hardness and friability of maize variety that can causes different and thermal damage during milling. Tested doughs showed WA values significantly different, Table 1. WA increased linearly with increasing DS content ($R^2 > 0.99$).

Figure 1 shows the oscillatory frequency sweep of doughs. In all cases, in the studied range, G´ and G´´ values increased with increasing angular frequency (ω). This behaviour can be attributed to the absence of binding agents in the dough (absence of gluten) and also because repulsive forces between starch granules are predominant[5]. For all maize flour doughs, G´ values were higher than G´´ indicating that elastic proportion was dominant over the viscous one, ($\tan\delta < 0.5$). YM flour dough showed the highest moduli and WM and PM flour doughs the lowest ones. This could be related to the high WA required for WM and PM flour doughs.

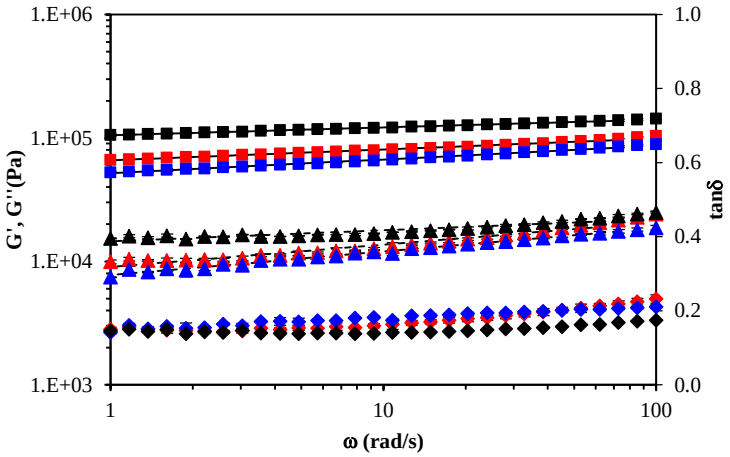

FIGURE 1. Experimental data of G´ (■), G´´ (▲) and tanδ (♦) of YM (black), WM (blue), PM (red).

In creep step, WM and PM doughs showed the highest J_0 (≈14 10^{-6} Pa^{-1}), Table 1. J_m increased with increasing DS, indicating that DS modified the viscoelastic behaviour of doughs. λ_c decreased with increasing DS. For recovery step, $J_{máx}$ increased with WA probably due to formation of weak material structures related to higher WA[6]. J_0 and J_m values were comparable and showed the same trend as those observed in creep step. Values of λ_r were higher than those observed for λ_c. This fact could be due to the operation outside the LVER in these tests. The J_r

/J_{max} ratio of doughs increased with WA and was higher in comparison to wheat doughs (65%) indicating a higher elastic character.

TABLE 1. D_w, DS, WA, and parameters of creep and recovery models, Eqs. (1) and (2)*

Parameters		YM	WM	PM
D_w (μm)		90	113	93
DS (% w/w, d.b.)		8.6±0.2^a	25.0±2.1^c	18.2±0.5^b
WA (%, d.b.)		63.0±1.0^a	90.0±2.0^c	81.1±1.4^b
Creep	J_0 (Pa^{-1})·10^6	9.1 ± 0.1^a	14.1 ± 0.2^b	14.2 ± 0.9^b
	J_m (Pa^{-1})·10^6	4.8 ± 0.1^a	11.2 ± 0.5^c	8.0 ± 0.3^b
	λ_c (s)	5.0 ± 0.1^c	1.5 ± 0.1^a	2.9 ± 0.2^b
	η_0 (Pa·s)·10^{-6}	7.3 ± 0.9^a	6.7 ± 0.2^a	7.4 ± 0.2^a
	R^2	0.98	0.95	0.96
Recovery	J_{max} (Pa^{-1})·10^6	21.7 ± 0.3^a	32.0 ± 1.4^b	30.5 ± 0.7^b
	J_0 (Pa^{-1})·10^6	9.6± 0.2^a	17.0 ± 1.4^b	18.3 ± 0.4^b
	J_m (Pa^{-1})·10^6	8.8 ± 0.1^a	11.2 ± 0.1^b	8.9 ± 0.2^a
	λ_r (s)	34.0 ± 1.4^c	17.0 ± 0.1^a	27.5 ± 0.7^b
	J_r/J_{max} (%)	83.1 ± 0.1^a	87.6 ± 1.3^c	86.5 ± 0.9^b
	R^2	0.95	0.85	0.91

*Data presented as means ± standard deviation. Values with different superscript letters in rows are significantly different, P≤0.05.

CONCLUSIONS

The results reveal that rheological properties of the corresponding doughs depend on maize variety. Water absorption increases linearly with increasing damaged starch even for flour from different types of maize. Oscillatory frequency sweep reveal that elastic behavior was predominant in relation to viscous component and viscoelastic moduli decrease with increasing water absorption.

ACKNOWLEDGEMENTS

The authors acknowledge the financial support to Ministerio de Economía y Competitividad of Spain and FEDER (CTQ 2013-43616/P).

REFERENCES AND NOTES

1. Revilla, P.; Landa, A.; Rodríguez, V.M.; Romay, M.C.; Ordás, A.; Malvar, R.A., *Journal of Agricultural Research*, **2008**, 6, 241-247.
2. ICC-Standard Methods. International Association for Cereal Chemistry, Vienna 337, **1996**.
3. ICC-Standard Methods. International Association for Cereal Chemistry, Vienna 173, **2008**.
4. Burgers, J.M., First Report on Viscosity and Plasticity. Nordemann Pub., New York, **1935**.
5. Sivaramakrishnan, H.P.; Senge, B.; Chattopadhyay, P.K., *Journal of Food Engineering*, **2004**, 62, 37-45.
6. Lazaridou, A.; Duta, D.; Papageorgiou, M.; Belc, N.; Biliaderis, C.G., *Journal of Food Engineering*, **2007**, 79, 1033-1047.

P7

Rheology of complex food emulsions with vegetable and animal proteins

Mara Pereira[1], Carla Graça[1], Sara Alves[2], Luís Raimundo[2], Anabela Raymundo[1], Isabel Sousa[1]

[1] (LEAF) – Centro de Investigação em Agronomia, Alimentos, Ambiente e Paisagem do ISA – ULisboa, Tapada da Ajuda 1349-017 Lisboa, Portugal

[2] CFG – Avda. Europa, 24; 28108 Alcobendas, Madrid, Espanha

Correspondence to: Isabel de Sousa (E-mail: isabelsousa@isa.ulisboa.pt)

ABSTRACT

The emulsions were produced with a mixture of animal and vegetal proteins and different processing conditions were tested. The values of firmness as the force peak obtained by a puncture test ranged from 0.85N to 2.80N, for P2 and P3 formulations, respectively. The minimal value for adhesiveness was -5.65N.s, for P2 formulation, and the highest value, -12.75N.s, was obtained for P3 formulation. At a controlled temperature of 20ºC, the emulsions produced with different processing methods presented similar flow behaviour. However, when heated from 20ºC to 90ºC the P4 formulation showed the highest decrease on viscosity. Therefore, when the flow curves at 40ºC were compared, the P4 material consistently presented the highest decrease on viscosity. This viscosity decrease was confirmed with rotation temperature ramps. Nevertheless, when emulsions were cooled back from 90ºC to 20ºC, the viscosity was recovered in all cases. The small amplitude oscillatory system (SAOS) measurements at 20ºC showed that all emulsions presented storage moduli (G') above loss moduli (G"), with similar behaviour and values. The mechanical spectra performed at 40ºC revealed that P3 presents some instability with a crossing point when G" becomes higher than G'. At the same conditions, P4, a material closer to a gel, showed the lowest value of G' and G'', and this can be an advantage in the filling process.

KEYWORDS

Emulsions, animal and vegetal proteins, texture, rheology behavior

INTRODUCTION

Emulsions are complex multiphase systems widely used in different industries, namely in the food industry. They are heterogeneous systems of two immiscible liquids and do not form spontaneously, these are metastable systems without thermodynamic stability [1]. Emulsion systems must therefore be carefully designed to overcome the instability mechanisms and provide sufficient stability over the lifetime of the product [2]. By adding substances known as emulsifiers and stabilizers, e.g. weighting agents, ripening inhibitors, or texture modifiers it is possible to form emulsions that are kinetically stable for a reasonable period of time [2]. Many types of food proteins can be used as emulsifiers due to their amphiphilic character, polymeric structure, and electrical charge characteristics. The amphiphilic character means that they are ambivalent with affinity to both water and oil, therefore they can adsorb to droplet surfaces during homogenization [3] and keeping part of the molecule in

contact with the disperse medium, leading to the formation of a strong layer at the surface of the droplet. The stability of an emulsion may be explained by rheological properties, an understanding of the relationship between the rheology and stability of emulsions is important to predict emulsion stability and to control product quality [4]. There is an interrelation between the rheology of interfacial surfactant layers and the stability of the emulsions because the latter is determined mainly by the elasticity (thermodynamic factor) and viscosity (kinetic factor) in droplet interactions [5].
The main goal of this work was to test the impact of different processing conditions on the flow and viscoelastic behaviour of the emulsions.

METHODS

Preparation of the emulsions

The emulsions were produced with animal and vegetal proteins. Different conditions were tested for pre-hydration of proteins and olive oil temperature. The emulsions were prepared in a thermo-processor (Bimby-Worwerk) for about 10 minutes at 6 position and 37 ºC, 3% of glucose and 2% of sodium ascorbate were added, to decrease the water activity and oxidation, respectively. The emulsions were coded as: P1 - hydration of proteins and olive oil at 21ºC; P2 - hydration of proteins at 21ºC and olive oil heating at 45ºC; P3 - hydration of proteins at 21ºC followed by heating at 70 ºC/45 min and olive oil at room temperature; P4 - hydration of proteins at 21ºC followed by heating at 70ºC/45min and olive oil heating at 45ºC.

Rheological measurements

Texture characterization

Texture parameters were determined from the texture profile analysis (TPA) using a Texturometer TA XT Plus (Stable Micro Systems), in puncture testing with a 25mm diameter acrylic cylindrical probe (15mm of penetration, 5s of waiting time and 1mm/ s of crosshead speed with 5kg of crossload). The experiments were carried out 24h after preparation of the emulsions kept in a cold room at 5ºC. Before performing any measurements, emulsions were allowed to equilibrate at 20ºC for 1h in a temperature-controlled room. Results of firmness (N) and adhesiveness (-N.s) were replicated at least four times, for each sample [6].

Rheological measurements

Rheological behaviour of the emulsions was evaluated in a controlled stress rheometer (Haake Mars III - Thermo Scientific), with an UTC-Peltier system. The flow curves (FC) were obtained at different temperature conditions, 20ºC and 40ºC, and the range of shear-rate used was $1x10^{-6}$ to $1x10^{3}$ s^{-1}. In rotation temperature ramp (RTR) the viscosity was measured when the emulsions were heated from 20ºC to 90ºC and cooled down from 90ºC to 20ºC. SAOS were performed with frequencies ranging

from $1x10^{-3}$ to $1x10^{2}$ Hz and 50 Pa for stress. The sensor used for all determinations was a serrated parallel-plate sensor (20, 1mm gap) system.

RESULTS AND CONCLUSIONS

Macrostructure of the emulsions was evaluated in terms of texture, using the TPA, the results to the firmness and adhesiveness parameters are presented in FIGURE 1 and FIGURE 2, respectively.

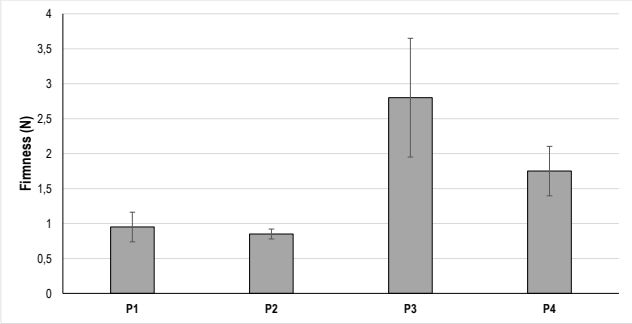

FIGURE 1 – Firmness of emulsions.

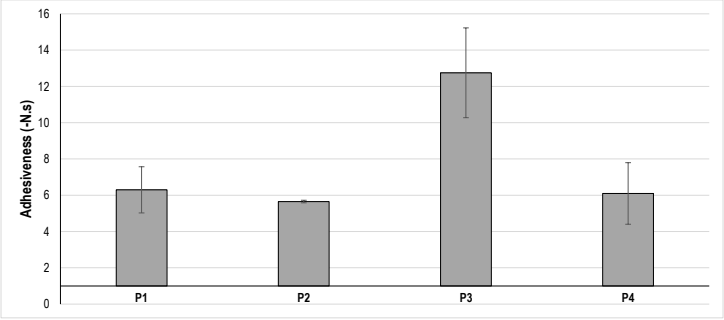

FIGURE 2 – Adhesiveness of emulsions.

The values of firmness obtained were between 0.85N and 2.8N, the minimal value corresponding to emulsion P2 and the highest value of firmness to P3. The minimal value for adhesiveness was -5.65N.s, for P2 emulsion, and the highest one for P3 with -12.75N.s. The extreme values of firmness and adhesiveness corresponding to the same samples, as it is usual in these systems.

The flow curves from the controlled stress rheometer were obtained at 20ºC and 40ºC, and are shown in FIGURE 3.

At 20ºC, the emulsions produced with different processing methods presented similar behaviours. However, when heated from 20ºC to 90ºC the P4 showed the highest decrease on viscosity. Therefore, when the FCs at 40ºC were compared, the P4 material consistently presented the highest decrease on viscosity. This viscosity decrease was confirmed with RTR. When emulsions were cooled from 90ºC to 20ºC, the viscosity was recovered in all cases (data not showed).

The results of SAOS, at 20ºC and 40ºC are presented in FIGURE 4.

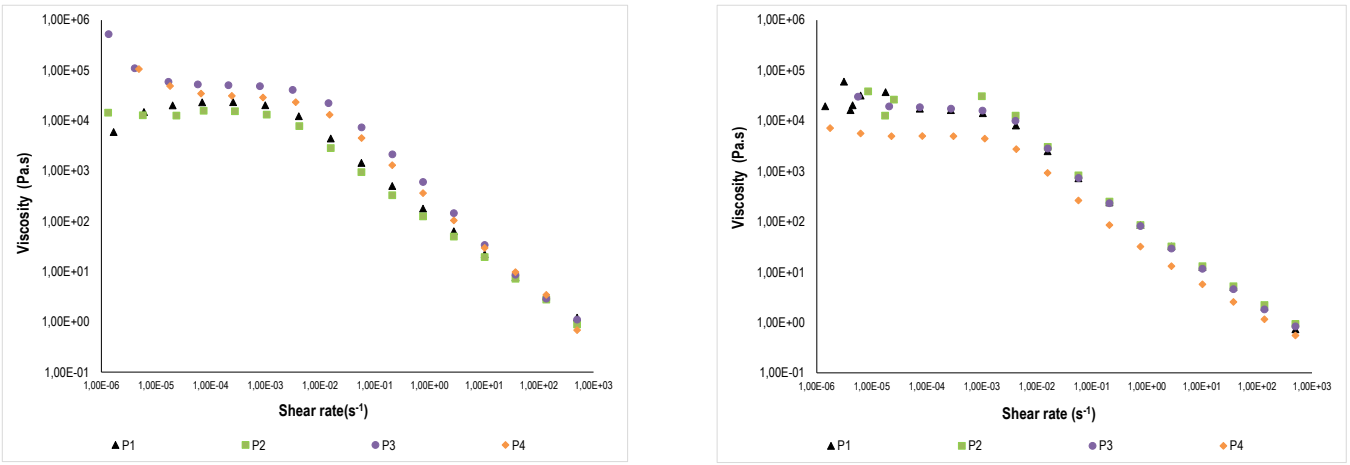

A B

FIGURE 3 – Flow curve at 20ºC (A) and 40ºC (B).

The SAOS at 20ºC showed that all emulsions present the storage modulus (G') higher than loss modulus (G"), with similar behaviour and values. The mechanical spectrum performed at 40ºC revealed that P3 presents some instability with G" becoming higher than G' with a crossing point. At the same conditions, P4, a material closer to a gel, showed the lowest value of G' and G", and this can be an advantage in the filling process.

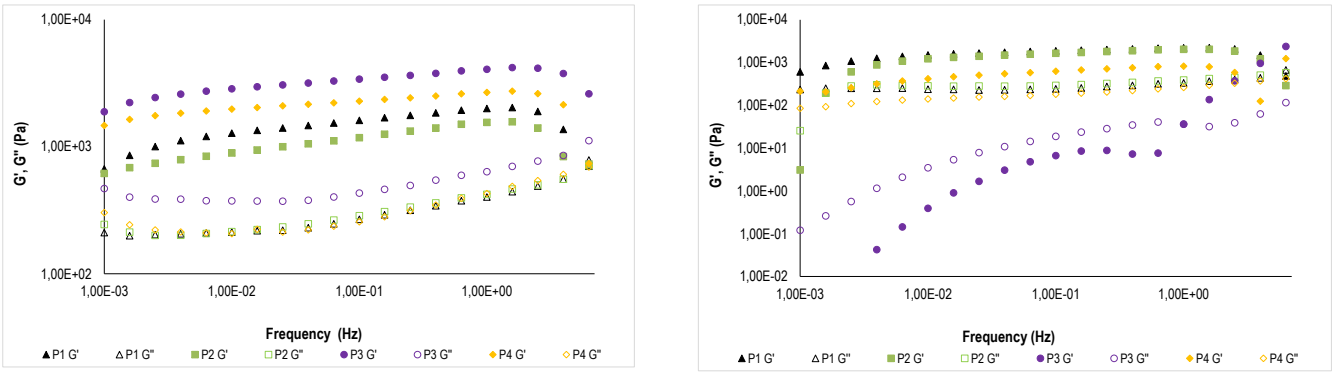

A **B**

FIGURE 4 – Mechanical spectra of the emulsions, at 20ºC (A) and 40ºC (B).

ACKNOWLEDGEMENTS

This work was supported by QREN – I&DT Project 38593.

REFERENCES

[1] Homayoonfal, M.; Khodaiyan, F.; Mousavi, M., *Modelling and optimising of physicochemical features of walnut-oil beverage emulsions by implementation of response surface methodology: Effect of preparation conditions on emulsion stability*. Food Chemistry, 2015, 174, 649 - 659

[2] Piorkowski, D.T.; McClements, D.J., *Beverage emulsions: Recent developments in formulation, production, and applications*. Food Hydrocolloids, 2014, 42, 5-41

[3] Qiu C.; Zhao, M.; McClements, D.J., *Improving the stability of wheat protein-stabilized emulsions: Effect of pectin and xanthan gum addition*. Food Hydrocolloids, 2015, 43, 377-387

[4] Udomrati, S.; Shoichi Gohtani, *Tapioca maltodextrin fatty acid ester as a potential stabilizer for Tween 80-stabilized oil-in-water emulsions*. Food Hydrocolloids, 2015, 44, 23-31

[5] Derkach, S.R, *Rheology of emulsions*. Advances in Colloid and Interface Science, 2009, 151, 1–23

[6] Nunes. M.C.; Raymundo, A.; Sousa, I., *Rheological behaviour and microstructure of pea protein/k-carrageenan/starch gels with different setting conditions*. Food Hydrocolloids, 2006, 20, 106-113

Development of a gluten-free mix for pizza base – rheological approach

Diana Narciso, Patrícia Fradinho, Isabel de Sousa, Anabela Raymundo

LEAF – Instituto Superior de Agronomia/Universidade de Lisboa, Tapada da Ajuda-Edifício Ferreira Lapa, 1349-017 Lisboa, Portugal

Correspondence to: Anabela Raymundo (anabraymundo@isa.ulisboa.pt)

ABSTRACT

The aim of this study is the development of a mix, for pizza base, designed for home preparation, increasing the market supply of gluten-free products without the high prices, normally associated with this kind of products. This is achieved through the use of rice by-products - broken rice and rice bran, which also contribute to the nutritional enrichment of the final product due to their dietary fiber content, polyunsaturated fatty acids, vitamins and minerals. The pizza base formulations were developed according to traditional recipes, replacing wheat flour with rice flour and rice bran. Other ingredients were also used to enhance the sensory characteristics of the pizza base developed. Since the manufacturing cost will influence the price of the final product paid by the consumer, the effect of xanthan gum use was also studied.

The rheological behaviour of developed doughs was assessed and compared with the one from commercial products and a control formulation with gluten.

The use of xanthan gum did not influence significantly the structure of dough. The storage modulus G' was greater than the loss modulus G" for all samples, showing a predominantly elastic behaviour. The gluten-free formulations showed lower frequency dependence of both modulli and a stronger structure than gluten doughs.

KEYWORDS: Pizza base, rice flour, xanthan gum, viscoelasticity, doughs

INTRODUCTION

Recently, there has been an increase of both the demand and supply of gluten-free products. However, the production of gluten-free bakery products presents a technological challenge, due

to the limited capacity of the gluten-free doughs in sustaining the CO_2 produced during fermentation, resulting in a poor viscoelastic dough.

To minimize this problem, the industry uses a mixture of hydrocolloids to improve the rheological characteristics of dough, and texture of products, increasing the costs dramatically. The aim of this work is the development of a formulation for gluten-free pizza dough through the use of by-products from the rice industry, namely broken rice and bran. If possible, the use of hydrocolloids (xanthan gum) will be discarded.

The use of economic ingredients and the reduced used of hydrocolloids will contribute to the development of a gluten-free product accessible to everyone, and also to the nutritional value of the final product, since rice bran is an excellent source of dietary fiber and oil rich in polyunsaturated acids.

EXPERIMENTAL

The ingredients used were selected based on their specific characteristics, market cost and gluten-free warranty. The dough was prepared with flour ground from broken rice and rice bran, both supplied from a rice industry. The other ingredients - egg, corn starch, oil, yeast, salt, sugar and xanthan gum – were purchased at local market.

The solid ingredients were placed in a food processor (Bimby, Vorwerk) and mixed. Then, water (37ºC), oil and egg were added and mixed together during 3 min. The fermentation took place at ambient temperature for 40 min. These conditions were chosen in order to be easily replicated by consumers at home.

The rheological behaviour of developed doughs – with xanthan gum (RXD) and without xanthan gum (RD) - was assessed and compared with the one from two commercial products: a gluten-free mix (CM) and whole flour mix with gluten (GM). A control formulation (GC) with wheat flour prepared in similar conditions as the developed doughs was also used.

The rheological behaviour of the doughs was assessed by small-amplitude oscillatory shear measurements in a Haake RS-75 controlled-stress rheometer. A serrated parallel plate sensor system with 20 mm diameter was used and a 1.5mm gap was applied.

After preparation the dough was transferred to the bottom plate. A stress sweep test was performed and the maximum shear stress amplitude value within the viscoelastic linear region (range of stress in which the structure is not destroyed) was used for the mechanical spectra.

Flow curves were determined using the same conditions, using a MARS III (Haake). Each formulation was tested at least in duplicate.

RESULTS AND DISCUSSION

The appearance of the developed doughs after preparation is presented in Figure 1. The effect of xanthan gum in the dough is clear, since the one with the hydrocolloid is moldable, an important characteristic because the consumer will have to shape the dough into a pizza-like form.

FIGURE 1. Pizza dough with (RXD) and without xanthan gum (RD).

The effect of xanthan gum addition on the dough viscosity is presented in Figure 2.

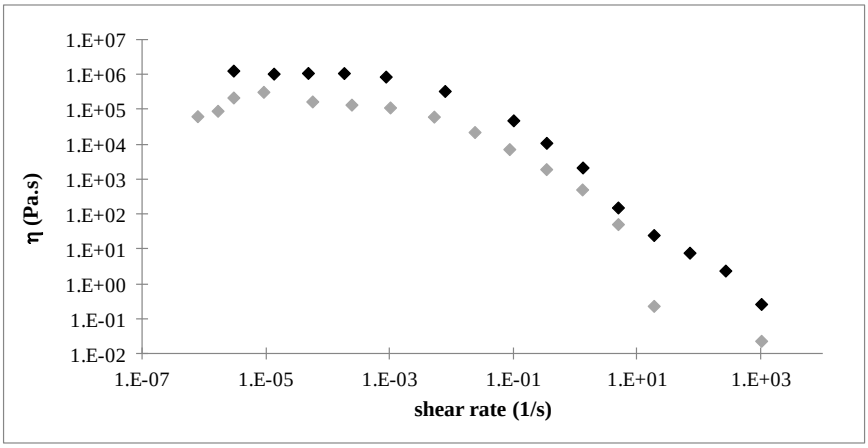

FIGURE 2. Flow curves of pizza base doughs with xanthan gum (◆ - RXD) and without xanthan gum (◆ - RD).

Both doughs show a similar flow curve pattern, with a newtonian plateau region at lower shear rates, followed by a shear-thinning zone. Gluten-free dough presents a slightly higher viscosity than the dough without hydrocolloid use. However, since xanthan gum has a high cost that will greatly influence the price of final mix, the subsequent product development was conducted without xanthan gum (RD).

The rheological behaviour of the gluten-free and commercial doughs was assessed and is depicted in Figure 3.

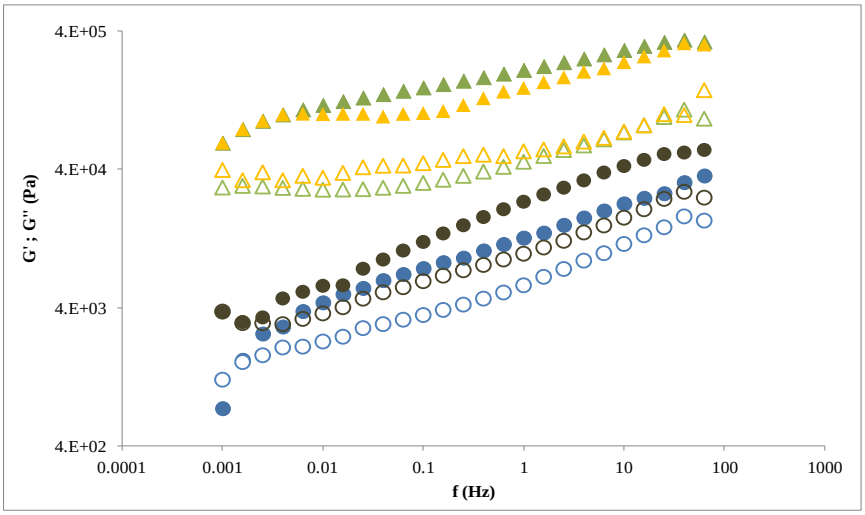

FIGURE 3. Mechanical spectra of the commercial and gluten-free doughs (● Gluten control (GC); ● Commercial gluten mix (GM); ▲ Commercial gluten-free mix (CM); ▲ Rice dough (RD); closed symbols-G'; open symbols–G'')

From the mechanical spectra of the doughs, it is observed that the elastic component (G') is always higher than the viscous component (G''), revealing a predominantly elastic behaviour of all doughs.

Regarding the rheological properties of the doughs, gluten formulations have a greater dependence of viscoelastic parameters (G 'and G' ') with frequency. Unlike the gluten-free formulations that have the most stable structures as the frequency increases. The gluten-free formulation developed shows values of G 'and G'' similar to the commercial gluten-free formulation (CM). Gluten-free dough also presents a wider gap between G' and G'' values, meaning that this dough has a stronger structure than gluten doughs.

CONCLUSIONS

It was possible to develop gluten-free dough without hydrocolloids, with similar rheological characteristics to commercial mix. This product is designed for easy preparation by the consumer. In this case, the consumer just adds water, oil and egg to the mix.

ACKNOWLEDGEMENTS

This work was supported by COMPETE program: QREN - "Arroz +" project n.38749.

Rheological study on slimming custards and milkshakes: Comparison of several commercial products

Manuel Muñoz[1], Alfonso Sánchez-Vicent[1], María Jesús Hernández[1], Jose Antonio Picó[2]

[1] Dep. Earth Physics and Thermodynamics, Fac. Physics, Univ. Valencia, 46100 Valencia (Spain).
[2] Korott, S.L. Research and Development, Polígono Santiago Payá, 03801 Alcoy (Spain).

Correspondence to: Jose Antonio Picó (E-mail: *japico@korott.com*)

ABSTRACT

Slimming milkshakes and custards with different flavors, manufactured by several trademarks, are compared in this work. Rheological properties measured at room temperature with a controlled stress rheometer (RS1, Thermo Haake) were analyzed. Important differences between brands were shown, especially in milkshakes. Most of milkshakes presented liquid consistencies; Newtonian or very low shear thinning. Custards were strongly shear thinning fluids, with gel like structure, and significant yield stresses and relative thixotropic areas. One of the brands distributed custards with different texture characteristics for the various flavors offered, while the custards of the other ones are more similar from the textural point of view. This fact could be responsible of a different sensation of satiety on the consumer, according to previous studies.

KEYWORDS: slimming food, satiating power, hydrocolloid, custard, milkshake

INTRODUCTION

Slimming foods are intended for use as a meal replacement in a weight-loss diet. These products do not in themselves contribute to weight loss, although they have the effect of not feeling hungry for a certain period of time, and they also provide a sufficient intake of nutrients[1]. Sales of enhanced satiety products had become more important in recent years in food market[2]. The composition of this kind of products normally includes milk, proteins, lipids, carbohydrates, fiber and hydrocolloids[1] among others. Texture of slimming foods plays a significant role in consumer acceptance, particularly since their satiating power seems to be directly related to their rheological properties[3,4]. In this work we compare some of these products in custard or in milkshake forms, developed by several commercial brands distributed in mass markets in Spain.

MATERIAL AND METHODS

Milkshakes and custards were prepared by dissolving the appropriated amount of commercial powder in skimmed milk with manual agitation. Products with different flavors manufactured by *Korott* ®, *SpecialLine*®, *MyBestFood*® and *biManán*® were analyzed (Table 1).

Rheological measurements were carried out in a controlled stress rheometer (RS1, Thermo Haake) with a thermostatic bath K10 and software Rheowin 4.2. A cone-plate 60 mm/2º sensor was used for milkshakes and 35 mm serrated parallel plates for custards. All measurements were performed in duplicate at 25 ºC. For all the systems, step flow curves in CR mode were performed between 1 and 100 s^{-1}. Then, after 1 min of shearing at 100 s^{-1}, down curves were recorded. For custards, steady flow curves in CS mode were also performed. Moreover, frequency sweeps in linear viscoelastic region (previously determined) were carried out.

RESULTS AND DISCUSSION

Texture of milkshakes and custards chosen was completely different, since milkshakes were liquid systems, and therefore, drinkable, while custards had a spoon-like consistency.

When comparing milkshakes, we observed the three *Korott* products presented similar textural characteristics, as they were slightly shear thinning fluids (fitting well to power law), while *My Best Food* milkshakes were much more liquid-like and almost Newtonian, just 10 times more viscous than water (Fig 1A).

On the other hand, it stands out the *Special Line* strawberry milkshake, with a behavior similar to custards (Fig 2A). Both in this case and custards flow curves were fitted to Carreau model

$$\eta = \eta_0 \Big/ \left[1+\left(\dot{\gamma}/\dot{\gamma}_c\right)^2\right]^s \qquad (1)$$

with similar shear thinning indexes, s≅0.4, and zero viscosities ranging from 1000 to 20000 Pa s.

Custards presented predominant elastic characteristics (G' > G"), as loss tangent indicated (Fig 2B), typical of gel like systems. Frequency dependence of storage modulus was satisfactorily fitted to power law functions

$$G' = G'_1 \, \nu^m \qquad (2)$$

Values of the parameter G'_1 (G' for 1 Hz) and m are shown in Table 1. It is interesting to point out that both lemon custards, from the two brands, were less firm, with lowest values of G_1' and highest *m*. They also presented the highest values of tan δ and the lowest values for η_0 (Fig. 2).

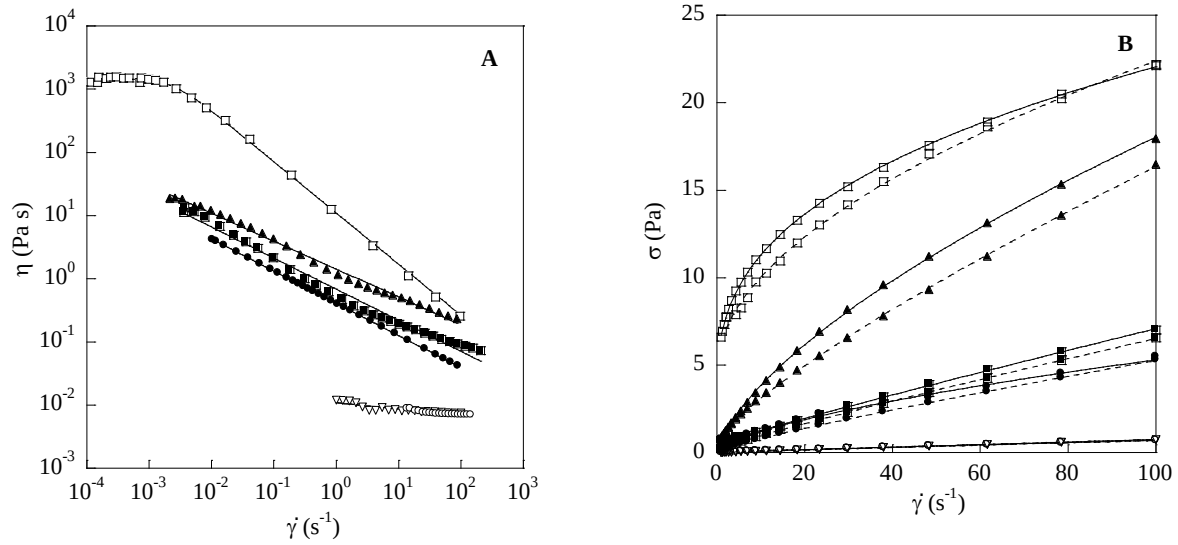

FIGURE 1. A) Steady flow curves in CS mode. B) Up flow curves and down curves after 1 min shearing. MILKHAKES: A) ▽Vanilla MyBestFood; ;○Chocolate MyBestFood; □Strawberry SpecialLine; ■Strawberry Korott; ; ●Chocolate Korott; ▲Cappuccino Korott.

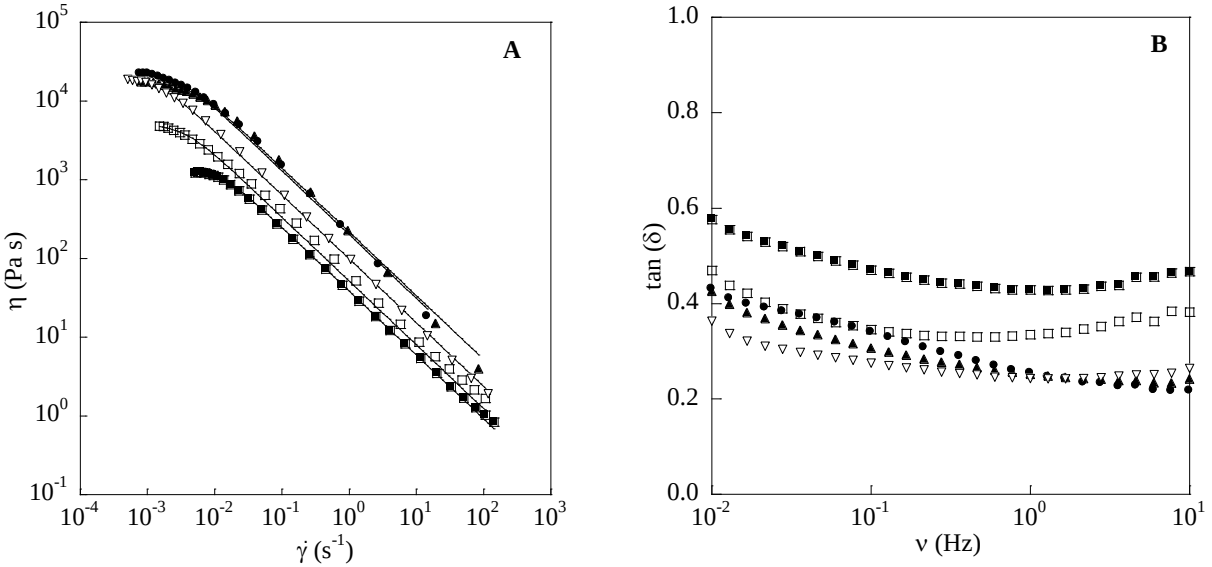

FIGURE 2. A) Flow curves fitted to Carreau model. B) Loss tangent versus frequency. CUSTARDS: ● Vanilla Korott**;** ■ Lemon Korott**;** ▲Chocolate Korott; □ Lemon BiManán; ▽Yogurt Cream BiManán.

Regarding to up and down curves performed in CR model, all systems measurements were fitted to Herschel Bulkley model (Fig. 1A)

$$\sigma = \sigma_0 + K\,\dot{\gamma}^n \qquad (2)$$

with the aim of estimating yield stresses. They were negligible for milkshakes, except for *Special Line* strawberry (Fig. 1B), on the contrary what happened for custards, which presented important values for these stresses (Table 1), especially for chocolate and vanilla custards.

Tarrega et al (2014) found viscosity at 100 s^{-1} and thixotropic area, S_T, were related to satiating power in semi-solid milk-based snacks[1], so we considered interesting to analyze these parameters in our custards (Table 1). Due to the differences in area enclosed by up curve, relative thixotropic areas[4] were considered (S_R). In our case it seemed that chocolate and vanilla custards could be the most satiating products, although sensory studies should be done to test it properly[4].

TABLE 1. Mean values and standard deviations of rheological parameters for milkshakes and custards.

Custards	σ_0 (Pa)	η_{100} (Pa s)	S_T (Pa s^{-1})	S_R (%)	G_1' (Pa)	m
Chocolate Korott	227 ± 12	3.08 ± 0.14	5600 ± 700	21.1	400 ± 30	0.188 ± 0.001
Vanilla Korott	184 ± 6	2.52 ± 0.06	5600 ± 500	24.1	450 ± 40	0.183 ± 0.014
Lemon Korott	42 ± 3	1.12 ± 0.05	1900 ± 500	21.1	58 ± 3	0.269 ± 0.015
Lemon BiManán	65.6 ± 0.3	1.81 ± 0.16	2600 ± 300	18.7	130 ± 10	0.220 ± 0.005
Yogurt Cream BiManán	85 ± 13	2.02 ± 0.12	2500 ± 200	14.7	350 ± 50	0.167 ± 0.003

CONCLUSIONS

The differences observed in milkshakes would be due to the hydrocolloids included in their formulation (guar gum in *Special Line*, and Xanthan gum in *Korott* –maybe in a smaller amount). These milkshakes are sold as a substitute of a meal, but although they provide the adequate amount of calories, they wouldn't have satiating power due to their low consistencies[2].

On the other hand, lemon custards (from the two brands analyzed) presented different textural properties than the rest of custards analyzed. This should be related to the preferences of consumers about texture associated to this flavor, what could determine the satiating power of the product[3].

REFERENCES AND NOTES

1. Tárrega, A.; Martínez, M.; Vélez-Ruiz, J.F.; Fiszman, S., Hydrocolloids as a tool for modulating the expected satiety of milkbased snacks. *Food Hydrocolloids*, **2014**, 39, 51-57.
2. Chambers, L.; McCrickerd, K.; Yeomans, M. R. Optimising foods for satiety. *Trends in Food Science & Technology*, **2015** ,41, 149-160.
3. Hogenkamp, P. S.; Stafleu, A.; Mars, M.; Brunstrom, J. M.; de Graaf, C. Texture, not flavor, determines expected satiation of dairy products. *Appetite*, **2011**, 57, 635-641.
4. Morell, P.; Fiszman, S.M.; Varela, P.; Hernando, I. Hydrocolloids for enhancing satiety: Relating oral digestion to rheology, structure and sensory perception. *Food Hydrocolloids*, **2014**, 41, 343-353.

P10

Rheological study on the Gofio/Aloe Vera juice system

E. García-López[1], J.F. Velázquez-Navarro[2], J. Rubio-Merino[3], F.J. Rubio-Hernández[1], A.I. Gómez-Merino[1]

[1]Departamento de Física Aplicada II, Universidad de Málaga, Málaga (Spain), [2]Departamento de Ingeniería Mecánica y Mecánica de Fluidos, Universidad de Málaga, Málaga (Spain), [3]Unidad Docente Multiprofesional de Atención Familiar y Comunitaria Distrito Málaga-Guadalhorce, Málaga (Spain)

Correspondence to: F.J. Rubio-Hernández (E-mail: *fjrubio@uma.es*)

ABSTRACT

Due to the potential application of *Aloe barbadensis Miller* (Aloe vera) plant in cosmetics, pharmaceutical and food industry, the study of its rheology has become in an important topic. Recently, many food- product producers have included it as nutritional supplement. The present study reports the rheological behavior when is associated with *Gofio*, a toasted grain mix (corn, wheat and barley) widely used in Canary Islands (Spain) diet. The samples have been prepared with *Aloe Vera* juice as the continuous phase in which Gofio is added forming a suspension. Rheological measurements were performed in order to study steady shear behavior of the samples, varying its mass percentage of Gofio from 5% to 30%. The steady shear response of the system has been analyzed through the steady shear flow curves, from which a non-Newtonian shear-thinning behavior is shown in every sample.

KEYWORDS Aloe vera juice, Gofio, Steady shear flow curves, Shear-thinning, SEM .

INTRODUCTION

Aloe Vera juice is a rich source of essential micronutrients, so it has wide applications in food, pharmaceutical and cosmetic products. Despite multiple investigations to the extracted gel of the plant, they all have been related to the study of its components and functionality, without delving into determining their rheological behavior[1]. Additionally, gofio is a basic food in Canary Islands diet. It is highly nutritious, with mealy appearance and produced primarily with wheat grains and corn which suffer different manufacturing processes, such as roasting, cooling and milling. Both products combined result in a mixture with possible food applications, besides the fact that it presents different rheological behaviours which result interesting to study by itself.

MATERIALS AND METHODS

The samples prepared for this study are composed of 3 components: plant of Aloe Vera (*Aloe Barbadensis Miller*), citric acid and canary gofio. It has been used a 3 years old plant in order to ensure that the content of polysaccharides and flavonoids reach its maximum levels[2]. The citric acid (PANREAC) was analytical grade. Finally, the canary gofio has been supplied by "Ramón Trujillo Cordero" brand. This material has been subjected to Scanning Electron Microscope (SEM), which shows that the material morphology is very similar to spherical geometry, as can be observed in the figure 1. Likewise, particles average size has been calculated by mean of computational processing images techniques, resulting in (11.6 ± 1.6) µm.

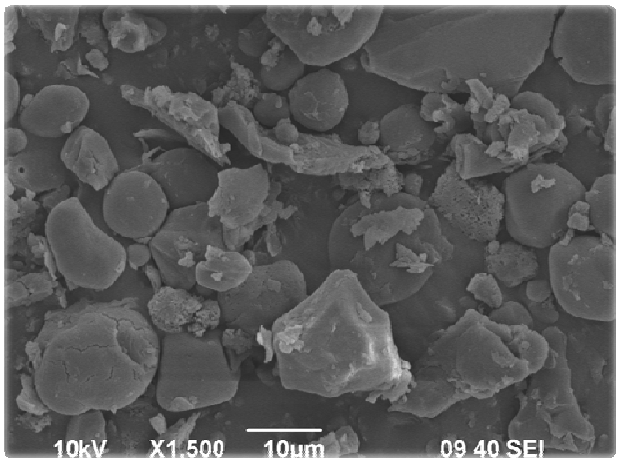

FIGURE 1. Gofio particles (SEM).

To form the dispersions a fresh and ripe leaf was cut from the Aloe Vera plant, separating the gel from the epidermis. Later, it was added an amount of citric acid equivalent to obtain a mass percentage equal to 0.089% so as to stabilize the Aloe Vera. The homogeneous mixture of these ingredients by using a beater is the medium where the gofio is going to be dispersed, supplying the necessary quantity to make dispersions of 0-30% w/w.

The rheological measurements have been carried out in a Malvern Gemini 150 rheometer (England) with coaxial cylinders geometry. The temperature has kept constant at (20.0±0.1)ºC during the experiments thanks to a Peltier system. A pre-shear protocol has been set before all the essays to ensure its repeatability and reproducibility. This protocol consists in a constant shear rate of 10 s^{-1} during 30 seconds. After this, the steady shear flow curve begins and the dispersions are subjected to a series of discrete shear rate values following a logarithmic distribution, from 0.1 s^{-1} to 200 s^{-1}.

RESULTS AND DISCUSSION

Steady shear viscosity of Gofio/*Aloe Vera* system

The results for steady shear flow curves obtained for each dispersion with different gofio %w/w is shown in Figure 2. Shear-thinning behavior is observed for all samples, being more evident and monotonous as the gofio mass percentage is greater. This behavior can be justified by the phenomena deriving from the manifestation of hydrodynamic resistance forces that arise due to displacement of gofio suspended in Aloe juice system when a shear rate is applied. These forces cause the break of the initial agglomerates into smaller aggregates, which suffer reorganization within the dispersing medium. This particles orient along the flow lines and, therefore, the apparent viscosity of the system decreases. In order to characterize the rheological properties in steady state of the suspensions of gofio in Aloe Vera, results have been fitted to Ostwald-de Waele model or power-law. This model is represented by equation (1).

$$\eta = K \cdot \dot{\gamma}^{n-1} \tag{1}$$

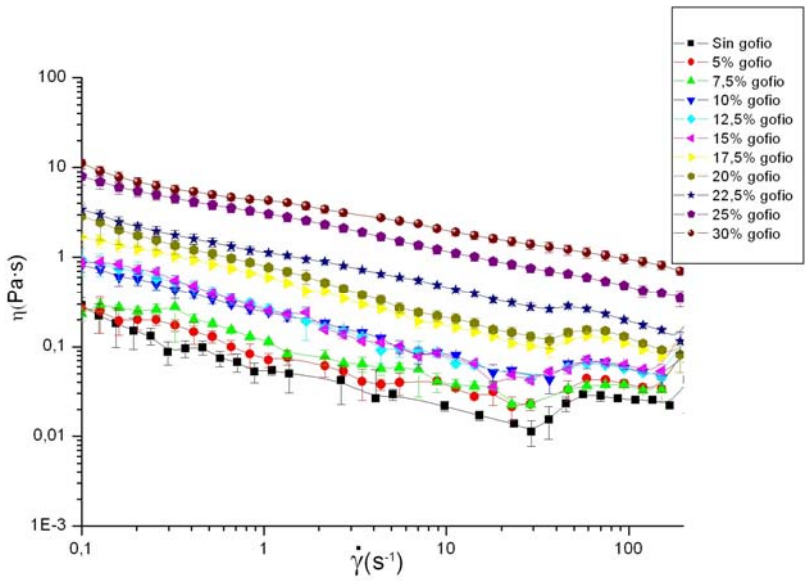

FIGURE 2. Viscosity evolution in steady flow curve

As it can be observed in the Table 1, K is higher than 1 when the gofio concentration is 22.5 %w/w or higher. As it was expected, the flow behavior index is lower than the unit in all cases, confirming the shear-thinning response for all samples. On the other hand, the larger the gofio concentration is, the higher the K values are. It is interesting to note that a small shear-thickening effect is observed in the dispersant phase, which disappears when the gofio concentration increases. Future works will be made in order to seek an explanation for this result.

TABLE 1. Ostwald de Waele parameters for different gofio-aloe juice systems.

Gofio (%w/w)	K ($Pa \cdot s^n$)	n
5.0	0.095±0.004	0.556±0.003
7.5	0.125±0.004	0.56±0.02
10.0	0.256±0.005	0.51±0.01
12.5	0.279±0.006	0.46±0.01
15.0	0.278±0.008	0.39±0.02
17.5	0.588±0.008	0.52±0.01
20.0	0.775±0.008	0.481±0.008
22.5	1.156±0.007	0.601±0.004
25.0	2.99±0.01	0.615±0.004
30.0	4.20±0.03	0.685±0.005

CONCLUSIONS

Aloe vera/gofio systems show shear-thinning behaviour for all the concentration range evaluated in this study, being satisfactory fitted by power law. This is due to the prominence of the hydrodynamics forces during shearing process.

REFERENCES AND NOTES

1. Lad, V.N.; Murthy, Z.V.P., Journal of Food Engineering, **2013**, 115, 279-284.
2. Hu, Y.; Xu, J.; Hu, Q., *Extracts*. J. Agric. Food Chem. , **2003**, 51 (26), 7788–7791.

Thermo-mechanical behavior of vegetable oils at very high shear rates

L. Goyos-Pérez[1], A.J. Pazmiño-Rentería[1], R. Delgado-García[1],
F.J. Rubio-Hernández[2], N.M. Páez-Flor[1], L.M. Carrión-Matamoros[1], A.I. Gómez-Merino[2]

[1]DECEM, Universidad de las Fuerzas Armadas, Avda. Gral. Rumiñaui s/n, Sangolquí (Ecuador) CP 170501
[2]Depto. de Física Aplicada II, Universidad de Málaga, C/Doctor Ortiz Ramos s/n, Málaga (Spain) CP 29071

Correspondence to: N.M. Páez-Flor (E-mail: *nmpaez@espe.edu.ec*)

ABSTRACT

Some experiments have been designed to discriminate the thermal and the mechanical causes of the viscosity variation of castor and coconut oils at very high shear rates. The mechanical behavior has been studied at shear rates close to $50000\ s^{-1}$ using a DH Rheometer (TA Instruments) equipped with plate-plate geometry. The temperature of the samples has been controlled with a Peltier system.

Our interest for this specific research is because these high shear rates are present in spraying processes for which we are checking several fluid materials.

It has been observed that the internal friction that develops in the material causes a rise in the sample temperature resulting in a decrease in the viscosity, which could be erroneously confused with a non-Newtonian behavior if it is assumed the process is isothermal. The comparison of the results obtained for both oils, under the same test conditions, has shown that the relevance of this behavior depends on the material. More precisely, the effect is more marked in the castor oil than in coconut oil.

KEYWORDS: straight vegetable oil, castor oil, coconut oil, viscosity, plate-plate geometry, high shear rate

INTRODUCTION

Biofuels have an important role in the future energy matrix because their renewable character and a cleaner energy perspective[1,2]. Unfortunately the viscosity of the straight vegetable oil causes combustion problems in diesel engines and burners[3-5]. Explored solutions for this problem comprise heating, blending with diesel fuel and more recently the emulsification[6-8]. All of these processes demand a precise knowledge of thermo-physical properties of the oil and its blends and emulsions to control the oil flow through the fuel system and its atomization. Different studies were performed to characterize the rheological behavior of straight vegetable oils and blends [9-11] but always limited to low shear rate values, below 5000 s^{-1}. These studies concluded the oils present a Newtonian behavior while some blends show non-Newtonian behavior[12,13]. The

present study has the aim to characterize the oils behavior under shear rates close to the atomization conditions and to establish the potential sources of erroneous behavior interpretation to properly evaluate the rheological test.

MATERIALS AND METHODS

Tests were performed using medical-grade of two oils: coconut and castor. The coconut oil was used to visualize the differences in relation with the castor oil, base of this study. The thermo-rheological properties were determined by using the rotational rheometer RH-2 Discovery (TA Instruments), with plate-plate geometry of 25 mm in diameter. Torque measurement resolution was 0.05 nNm. This configuration was able to reduce the gap till a value which ensures a shear rate value as high as 49000 s^{-1}. This configuration also minimizes the possibilities of secondary flows which could appear in the concentric cylinders and cone-plate geometries. The temperature measurement and control was performed by a Peltier device with an accuracy of ± 0.1 °C. All measurements were repeated at least three times and the results were averaged for the subsequent analysis.

RESULTS AND DISCUSSION

A flow ramp test was performed to castor oil at 20, 25, 50 and 80 ^{o}C. Results are shown in Fig. 1 (viscosity curve). Castor oil behaves as a Newtonian fluid at temperature of 80 ^{o}C, as it is expected. The slight decrease in the viscosity at the beginning of the test is probably due to the flow-out of the oil from the geometry because the little gap used and the high temperature applied. During the rest of the test there are only very small changes in the viscosity value. However, the flow ramp at 20 ^{o}C shows a continuous and significant reduction in viscosity, changing from 0.822 Pa·s to 0.433 Pa·s. This viscosity reduction could be erroneously confused with shear thinning behavior[14]. The explanation we propose for this result lies in the characteristics of the test itself and the density of the oil. Certainly, the “isothermal test” is not really isothermal. The equipment ensures the temperature settled only in the surroundings of the Peltier device or, in a most specific manner, in the surroundings of the temperature sensor position. As well a zone is far away from this position the possibility of a different temperature increases. This risk may be negligible under typical gaps values but, when an extremely little gap

is used to achieve high shear stress rate, the risk can becomes greater. Additionally, the use of a high stress rate test on high density fluids enhances the internal friction forces in the fluid and increases the temperature in zones not contiguous to the Peltier device.

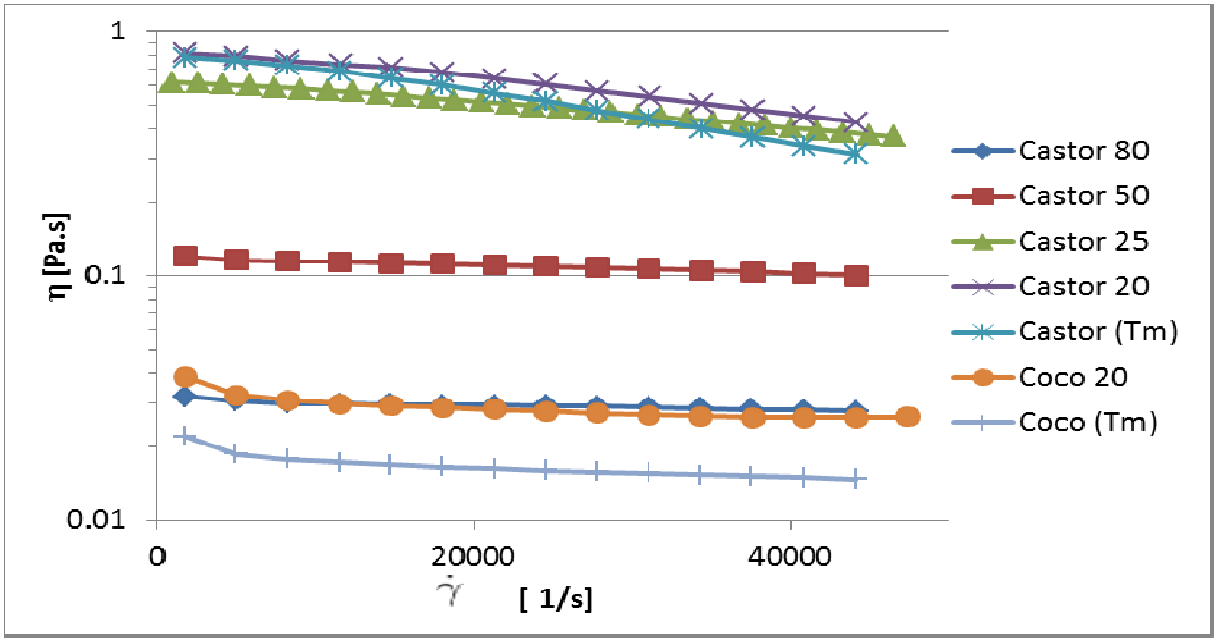

Figure 1. Steady viscosity curve for castor and coconut oils.

To confirm this hypothesis a non-controlled temperature test (Tm) was performed. This test started at room temperature (21 ^{o}C) and has been performed in the same way the isothermal one but without any temperature control. The Peltier device only limited to record the temperature of the sample during the test. Results obtained for coconut and castor oils are over imposed in Figure 1. During this test the temperature of the castor oil increased continuously and finally reached a value of 26.7 ^{o}C. The viscosity drops to a value of 0.273 Pa·s, slightly lower than the value corresponding to the 25 ^{o}C isothermal flow test, which is coherent with the temperature dependence of the viscosity of a liquid. This agreement between the isothermal and non-isothermal tests eliminates the possibility to think about a behavior intrinsically dependent of the fluid status and enhances the role of the temperature increase in the behavior.

The same test was performed using coconut oil. Results are over imposed in the Figure 1. The behavior of coconut oil when an isothermal test at 20 ^{o}C is applied evidences the expected Newtonian behavior. The non-controlled temperature test shows, however, the same Newtonian

behavior but reflects an increase of the temperature in the sample (around 2 ^{o}C). This different result is due to that there was no remarkable internal friction because the lower density of the coconut oil.

CONCLUSIONS

A flow ramp test was performed to castor oil at 20, 25, 50 and 80 ^{o} C. The flow ramp at 20 ^{o}C shows a continuous and significant reduction in viscosity which could be erroneously confused with shear thinning behavior. We have justified this result showing that the assumed "isothermal test" is not really isothermal. This hypothesis has been confirmed making a non-controlled temperature test with castor oil and also with coconut oil. These results have lead to the main conclusion of this work, i.e. the assumption of "isothermal test" in shear rheometry tests at very high shear rates is wrong. This result is enhanced in materials with a higher density value.

ACKNOWLEDGEMENTS

The authors acknowledge the contribution of Programa Prometeo, SENESCYT, by the scholarship granted to L.G.P.

REFERENCES

1 A. K. Hossain, P. A. Davies, *Renewable Energy* **2010**, *35*, 1-13.
2 A. S. Ramadhas, S. Jayaraj, C. Muraleedharan, *Renewable Energy* **2004**, *29*, 727–742.
3 J. Galle, S. Verhelst, R. Sierens, L. Goyos, R. Castaneda, M. Verhaege, L. Vervaeke, M. Bastiaen, *Biomass & Bioenergy* **2011**, doi:10.1016/j.biombioe.2012.01.041.
4 R. D. Misra, M. S. Murthy, *Renewable and Sustainable Energy Reviews* **2010**, *14*, 3005-3013.
5 S. Nettles-Anderson, D. Olsen, *SAE Tech. Paper Ser.* **2009**.
6 E. A. Melo-Espinosa, R. Piloto-Rodríguez, L. Goyos-Pérez, R. Sierens, S.Verhelst, *Renewable and Sustainable Energy Reviews* **2015**, *47*, 623–633.
7 S. Bajpai, P. K. Sahoo, L. M. Das, *Fuel* **2009**, *88*, 705–711.
8 S. Bari, T. H. Lim, C. W. Yu, *Renewable Energy* **2002**, *27*, 339-351.
9 L. M. Diamante, T. Lan, *Journal of Food Processing* **2014**, *2014*, Article ID 234583, 6 pages.
10 B. Esteban, J.-R. Riba, G. Baquero, A. Rius, R. Puig, *Biomass and bioenergy* **2012**, *42*, 164-171.
11 H. Yalcin, O. S. Toker, M. Dogan, *Journal of Oil Science* **2012**, *61*, 181-187.
12 W. W. Focke, L. Moyo, F. J. W. J. Labuschagne, N. G. Hoosen, S. Ramjee, M. Saphiannikova, *Colloids and Surfaces A: Physicochemical and Engineering Aspects* **2014**, *443*, 391–397.
13 C. Bower, C. Gallegos, M. R. Mackley, J. M. Madiedo, *Rheol. Acta* **1999**, *38*, 145-159.
14 C. J. Pipe, T. S. Majmudar, G. H. McKinley, *Rheol. Acta* **2008**, *47*, 612–642.

P12

Rheological characteristics of chia - flaxseed composite paste

F.G. Gómez-Merino[1], J. Aguiar, J.M. Jiménez-Delgado[1], J. Rubio-Merino[3], N.M. Páez-Flor[2], A.I. Gómez-Merino[1], F.J. Rubio-Hernández[1]

[1]Departamento de Física Aplicada II, Universidad de Málaga, Málaga (Spain) CP 29071

[2]DECEM, Universidad de las Fuerzas Armadas, Sangolquí (Ecuador) CP 170501

[3] Unidad Docente Multiprofesional de Atención Familiar y Comunitaria Distrito Málaga-Guadalhorce, Málaga (Spain)

Correspondence to: A.I. Gómez-Merino (E-mail: *aimerino@uma.es*)

ABSTRACT

The flow and viscoelastic characteristics of chia-flaxseed composite paste were determined. Moreover, the effects of pH (4.4-5.5) and olive oil concentration (0-0.5) on rheology and physical stability of the resulting emulsions were studied. Oscillatory measurements showed that the mixture exhibited gel-like behaviour.

KEYWORDS: Functional food, Flaxseeds, Chia seeds, Hydrocolloids, Rheology

INTRODUCTION

Due to the increased awareness of consumers towards health; a demand for functional foods has risen dramatically. Flaxseed (Linum usitatissimum) and Chia (Salvia hispanica L.) seeds are used as a potential source for functional food due to its unique nutrient profile. Chia seeds are composed of proteins, lipids, carbohydrates and have high fiber content. These seeds contain a large amount of antioxidants, minerals and vitamins. Both chia and flaxseeds are rich in polyunsaturated omega-3 and omega-6 fatty acids, which constitute the central nervous system, total fatty acids, α-linolenic acid (ALA)[1].

Hydrocolloids are a diverse group of long-chain polymers that are readily dispersive, fully or partially soluble, and prone to swell in water. They change the physical properties of the solution to form gels, or enable thickening, emulsification, coating, and stabilization[2]. The aim of the present work is to characterize the rheological properties of chia-flaxseed composite paste as a possible substitute of eggs, yoghurt, etc. or to enhance the nutritional and sensorial properties

of foods. The effect of some conditions such as olive oil concentration, pH, and ionic strength was evaluated.

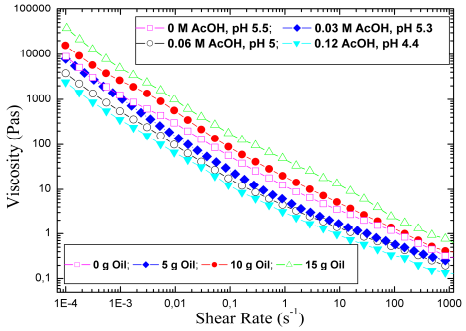

Figure 1. Viscosity curve of the chia-flaxseed composite paste.

MATERIALS AND METHODS

Commercially ecological chia and flaxseed were used in this study. The content of chia was: fat 31.0 % (omega-3-18.6%) ; protein 20.0, carbohydrates 39.9 %; salt content 0.04 %; and flaxseed was: fat 42.2 %; carbohydrates 28.8%; protein 18.3 %; salt content 0.0075; milled chia-flaxseed particles presented a size distribution between 200-1000 μm, obtained by DLS measurements. Samples were prepared by mixing 250 g of chia:flaxseed (1:1) composite flour in 20 ml of deionised water. The mixture was stirred for two hours at 500 rpm. For all samples 1M of NaCl was added and the influence of acetic acid and olive oil was tested. The resulting paste was left overnight stored at 4 ºC. Rheological experiments were carried out with a Peltier system for the control of the temperature, on a MARS III (Thermo-Haake, Germany) using a plate-plate sensor system with a diameter of 20 mm. Experiments were conducted under steady shear. Flow curves were conducted under steady shear. Strain sweep was performed to determine the linear viscoelastic region at 1 Hz. Frequency sweep was carried out at a range of 0.01-10 Hz. Three measurement replicates were recorded for each sample. All measurements were performed at 25.0±0.1 ºC.

RESULTS AND DISCUSSION

It has been described elsewhere a tentative structure of the basic unit of the chia polysaccharide (Lin et al. (1994)) as a tetrasaccharide with 4-O-metil-α-D-glucoronopyranosyl residues occurring as branches of β-D-xylopyranosyl on the main chain and the flaxseed mucilage components[3] as pectic-like polisaccharides containing L-rhamnose, D-galactose and D-galacturonic acid as well as β-D-1,4-xylan backbone of the arabinoxylan component. When the composite milled seeds are in contact with water the mucilage small filaments appear as a completely developed filiform structure which is uniformly distributed forming a framework where other molecules could be coupled[4]. Fig. 1 shows the viscosity curve of the chia-flaxseed

composite paste. In all cases [NaCl] 1 M was added and the total volume of the liquid phase was kept constant. It exhibits pseudoplastic flow behaviour, as described elsewhere[5]. Besides, the oil

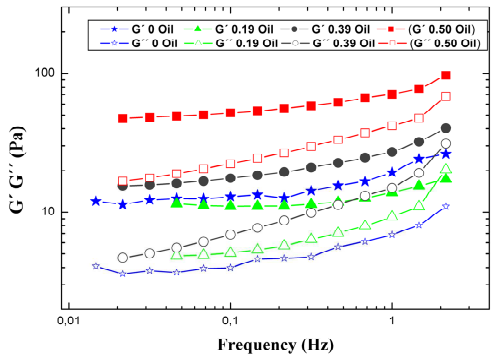

Figure 2. Frequency sweep, γ=0.05. Oil addition effect.

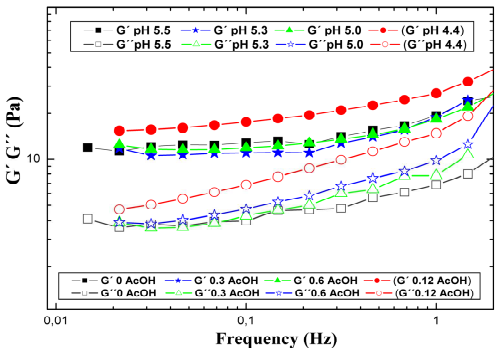

Figure 3. Frequency sweep, γ=0.05. pH effect.

addition leads to an increase in the viscosity of the paste. This result is reasonable because the water-oil emulsion increments the system viscosity. Although rigid hydrocolloids are not considered classical emulsifiers they can be regarded as stabilizers due to their hydrophilicity, high molecular weight and gelation behavior. However, they retard precipitation of dispersed solid particles and coalescence of oil droplets[3]. Therefore, the increasing of viscosity can be tentatively explained considering the mucilage structure as the framework in which the oil drops are trapped. The proteins present in chia and flaxseed can possess flexible molecular structures (spheroproteins) which, when denatured, result in rapid adsorption and rearrangement at the interface to give a coherent macromolecular protective layer surrounding the oil drop and preventing coalescence. But when the amount of oil increases and the continuous phase is olive oil the hydrocolloid gel structure is not able to trap all the available oil drops and the emulsion becomes unstable. On the other hand, the addition of acetic acid affects also the viscosity of the paste. Thus, from Fig 1, the pH effect can also be observed. It was always kept under the protein isoelectric point (IEP), pH 7, which promotes the system stability. The less viscous paste corresponds to the lowest pH value, 4.4. The explanation of this behaviour resides in the higher charge of the protein molecules due to the protonation of the carboxyl group which facilitate its emulsifier action. As a result, rigid gels are formed at acidic pH values. In some cases, denaturation can be shifted to lower temperatures with decreasing pH. Another interesting result is the compatibility of protein-hydrocolloid even at high ionic strength, 1 M NaCl. Figs. 2 and 3 depict the frequency sweep in the linear elastic region of the same samples shown in Fig.1. In all

cases a gel-like structure is formed since the elastic modulus is always greater than the loss modulus. In fact, it is the emulsion structure and in this case the system is weakly structured. Fig. 2 compares the influence of the olive oil addition to the mixture. Despite the rheological characteristics of the tested samples are quite similar to that of chia-flaxseed composite the increase of olive oil reinforces the gel-like structure until the limit of the emulsion stability. In this system, oil volume fractions higher than 0.5 make the mixture unstable. Likewise, the pH slightly modifies the elastic properties of the mixture. But if a denaturation of the proteins occurs an increase in the elastic modulus, G´, will be expected[6]. Therefore, according to Fig. 3 moderate conditions of pH and ionic strength do not considerably affect the elastic properties of this system.

CONCLUSIONS

The flow behaviour and microstructure characterization of the chia-flaxseed composite paste as a possible functional food was studied. The addition of olive oil, sodium cloride and acetic acid (pH) was examined for different purposes: salad dressing, beverages, egg white replacement, etc. Under the pH and olive oil volume fraction conditions studied a good compatibility of the different components (hydrocolloids and proteins) was found.

Although this previous work suggests promising results a more detailed study should be carried out in order to get better knowledge of the different processes that take place during mixing components, heating, etc. Under this point of view temperature influence as well as interface and spectroscopic studies will be considered.

REFERENCES

1. Ayerza, R.; Coates, W., *Tropical Science,* **2004,** *44*, 131–135.
2. Pin, J.M.; Nie, S.P., *Food Hydrocolloids*, **2015**, doi:10.1016/j.foodhyd.2015.01.035
3. Cui, W., Mazza G.; Biliaderis C.G., J. *Agric. Food Chem.*, **1994**, *42*, 1891–1895.
4. Muñoz, L.A.; Cobos A.; Diaz, O.; Aguilera, J.M., *Journal of Food Engineering,* **2012**,*108,* 216-224.
5. Qian, K.; Cui, S.; Wu, Y.; Goff, H., *Food hydrocolloids*, **2012**, 28, 275-283.
6. Nishinari, K.; Fang, Y.; Guo, S.; Phillips, G. O., *Food Hydrocolloids*, 2012, *39*, 301-318.

Acorn bread development – texture characterization

Nuno Alvarenga[1,2], Bruno Nunes[1], Nuno Burrica[1], Bárbara Candeias[1], Neide Loução[1] João Dias[1] e Maria João Carvalho[1]

[1]*IPBeja - Escola Superior Agrária Rua Pedro Soares, 7801-902 Beja – Portugal*

[2]*LEAF – ISA-UL, Tapada da Ajuda, 1349-017 Lisboa, Portugal*

Correspondence to: Nuno Alvarenga (bartolomeu.alvarenga@ipbeja.pt)

ABSTRACT

In Portugal, bread is a food historically indispensable on daily diet, present in all regions, under different recipes. Since acorn it's a product that isn't much used in human diet, was decided to produce a different type of bread. It were produced three types of bread: one with 25% of acorn flour and 75% of wheat flour with 1.5% of salt (Sodium chloride), a second one with 50% of acorn flour and 50% of wheat flour with 1.5% of salt, and a third one with 50% of acorn flour and 50% of wheat flour with 2.0% of salt. So the main goal was to compare the differences between the breads with different acorn flour percentages and how the salt could affect the bread, mainly its texture, nutritional and hedonic sensory analysis. Nutritionally it's possible to find some differences between moisture and proteins content in all breads ($P<0.05$). The driest bread was the bread with 2.0% of salt and the bread with more water was the bread with 50% of acorn flour with 1.5% of salt. The bread with 25% of acorn flour had the highest protein content, due to the high content on wheat flour. Analysing the color, the bread with 25% of acorn flour is the lighter bread, but there are no significate difference between this one and the bread with 2% of salt, as expected. In terms of the breads rheology behaviour, it's possible to see that the bread with 25% of acorn flour was the softest of all three breads, with a 9.90 N of hardness and only 56.31 N.mm of compression work. Comparing the breads with 50% of acorn bread, it's possible to see that the bread with 2.0% of salt was harder than the bread with 1.5% of salt. The compression work was also higher in the bread with 2.0% of salt than the bread with 1.5% of salt. Finally, the bread with more sensory acceptance was the bread with 50% of acorn flour and with 1.5% of salt.

KEYWORDS: Acorn, Bread, Rheology, Sensory Analysis, Salt

INTRODUCTION

Worldwide bread consumption accounts for one of the largest consumed foodstuffs, it's over 20 billion pounds (9 billion kg) of bread being produced annually [1]. In Portugal, bread is a food historically indispensable on daily diet, present in all regions, under different recipes, manufacturing, shapes and flavour. The whole wheat bread offers a substantial amount of mineral salts and fibres, because of economical and nutritional

reasons, with a constant increase of consumption [2]. Wheat is a very important cereal crop for human food production. This reflects the unique ability of wheat flour to produce viscoelastic dough when it is mixed with water. The principal characteristic that governs the wide usage of wheat flour is the viscoelasticity of the gluten network formed by its major protein fractions: the polymeric glutenins and the monomeric gliadins [3]. The structure of gluten proteins and their interactions can also be affected by solvent environment upon hydration, including the presence of salt. This is because salt acts as a co-solute and influences the hydration of wheat proteins and starch under the particular moisture conditions during the manufacture of a diverse range of products including bread, breakfast cereal, pasta, and Asian noodles [3]. Salt plays an important role in baked dough products and related processes. It is generally used at levels of about 1–2% (based on flour weight), and acts as a flavour enhancer and as stabilizer for the yeast fermentation rate, but it also plays an important role in baked dough products. Up until now, most of the studies have been focused on the effects of salt on the rheological properties of wheat flour dough, however, it seems that firstly, salt affects the formation of the gluten network during the initial hydration of the gluten proteins when wheat flour is mixed with water and then the rheological properties as a result of the gluten network formed in the presence of salt [3]. Acorn have been a part of the local diet for some time, furnishing up to 25% of the food consumed by the poorer classes of Italy and Spain, and are consumed in the form of bread cake and as a coffee substitute [4]. The use of acorn in local diet and empirical treatment of some human diseases such as diarrhea can be use by some people, like the Iranians, but due to its bitter constituents, wooden texture and astringent taste, acorn is scarcely used in normal diet. However, it's wide spread availability and empirical use for medical purposes suggest some possibilities of using acorn in food and drug industries [5]. Analysing the microstructure of rehydrated water-wash (WW), salt-wash (SW) and fresh wet gluten, the gluten network formed when NaCl was used in the mixing of the flour, a fibrous structure was observed in contrast to those without NaCl for which large aggregates of gluten were seen. This study also showed, by dynamic oscillatory rheology, that the gluten structure exhibited relatively less elastic behaviour or more viscous behaviour when gluten was prepared in presence of NaCl [3].

The sensory quality of bread, an important component of total product quality, can be evaluated by analytical (objective) methods, namely with texture instrumental methods, however, it's also required a well-trained testing panel and the use of specific and

adequate attributes that are easily perceived and differentiated for different bread samples [6]. So the main goal of this project was to see and compare the differences between the breads with different acorn flour percentages and how the salt could affect the bread, mainly its texture, nutritional and hedonic sensory analysis.

MATERIAL AND METHODS

It were produced three types of bread: one with 25% of acorn flour and 75% of wheat flour with 1.5% of salt (Sodium chloride), a second one with 50% of acorn flour and 50% of wheat flour with 1.5% of salt, and a third one with 50% of acorn flour and 50% of wheat flour with 2.0% of salt. The hedonic method was carried out in a single day and the subjects were asked to rate each sample using a numerical scale with the extremes from 1- "Extremely disliked" and 9 - "Extremely liked" [7]. In this sensory session it was tend to be perceived in the following order: appearance, color, crust hardness, crumb texture and flavour [8].

A texture analyser TAHD*i* (Stable Micro Systems, Godalming, UK), equipped with a 250 N load cell, was used to perform the texture analysis at 20±1 °C. The procedure was implemented by slices of 20 mm compression, with a 20 mm diameter aluminium cylindrical probe, being the depth of compression 10mm. The crossed speed was 1mm s^{-1}. Texture measurements were performed in quintuplicate. Hardness values were obtained from the force vs. time texturograms [9].

RESULTS DISCUSSION

Nutritionally it's possible to find some differences between moisture and proteins content in all breads ($P<0.05$). The driest bread was the bread with 2.0% of salt and the bread with more water was the bread with 50% of acorn flour with 1.5% of salt. Related with proteins content the bread with 25% of acorn flour had the highest content, due to the high content on wheat flour. Relatively to ash content, fat, fibre and carbohydrates there are no significate difference in all three breads. Analysing the color, the bread with 25% of acorn flour is the lighter bread, but there are no significate difference between this one and the bread with 2% of salt, as expected. In terms of the breads rheology behaviour, it's possible to see that the bread with 25% of acorn flour was the softest of all three breads, with a 9.90 N of hardness. Comparing the breads with 50% of acorn flour, it's possible to see that the bread with 2.0% of salt was harder than the bread with

1.5% of salt (Figure 1a) but the bread with 50% of acorn flour and with 1.5% of salt The most accepted in sensory analysis (Fig 1b).

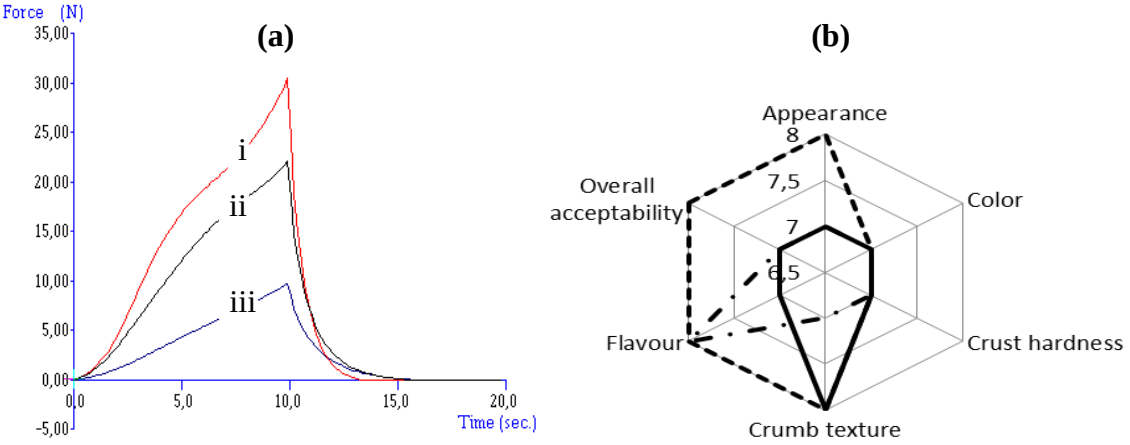

Figure 1. (a) Texture profile and (b) sensory analysis of breads with i) 50% of acorn flour and 2% salt ——— PB50%/2,0%, ii) 50% of acorn flour and 1.5 % salt - - - - PB50%/1,5% and iii) 25% of acorn flour and 1.5 % salt — · — PB25%/1,5%.

CONCLUSIONS

In terms of the breads rheology behaviour, it's possible to see that the bread with 25% of acorn flour was the softest of all three breads. Comparing the breads with 50% of acorn bread, it's possible to see that the bread with 2.0% of salt was harder than the bread with 1.5% of salt. Finally, the bread with more sensory acceptance was the bread with 50% of acorn flour and with 1.5% of salt.

REFERENCES

[1] – Heenan, S., Dufour, J., Hamid, N., Harvey, W., Delahunty, C. (2008). *Food Research International*, **41** 989-997

[2] – Battochio, J., Cardoso, J., Kikuchi, M., Macchione, M., modolo, J., Paixão, A., Pinchelli, A., Silva, A., Sousa, V., Wada, J., Wada, J., Bolini, H. (2006). *Ciênc. Tecnol. Aliment.*, **26** 428-433

[3] – Tuhumury, H.C.D., Small.D.M., Day. L. (2014). *Journal of Cereal Science*, **60** 229-237

[4] – Rakić, S., Povrenović, D., Tešević, V., Simić, M., Maletić, R. (2006). *Journal of Food Engineering*, **74** 416-423

[5] – Tadayoni, M., Sheikh-Zeinoddin, M., Soleimanian-Zad, S. (2015). *International Journal of Biological Macromolecules*, **72** 179-185

[6] – Callejo, M., Vargas-Kostiuk, M., Rodríguez-Quijano, M. (2015). *Journal of Cereal Science*, **61** 55-62

[7] M. Laureati B. Giussani, E. Pagliarini (2012). *Food Research International* **46** 326–333.

[8] – Kihlberg, I., Öström, Å., Johansson, L., Risvik, E. (2006). *Journal of Cereal Science*, **43** 15-30.

[9] – Alvarenga, N., Canada, J. Sousa, I. (2011). *Journal of Dairy Research*, **78** 80–87.

P14

Effect of chia flour addition on rheological behaviour of quinoa flour dough

F.G. Gómez-Merino[1], J. Aguiar, J.M. Jiménez-Delgado [1], J. Rubio-Merino[3], N.M. Páez-Flor[2], A.I. Gómez-Merino[1], F.J. Rubio-Hernández[1]

[1]Departamento de Física Aplicada II, Universidad de Málaga, Málaga (Spain) CP 29071

[2]DECEM, Universidad de las Fuerzas Armadas, Avda. Gral. Rumiñaui s/n, Sangolquí (Ecuador) CP 170501
[3] Unidad Docente Multiprofesional de Atención Familiar y Comunitaria Distrito Málaga-Guadalhorce,Málaga (Spain)
Correspondence to: A.I. Gómez-Merino (E-mail: *aimerino@uma.es*)

ABSTRACT

The flow and viscoelastic properties of quinoa-chia flour for bread making were studied. The addition of chia flour was 5, 10, 20 and 30 % of the solid weight. The viscosity of the mixtures was higher than the wheat dough. Oscillatory measurements showed that the doughs with chia presented gel-like behaviour due to its elastic properties. Compared to quinoa this formulation exhibited an increase in the volume and good sensory acceptance.

KEYWORDS: Functional food, Quinoa, Chia seeds, Hydrocolloids, Rheology

INTRODUCTION

Quinoa (*Chenopodium quinoa* Willd.), which is considered a pseudocereal or pseudograin, has been recognized as a complete food due to its protein content (15%) but also from its great amino acid balance. Besides, it is an important source of minerals, vitamins, polyphenols, phytosterols, and flavonoids with possible nutraceutical benefits. For that reason and for the absence of gluten, quinoa has recently been used as a novel functional food[1]. But the absence of gluten, in these flours, results in major problems for many pasta and bakery products. Attempts to use proteins from alternative flours as a partial substitute in wheat products have generally been unsuccessful, accounted for the viscoelastic properties of wheat gluten proteins. Hydrocolloids are a diverse group of long-chain polymers that are readily dispersive, fully or partially soluble, and prone to swell in water and can form gels, or enable thickening, emulsification, coating, and stabilization. Chia (Salvia hispanica L.) seeds are used as a potential source for functional food due to its unique nutrient profile. It contains proteins, lipids,

carbohydrates, high fiber content (hydrocolloids) and polyunsaturated omega-3 and omega-6 fatty acids. The main objetive of this work is to study the rheological characteristics of quinoa-chia for bread making. Thus, steady shear and dynamic oscillatory tests were performed.

MATERIALS AND METHODS

Commercially ecological chia seeds were used in this study. The content of chia is: fat 31.0% (omega-3-18.6%); protein 20.0%, carbohydrates 39.9 %; salt content 0.04 %. Commercially ecological quinoa flour has protein 20.0%, carbohydrates 60.8 %; fat 5% and fiber 6.6 %. Samples with different content of chia flour were prepared mixing a certain amount of chia flour in 10 ml of deionised water. The mixture was stirred for two hours at 500 rpm until the mucilage was released. An adequate amount of quinoa flour was added until 8.5 g of solid was completed and stirred for 2 more hours. The resulting dough was left overnight and stored at 4 ºC. The samples contained 5, 10, 20 and 30 % of chia flour. Rheological experiments were carried out with a Peltier system for the control of the temperature, on a MARS III (Thermo-Haake, Germany) using paralel plate (serrated) sensor system with a diameter of 20mm. Flow curves were conducted under steady shear. Strain sweep was performed to determine the linear viscoelastic region at 1 Hz. The frequency sweep was carried out at a range of 0.01-10 Hz. Three measurement replicates were recorded for each sample. All measurements were performed at 25.0±0.1 ºC.

RESULTS AND DISCUSSION

The rheological behaviour of gluten dough depends on its composition and microstructure i.e. spatial arrangement of its constituents. Dough development involves the hydration of gluten protein, the predominant fraction controlling the viscoelastic properties of dough. A very simplified model of gluten at the molecular level consists of two classes of protein: linear proteins, glutenins, and globular proteins, gliadins, which can be represented as spheres. The linear proteins interact with each other via the loop and train mechanism and by disulphide bonding[2]. As a first approximation, the chains are imagined to interact with the globular proteins by non-bonding forces such as Van de Waals interactions. During mixing, glutenins tend to align and form cross-links between gliadins molecules, leading to an increase in dough strength. The amount of glutenin in flour was found to be positively correlated with dough strength while

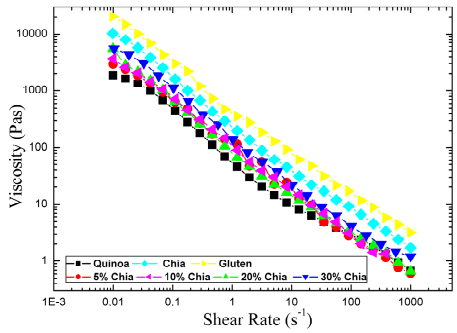

Figure 1. Viscosity curve of quinoa-chia dough.

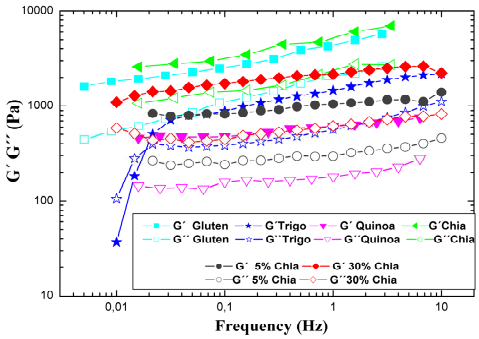

Figure 2. Frequency sweep, γ=0.05.

gliadin promotes elongational resistance and dough extensibility. The hydrated gluten protein network provides a framework for holding starch granules and trapping air cells. Wheat flour dough is regarded as a composite material of starch granules embedded in a continuous gluten protein network, which confers viscoelastic properties. However, quinoa proteins are mainly globulin or spheroproteins (70 % of total proteins) which do not provide dough elasticity. Chia seeds contain a significant quantity of oil as a linolenic acid (omega 3) and also dietary fiber, a polysaccharide with a high molecular weight. A tentative structure of the basic unit of the polysaccharide was proposed by as a tetrasaccharide with 4-O-metil-α-D-glucoronopyranosyl residues occurring as branches of β-D-xylopyranosyl on the main chain. Immediately the milled seeds are in contact with water, small filaments appear on the surface that began to stretch slowly until they become fully extended. When the seeds are totally hydrated, these filaments (mucilage fibers) are completely developed in a filiform structure which is uniformly distributed forming a framework where other molecules, i.e. globulins, starch, etc. can be trapped[3, 4]. The presence of elongated branched aggregates results in an increasing of the system viscosity. Fig. 1 shows the viscosity curves of the different tested samples. Considering the microstructure above explained, the high viscosity of gluten can be easily explained due to the solid-like behaviour of the gluten protein network. Chia mucilage has a similar rheological behaviour to gluten although is not as rigid as gluten. This characteristic improves the texture quality of the dough. As we can see in this figure, wheat dough is less viscous than gluten or chia and quinoa-water paste is the least viscous, for the same solid concentration. Actually, the viscosity of the mixtures quinoa-chia is in the suitable values taking into account that chia needs water to release the mucilage. Therefore, for commercial purposes, in the mixtures quinoa-chia, for the same solid quantity, more water should be added to prepare the dough. The results of the strain sweep are shown in Table 2. Gluten has the largest linear elastic region and the highest crossover stress value, which is

consistent with its elastic solid-like behaviour. On the other hand, quinoa flour exhibits the smallest values of these parameters as a consequence of the major content of spheroproteins in its microstructure which do not provide elastc properties to the dough. Fig. 2 shows the frequency sweep of the different doughs. Gluten and chia display similar values of the elastic and viscous moduli while quinoa shows the smallest values. In all cases, the elastic modulus (G´) is higher than the viscous modulus (G´´). But wheat flour presents a cross point at low frequencies in which G´´ exceeds G´, in agreement with the Maxwell elastic model. The mixtures quinoa-chia display values of G´ and G´´ between those exhibited by quinoa and chia, as it can be expected[5,6]. The explanation of this fact can be found in the interaction of the hydrocolloid filiform framework with the spheroproteins and starch present in quinoa flour giving place to a more consistent cross-linked structure.

TABLE 1. Strain sweep at 1 Hz

	Quinoa	5% Chia	10% Chia	20% Chia	30% Chia	Chia	Wheat	Gluten
$\gamma_{linear\text{-}limit}$ (10^{-4}) (-)	39.5±0.1	46.3±0.1	(41.2±0.1)	(46.5±0.1)	(55.9±0.1)	46.6±0.1	69.2±0.1	315±1
$\tau_{crossoverpoint}$ (Pa)	18.5±0.2	20.8±0.2	43.8±0.2	61.2±0.2	81.5±0.2	115.4±0.2	23.8±0.2	15330±1

CONCLUSIONS

The flow properties of quinoa-chia dough were studied. In all the tested samples, the elastic properties of the resulting dough were improved. After baking, the addition of chia increased the volume of the loaf and exhibited good sensory acceptance. In future work the temperature influence as well as salt addition and flavour enhancers will be considered.

REFERENCES

1. Lilian E. Abugoch J., *Advances in Food and Nutrition Research*, ***2009***, *58 1-31.*
2. Shewry, P-S.; Popineau, Y.; Lafiandrax, D.; Belton, P., *Trends in Food Science & Technology 11,* 2001, 433–441.
3. Muñoz, L.A.; Cobos A.; Diaz, O.; Aguilera, J.M., *Journal of Food Engineering,* **2012**, *108,* 216–224.
4. Nishinari, K.; Fang, Y.; Guo, S.; Phillips, G. O., *Food Hydrocolloids*, 2012, *39*, 301-318.
5. Qian, K.; Cui, S.; Wu, Y.; Goff, H., *Food hydrocolloids*, **2012**, 28, 275-283.
6. Lamacchia, C.; Chillo, S.; Lamparelli, S.; Suriano, N., La Notte, E.; Del Nobile, M. A., *Journal of food engineering*, **2010**, *96*, 97-106

Influence of Modified Atmosphere Packing in texture of a typical Portuguese whey cheese cake "queijadas"

Nuno Alvarenga[1,2], Sara Nunes[1], Manuela Costa[1], Carlos Ribeiro[1] e Maria João Carvalho[1]

[1]*IPBeja - Escola Superior Agrária Rua Pedro Soares, 7801-902 Beja – Portugal*

[2]*LEAF – ISA-UL, Tapada da Ajuda, 1349-017 Lisboa, Portugal*

Correspondence to: Nuno Alvarenga (bartolomeu.alvarenga@ipbeja.pt)

ABSTRACT

The objective of this work, was determinate the shelf life of a typical Portuguese whey cheese cake named "Queijadas" produced with ewe's whey cheese, honey and lemon. After manufacture of samples, Modified Atmosphere Packaging (MAP) was used, with different gases, like CO_2, N_2 and O_2 on samples, in two different storages temperatures (20ºC and 26ºC). During 30 days it was studied the water activity, the texture, the microbiology, moisture, ash content, fat content, protein, fiber, the level of O_2 and CO_2 on the different samples in different modified atmosphere packaging and the sensory analysis to see the overall acceptability from the consumers. In this work it will be emphasized the texture and sensory analysis. It was concluding that the suitable modified atmosphere packaging was the CO_2 for 22 days of storage at 20ºC, which allowed to stablish its shelf life, since this sample showed more acceptance and hardness stability, during the time of work. It is important to remark that the only samples that preserved the textural and sensory quality during 30 days were the samples packed in MAP with CO_2 (at 20 and 26 ºC).

KEYWORDS: "Queijadas", Modified Atmosphere Packaging (MAP), Water Activity, Texture and Sensory Analysis

INTRODUCTION

In the last few years there had been a huge research of traditional products made with raw materials from each region, and one of those final products applications can be for instance cakes manufacturing. Cakes are baked products highly appreciated by the consumers worldwide, being characterized by a dense, tender crumb and sweet taste [1]. Among several traditional recipes from Alentejo province, there are specific cakes named "Queijadas" which are considered stuffing cakes, being the stuff made with whey cheese and eggs. These ingredients make those cakes very perishable, which fact led to one of this research study goals, the evaluation of shelf life in different Modified Atmosphere Packaging (MAP) at different storage temperatures. MAP may be defined as 'the enclosure of food products in gas-barrier materials, in which the gaseous environment has been changed' [2] in order to inhibit spoilage agents and therefore

either maintain a higher quality within a perishable food during its natural life or actually extend the shelf-life. This technique was specifically designed to overcome some of the problems associated with (or in fact caused by) vacuum packaging, namely to inhibit a wider range of microbiological spoilage agents and avoid compression damage. With vacuum packaging the products are usually chill stored to maximise the inhibitory effect. Three gases are generally used-oxygen (O_2) nitrogen (N_2) and carbon dioxide (CO_2), each of which has a specific function.

Texture is defined as the attributes of a substance resulting from a combination of physical properties and perceived as the senses of touch, sight and hearing and the evaluation of the foods texture is driven in the cause of mastication [3]. A product texture can be evaluated by physicochemical properties measured objectively and by sensory methods, and thus the relationship between consumer preferences and rheological properties of foods is a key part of the science of rheology [4]. The objective of this work, was to develop a typical Portuguese whey cheese cake named "Queijadas" produced with ewe's whey cheese, honey and lemon and research the influence of package time and conditions in texture and acceptability.

MATERIAL AND METHODS

These "Queijadas" were considered stuffing cakes, being the stuff made with traditional ewe's whey cheese and eggs, which make it very perishable. Due to rights of enterprise, the formula cannot be reported. After samples manufacture, Modified Atmosphere Packaging (MAP) was used, with different gases mixtures of CO_2, N_2 and O_2 on samples, and storage at two different temperatures (20ºC and 26ºC). During 30 days it was studied the water activity, the texture, total count microorganisms at 30ºC, moisture content, ash content, fat content, protein, fibber, the level of O_2 and CO_2 on the samples with different modified atmosphere packaging and sensory analysis to evaluate the overall acceptability from the consumers. In this work it will be emphasized the texture and sensory analysis.

Cake acceptability was conducted with 70 volunteer panellists of 18–60 years of age from staff, undergraduate and postgraduate students and employees from IPBeja. All the panellists, who were regular cake consumers, were asked to evaluate the samples on the basis of acceptance of cake appearance, aroma, taste, texture and overall liking on a seven-point hedonic scale (1=very disliked, 7=very liked) in manufacturing day.

A texture analyser TAHDi (Stable Micro Systems, Godalming, UK), equipped with a 250 N load cell, was used to perform the texture analysis at 20±1 °C. The procedure was implemented by puncture with a 3 mm diameter aluminium cylindrical probe, at a penetration depth of 10mm (the height of the sample was 30 mm), with a crossed speed of 1mm s^{-1}. Texture measurements were performed in quintuplicate. Hardness values were obtained from the force vs. time texturograms [5].

RESULTS DISCUSSION

In Table 1, it was established that the favourite sample was the QM with the traditional ingredients, which had the highest scores in appearance, colour, texture and aroma, and then preceded by sample K with the same recipe but without traditional products.

Table 1- Sensory Parameters on samples K and QM

SAMPLE	APPEARANCE	COLOUR	TEXTURE	AROMA	FLAVOUR	OVERALL ACCEPTABILITY
K	6,08(1,15)	6,04(1,22)	6,02(1,16)	6,26(1,01)	6,51(0,83)	6,36(0,64)
QM	6,63(0,56)	6,45(0,58)	6,31(0,81)	6,36(0,71)	6,40(0,77)	6,40(0,98)

Legend: K – receipt without traditional whey cheese and honey. QM – receipt with traditional whey cheese and honey

Figure 1 shows a texture profile of all samples storage at 20ºC and 26ºC in MAP CO_2, N_2 e O_2 through 30 days. It was noticeable that CO_2 samples were very stable in hardness along time but at 30 days and at both storage temperature the increase in hardness was remarkable.

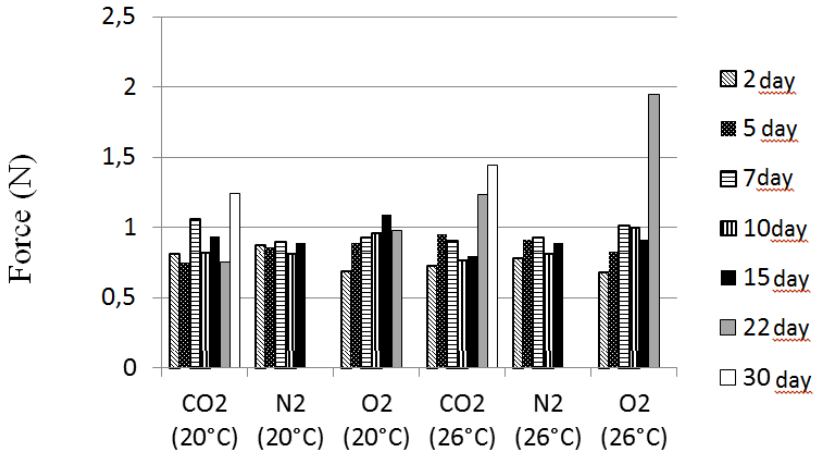

Figure 1- Hardness values on samples storage at 20ºC and 26ºC in MAP CO_2, N_2 e O_2.

In the figure 2, it's perceptible that the samples in general terms with more hardness in terms of the average along time were the samples with the O_2 atmosphere at 26ºC,

concluding that this is not an ideal gas in terms of results in texture. The packaging with N_2 atmosphere had the steadiest results during the storage days at both temperatures.

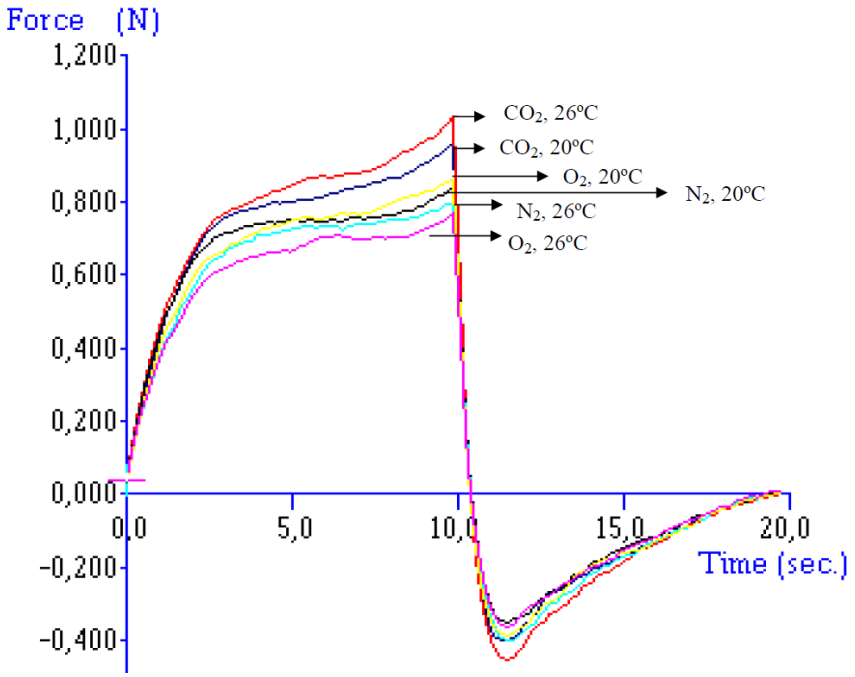

Figure 2 – Average texture profile of samples storage at 20ºC and 26ºC in MAP CO_2, N_2 e O_2.

CONCLUSION

It was concluding that the suitable modified atmosphere packaging was the CO_2 for 22 days of storage at 20ºC, which allowed to stablish its shelf life, since this sample had shown more acceptance and hardness steadiness, during this research time. It is important to remark that the only samples that preserved the textural and sensory quality during 30 days were the samples Package in MAP with CO_2 (at 20 and 26 ºC). Even in terms of hardness the samples package in MAP with N_2 was stablish, in terms of microbiology analysis (data not shown) it was observed high microbiological contamination and, for that reason, it wasn't acceptable.

REFERENCES

[1] Paraskevopoulou, A., Amvrosiadou, S., Biliaderis, C., & Kiosseoglou, V. (2014). *Food Research International*, **62** 492–499.
[2] Young H, MacFie H, Light, N. (1988) *Effect of packaging and storage Technology: A Review.*
[3] Jowitt, R. (1974). Journal of Texture Studies, **5** 351–358.
[4] Menjivar, J. A. (1990). Fundamental aspects of dough rheology. In H. Faridi & J. M. Faubion (Eds.), Dough rheology and baked product texture (pp. 1–28). New York: Van Nostrand Reinhold.
[5] Alvarenga, N., Canada, J. Sousa, I. (2011). Journal of Dairy Research, **78** 80–87.

Wall slip on rheological measurements of injection grouts

Luis G. Baltazar[1], Fernando M.A. Henriques[1], Tiago Cardoso[1], Maria Teresa Cidade[2]

[1] Dpto Engenharia Civil, Faculdade de Ciências e Tecnologia, Universidade Nova de Lisboa, 2829-516 Caparica, Portugal

[2]Dpto. Ciência dos Materiais and Cenimat/I3N, Faculdade de Ciências e Tecnologia, Universidade Nova de Lisboa, 2829-516 Caparica, Portugal

Correspondence to: Luis G. Baltazar (luis.baltazar@fct.unl.pt)

ABSTRACT

In this study, the degree of wall slip on rheological measurements of injection grouts is investigated. Grouts can be seen as suspensions of binder particles in water which have a considerable fluidity in order to be successfully injected in many applications in civil engineering works such as consolidation of stone masonry walls. For the determination of wall slip in a rotational rheometer with parallel plates, stress controlled measurements at various gaps and different shear stress were carried out. Overall, our results revealed that wall slip is function of the shear stress and the grout composition. It was also found that the parallel plate with emery paper glued can be a solution to mitigate the slip. Results from this study can help to define an adequate measurement protocol to correctly infer the rheological properties of injection grouts by using parallel plates.

KEYWORDS: wall slip, injection grout, parallel plates, stone masonry

INTRODUCTION

Stone masonry is a constructive technique invented thousands of years ago. Its simplicity and durability lead to an extensive use and it represents the large majority of old buildings in many urban centers across Europe. Stone masonry, a non-homogeneous and non-monolithic composite material, has particular weakness which, associated with the absence of maintenance, increase the vulnerability of its structural integrity. Grout injection is an interesting solution to repair and reinforce old stone masonry walls, particularly those built with two exterior skins of stonework and a ruble core (see Fig 1a). This consolidation method is defined as the introduction of a fluid material injected under pressure into the masonry inner core (Fig. 1). Injection grouts aim to fill cracks, voids and at same time enable the bonding between masonry elements which is essential towards masonry integrity (monolithic behavior).

Grouts can be represented as biphasic system consisting of suspended particles (binder) in a continuous fluid phase (water). The efficacy of the grouts depends mainly on the injectability properties. Therefore, it is essential to evaluate the effectiveness of the injection grouts in terms of keeping their adequate properties. For that purpose controlling the rheological properties of grouts is crucial for successfully grouting process [1,2]. Notwithstanding, during rheological measurements many phenomena can arise which can lead to test results having no value at all. Several authors [3,4,5] have shown that wall slip can play a significant role during the rheological measurements of cementitious materials leading to an underestimation of the yield stress values and inaccurate viscosity results. The aim of the present research is to determine the degree of wall slip effect during rheological measurements of injection grouts in order to define an adequate measurement protocol.

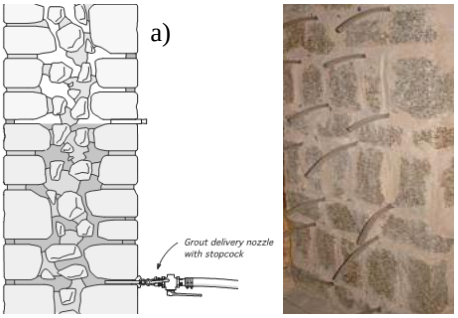

FIGURE 1 a) Example of a section of stone masonry wall core being grouted. b) Stone masonry with injection pipes.

METHODS

Rheological measurements were performed with a rotational rheometer (Bohlin Gemini HR^{nano}), equipped with a plate-plate geometry (with Ø = 40mm). The best way to confirm the presence of wall slip is taking measurements with smooth and serrated plates. However, in this case the authors did not have both geometry types available for such a comparison and so they have used an application note of Malvern[6], which says that evidence of slip can be obtained by performing stress controlled measurements at different gaps. If slip occurs then the slip velocity (V_s) will depend only on the applied shear stress (σ) but not on the gap (h). Thus by varying the gap and keeping the stress constant it is possible to determine the slip velocity and the true shear rate using Equation 1. This can be performed by plotting the measured shear rate against 1/h which should result in a straight line with gradient 2.V_s and intercept γ.

$$\gamma_m = \frac{V}{h} = \frac{2.V_s}{h} + \gamma \quad (1)$$

Where V is the velocity of the upper plate; γ_m is the measured shear rate and γ is the true shear rate.

All rheological measurements were carried out at 20°C. Single shear measurements at various gaps of 1mm, 1.5mm, 2mm and 3mm using constant applied stresses of 10 Pa, 15 Pa and 20 Pa were conducted. The measured shear rate was then plotted against the inverse gap and a linear regression model fitted. This way the slip velocity and true shear rate can be estimated from the gradient and intercept respectively.

MATERIALS

The experimental program was conducted using a natural hydraulic lime (NHL) produced according to the European standard EN459-1:2010 and the following water/binder ratios (w/b) 0.45, 0.50 and 0.55 was used. NHL was chosen as binder, since it is a hydraulic binder that presents chemical and physical properties closer to those of preexisting materials in old masonries. A commercially available polycarboxylate ether superplasticizer (conforming to ASTM C494-05 Type F) with a constant dosage of 1wt% was used.

RESULTS AND DISCUSSION

Example of measured shear rate versus inverse gap is presented in Fig. 2 for NHL-based grout with water/binder ratio of 0.45 at different shear stresses. As previously mentioned to estimate the slip velocity a linear model fit was applied to the data with gradient of the line equal to 2.Vs and the intercept equal to the true shear rate. For the grout with water/binder of 0.45 the slip velocity was estimated to be 2.2mm/s, 3.8mm/s and 5.2mm/s and the true shear rate 0.7s^{-1}, 1.4s^{-1} and 1.7s^{-1} for the shear stress of 10Pa, 15Pa and 20Pa, respectively. This is quite lower than the measured shear rate range 2-5 s^{-1}, 4-9 s^{-1} and 5-12 s^{-1} for each shear stress, which suggest a significant degree of wall slip.

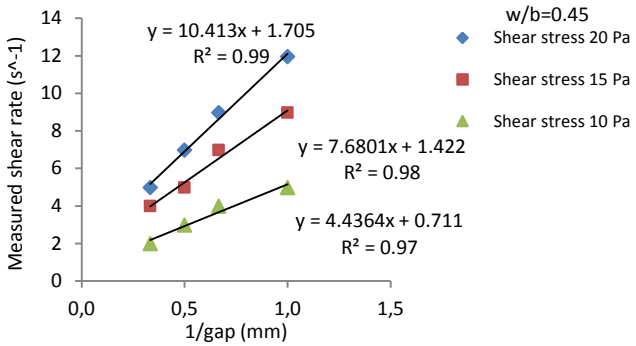

FIGURE 2 Measured shear rate *vs* 1/gap at different shear stress for the grout with w/b of 0.45.

The profiles of measured shear rate versus gap obtained for the other water/binder ratios are presented in Fig 3 and Fig. 4. From Fig 3, it can be seen that for the shear stress of 10Pa an approximately constant shear rate at each gap was obtained, which means no wall slip occurred. On the contrary, the higher shear stresses show a slight gradient (slip velocity) with higher shear rate reported at bigger gaps which is attributed to wall slip. It should be noted that for the shear stress of 15Pa the wall slip only begins at the biggest gap.

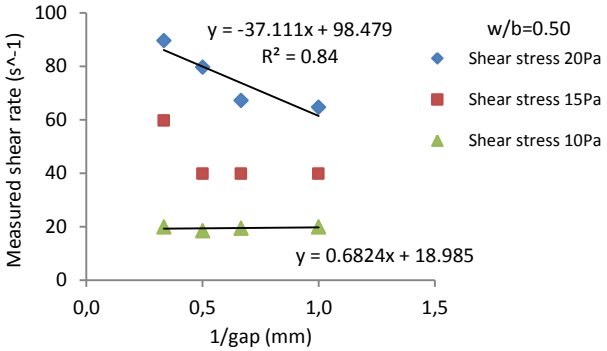

FIGURE 3 Measured shear rate *vs* 1/gap at different shear stress for the grout with w/b of 0.50.

From the results presented it is clear that the degree of wall slip (i.e. slip viscosity) increases with increasing shear stress. Moreover, it can also be observed that the trend of the curve shear rate *vs* 1/gap is function of the water/binder content. At the lower water/binder content (w/b=0.45) the slope is positive which means that the wall slip is likely to cause an overestimation of rheological parameters. As the water/binder content is increased the slope of the curve becomes negative meaning a tendency to underestimation of the parameters as result of the wall slip. This behavior is associated with greater tendency to segregation as the amount of free water in the suspension increases. This can be explained by the uniform settlement of binder particles, leaving a thin layer of water over the surface. Therefore local properties are changed, leading to an improper evaluation of yield stress, which can be over or under estimated as evidenced by the different slope sign of the linear models.

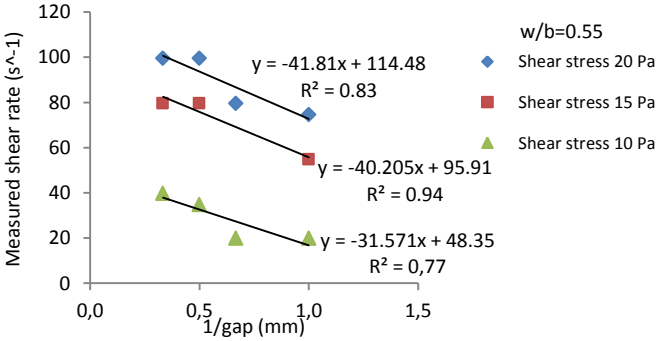

FIGURE 4 Measured shear rate *vs* 1/gap at different shear stress for the grout with w/b of 0.55.

Considering the above results, serrated plates should be used to avoid slip. Since the authors did not have serrated plates available, some measurements with plates with emery papers glued were performed. This is an ongoing work but the preliminary results are quite promising. From Fig 5 it is clear the difference between the flow curves obtained with smooth parallel plate and the one with emery paper glued. There is no doubt that the sharp change in trend of the flow curve obtained with smooth plates (see Fig 5a) is related to slip at plate-grout interface. While for the plate with emery paper glued a gradual deviation of the stress curve from linearity as the shear rate increases is verified. Thus, it can be stated that the emery paper glued to the smooth plates can be a good solution to avoid slip during rheological measurements of injection grouts.

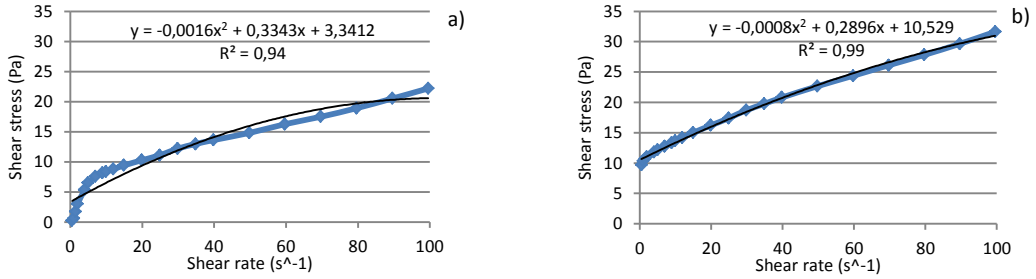

FIGURE 5 Influence of geometry roughness on the flow curve behavior for the grout with w/b=0.50 at a gap of 3mm a) smooth parallel plate and b) parallel plate with emery paper glued.

CONCLUSIONS

In the light of the achieved results, it is clear that for rheological measurements of injection grouts using a rotational rheometer equipped with smooth parallel plates some aspect have to be taken into account in order to avoid getting significant error in the results. A suitable choice of shear stress range applied during the rheological measurement should be made, since the higher shear stress increases the degree of wall slip. Moreover, a proper formulation of the grout is also recommended in order to avoid grouts with higher tendency to segregate that promote the wall slip. Preliminary measurements performed with parallel plate with emery paper glued reveal to be a viable way to avoid the slip. The results and procedures reported in this paper can therefore be used to estimate the degree of slip of a specific grout composition and indicate whether the use of roughened plates is required.

REFERENCES

1. Baltazar, L.G., Henriques, F.M.A., Jorne, F., Cidade, M.T., *Rheologica Acta*, **2013**, 50(2), 127-138.
2. Baltazar, L.G., Henriques, F.M.A., Jorne, F., Cidade, M.T., *Construction and Building Materials*, **2014**, 50, 584-597.
3. Banfill P.F.G., Rheology of fresh cement and concrete, In Rheol. Rev., British Society of Rheology, Uk, **2006**.
4. Nehdi M., Rahman M-A., *Cement and Concrete Research*, **2004**, 34, 1993-2007.
5. Saak, A.W., Jennings, H.M., Shah, S.P., *Cement and Concrete Research*, **2001**, 31, 205-212.
6. Malvern - Application Note. Overcoming and quantifying 'Wall Slip' in measurements made on a rotational rheometer. Malvern Instruments – Spectris plc - the Precision Instrumentation and Controls Company, **2012**.

P42

RHEOLOGICAL BEHAVIOR OF KAOLIN DISPERSIONS IN A NON-NEWTONIAN FLUID

F.J. Sánchez-Luque[1], J.F. Velázquez-Navarro[2], F.J. Rubio-Hernández[1], A.I. Gómez-Merino[1], N.M. Páez-Flor[3]

[1]Departamento de Física Aplicada II, Universidad de Málaga, Málaga (Spain) , [2]Departamento de Ingeniería Mecánica y Mecánica de Fluidos, Universidad de Málaga, Málaga (Spain) , [3]DECEM, Universidad de las Fuerzas Armadas, Sangolquí (Ecuador)

Correspondence to: J.F. Velázquez-Navarro (E-mail: *josevelazquez@uma.es*)

ABSTRACT

Kaolin is one of the most used clays in a very wide range of industries. One of the most widespread ways to use it is by forming a suspension in different liquid mediums. The efficiency of these types of suspensions will depend on two main factors: as its homogeneity and stability, as its mechanical response under varied conditions[1]. The suspensions are composed of a liquid medium (silica sol) and floating particles (kaolin). The silica sol is composed by $90\%\ w/w$ of deionised water and $10\%\ w/w$ of silica oxide. The kaolin concentration varies between 5 and $25\%\ w/w$, so as to observe how this fact affects to the rheological behaviour shown under different conditions.The stationary responses of the samples has been measured by mean of stationary flow curves. They have clearly shown a shear-thinning behaviour in all cases, and as it was expected, an increase of the viscosity while the kaolin concentration rises. Mooney fitting curves have been applied in order to characterize the behavior and main characteristics of the dispersions through their intrinsic viscosity values.

KEYWORDS : Diluted suspensions , kaolin, Mooney model, stationary flow curve, shear-thinning.

INTRODUCTION

Kaolin is normally applied in suspensions by using different liquid media, whose performance will depend mainly on the homogeneity and stability of the dispersion[2], and also, in the mechanical response under different conditions. In order to ensure that these properties are optimal, dispersants are widely used, such as silica sol[3]. Regarding of this, the aim of the present work is to determine the influence of the kaolin concentration on the rheological behavior and suspension properties for these materials.

MATERIALS AND METHODS

The materials involved in this study were kaolin (NC-35), silica fumed (DEGUSSA) and deionized water. The following samples have been analyzed: silica sol, 5% kaolin w/w, 10%, 15%, 20%, 25%. To prepare the dispersions, the silica sol (10% w/w silica oxide) has been stirred 2 hours and then sonicated about 20 minutes to avoid aggregates formation. After that the amount of kaolin has been added and stirred 3-5 minutes additionally. Malvern Gemini 150 rheometer (coaxial cylinders geometry) has been employed to measure the suspensions up to 15% w/w kaolin. For the most concentrated suspensions (20 and 25% w/w), due to their high viscosity, a Haake RS600 rheometer with a plate-plate geometry were used.

In order to ensure the homogeneity and stability of the studied samples, it has been set a strict protocol to prepare them, with the purpose of standardize the whole process avoiding randomness factors. Firstly, all samples were pre-sheared 60 s at 50 s^{-1}, making sure that the stationary state was always reached. Then the stationary flow curves were performed in which the material will be subjected to different increasing shear rates, until reach the maximum rate. Each step will remain time enough until the stationary state is reached.

RESULTS AND DISCUSSION

Figure 1 shows the evolution of the viscosity in all suspensions in function of the shear rate.

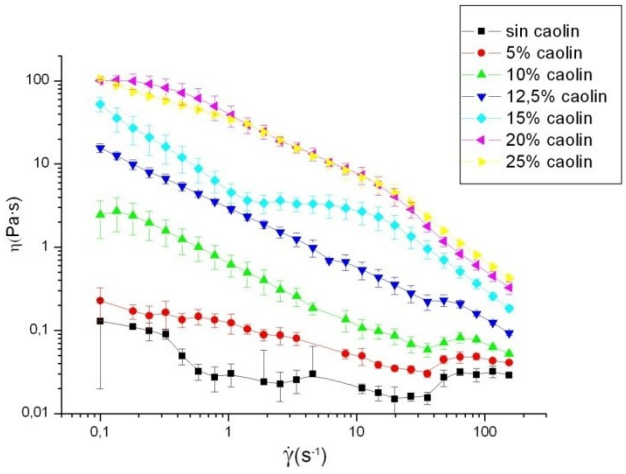

FIGURE 1 Evolution of the viscosity in the stationary flow curve.

A shear-thinning behavior is observed in all samples and it also shown that, the higher the kaolin concentration is, more pronounced is this response. For this, in order to understand better the material performance, Mooney model (equation 1) was fitted for different shear rates for all dispersions up to 15% w/w kaolin.

$$\eta_r = \exp\left(\frac{[\eta]\varphi}{1-\left(\varphi/\varphi_m\right)}\right) \quad (1)$$

The curves obtained in this way are shown in the figure 2. According to these trends, table 1 values has been computed from the fit parameters for each case.

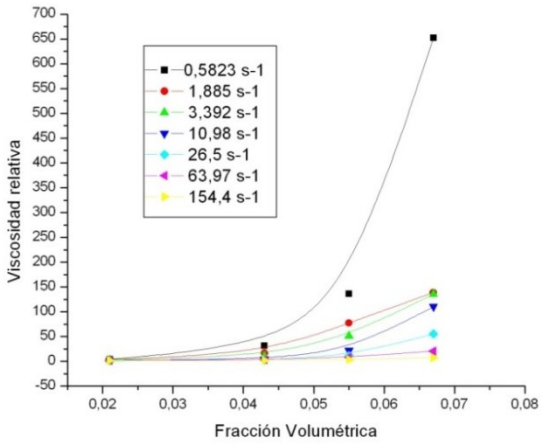

FIGURE 2 Relative viscosity-volumetric fraction curves.

TABLE 1 Parameters fitted using Mooney equation.

$\dot{\gamma}$ (s^{-1})	$[\eta]$	ϕ	R^2
0.6	64,3	0.20	0,99989
1.9	49,5	0.20	0.89150
3.4	40.7	0.15	0.97355
10.9	28.0	0.11	0.99893
26.5	19.1	0.10	0.99864
64.0	22.0	0.13	0.99660
154.4	12.4	0.11	0.99351

It can be claimed that a critical shear rate exists ($\dot{\gamma}_c$), which limits two regions: the low shear rates zone where the shear thinning is more evident (more pronounced curves in the figure 2),

and high shear rates zone where the response is almost typical Newtonian one. This critical shear rate is in this case around 2 s^{-1}. The curves belonging to the low shear rates trends to a vertical asymptote, which is located at 0,075 (the maximum volume concentration accepted by the medium). The samples of 20 and 25% of kaolin, corresponding to ϕ equal to 0,09 and 0,12 respectively, are over this medium limit. In that situation, there is more kaolin mass than which the liquid phase is able to remain, so the homogeneity and stability of the samples are lost. On the other hand, the values of $[\eta]$ (table 1) are very high (inversely proportional to the shear rate), and the maximum packing fraction (ϕ_M) values are low in all cases. The high values of $[\eta]$ are the evidence of high poly-disperse suspension. The kaolin particles are planes, like oval "plates" with a very high relation between its length and thickness. On the other side, silica oxide particles are spheroids of a non-regular shape and surface, in consequence, both of these parameters (ϕ_M and $[\eta]$) will keep in low and high values respectively[4].

CONCLUSIONS

The silica sol could be a proper dispersant for dispersions up to 15% kaolin w/w, from this amount, the samples turn to thick mixtures where the homogeneity and stability cannot be guaranteed and, therefore, they are not suitable for industrial purposes. On the other side, these dispersions has demonstrated to be vey poly-disperse due to particles relative shapes as is shown by Mooney fit parameters.

REFERENCES AND NOTES

1. M. Loginov, O. Larue, N. Lebovka, E. Vorobiev, *Fluidity of highly concentrated kaolin suspensions: influence of particle concentration and presence of dispersant.* Colloids Surfaces A , **2008**, 325, 64-71.

2. Le Bell, J.C., Hurskainen, V.T., Stenius, P.J. *The influence of sodium lignosulphonates on the stability of kaolin dispersions.* J. Colloid Interface Sci., 1976, 55, 60-68.

3. Zhi, Z., Xuxhen, L., Peng, S. *Dispersion of kaolin powders in silica sols.* Appl. Clay Sci., **2010**, 49, 51-54.

4. Larson. R.G., The Structure and Rheology of Complex Fluids; Keith E. Gubbins, Ed.; Oxford University Press: New York, Oxford, **1999**

P44

Rheological characterization of green emulsions developed with several emulsification methods

M. José Martín-Piñero[1], Luis A. Trujillo-Cayado[1], M. Carmen García[1], M. Carmen Alfaro[1*], José Muñoz[1]

[1] Reología Aplicada. Tecnología de Coloides. Departamento de Ingeniería Química. Facultad de Química. Universidad de Sevilla. C/ P. García González, 1, 41012, Sevilla, Spain.

Correspondence to: M. Carmen Alfaro (E-mail: alfaro@us.es)

ABSTRACT

The goal of this work was to investigate the influence of the emulsification method on the rheological properties and physical stability of 30 % oil-in-water emulsions formulated with a mixture of two green solvents as oil phase. We report the effect of homogenization speed in two rotor-stator devices and pressure in a high-pressure valve homogenizer on the rheology and physical stability of emulsions. Flow curves of emulsions showed slight shear thinning behavior and viscoelastic responses could not be detected. The higher the energy input the more viscous and shear thinning were the emulsions. Samples prepared with rotor-stator devices showed lower apparent viscosities and higher power law indexes than those developed with the high-pressure valve homogenizer used. The emulsion with the highest fraction of smaller droplets and the highest physical stability was achieved using the high-pressure valve homogenizer at 15000 psi.

KEYWORDS: Emulsion, Shear thinning, Non-Newtonian, Shear flow, Rheology, Green solvent.

INTRODUCTION

Droplet size distribution is one of the most important factors in determining properties like rheology and physical stability of emulsions. Current equipments used for emulsification involve rotor-stator devices, membranes, colloid mills and high-pressure homogenizers. Emulsions were formulated with a fatty acid dimethylamide (FAD). FADs have been recognized as green solvents because they are obtained from renewable raw materials and in addition exhibit excellent EHS properties. α-Pinene is a biosolvent that may be obtained from pine resins or distillation and can be formulated as stable oil-in-water (O/W) emulsions with the help of

biopolymers[2]. The goal of this work was to investigate the influence of emulsification method on the rheological properties, droplet size distribution and physical stability of O/W emulsions formulated with a mixture of green solvents as oil phase and an emulsifier useful for eco-labeling. We compare the properties of emulsions prepared using two rotor-stator devices to those prepared with a high-pressure valve homogenizer (HPvH) at several processing variables.

MATERIALS AND METHODS

Lauryl N,N-dimethylamide (Agnique AMD-12^{TM}) and α-pinene, supplied by BASF and Sigma-Aldrich respectively, were used as the oil phase using an AMD-12^{TM}/α-pinene mass ratio of 75/25[2]. A polyoxyethylene glycerol ester (HLB: 13) derived from cocoa oil (glycereth-17 cocoate, Levenol C-201^{TM}, from KAO) was used as emulsifier. Emulsions were produced by homogenizing 30 wt% oil (total concentration) with 70 wt% aqueous phase containing 3 wt% surfactant. Samples were prepared with rotor-stator devices by applying a rotational speed in the (4000 - 8000) rpm range for 120 s at room temperature. The performance of the Ultraturrax T50 (UT-T50) equipped with a G45F toothed dispersion unit was compared to that of the Silverson L5M (SL5M) equipped with a high shear screen. Coarse emulsions prepared using the UT-T50 at 4000 rpm were immediately passed once through the Avestin Emulsiflex C5 HPvH. Homogenization pressures considered were 5000 and 15000 psi (34.5 & 103 MPa, respectively). A heat exchanger was used with water flowing at inlet temperature of 20ºC to cool the emulsions.

The rheological measurements were carried out with a controlled-stress rheometer (Haake-MARS) using a sandblasted Z20 coaxial cylinder geometry to avoid slip-effects (T = 20°C). Droplet size distribution measurements were performed using a laser diffraction instrument (Malvern Mastersizer X). Multiple light scattering scans were carried out with a Turbiscan Lab-expert to obtain information on the destabilization kinetics and the main mechanism involved.

RESULTS AND DISCUSSIONS

Figure 1A shows the droplet size distributions (DSDs) of emulsions aged for 24 h prepared with the processing variables that yielded the lowest droplet mean diameter for each emulsification method used. All emulsions prepared with rotor-stator devices exhibited monomodal DSDs. The SL5M, which is equipped with a high shear screen, yielded slightly lower oil droplet diameters than the UT-T50/G45F at the same homogenization rates. By contrast,

samples prepared with the HPvH showed a small second peak due to the occurrence of recoalescence which, in turn, is a consequence of some over-processing. Fortunately, the HPvH provided a markedly higher fraction of droplets with smaller diameters.

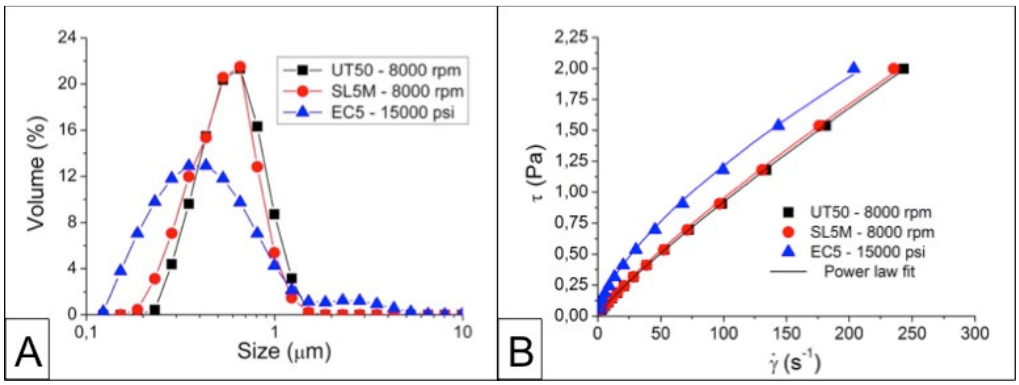

FIGURE 1. (A) Droplet size distributions at room temperature and (B) flow curves (T = 20°C) for selected emulsions aged for 24 hours as a function of the different emulsification processes.

All the emulsions exhibited shear-thinning flow behavior (see figure 1B), which fitted the power-law equation:

$$\tau = \tau_1 \cdot \left(\frac{\dot{\gamma}}{1s^{-1}} \right)^n \qquad \text{Eq. (1)}$$

where τ is the shear stress, τ_1 is the shear stress value at $1s^{-1}$, $\dot{\gamma}$ is the shear rate and n is the power law index. The fluid-like behaviour of these emulsions was supported by their low apparent viscosity values (η_{2Pa} ranged from 7.21 to 9.82 mPa·s at 20°C). τ_1 values were similar for all emulsions prepared with HPvH but slightly higher than those obtained for emulsions prepared with rotor-stator devices. These results are consistent with the occurrence of lower mean diameters (data not shown). Power law indexes for emulsions prepared with rotor-stator devices were significantly higher (i.e. they are less shear thinning) than those of emulsions prepared with HPvH. None of these emulsions showed measurable linear viscoelastic properties.

Multiple light scattering demonstrated that the emulsions with smaller droplet sizes exhibited enhanced stability against creaming. The most stable emulsion was that prepared with the Avestin Emulsiflex C5 at 15000 psi.

TABLE 1. Power law fitting parameters for flow curves of the emulsions studied at 20ºC.

Method		τ_1 (Pa)	n	η_{2Pa} (mPa·s)
UT50	4000 rpm	0.013	0.89	7.21
	8000 rpm	0.017	0.86	8.21
SL5M	4000 rpm	0.013	0.89	7.13
	8000 rpm	0.019	0.85	8.49
EC5	5000 psi	0.042	0.70	8.79
	15000 psi	0.056	0.67	9.82

CONCLUSIONS

The higher fractions of smaller droplets were achieved by using the high-pressure valve homogenizer. Flow curves were sensitive to emulsification method and all emulsions exhibited shear-thinning behaviour. None of them exhibited linear viscoelastic properties. The emulsions obtained by high-pressure valve homogenizer showed higher apparent viscosity and more marked shear-thinning properties than those prepared with rotor-stator homogenizers, which is consistent with their lower mean droplet diameters. These properties resulted in enhanced physical stability against creaming. The optimum results were those of the emulsion prepared with the high-pressure valve homogenizer at 15000 psi (103 MPa).

ACKNOWLEDGEMENTS

The financial support received (Project CTQ2011-27371) from the Spanish Ministerio de Economía y Competitividad (MINECO) and from the European Commission (FEDER Programme) is kindly acknowledged.

REFERENCES

1. García, M.C; Alfaro, M.C; Calero, N.; Muñoz, J., Influence of polysaccharides on the rheology and stabilization of α-pinene emulsions. *Carbohydrate polymers*, **2014**, *105*, 177-183.
2. Santos, J.; Trujillo-Cayado, L. A.; Calero, N.; Muñoz, J., Physical characterization of eco-friendly O/W emulsions developed through a strategy based on product engineering principles. *AIChE Journal*, **2014**, *60*, 2644-2653.

Rheological Properties of Muffin Batter Reformulated with Chickpea Flour

María Dolores Alvarez[1], Raúl Fuentes[1], Beatriz Herranz[1], Francisco Cuesta[2], Wenceslao Canet[1]

[1]Department of Characterization, Quality, and Safety, Institute of Food Science, Technology and Nutrition (ICTAN-CSIC), José Antonio Novais 10, 28040 Madrid, Spain

[2]Department of Products, Institute of Food Science, Technology and Nutrition (ICTAN-CSIC), José Antonio Novais 10, 28040 Madrid, Spain

Correspondence to: María Dolores Alvarez (E-mail: *mayoyes@ictan.csic.es*)

ABSTRACT

The effect on the rheological properties of muffin batter of replacing wheat flour (WF) with chickpea flour (CF) was studied by using oscillatory and steady state shear tests. CF was used to replace the WF in the batter partially (25, 50, and 75% w/w; 25%CF, 50%CF, and 75%CF samples) or totally (100% w/w, 100%CF batter), and compared with a control made only with wheat flour (100%WF batter). SAOS measurements indicate that 100%WF batter can be characterized as a weak gel, while batters with partial and total WF replacement presented a structure between those of a concentrated biopolymer and a weak gel with higher loss tangent (tan δ) values. Zero-order reaction kinetics described batter gelatinization process well, and activation energies were obtained for all the batters. Extent of thixotropy and rebuild time decreased significantly with increases in the WF replacement level. Complex and apparent viscosities failed to follow the Cox–Merz rule.

KEYWORDS Chickpea flour, Muffin batter, Viscoelasticity, Thixotropy, Viscosity; Cox–Merz rule

INTRODUCTION

Muffin batter is a complex fat-in-water emulsion composed of an egg–sucrose–water–fat mixture as the continuous phase and bubbles as the discontinuous phase in which flour particles are dispersed[1]. A muffin recipe is mainly composed of WF, sucrose, vegetable oil, egg, and milk[2]. People with celiac disease are unable to consume this type of baked product. Moreover, many gluten-free products available on the market are often of poor technological quality[3]. Chickpea (*Cicer arietinum* L.) is one of the top five important legumes on the basis of whole grain production[4]. Potential for increased use of chickpea is related to its relatively low cost, relatively high protein content (~18.3–28.9%), high protein digestibility (76–78%), and other desirable functionalities[5].

The aim of this work was to evaluate the suitability of CF to replace different percentages of WF in muffins, and to study its functionality in the linear viscoelastic properties (oscillatory tests)

and the flow behavior (steady-state shear tests) of the batter as a prior step to evaluating other properties (texture and sensory acceptability) of the baked muffin.

EXPERIMENTAL DATA

Batter Preparation

Five muffin formulations were prepared with the ingredients and amounts shown in Table 1. The batter was prepared in a KPM5 professional mixer (Kitchen Aid, St. Joseph, Michigan, USA).

TABLE 1 Formulations of control muffin batter prepared with 100% of wheat flour (WF) and batters prepared with increasing quantities of chickpea flour (CF) as WF replacer

Ingredients (g 100 g^{-1} flour)	100%WF	25%CF	50%CF	75%CF	100%CF
WF	100	75	50	25	0
CF	0	25	50	75	100
Whole egg	81	81	81	81	81
Sucrose	100	100	100	100	100
Salt	0.75	0.75	0.75	0.75	0.75
Milk	50	50	50	50	50
Oil	46	46	46	46	46
Natural lemon juice	3	3	3	3	3
Sodium bicarbonate	4	4	4	4	4

Rheological Properties of Muffin Batter (SAOS and Steady Shear Rheological Measurements)

SAOS and flow tests were performed using either a Bohlin CVR 50 controlled stress rheometer (Bohlin Instruments Ltd., Cirencester, UK) or a Kinexus pro rotational rheometer (Malvern Instruments Ltd, Worcestershire, UK). Measurements were obtained using parallel-plate geometry (40 mm diameter, 1 mm gap). Stress sweep, frequency sweep, and temperature sweep tests were carried out under SAOS mode. To study flow time dependence, the hysteresis loop was obtained. Before analyzing flow behavior, the structure responsible for thixotropy was previously destroyed by shearing[6]. Viscometry rebuild analysis was also carried out.

RESULTS AND DISCUSSION

SAOS Measurements and Viscous Shear Flow of Muffin Batter

Batters made with CF at 25–100% levels are more deformable, with a higher degree of conformational flexibility than 100%WF batter, reflecting loss of both rigidity and elasticity (high tan δ) as higher WF percentages are replaced by CF. Increase in the G'_0 and G''_0 values

(intercepts of linear regressions of power-type relationship of lnω vs. lnG'_0 and lnG''_0, respectively) with increasing WF replacement was accompanied by an increase in the n' and n'' values (slopes of the cited linear regressions), therefore reflecting higher ω dependence associated with reduced stability of the protein network[7]. Power law fits showed that there were no significant differences between the G' and G'' values of 100%WF and 100%CF batters throughout the ω range studied. Both batters, with 0 and 100% replacement levels, also had similar gel points.

FIGURE 1 Mechanical spectra data for muffin control batter and batters with wheat flour (WF) replaced by different percentages of chickpea flour (CF).

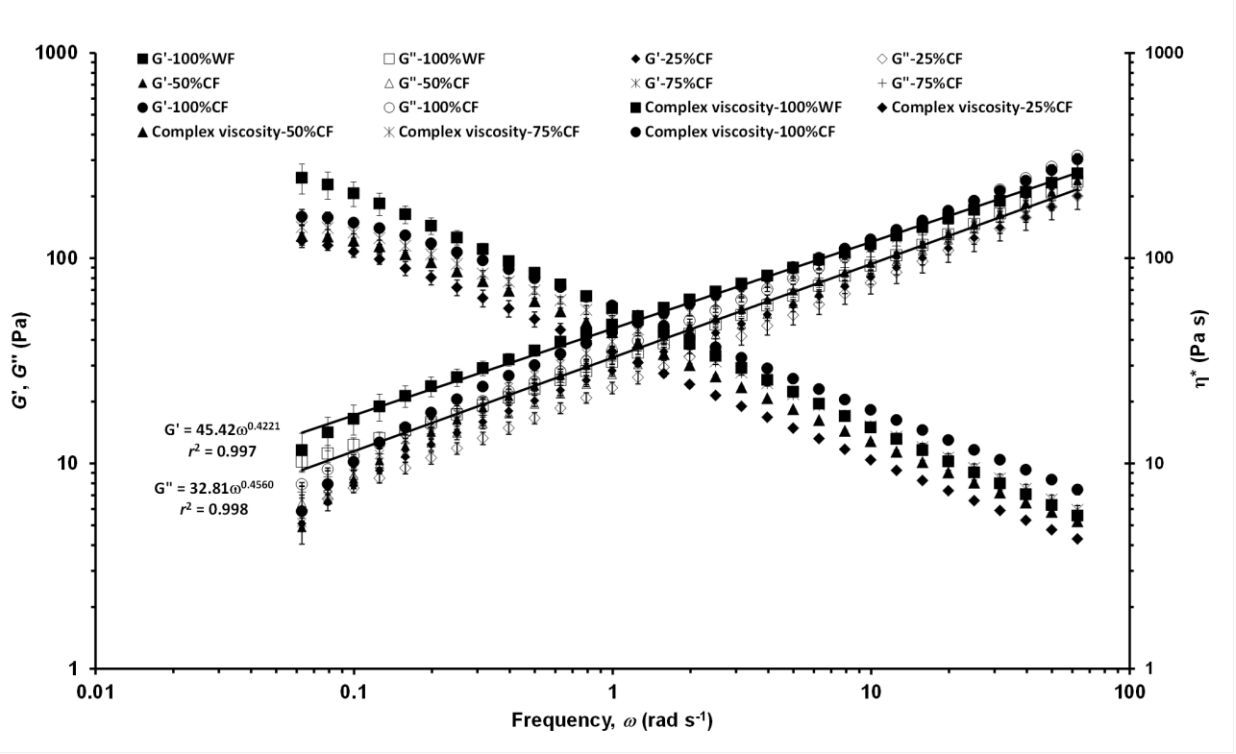

Batter gelatinization under non-isothermal conditions was well described by first-order reaction kinetics. The lower activation energy (113.43 kJ mol^{-1}) of 100%WF batter implies that it was more favorable for gelatinization. Under viscous flow, 100%WF batter was the most thixotropic (Table 2), with the lowest viscosity recovery percentage and resistance to flow, the longest rebuild time, and the highest fluidity. Shearing reduced 94% of the flow time dependence in 100%WF batter, whereas in 100%CF sample the hysteresis loop increased. All four CF formulae exhibited a short, rapid build-up of viscosity to a highly structured state after shearing.

Flow data fitted well to Herschel–Bulkley model, which showed that gluten-free batter had the highest yield stress, pseudoplasticity, and viscosity. Power type modification of the Cox–Merz rule can be successfully used for all the muffin batters studied. Specific gravity values (data not shown) would appear to indicate a higher incorporation of air into the 100%CF batter. However, 100% WF replacement is accompanied by an increase in the weakening of the muffin crumb structure, associated with inadequate gas retention.

TABLE 2 Effect of wheat flour replacement on hysteresis areas and rheological parameters of Herschel–Bulkley model describing flow curves of the muffin batter at 25 °C.

Formula	Hysteresis area before shearing (Pa s^{-1})	Hysteresis area after shearing (Pa s^{-1})	σ0 (Pa)	K (Pa sn)	n	R^2
100%WF	1974.3±353.1[a]	115.8±47.2[b]	4.23±0.47[b]	8.60±0.64[b]	0.760±0.013[b,c]	1.000
25%CF	1438.5±65.9[b]	191.9±73.7[b]	4.49±1.56[b]	8.56±1.76[b]	0.780±0.031[a,b]	0.999
50%CF	1034.4±281.8[b]	202.0±118.6[b]	3.22±0.29[b]	8.65±0.26[b]	0.804±0.006[a]	1.000
75%CF	504.1±145.7[c]	297.5±105.8[a,b]	4.89±0.69[b]	10.02±1.34[b]	0.793±0.023[a,b]	1.000
100%CF	357.0±71.1[c]	428.8±44.9[a]	12.57±0.81[a]	19.91±2.00[a]	0.729±0.005[c]	0.999

[a-c] Different letters in the same column mean significant differences ($P < 0.05$) among samples according to Bonferroni multiple range test. WF: wheat flour; CF: chickpea flour. σ_0, yield stress; *n*, flow behavior index; *K*, consistency index.

ACKNOWLEDGEMENTS

The authors wish to thank the Spanish Ministry of Economy and Competitiveness (AGL2011-28569).

REFERENCES

1. Matos, M.E.; Sanz, T.; Rosell, C.M., *Food Hydrocolloids*, **2014**, *35*, 150-158.
2. Sanz, T.; Salvador, A.; Baixauli, R.; Fiszman, S.M, *European Food Research and Technology*, **2009**, *229*, 197-204.
3. Mariotti, M.; Lucisano, M.; Pagani, M.A.; Ng, P.K.W., *Food Research International*, **2009**, *42*, 963-975.
4. Matos, M.E.; Rosell, C.M., *Plant Food for Human Nutrition*, **2011**, *66*, 224-230.
5. Hefnawy, T.M.H.; El-Shourbagy, G.A.; Ramadan, M.F., *International Food Research Journal*, **2012**, *19*, 521-525.
6. Tárrega, A.; Durán, L.; Costell, E., *International Dairy Journal*, **2004**, *14*, 345–353.
7. Moresi, M.; Brubo, M.; Parente, E., *Journal of Food Engineering,* **2004**, *64*, 179–186.

P46

Viscous flow behavior of polyethylene modified bitumen emulsions

Claudia Roman, Antonio Abad Cuadri, Moisés García-Morales, Francisco Javier Navarro, Francisco José Martínez-Boza and Pedro Partal

Dpto de Ingeniería Química, Centro de Investigación en Tecnología de Productos y Procesos Químicos (Pro2TecS), Campus de 'El Carmen', Universidad de Huelva, 21071, Huelva (Spain)

Correspondence to: Claudia Roman (E-mail: *claudia.roman@diq.uhu.es*)

ABSTRACT

With the goals of preventing the phase separation which may occur when polymer modified bitumens (PMBs) are stored at very high temperatures and minimizing the energy consumption involved in the fabrication of their asphalt mixes, PMBs can be conditioned in the form of their corresponding O/W emulsions. With this regard, five polyethylene modified bitumen emulsions were prepared and their viscous flow behavior at 25ºC evaluated. The resultant emulsions presented a low Sauter mean diameter (2-4 μm). Likewise, all flow curves firstly showed a shear-thinning behavior, followed by a high-shear-rate-limiting viscosity, which increased as bitumen-polymer phase concentration increased.

KEYWORDS

Bitumen, emulsion, polyethylene, viscosity, product formulation.

INTRODUCTION

Bitumen has been largely used as a binder of mineral aggregates in road paving [1]. Traditional asphalt mixtures are always produced at high temperatures, never below 150ºC. Very often, the performance of bitumen is improved by addition of different types of substances, among which polymers are mostly utilized. Polyethylenes have shown to improve the high temperature performance of bitumen, by reducing the formation of ruts in the pavement. However, bitumen modified with polyethylenes may encounter serious problems: a) its application involves even higher paving temperatures than plain bitumen; b) there exists a high risk of polymer separation when these binders are stored at high temperature.

Alternatively, different types of reduced-temperature technologies have emerged over the last decades. In particular, cold-mix asphalts consist in coating the mineral aggregates with an emulsion formed by very fine bitumen droplets dispersed in water and stabilized with a surfactant. This technology may prevent phase segregation, since the polymer is embedded in bitumen droplets suspended in aqueous phase [2]. Moreover, PMB emulsions present much lower viscosities than bitumen itself and can be applied at temperatures between 25 and 60ºC.

With a view to their potential application, five PMB emulsions modified with recycled LDPE were prepared and the influence of bitumen phase polymer concentration and solids content on their viscous flow behavior, at 25ºC, was evaluated.

EXPERIMENTAL

Bitumen with penetration grade 160/220, supplied by Repsol S.A., and recycled LDPE, kindly donated by Cordoplas S.A., were the main materials for the PMB emulsions. The surfactant, an alkyltrimethylenediamine derived from N-tallow, was also provided by Repsol S.A.

The preparation of the PMB emulsions consisted of a first step of bitumen modification with recycled LDPE (bitumen phase) and a further step of emulsification into an aqueous solution of surfactant (water phase). The bitumen modification was conducted with a Silverson L5M (U.K.) high-shear homogeneizer, under optimized blending conditions of 170ºC, 1 hour and 5000 rpm. Recycled LDPE concentrations (in the bitumen phase) studied ranged from 2 to 5 wt.%. The emulsification was carried out in a continuous plant equipped with a Denimotech DT 03 (Denmark) colloidal mill, and a sample collector vessel which can be pressurized. Optimized emulsifying conditions were temperatures in the range 165-175ºC (depending on polymer concentration), pressure of 7.5 bar and speed of 9000 rpm. In any case, the water phase flow rate was fixed and the LDPE-bitumen phase flow rate was varied so that different solids contents were obtained. The surfactant content was always set to between 0.75 and 1 wt.%. A non-modified emulsion is included for reference.

With respect to characterization, steady viscous flow curves, droplet size distribution and solids content were evaluated. Viscous flow curves, at 25ºC, were performed with a controlled stress Thermo-Haake MARS II (Germany) rheometer equipped with concentric cylinders geometry type Z20 DIN-53019. The droplet size distribution and Sauter average diameters were measured

with a Malvern Mastersizer 2000 (U.K.) laser diffraction analyzer, with previous dilution of the emulsion into water. The solids content, in wt.%, was calculated from the weights of an emulsion sample and its residue when it was set in an oven at 110ºC overnight.

RESULTS AND DISCUSSION

The different emulsions in Table 1 are identified by the bitumen phase polymer concentration: 0, 2, 4 and 5 wt.% (E0, E2, E4 and E5, respectively). Three different emulsions with varying solid contents were prepared for 5 wt.% polymer (E5-1, E5-2 and E5-3).

With regard to the droplet size distribution (DSD), PMB emulsions up to 4 wt.% LDPE showed one single peak, whilst a multimodal distribution was observed for 5 wt.%. Also, the former emulsions presented Sauter mean diameters ($D_{3,2}$) between 4.1-4.4 μm, whilst the latter ones demonstrated smaller values (2.1-1.8 μm).

TABLE 1 Values of solids content, $D_{3,2}$ and limiting viscosity for the five PMB emulsions studied.

	E0	**E2**	**E4**	**E5-1**	**E5-2**	**E5-3**
Polymer in bitumen phase (wt.%)	0	2	4	5	5	5
Solids content (wt.%)	50.6	50.0	55.0	48.2	55.7	62.8
Sauter mean diameter (μm)	4.1	4.2	4.4	2.1	1.8	1.8
$\eta\infty$ (mPa·s)	5	15	24	10	16	25

On the other hand, the evolution of viscosity, at 25ºC, with shear rate shown in Figure 1 consisted of a shear thinning drop followed by a constant high-shear-rate-limiting viscosity beyond a threshold value of shear rate, which can be described by the Sisko's model:

$$\eta(\dot{\gamma}) = k_s \cdot \dot{\gamma}^{n-1} + \eta_\infty \qquad (1)$$

Values of η_∞ have been calculated from Figure 1 and presented in Table 1. According to this table, these limiting viscosities seem to be influenced by both polymer concentration in the bitumen phase and the solids content in the emulsion. Thus, by comparing emulsions E0 and E2 (with similar solids contents and Sauter mean diameters), the addition of 2 wt.% LDPE led to a limiting viscosity increase from 5 to 15 mPa·s. On the other hand, the limiting viscosity increased further, from 15 to 24 mPa·s when the polymer concentration was raised to 4 wt.%, also affected by a higher solid content of 55 wt.%. As for, the three emulsions with the same polymer concentration in the bitumen phase of 5 wt.% (with comparable Sauter average

diameters), the effect of the solids content is clearly observed. Hence, E5-3 (solids content of 62.5 wt.%) presents the highest limiting viscosity, of 25 mPa·s, followed by E5-2 (solids content of 55.7 wt.%) and E5-1 (solids content of 48.4 wt.%), with limiting viscosities of 16 and 10 mPa·s, respectively.

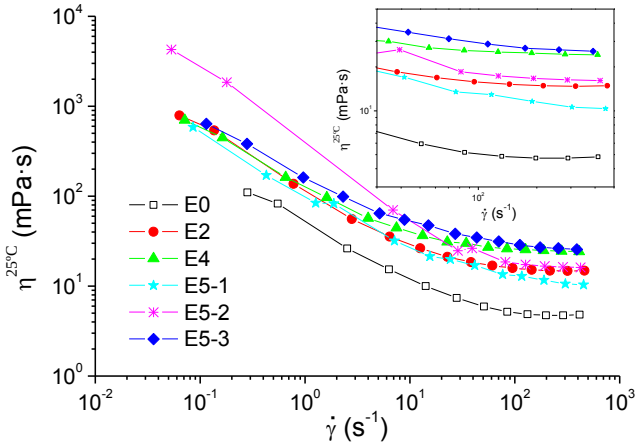

FIGURE 1 Viscosity curves in steady state, at 25ºC, for the five PMB emulsions studied.

CONCLUSIONS

The fabrication of O/W emulsions of LDPE-modified bitumens was accomplished by an in-line emulsification procedure at high temperature and pressure. The resultant emulsions presented a low Sauter mean diameter (2-4 μm) and a shear-thinning behaviour followed by a high-shear-rate-limiting viscosity, which increased as bitumen-polymer phase concentration increased .

ACKNOWLEDGEMENTS

This work was funded by MINECO-FEDER (Subprogram INNPACTO project IPT-2012-0316-370000). Authors gratefully acknowledge their support.

REFERENCES

1. Read, J., Whiteoak, D., The Shell Bitumen Handbook (Fifth Ed.); Thomas Telford Publishing: London, **2003**
2. Lesueur, D. In Polymer Modified Bitumen; McNally, T., Ed.; Woodhead Publishing: Cambridge, **2011**; Chapter 2, pp 25-42.

P47

Autoplasticised PVC using the strategy of PVC/PBA copolymers: Rheology and microestructure

María Eugenia Muñoz[a], Itxaso Calafel[a], Antxon Santamaría[a], Miquel Boix[b], Jose Ignacio Conde[b], Belén Pascual[b].

[a] POLYMAT, Departamento de Ciencia y Tecnología de Polímeros, UPV/EHU. Avenida de Tolosa 72, E-20018, San Sebastián. Spain

[b] ERCROS SA, Departamento de Innovación y Tecnología de la División de Plásticos, Diagonal 595, 08014, Barcelona. Spain

Correspondence to: Maria Eugenia Muñoz (E-mail: *mariaeugenia.munoz@ehu.es*)

ABSTRACT

The synthesis of poly (vinyl chloride), PVC, copolymers by living radical polymerization constitutes a novel strategy developed to obtain self-pasticised PVCs, that can avoid the problems derived from the migration of conventional plasticisers, like phthalates. In this work, random and block copolymers, with 0-40% weight of BA content, are investigated. In the case of the block copolymers, microphase separation and the presence of crystals lead to a thermorheologically complex behaviour, in contrast with the simplicity observed for random copolymers. The viscosity of the copolymers determined by extrusion capillary rheometry, under conditions similar to polymer processing, was also investigated showing the advantages of the self-plasticised material.

KEYWORDS

PVC Copolymers; Thermorheological complexity; Dynamic viscoelasticity; Viscosity function; Self-plasticization

INTRODUCTION

PVC particles have crystallites of varying sizes, which only melt completely above approximately 230ºC[1]. This factor, together with its low thermal stability above 190ºC, obliges

to process PVC in a partially crystalline state. To avoid this difficulty, plasticisers such as diethyl- (2-ethylhexyl) phthalate (more known as DOP) have been traditionally used, but the migration of these low molecular weight molecules causes salubriousness problems. Plasticisation or reduction of the glass transition temperature, Tg, of PVC has been also reached by means of blends, for instance with EVA copolymer[2] or by internal plasticisation with PBA in PVC-PBA copolymers obtained by radical block polymerization[3].

A very interesting success of the Single Electron Transfer-Degenerative Chain Transfer Living Radical Polymerization (SET- DTLRP) concerns the synthesis of tri-block copolymers (ABA) of poly(vinyl chloride) (PVC) and poly(n-butyl acrylate) (PBA), that is, PVC-b-PBA-b-PVC[4]. In contrast with the relatively known block copolymers, the synthesis of PVC-PBA based random copolymers by living radical polymerization (SET-DTLRP) has been very recently claimed[5].

The aim of this paper is to investigate both block and random PVC-PBA copolymers, considering them as self-plasticised materials. This implies a rheological study focusing on the correlation *microestructure-rheology-processing*, which involves linear viscoelastic measurements, as well as continuous capillary flow tests.

EXPERIMENTAL PART

Samples preparation and Characterization

Details of the synthesis and polymerization, as well as methods used for characterization, are given elsewher[4,5].

Rheological measurements

The dynamic viscoelastic behavior of the samples in the molten state was investigated using a ARG-2 rheometer with a parallel-plate fixture (25mm diameter).

Extrusion flow experiments were performed in a Göttfert 2002 rheometer. The viscosity curves, i.e. viscosity as a function of shear rate, were obtained.

RESULTS AND DISCUSSION

In block copolymers, phase separation and the presence of small crystals, detected by DSC, is reflected in the viscoelastic behavior, at temperatures above the melting of the main crystals[4]. To the difference to random copolymers, block copolymers give a thermorheologically complex behavior, since time-temperature superposition does not hold (Figure 1).

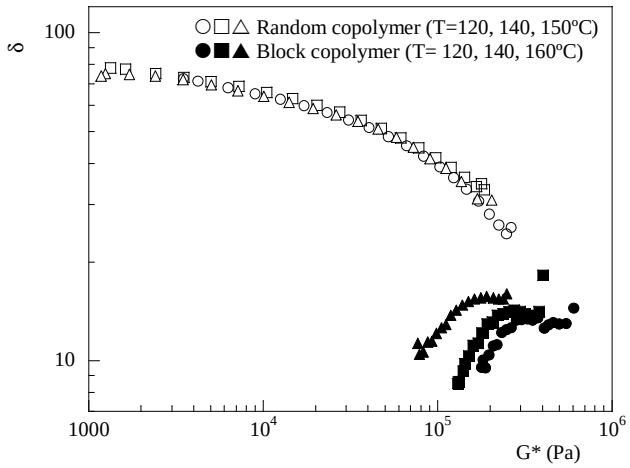

Figure 1: Loss factor (δ) vs complex modulus (G*) for 60PVC-40BA random copolymer (open symbols) and 30PVC-40PBA-30PVC block copolymer (full symbols).

For random copolymers, plots like those shown in Figure 1 allow determining the entanglement modulus, G_N^0, which is the value of the elastic modulus as δ tends to zero. This in turn leads to obtain the packing length and other structural parameters. However, block copolymers act as complex fluids and so the correlation between rheology and chain structure cannot be investigated. Alternatively, in Figure 2 the continuous flow viscosity function, $\eta(\dot{\gamma})$, is shown, together with the complex viscosity, η* (ω), determined in oscillatory flow (Cox-Merz rule).

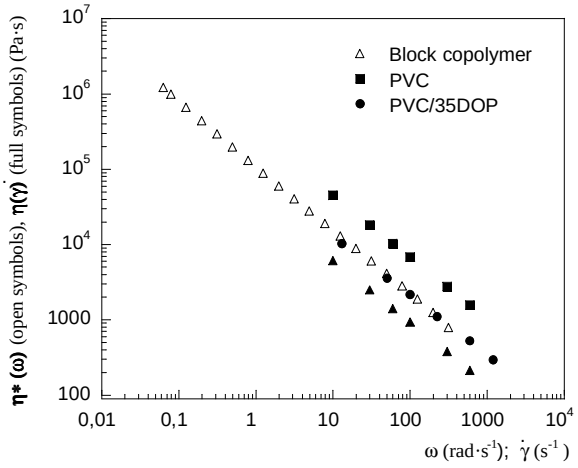

Figure 2: Test of the Cox-Merz rule for 30PVC-40PBA-30PVC block copolymer (△,▲). For comparison purposes $\eta(\dot{\gamma})$ vs $\dot{\gamma}(s^{-1})$ of conventional PVCs are included: PVC (■) and PVC/35DOP (●).

CONCLUSIONS

The main feature of the investigated materials is their capacity to self-plasticise, owed to the presence of PBA. Extrusion flow results demonstrate that the viscosity can be reduced to the levels of conventional PVC which contains 35% DOP plasticiser. Phase separation and *rheology-microestructure* correlation is analysed using oscillatory flows. Two remarks can be done:

a) No concordance between both viscosities is observed, as could be expected for a complex system.

b) The self-plasticised effect is noted, as low viscosity values are observed in the block copolymer, as compared with pure PVC and plasticised PVC/DOP.

ACKNOWLEDGEMENTS

UPV/EHU (UFI 11/56) and GIC IT-586-13 (Basque Government).

REFERENCES AND NOTES

1. A. M. Zdilar, R. I. Tanner, *J. Rheol.* **1994**, *38*, 909-920.
2.- R. Hernández, J. A. del Agua, J. J. Peña, A. Santamaría, J. *Polym. Eng. Sci.* **1996**, *36*, 2570-2578.
3. N. Overberg, G. Weinand, G. Smets, *J. Polym. Sci., Part A: Polym. Chem.* **2006**, *16,* 3107-3121.
4. I. Calafel, M. E. Muñoz, A. Santamaría, M. Boix, J. I. Conde, B. Pascual, *J. Vinyl Addit. Technol.* **2015**, *21*, 24-32.
5. R. Obeso, B. Pascual, J. M. Asua, (Ercros S.A.). WO2013014158A1, Jun 19, 2014.

P48

Improving the rheological performance of bituminous mastics by LDPE and SBS modification

Antonio Abad Cuadri, Claudia Roman, Ievgenii Liashenko, Moisés García-Morales, Inmaculada Martínez, Pedro Partal

Departamento de Ingeniería Química, Centro de Investigación en Tecnología de Productos y Procesos Químicos (Pro^{2}TecS), Campus de "El Carmen", Universidad de Huelva, 21071, Huelva, Spain

Correspondence to: Pedro Partal (E-mail: *partal@uhu.es*)

ABSTRACT

This research presents a comparative analysis between asphaltic mastics, containing a filler/bitumen ratio of 65/35, from bituminous binders which were previously modified by addition of either a thermoplastic elastomer Styrene-Butadiene-Styrene (SBS) or recycled low density polyethylene (LDPE). LDPE-mastic showed an enhancement in the linear viscoelastic behaviour at medium-high temperature range (45-65 ºC), if compared to SBS-mastic. Additionally, if a deformation outside the linear viscoelastic (LVE) range is applied, LDPE-mastics present an improved capacity of recovery when they return to the LVE.

KEYWORDS

Bituminous mastics; polymer modification; rheological properties; product design.

INTRODUCTION

In bituminous asphalt mixes, mineral fillers (with a particle size below 75 μm) typically represent from 2 to 12 wt.% on their total mineral matter[1]. Hence, a bitumen/filler blend (commonly referred to as mastic) naturally forms when bitumen and aggregates are mixed. Consequently, bitumen is the only deformable component and forms the continuous matrix of the mastic (and, the asphalt mixtures) contributing significantly to road performance[2].

Not much work has been done on polymer-modified bituminous mastics, and the effect that polymer modification exerts on the mastic performance. With the aim of improving knowlegde

on this subject, asphaltic mastics, containing a filler/bitumen ratio of 65/35, were prepared from bituminous binders which were previously modified by addition of either a thermoplastic elastomer SBS or recycled LDPE. Rheological characterization, through linear and non-linear viscoelasticy tests, revealed that polymer type exerts a significant influence on the binder contribution to the overall rheological properties of the mastics.

EXPERIMENTAL SECTION

Materials

Two base bitumens with penetrations values (according to EN 1426:2007) of 50 and 73 dmm, respectively, were selected. In addition, two different types of polymers have been considered as bitumen modifying agents: a) a thermoplastic elastomer SBS triblock copolymer (trade name "C-401"), supplied by Dynasol S.A.; and b) a recycled LDPE, provided by Cordoplas S.A. Finally, the mineral filler obtained from a stone quarry, with a particle size between 45 and 105 μm, has been used as reinforcing filler in the preparation of the asphaltic mastics.

Samples processing

Prior to the preparation of the mastics, bitumen 70/100 was modified by addition of either SBS or LDPE. Bitumen modification was carried out with a Silverson L5M homogenizer at 3500 rpm by mixing bitumen 70/100 and 3 wt.% SBS or LDPE, for 1.5 h, and at a processing temperature of 180 or 170 ºC, respectively (under these conditions, the loss of highly components from the bitumen may be considered negligible). After this stage, the adequate amount of filler was mixed with the modified binders for 1 h, getting asphaltic mastics with a filler/bitumen ratio of 65/35. These mastics are compared to an unmodified mastic prepared from bitumen 50/70. Thus, the three base binders present similar penetrations (50, 48 and 63 dmm), and the comparison of the overall rheological properties is not influenced by binders with different hardnesses.

Tests and measurements

Frequency sweep tests, in shear mode, within the linear viscoelasticity region (LVE), from 0.03 to 100 rad/s, and recoverability tests, were performed using a controlled-stress rheometer Physica MCR-301 (Anton Paar, Austria) at 55 ºC. Recoverability tests were proposed to assess material nonlinear viscoelastic performance, by means of three 30 min intervals of dynamic loading at a

fixed frequency and different deformations, with the one in between outside the LVE region. In order to ensure accurate results, at least two replicates were conducted for every sample.

RESULTS AND DISCUSSION

Dynamic mechanical spectra, at 55 ºC, of the different mastics studied are shown in Figures 1A and 1B. At 55 ºC, bitumen softens sufficiently, and hence, the polymer significantly contributes to the bulk rheological behaviour of the bituminous mastics.

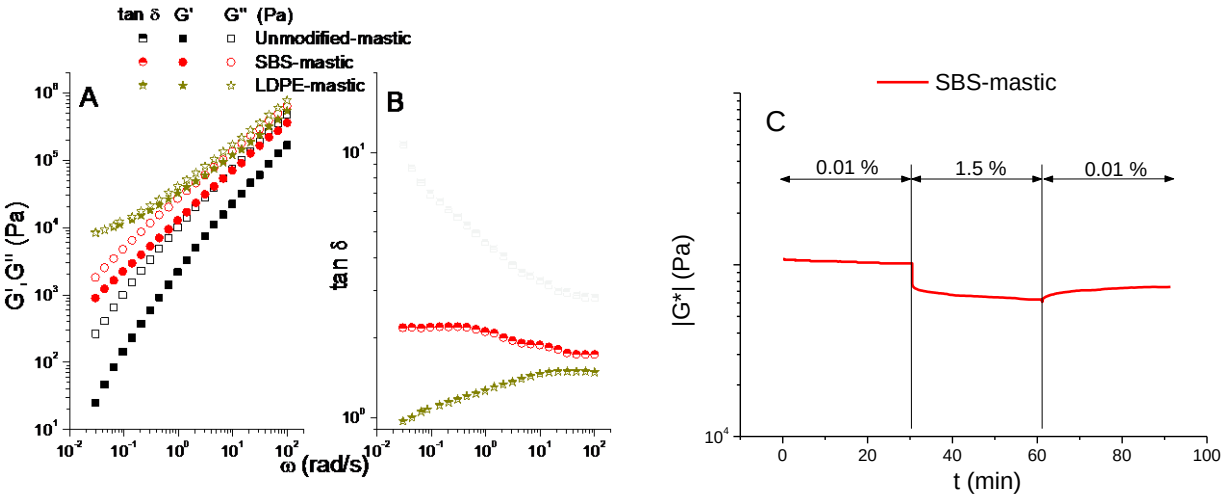

FIGURE 1. Frequency sweep tests in the linear viscoelastic range, at 55 ºC, for unmodified and polymer-modified mastics (Fig 1A,1B). Evolution of the Complex modulus decay after changing deformation values for SBS-mastic (Fig. 1C).

As can be observed, at 55 ºC, unmodified mastic curves tend to a terminal flow region at the lowest frequencies studied, being G' and G'' nearly proportional to ω^2 and ω^1, respectively. The addition of polymers (recycled LDPE or SBS) to the neat bitumen increases both moduli over the entire range of frequency studied for their corresponding mastics. It is well known that the polymer may dissolve and/or disperse into the maltenic medium, enhancing the properties of the blends[1]. It can be noticed that, for the SBS-mastic, both moduli are parallel lines, as supported by a relatively constant value of loss tangent, tan δ, shown in Figure 1B. In addition, LDPE-mastic shows the highest values of both moduli at low/intermediate frequencies. This observation indicates a remarkable enhancement of the rheological properties for LDPE-mastic in relation to those shown by unmodified mastic or SBS-mastic. Thus, the results obtained with the LDPE-mastic could be attributed to a binder with enhanced elasticity, as can be seen in Figure 1B, where the values of the loss tangent (tan δ) are the lowest within the entire frequency range studied.

The non-linear viscoelastic behaviour of mastics was studied through recoverability tests, which display the evolution of the complex modulus (|G*|) with the elapsed time, at 55 ºC, submitted at different deformation cycles (see Figure 1C). The percentage values of recovery and destruction (Table 1) were calculated from the steady-state complex modulus (G_0^*, G_1^* and G_2^*) attained for the first, second and third deformation value applied, being G_0^* and G_2^* obtained at deformations within LVE and G_1^* measured in the non-linear viscoelasticity region.

TABLE 1 Rheological destruction and recovery percentages for the asphaltic mastics studied.

	Destruction[a] (%)	Recovery[b] (%)
Unmodified -mastic	29.6	17.3
SBS-mastic	38.4	29.3
LDPE-mastic	66.6	63.9

[a] (%)Destruction = $[(G^*_0 - G^*_1) / G^*_0] \times 100$; [b] (%)Recovery= $[(G^*_2 - G^*_1) / (G^*_0 - G^*_1)] \times 100$

As can be deduced from Table 1, the highest destruction and recovery percentages values are observed for the LDPE-mastics. Thus, if a deformation outside the LVE is applied, mastics prepared from a binder modified with recycled LDPE present a higher capacity of recovery to SBS-mastic, when they return to the LVE range.

CONCLUSIONS

Asphaltic mastics prepared from LDPE and SBS modified binders showed a significant enhancement in the rheological properties at medium-high (45-60 ºC) in-service temperatures. Such an improvement can be deduced from both dynamic mechanical spectra conducted in the linear viscoelastic region and recoverability tests at 55 ºC.

ACKNOWLEDGEMENTS

This work was funded by MINECO-FEDER (Subprogram INNPACTO project IPT-2012-0316-370000). Authors gratefully acknowledge their support.

REFERENCES

1. Lesueur, D., Advances in Colloid and Interface Science, 2009, 145, 42-82.
2. Adedeji, A.; Grünfelder, T.;Macosko, C.W.; Stroup-Gardiner, M.; Newcomb, D.E., Polymer Engineering Science, 1996, 36, 1707-1723.

Stability and rheology of ecological submicron emulsions as influenced by dispersed phase concentration

Luis A. Trujillo-Cayado[1], Mª Carmen Alfaro[1], José Muñoz[1]

[1] Reología Aplicada. Tecnología de Coloides. Departamento de Ingeniería Química. Facultad de Química. Universidad de Sevilla. C/ P. García González, 1, 41012, Sevilla, Spain.

Correspondence to: María Carmen Alfaro Rodríguez (E-mail: *alfaro@us.es*)

ABSTRACT

In this study, we examined the influence of dispersed phase concentration on the rheology, droplet size distribution and physical stability of submicron emulsions. The formulation consists of a mixture of green solvents (N,N dimethyldecanamide and α-pinene) as dispersed phase and a non-ionic polyoxyethylene glycerol ester as emulsifier. Rheology provides useful information on the physical stability and handling properties of emulsions. We report the effect of aging time on a) steady shear flow, b) viscoelasticity, c) droplet size distribution and d) physical stability of emulsions. The rheological properties assessed were significantly influenced by the dispersed phase concentration. All emulsions exhibited shear thinning behavior and viscoelastic properties above of 35 wt% dispersed phase. The laser diffraction technique revealed submicron droplet sizes for all studied emulsions, which tended to grow with aging time by coalescence in the most concentrated emulsions.

KEYWORDS: Emulsion, Dispersed phase, Green solvent, Rheology, Viscoelasticity

INTRODUCTION

The oil phase of an emulsion is one the points of current progress in innovate formulations. From this point of view the use of green solvents is now an area of great interest. Different organic solvents vary in their molecular characteristics that lead to changes in their properties such as density, melting point, polarity, viscosity and solubility in water. Many of these properties have a major influence on the formation, stability and functionality of emulsions[1]. For example, the solubility in water of an oil phase determines the physical stability of an emulsion

to Ostwald ripening phenomenon due to diffusion of solvent molecules through the continuous phase. In addition, the concentration of oil droplets in an oil-in-water emulsion influences its physical stability and rheological properties. Droplet concentration is usually characterized in terms of the dispersed phase mass fraction (ϕ_m), which is the mass of the oil phase (m_{oil}) divided by the total mass of emulsion (m_E):

$$\phi_m(\%) = 100 \cdot \frac{m_{oil}}{m_E} \qquad \text{Eq. (1)}$$

An eco-friendly emulsion may contain a variety of different green solvents as oil phase, such as essential oils, terpenes and fatty acid dimethylamides. In this study, we examined the influence of dispersed phase concentration on the rheology, droplet size distribution and physical stability of submicron emulsions.

MATERIALS AND METHODS

Oil-in-water emulsions with 3 wt% surfactant (glycereth-17 cocoate) and different dispersed phase concentrations (from 30 wt% to 50 wt%) were prepared using as a oil phase a mixture of green solvents, N,N-dimethyl decanamide (AMD-10^{TM}) and α-pinene, with a mass ratio of 75/25 respectively. Emulsions were produced by homogenization with a rotor-stator device (Silverson L5M) using a rotational speed of 7500 rpm for 120 s at room temperature.

Characterization of the flow behavior was carried out with a controlled stress rheometer (Haake-MARS) using a sandblasted Z20 coaxial cylinder geometry (Ri=1cm, Re/Ri=1.085) to avoid slip-effects. The same rheometer with a sandblasted double-cone sensor (60 mm, 1°) was used to perform frequency sweep tests from 20 to 0.05 rad/s by selecting a stress within the linear range. Equilibration time prior to rheological tests was 5 min. Test temperature = 20°C.

Droplet size distribution measurements were performed using a static light scattering instrument (Malvern Mastersizer X) for about 30 days.

RESULTS AND DISCUSSIONS

Figure 1 shows the Sauter mean diameters ($D_{3,2}$) of emulsions with different dispersed phase concentration aged for 1 and 30 days. For all emulsions submicron mean diameters were

achieved. The emulsions aged 24 hours show a marked increase of $D_{3,2}$ by increasing the concentration of dispersed phase from 45 to 50wt%. Taking into account the time evolution for 30 days of $D_{3,2}$ for the five emulsions, the results obtained pointed to the occurrence of some coalescence for emulsions containing 45 and 50 wt% oil phase.

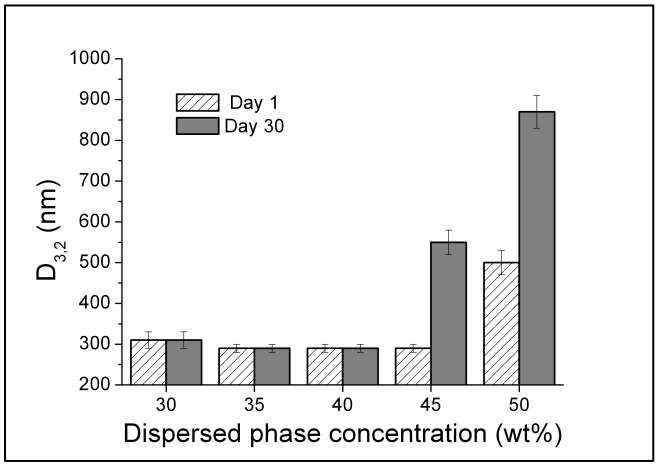

FIGURE 1. Sauter mean diameter ($D_{3,2}$) for all emulsions aged for 1 and 30 days as a function of the dispersed phase concentration.

Figure 2A shows the viscosity curves fitted to the Cross model for the emulsions studied aged for 24 hours as a function of oil phase concentration. All emulsions in the studied concentration range exhibited shear-thinning behaviour. An increase of the dispersed phase concentration from 30 to 45 wt% yielded an increase of the zero shear viscosity and a decrease of the flow index. The decrease in viscosity values for the 50 wt% emulsion aged for 1 day may be due to the higher mean droplet diameter.

Figure 2B shows the frequency influence on the linear viscoelastic functions, G' and G", for the emulsions aged that exhibited measurable linear viscoelastic range as a function of time. The results obtained corresponded to the so-called plateau relaxation zone. The emulsion containing 35 wt% of dispersed phase shows lower values of G" than G' in the higher frequency regime and G" is greater than G' in the lower frequency regime as a consequence of a crossover point between G' and G". All samples above 35 wt% dispersed phase displayed clear viscoelastic properties with a predominance of the elastic over the viscous component in the frequency range studied. G´ turned out to be relatively independent of frequency, which is typical of gel-like materials. The addition of oil phase caused the formation of a weaker structure above 45 wt%,

which is consistent with laser diffraction and flow curves results.

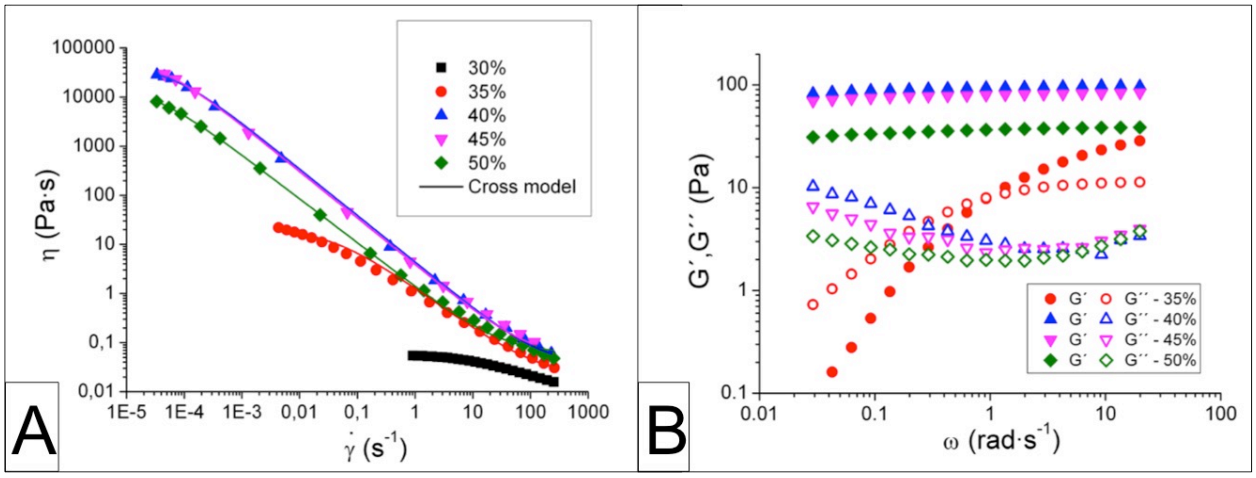

FIGURE 2. (A) Flow curves and (B) mechanical spectra for all emulsions aged for 24 hours as a function of dispersed phase concentration.

CONCLUSIONS

The rheological properties assessed were significantly influenced by the dispersed phase concentration. All emulsions exhibited shear thinning behavior, which fitted the Cross model. An increase the dispersed phase concentration from 30 to 45 wt% yielded an increase of the zero shear viscosity and a decrease of the flow index. All samples above 35 wt% dispersed phase displayed clear viscoelastic properties with a predominance of the elastic over the viscous component in the frequency range studied. The laser diffraction technique revealed submicron droplet sizes for all studied emulsions, which tended to grow with aging time by coalescence in the most concentrated emulsions.

ACKNOWLEDGEMENTS

The financial support received (Project CTQ2011-27371) from the Spanish Ministerio de Economía y Competitividad and from the European Commission (FEDER Programme) is kindly acknowledged.

REFERENCES AND NOTES

1. McClements, DJ.; Rao, J., Food-grade nanoemulsions: formulation, fabrication, properties, performance, biological fate, and potential toxicity. *Critical Reviews in Food Science and Nutrition*, **2011**, 51, 285-330.

P50

Influence of homogenization rate on the rheology and stability of emulsions formulated with a mixture of green solvents.

Nuria Calero[1], Jenifer Santos[1], José Muñoz[1].

[1]Reología Aplicada. Tecnología de Coloides. Departamento de Ingeniería Química. Facultad de Química. Universidad de Sevilla c/ P. García González, 1, E41012, Sevilla España.

Correspondence to: Nuria Calero (E-mail: *nuriacalero@us.es*)

ABSTRACT

There is a need to replace the traditional organic solvents by more environmentally favourable solvents in process engineering, cleaning as well as in other formulated products[1]. The goal of this study was to assess the processing conditions which slow down the destabilization kinetics of green emulsions by means of rheological techniques, assisted by laser diffraction. Fatty acid dimethylamides (FAD) are green solvents derived from biomass that find application in agrochemical emulsificable concentrates. D-Limonene (D-L) is a naturally occurring hydrocarbon which can be derived from the rinders of citrus fruits and shows good biodegradability. In this research an optimised ratio of FAD and D-L solvents was used as dispersed phase of O/W emulsions[2]. Lab-scale emulsions were prepared, with a Silverson homogenizer equipped with an emulsor mesh screen, at several rotational speeds (Ω). The specific target of this study was to determine the optimum Ω which results in enhanced stability. Regardless of the Ω used, flow curves of emulsions at 20ºC showed Cross-type behaviour. Emulsions processed above a critical Ωc exhibited weak-gel viscoelastic properties when studied under SAOS. A decrease of plateau modulus was a clear indication of the occurrence of some coalescence, which was also confirmed by the increase in droplet sizes measured by laser diffraction. We demonstrate that the optimum homogenization rate was around 4000 rpm on account of the lack of coalescence.

KEYWORDS: eco-friendly emulsions, rheology, laser diffraction, stability.

INTRODUCTION

The toxicity of traditional organic solvents limits its application in emulsions for agrochemical use. Hence, in order to avoid the use of toxic solvents in the production of

agrochemical products, active ingredient used in pesticides should be dissolved in a natural and nontoxic solvent. In this regards, L-limonene, a safe, highly effective, and biodegradable natural extraction from peel of citrus fruits, is a good solvent alternative for this application. In addition, N,N-dimethyldecanamide has attracted the attention recently due to its good characteristics like eco-friendly solvent.

The main objective of this work was the study of the influence of homogenization rate on the physical stability of slightly concentrated O/W emulsions formulated with two green solvents (N,N-dimethyldecanamide and D-limonene) and a polyoxyethylene glycerol ester as emulsifier.

MATERIALS AND METHODS

Materials

N,N-Dimethyldecanamide (Agnique AMD-10^{TM}, BASF), D-Limonene (Sigma Aldrich) and Glycereth-17 Cocoate (HLB:13)(KAO) as emulsifier, were used. Its trade name is Levenol C-201^{TM}. RD antifoam emulsion (DOW CORNING$^{®}$) was used as antifoaming agent. Deionized water was used for the preparation of all emulsions.

Methods

Emulsions development

Emulsions containing 4 wt % Levenol C-201 as emulsifier, 0.1 wt % antifoam emulsion and 40 wt% mixture of solvents were prepared. The ratio used was 75 wt% AMD-10 and 25 wt% D-Limonene, which was previously demonstrated to be the optimum. These O/W emulsions were carried out using a Silverson L5M at different homogenization rates (4000-8000 rpm) during 60 s.

Laser diffraction measurements

Size distribution of oil droplets were determined by laser diffraction using Mastersizer X (Malvern, Worcestershire, UK). The mean droplet diameters was expressed as Sauter diameter ($D_{2,3}$) an volumetric diameter ($D_{4,3}$):

$$D[M,N] = \left[\frac{\int D^M\, n(D)dD}{\int D^N n\,(D)dD}\right]^{\frac{1}{M-N}} \quad (1)$$

Rheological measurements

Rheological experiments were conducted with a Haake MARS controlled-stress rheometer (Thermo-Scientific, Germany), equipped with a sand-blasted double cone/1º to avoid slip effects. Flow curves were carried out from 0.05 to 5 Pa at 20ºC. Frequency sweeps were conducted from 0.05 to 20 rad/s selecting a stress well within the linear range.

RESULTS AND DISCUSSION

Figure 1A shows flow behavior for studied emulsions as a function of homogenization rate. All emulsions showed shear-thinning behavior that fitted fairly well to Cross model.

$$\eta = \frac{\eta_0}{1+\left(\frac{\dot{\gamma}}{\dot{\gamma}_c}\right)^{1-n}} \qquad (2)$$

Where η_o is zero shear viscosity, $\dot{\gamma}_c$, critical shear rate and n the flow index. Two levels in zero shear viscosity were observed. Emulsions processed above 6000 rpm showed higher η_o than emulsions processed at lower homogenization rates. This supports laser diffraction results. In addition, only emulsions processed above 5000 rpm exhibited viscoelastic properties where storage modulus are higher than loss modulus in every frequency. This fact may be explained by a flocculation process. Plateau zone was observed in all frequency sweeps with a characteristic plateau modulus, G_N^0. Figure 1B shows plateau modulus as a function of homogenization rate with aging time. G_N^0 for 1-day.aged emulsions processed at 6000 and 7000 rpm did not show any significant differences. However, 8000 rpm emulsion showed lower G_N^0 than the others. This fact may be related to a break of flocs since the volumetric diameter was very similar (see fig 2). Furthermore, all emulsions exhibited a decrease of G_N^0 with aging time. Thus, a coalescence phenomenon could be taking place.

Figure 2 shows volumetric diameter as a function of homogenization rate at 1 and 30 days of aging time. There is a decrease of volumetric diameter with homogenization rate at one-day aging time. However, a trend to level off at higher homogenization rates was also observed. In addition, there is an increase in the droplet size from day 1 to 40 for emulsions processed above 5000 rpm. This fact may be related to a flocculation process, which explains the higher viscoelastic properties of these emulsions.

CONCLUSIONS

Submicron emulsions were obtained using a rotor-stator device. All emulsions exhibited shear-thinning behaviour and emulsions above 5000 rpm showed viscoelastic properties. These viscoelastic emulsions showed an increase of droplet size by laser diffraction. Rheology measurements supports this fact. Taking into account these results, we demonstrated that the optimum homogenization rate for these 40 wt% eco-friendly emulsions was 4000 rpm due to the lack of coalescence.

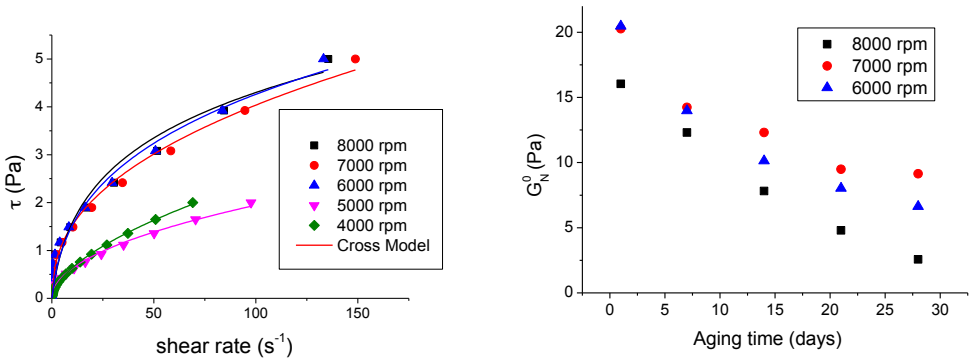

Figure 1.A) Flow curves for 40 wt% emulsions as a function of homogenization rate. B) Influence of aging time on plateau modulus for emulsions processed at different homogenization rate.

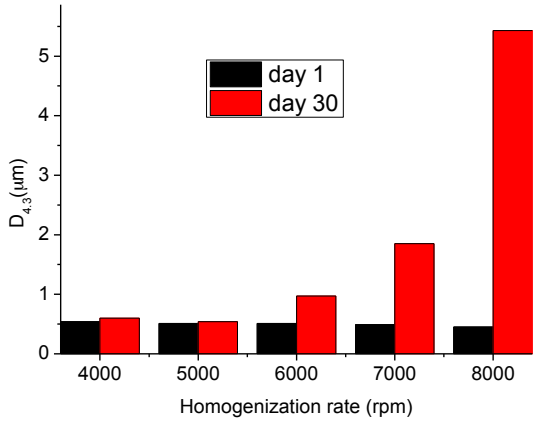

Figure 2.Volumetric mean diameter for emulsions processed at different homogenization rates at 1 and 40 days of aging time.

ACKNOWLEDGEMENTS

The financial support received (Project CTQ2011-27371) from the Spanish Ministerio de Economía y Competitividad, the European Commission (FEDER Programme) and from V Plan Propio Universidad de Sevilla is kindly acknowledged.

REFERENCES

1. Gani, R.; Jiménez-González, C.; ten Kate, A.; Crafts, P. A.; Jones, M.; Powell, L; & Cordiner, J. L., *Chemical engineering*, **2006**, 113, 30-43.

2. Santos, J.; Trujillo-Cayado, L. A.; Calero, N.; & Muñoz, J., *AIChE Journal*, **2014**, 60, 2644-2653.

IBER REO 15 Coimbra 2015

P30

Small and large amplitud oscillatory shear measurements of Advanced Performance xanthan gum solutions. Effect of xanthan gum concentration

Pablo Ramírez[1], Aurora Lucas Curado[1], José Antonio Carmona[1], Nuria Calero[1], José Muñoz[1]

[1]Departamento de Ingeniería Química. Facultad de Química. Universidad de Sevilla c/ P. García González, 1, E41012, Sevilla, Spain.

Correspondence to: Pablo Ramírez (E-mail: *pramirez@us.es*)

ABSTRACT

The idea behind LAOS is an attempt to describe the mechanical behaviour of complex fluids at large deformations, well beyond the linear viscoelastic region, which are closer to real processing conditions. Furthermore, large amplitude oscillatory shear (LAOS) has proven to be a sensitive technique in order to detect microstructural changes in complex fluids such as biopolymer networks, colloidal gels, etc. We illustrate the applications of LAOS with an "advanced performance" xanthan gum aqueous dispersions at different concentrations (from 0.15% (m/m) to 0.40% (m/m)), on account of the great technological interest of this bacterial polysaccharide. The influence of concentration on the viscoelastic properties of aqueous xanthan gum dispersions was studied by means of both techniques, SAOS and LAOS. Within linear viscoelastic range, the "advanced performance" xanthan gum demonstrated that possesses less fluid-like behaviour than conventional gum. More interestingly, the combination of the use of both rheological measurements allowed us to detect a structural transition within the concentration range studied.

KEYWORDS: Xanthan gum; LAOS; Non-linear viscoelasticity; Chebyshev coefficients; Weak-gel.

INTRODUCTION

Although SAOS tests are a useful tool to obtain a convenient rheological characterization of complex fluids in most real operations the deformation is well beyond the linear viscoelastic region and therefore linear viscoelastic characterization lacks information to fully understand practical polymer processing. Thus, LAOS tests are being increasingly important due to their usefulness in describing the elastic and viscous properties of complex fluids at large deformations[1,2].

The objective of this work was to study the influence of polymer concentration on the rheological properties of aqueous solutions of a commercial “advanced performance” xanthan gum (APXG). This rheological study involves small amplitude oscillatory shear (SAOS) and

large amplitude oscillatory shear (LAOS). The non-linear oscillatory response was analyzed using the third-order Chebyshev coefficients (e_3 and υ_3) may then be used to determine material nonlinear viscoelastic behaviour. Thus, material viscoelastic behaviour is classified in six categories: strain-softening (e_3<0), strain-stiffening (e_3>0), linear elastic e_3=0, shear thinning (υ_3<0), shear thickening (υ_3>0) and linear viscous υ_3=0 [3].

MATERIALS

KELTROL® Advanced Performance "Food Grade" xanthan gum, generously donated by CP Kelco, was used to prepare xanthan gum solutions. Xanthan gum solutions with concentrations ranging from 0.15% to 0.40% (m/m) were prepared by slowly adding the required amount of polymer powder. The solutions studied were prepared with ultrapure Milli-Q water. 0.1% (m/m) sodium azide was added to the solutions to prevent the growth of microorganisms. All ingredients were used as received.

RESULTS AND DISCUSSION

SAOS

Figure 1 shows G*and tan(δ) as a function of frequency within LVR (strain = 5%) for the two limiting concentrations studied. When increasing polymer concentration G* increases whereas tan(δ) decreases with values lower than one in all the frequency range studied, corresponding to a weak-gel behaviour. Nevertheless, there is a tendency to reach the crossover frequency that determines the onset of the terminal relaxation zone when moving towards lower frequencies for the lowest xanthan gum concentration. Furthermore a comparison of frequency sweeps for both the APXG used in the present study and a conventional one produced by the same Company (CP Kelco) for the same concentration of xanthan gum 0.40% (m/m) and ionic strength[4] showed that the conventional xanthan gum has a more fluid-like behaviour.

It is interesting to note that the Cox- Merz rule was followed for the lowest concentration of xanthan gum (0.15 % (m/m)), while it failed for the rest of concentrations studied. In this case the departure could be related to the occurrence of a structured system, supporting that the weak-gel structure was clearly set.

LAOS

Further information on the influence of the xanthan gum concentration on the microstructure of xanthan gum can be obtained by analysing the third-order Chebyshev coefficients (e_3 and υ_3). Figures 2a and 2b show the parameters e_3 and υ_3 used to evaluate the intracycle elastic and viscous non-linearities for the two limiting concentrations studied. Thus, the non-linear viscoelastic region can be divided into three parts according to the intracycles parameters. Region (A) Strain softening (e_3 < 0) + Shear thickening (υ_3 > 0); Region (B) Strain stiffening (e_3 > 0) + Shear thickening (υ_3 > 0) and Region (C) Strain stiffening (e_3 > 0) + Shear thinning

($\upsilon_3 < 0$). Furthermore, when υ_3 was plotted as a function of xanthan gum concentration two linear tendencies were observed, which could be related to a change in the behaviour of the polymer solution indicating the occurrence of two regimes. The drastic change in the slope was found in the 0.20% to 025% (m/m) range.

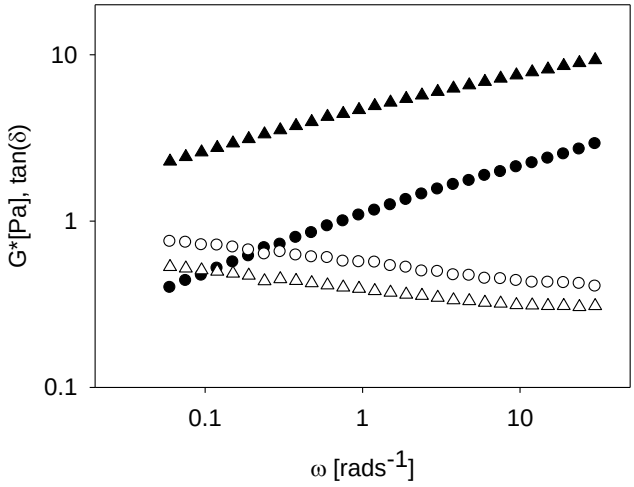

FIGURE 1. Complex modulus, G*(close symbols) and loss tangent, tan(δ) (open symbols) as a function of frequency for xanthan gum concentrations of 0.15 %(m/m) (circles) and 0.40 %(m/m) (triangles)T=20ºC.

CONCLUSIONS

All the studied systems showed a weak-gel behaviour that increase with concentration. The comparison of the mechanical spectrum for the Advanced Performance Xanthan Gum with a conventional one showed that the viscous component of the latter was more important than the one for the Advanced Performance.

The second evidence supporting a structural change was the deviations from the Cox-Merz rule for the concentrations above 0.20% (m/m), which indicates the occurrence of a more development structure.

A complete rheological characterization of the systems was achieved by analysing the parameters deduced from local methods. The plot of the maximum value of third-order –viscous Chebyshev coefficient (υ_3) obtained by LAOS against concentration supported the aforementioned change of the viscoelastic behaviour associated to the modification of the gum structure.

Finally, the non-linear viscoelastic region can be divided into three parts according to the intracycles parameters. Thus, region (A) Strain softening ($e_3 < 0$) + Shear thickening ($\upsilon_3 > 0$); Region (B) Strain stiffening ($e_3 > 0$) + Shear thickening ($\upsilon_3 > 0$) and Region (C) Strain stiffening ($e_3 > 0$) + Shear thinning ($\upsilon_3 < 0$).

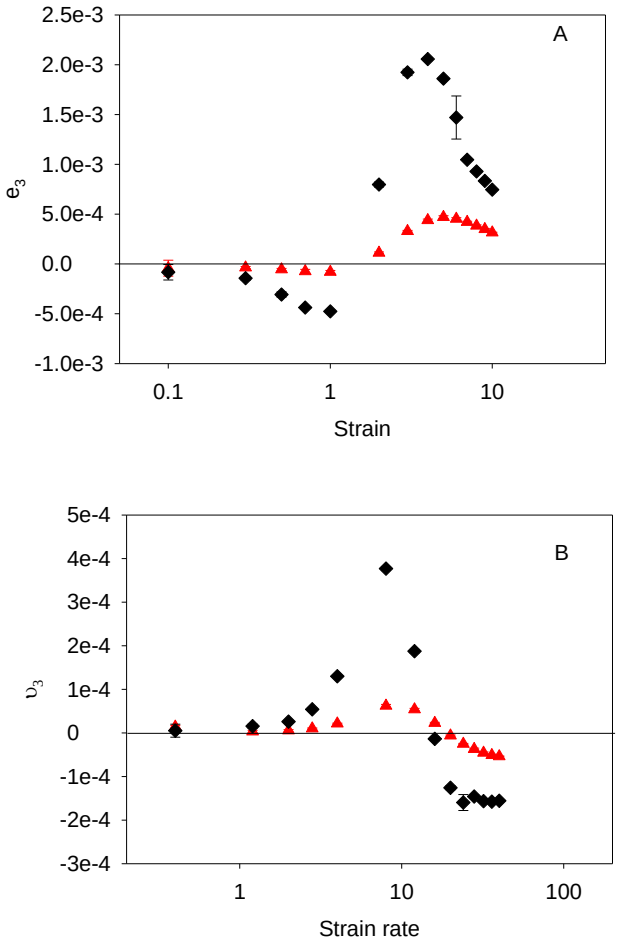

FIGURE 2. Oscillatory shear tests of xanthan gum at 4 rad/s analysed by means of LAOS parameters for 0.15 % (m/m) (triangles) and 0.40% (m/m) (diamonds). A) Third-order elastic Chebyshev coefficient, e_3. B) Third-order viscous Chebyshev coefficient, υ_3. T = 20ºC. The error bars are included in the figure.

ACKNOWLEDGEMENTS

The financial support received (Project CTQ2011-27371) from the Spanish Ministerio de Economía y Competitividad (MINECO) and from the European Commission (FEDER Programme) is kindly acknowledged.

REFERENCES

1. Carmona, J.A. ; Ramírez, P. ; Calero, N. ; Muñoz, J. Journal of Food Engineering, **2014**, *126*, 165.
2. Ewoldt, R.H. ; Winter, P. ; Maxey, J. ; McKinley, G.H. Rheologica Acta **2010**, *49*, 191.
3. Ewoldt, R.H. ; Hosoi, A.E. ; McKinley, G.H. Journal of Rheology **2008**, *52*, 1427.
4. Wyatt, N. B. ; Gunther, C. M.; Liberatore, M. W. Journal of Non-Newtonian Fluid Mechanics, **2011**, *166*, 25.

P31

Correlation of glycerol viscosity with temperature

Abel G. M. Ferreira[1], Ana P. V. Egas[1], Ana C. Costa[2], Danielly C. Abreu[2]

[1]*Department of Chemical Engineering, University of Coimbra, Polo II, Rua Silvio Lima, 3030-970 Coimbra, Portugal.*

[2] *Departamento de Engenharia Química, Universidade Federal de São João del-Rei Campus Alto Paraopeba - C.A.P,Rod.: MG 443, KM 7 Ouro Branco - MG 36420-000, Brasil.*

Correspondence to: Abel G. M. Ferreira (E-mail: abel@eq.uc.pt)

ABSTRACT

The dynamic viscosity of glycerol was measured in the range T= (293 to 394) K and atmospheric pressure using a Brookfield Thermosel system. To produce an extensive viscosity database for this substance, the data obtained in this study were combined with published data from the literature covering the range of temperature from near the glass transition temperature (190 K) up to 394 K. The Vogel-Tamman-Fulcher (VTF) equation and the Bond Strength-Coordination Number Flutuation (BSCNF) model, were both used to correlate the values selected in the database. From BSCNF the structural effects taking place near the glass transition were discussed.

KEYWORDS: Glycerol, Viscosity, Glass transition, BSCNF model, VTF equation

INTRODUCTION

Glycerol is one of the most extensively studied hydrogen-bonded systems. The presence of three hydroxy groups in the molecule gives rise to particularly rich and complex conformational and structural behaviour and it is one of the archetypal glass-forming liquids. The nature of its glass transition has been the object of several experimental investigations. In particular, the viscosity has been measured using different type of viscometers and consequently there is some disagreement in data from the various sources.

EXPERIMENTAL

Glycerol was obtained from ACROS (Cas No: 142-82-5) with mass fraction purity of 0.9987. Since glycerol is highly hygroscopic, samples were further degassed ultrasonically and dried over freshly activated molecular sieves supplied by Aldrich. Dynamic viscosity measurements were made in the range 20 to 121 ºC using a Brookfield Thermosel system with a rotational DV-II+ (model LVDV-11) viscometer. Temperature was controlled to ±0.5 K.

THEORY

The glass-forming liquid is formed by an agglomeration of clusters or structural units which are

bound to others by a certain bond strength retaining its spatial random connectivity. Thermally activated viscous flow occurs due to bond-breaking and bond-switching. Aniya et al.[1] developed the BSCNF viscosity model which is characterized by Gaussian distributions of the binding energy (E) and the coordination number (z) between structural units. The binding energy and coordination number are $E=E_0+\Delta E$ and $z= z_0+\Delta z$, respectively, where E_0 and z_0 are average values and ΔE and Δz are fluctuations. The viscosity in BSCNF is

$$\ln\left(\frac{\eta}{\eta_\infty}\right)=\frac{Cx+Cx^2\left\{\left[\ln\left(\frac{\eta_g}{\eta_\infty}\right)+0.5\ln(1-B)\right]\left(\frac{1-B}{C}\right)-1\right\}}{1-Bx^2}-0.5\ln(1-Bx^2) \qquad (1)$$

where $B=\left[\frac{(\Delta E)(\Delta Z)}{RT_g}\right]^2$, $C=\frac{E_0Z_0}{RT_g}$, x = T_g/T (T_g is the glass transition temperature, $\eta_g=10^{12}$ Pa.s and $\eta_\infty=10^{-5}$ Pa.s. The fragility index, $m=[d \log \eta /d(T_g/T)]_{T=Tg}$, from equation (1) is

$$m=\frac{1}{\ln(10)}\frac{\left\{B-C+2\left[\ln\left(\frac{\eta_g}{\eta_\infty}\right)+0.5\ln(1-B)\right]\right\}}{1-B} \qquad (2)$$

According to BSCNF theory, parameters B and C obey the relation[1]

$$C=\frac{2\gamma(1-B)}{2\gamma+\sqrt{B}\,(1+\gamma^2)}\left[\ln\left(\frac{\eta_g}{\eta_\infty}\right)+0.5\ln(1-B)\right],\ \gamma=\frac{|\Delta E|/E_0}{|\Delta z|/z_0} \qquad (3)$$

When γ= 1, equation (1) simplifies and the only parameter to be found is B (=B*) ($\ln(\eta_g/\eta_\infty)$ can be considered also as a varying parameter). This model will be referred here as BSCNF1. The Vogel-Fulcher-Tammann (VFT) equation[2-4]

$$\log\eta=A_{VTF}+\frac{B_{VTF}}{T-T_0} \qquad (4)$$

is one of the most commonly used expressions for the analysis of the temperature dependence of viscosity. $A_{VTF} = \log(\eta_\infty)$ is the value of the viscosity at the high temperature limit. B_{VTF} (=DT_0) and T_0 are fitting parameters. D is the strength parameter and T_0 is the Vogel temperature. An important quantity obtained from BSCNF model is the number of structural units broken $N_B= E_\eta / (E_0z_0)$ where E_η is the activation energy for the viscous flow and (E_0z_0) is the average total binding energy per one structural unit. Following Ikeda and Aniya[5] N_B gives the number of the structural units involved in

the thermally activated viscous flow, and it is expected to provide the degree of fluidity within the glass-forming liquids. From BSCNF model,

$$N_B = \frac{B^* - C^* + 2\left[\ln\left(\frac{\eta_g}{\eta_\infty}\right) + 0.5\ln(1-B^*)\right]}{(1-B^*)C^*} \qquad (5)$$

RESULTS

In table 1 the parameters of BSCNF and VTF models obtained by least squares fitting are presented. The fragility m and N_B are also presented. In figures 1 and 2 the experimental data are compared with the model equations.

TABLE 1. Parameters of BSCNF and VTF models of viscosity.

Model	B	C	B*	C* [b]	$\ln(\eta_g/\eta_\infty)$	m	T_g/K[c]	N_B	A_{VTF}	B_{VTF} (D_{VTF})	T_0	m_{VTF}
BSCNF	0.5576	7.7623	-	-	39.1440	69.0	190	-	-	-	-	-
BSCNF1	-	-	0.5346	9.6665	36.3392	58.6	190	14.0	-	-	-	-
VTF-5 [a]	-	-	-	-	-	-	-		-5.0	806.16 (5.8022)	138.94	58.8
VTF-6 [a]	-	-	-	-	-	-	-	-	-6.0	1028.99(8.0803)	127.345	-

[a] VTF-5 ($\eta_\infty=10^{-5}$) and VTF-6 ($\eta_\infty=10^{-6}$); [b] C* calculated from equation (3) with γ=1. [c]From calorimetric techniques.

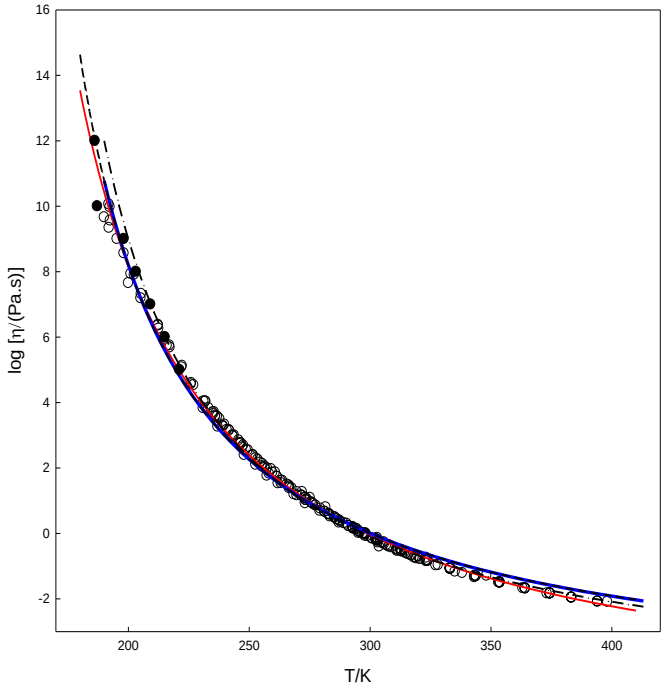

FIGURE 1. Experimental viscosity of glycerol as a function of temperature: ○, data used in the fittings; ●, Parks and Gilkey[6]; —·—, BSCNF; - - - -, BSCNF (γ=1); —, VTF ($\eta_\infty=10^{-6}$ Pa.s); —, VTF ($\eta_\infty=10^{-5}$ Pa.s).

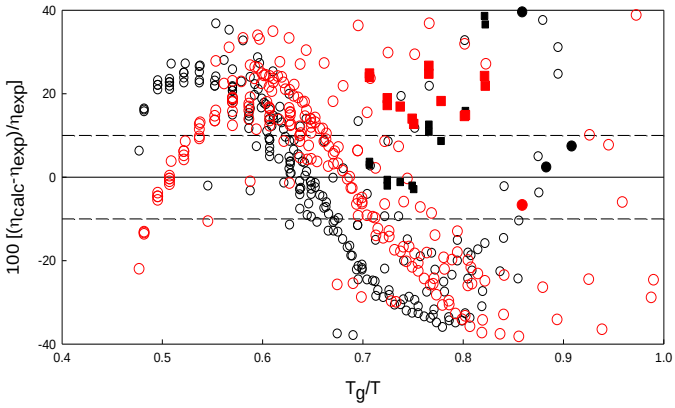

FIGURE 2. Relative deviations between calculated viscosity $\eta_{(calc)}$, and the measured values from literature, $\eta_{,exp}$: ○, fitting with BSCNF; ○, fitting with VTF ($\eta_\infty=10^{-6}$ Pa.s); ●, deviations from Parks and Gilkey[6] (BSCNF); ■, deviations from Tammann and Hesse[4] (BSCNF); ●, deviations from Parks and Gilkey with VTF ($\eta_\infty=10^{-6}$ Pa.s); ■, deviations from Tammann and Hesse[4] with VTF ($\eta_\infty=10^{-6}$ Pa.s).

CONCLUSIONS

From figure 2 it can be seen that the BSCNF and VTF models can represent the experimental viscosity data from literature with variable performance with relative deviations from zero up to 20%. This variation is explained in part by the discrepancy of data from the various authors and in other hand by the fail of models to describe data in wide range of temperature starting from T_g. Despite the scarcity of data in the approach to the glass transition temperature the tested models give reasonable results in the medium temperature range. It is interesting to note that the old data of Parks and Gilkey (1929) can be represented by BSCNF model close to the glass transition. The fragility index obtained in this work (m=59) (m=53)[7] characterizes glycerol as a moderate fragile liquid. The physical basis of BSCNF theory is an important aspect possibly more significant than the intrinsic precision of fitting with this model. The value N_B=14 suggests that bonds corresponding to about 14 structural units must be broken in order to observe the viscous flow in the glass transition range.

ACKNOWLEDGEMENTS

The authors are grateful to Prof. K. Schröter (Institute of Physics, University Halle, Germany), Prof. M. E. Möbius (Scholl of Physics, Trinity College, Dublin, Ireland) and Prof. Stefan Klotz, CNRS, Université Pierre et Marie Currie, Paris, France) for having sent the viscosity data.

REFERENCES

1. Ikeda, M.; Aniya, M., Bond Strength-Coordination Number Fluctuation Model of Viscosity: An Alternative Model for the Vogel-Fulcher-Tammann Equation and an Application to Bulk Metallic Glass Forming Liquids, Materials, **2010**, 3, 5246-5262.
2. Vogel, H., Das Temperaturabhängigkeitsgesetz der Viskosität von Flüssigkeiten, Phys. Z **1921**, 22, 645–646 .
3. Fulcher, G. S., Analysis of recent measurements of the viscosity of glasses, J. Am. Ceram. Soc. **1925**, J 8, 339–355.
4. Tammann, G.; Hesse, W., Die Abhängigkeit der Viscosität von der Temperatur bie unterkühlten Flüssigkeiten, Z. Anorg. Allg. Chem. **1926**, 156, 245–257.
5. Ikeda, M.; Aniya, M., Correlation between fragility and cooperativity in bulk metallic glass-forming liquids, Intermetallics, **2010**, 18, 1796-1799.
6. Parks, G. S.; Gilkey, W. A., Studies on glass.IV. Some viscosity data on liquid glucose-glycerol solutions. J. Phys. Chem. **1929**, 33, 1428-1437.
7. Huang, D.; McKenna, G. B., New insights into the fragility dilemma in liquids, J. Chem. Phys. **2001**, 114, 5621-5630.

P32

Rheological Implementation of the Joule Effect in Conductive liquids. Application to thermosets curing.

C. Gracia Fernández[1], S. Gómez Barreiro[2], J. López Beceiro[2], R. Artiaga[2]

[1]*TA Instruments-Waters Cromatografía, 28108 Alconbendas Madrid, Spain*

[2]*University of A Coruña, Higher Polytechnic School, Campues de Esteiro, Ferro 15403, Spain*

Correspondence to: Author Name (cgracia@tainstruments.com)

ABSTRACT

The main target of the present work is to monitorize the curing of a bicomponent thermoset by rheology when an electrical current going trought the sample produces heat by the Joule effect. So the first point was to increase the conductivity of the material. In order to get the necessary minimum electrical conductivity, Multiwall carbon nanotubes (MWCNTs) where introduced in the thermoset Matrix. The concentration used was 3 %. Rheological experiments ensure that that concentration is higher than the percolation concentration. In order to motorize the curing, at the same time that the DV voltaje is applied, the system has being integrated in a Rheometer DHR2 (TA Instruments, DE, USA). The geometry used has being 25 mm disposable parallel plates. Both plates have being soldered to the negative and positive sides of a DC source. The voltage difference up to 75 V produces the current intensity that will produce the heat by joule effect. Multifrequency time sweep experiments provide the viscoelastic profile during the curing process.

KEYWORDS thermoset, MWCNTs, Joule effect, gelification, conductivity

INTRODUCTION

The curing of thermosets is a research field widely studied in the literature. Most of them are heat induced typically by convection. Moreover, there are curing applications that use UV light. One of the main disadvantages of this technique is the low penetration index of the UV light. Therefore, the curing is produced mainly in the Surface what it is useful in coatings but not so much is structural parts.

The Joule effect is another way to produce heat that has not being deeply studied in the thermoset field. Some authors have used the carbon fibbers that are present in some composites to conduct the electricity that finally produces the heat by Joule effect.

Materials

Epoxy/Hardener: BEPOX 1622 (Gairesa, Valdoviño Spain). Proportion 2.38 to 1 in weight.

MWCNTs: from Aldrich; 6-9 nm x 5 microns

Rheometer: DHR TA Instruments (DE USA).

DETA accessory: Disposable geometries 25 mm. Agilent brigde LCRmeter 4980A, freq range from 20 Hz to 2 MHz. Voltage range from 0.005 to 20 V. maximum output Intensity 200 mA.

DC voltage source: MYWAVE MPD-7505 POWER SUPPLY. 0 – 75 V. 0 – 5 A.

Dispersion machine: heidolph diax 900, 8,000-26,000 rpm

MATLAB: control the DC source through t the intensity. P = 0.05, I = 0.01; D = 0.01

The final mixture between the 3 components, epoxy resin, hardener and MWCNTs has being made by mechanical agitation and ultrasounds.

RESULTS

As it is shown in Figure 1, the 3 % of MWCNTs increases the resin conductivity around 4 orders of magnitude. It is very interesting to observe that the complete cured sample has the highest conductivity

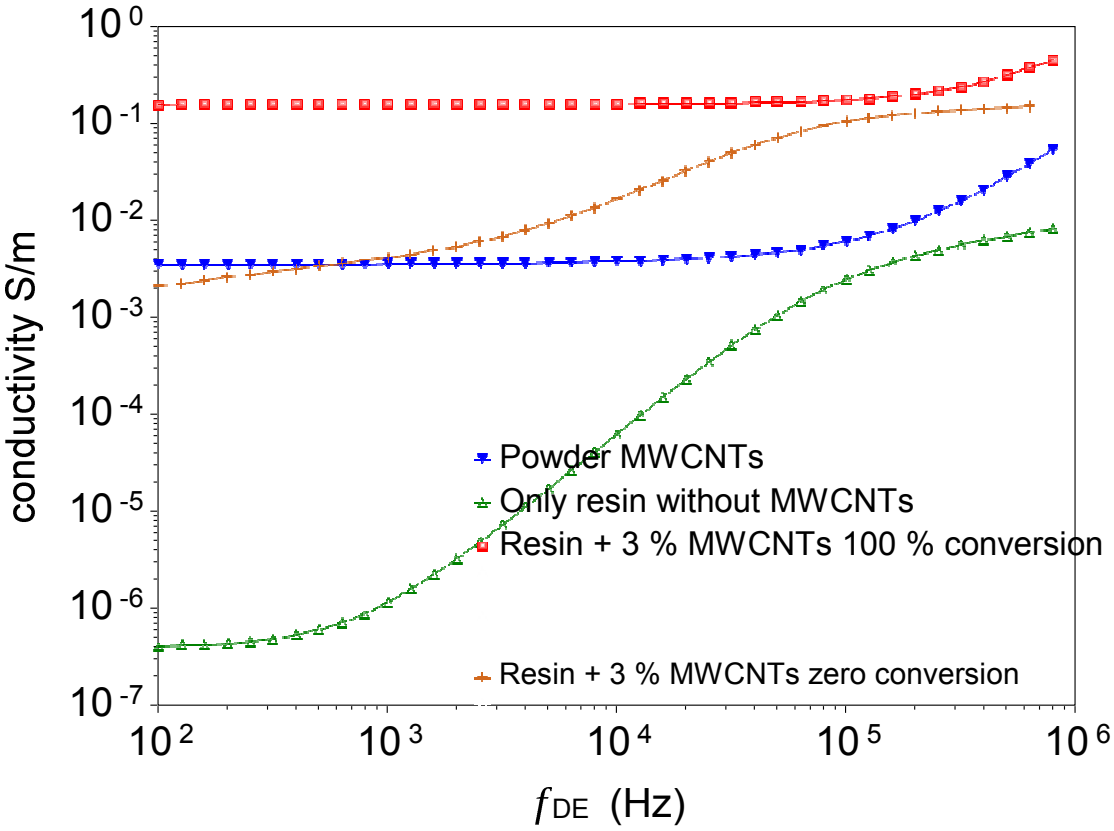

Figure 1. Conductivity versus frequency for the MWCNTs powder, resin without MWCNTs, and resin + 3 % MWCNNTs at zero and 100 % conversion.

So, using the DC source and the adequate PID control (P = 0.05, I = 0.01; D = 0.0)1, we were able to make Dynamic and isothermal temperature profiles. The voltage range was between 10 and 20 V and current intensities between 0.2 and 1 A. The results are presented in Figure 2.

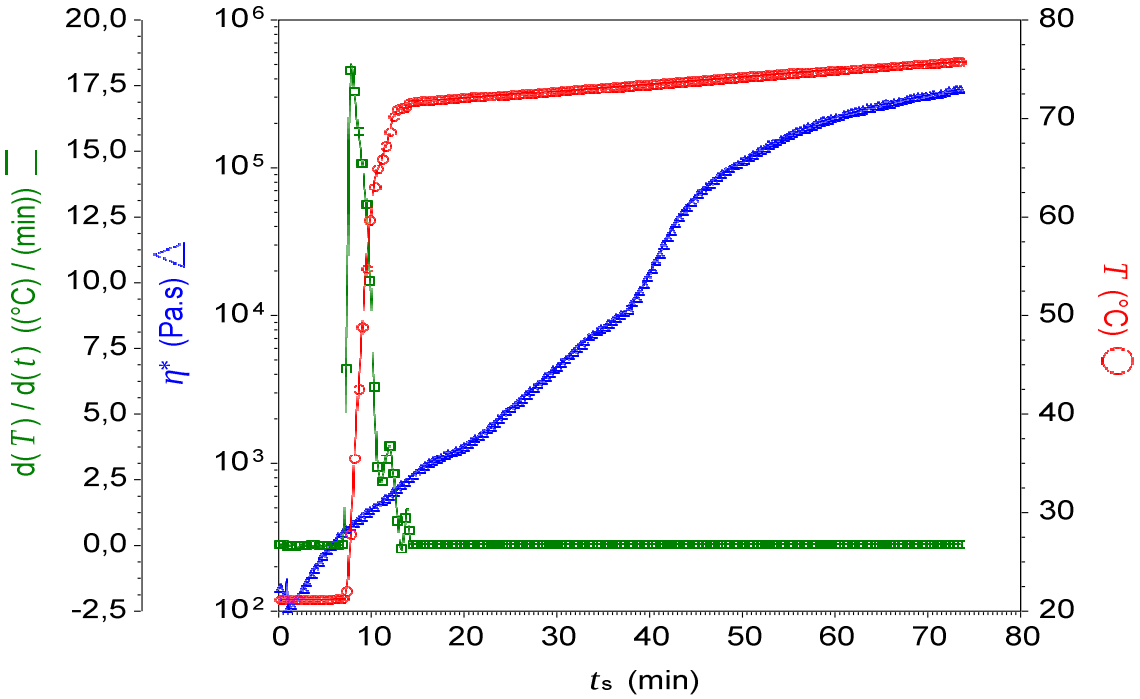

Fgure 2. Temperature, heating rate and complex viscosity versus time.

It is possible to observe in Figure 2 that the PID parameters chosen provide a very accurate temperature control with heating rates up to 17ºC/min and down to 0.2 C/min.

In order to obtain the gelation time, we performed a multifrequency experiment at 1, 2 and 5 rad/s. Results are shown in Figure 3.

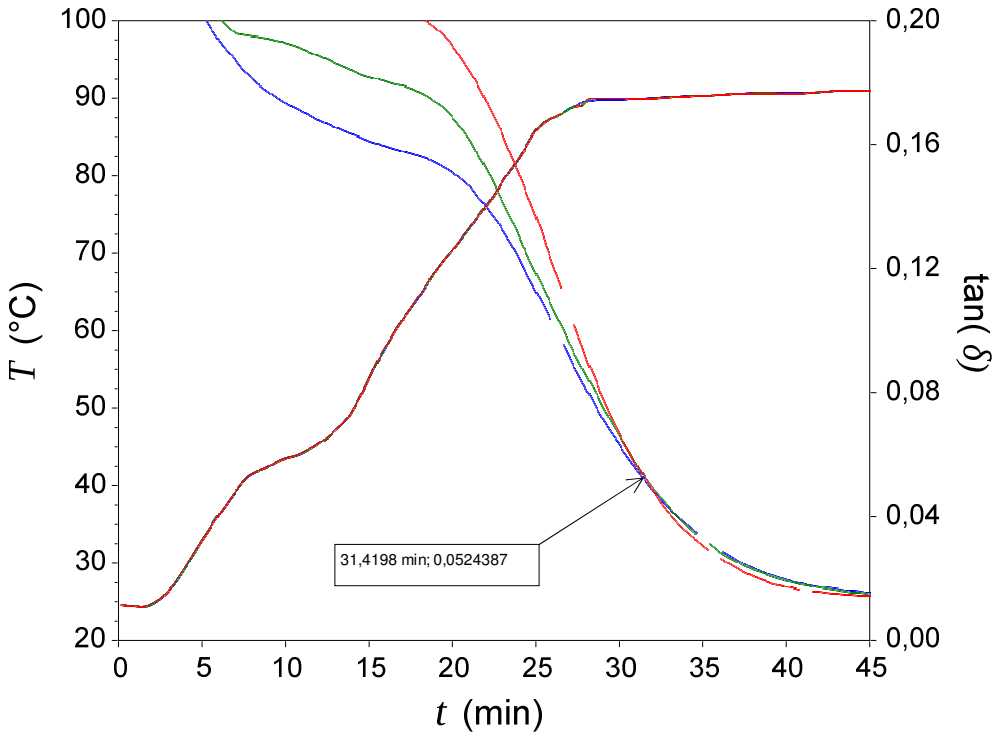

Figure3. Tan delta and Temperature versus time.

It is possible to observe in Figure 2 that the crossover of tan delta at the 3 frequencies occurs at 31. 41 min so 6 min after to reach the isothermal temperature at 90º C

CONCLUSIONS

The curing by Joule effect was successfully implemented in The Rheometer DHR using the Disposable plates of the DETA accessory. This technique allows the rheological measurement at one frequency or in multifrequency of a conductive thermoset.

In order to increase the conductivity, MWCNTs were successfully added at a concentration of 3 %. The conductivity increased around 4 decades.

REFERENCES

[1] B. Mas, J. P. Fernández-Blazquez, J. Duval, H. Bunyan; J.J. Vilatela, Carbon, 63: 523-529 (2013).

P33

Characterization of polyelectrolytes through dilution viscometry

Raquel Costa[1] Ąnita Lourenço[1,2], Rita Garrido[1], David Hunkeler[2], Manuel Banobre[3], Maria G. Rasteiro[1]

[1]Chemical Engineering Department, University of Coimbra, Rua Sílvio Lima, 3030-790 Coimbra, Portugal

[2]AquaTech, 1237 Avully, Geneva, Switzerland

[3]International Iberian Nanotechnology Laboratory, 4715-330 Braga, Portugal

Correspondence to: Maria G. Rasteiro (E-mail: *mgr@eq.uc.pt*)

ABSTRACT

Charged macromolecules with high molar mass tend to pose characterization difficulties. Dilution viscometry can be a reliable technique to characterize polyelectrolytes providing their intrinsic viscosity. The intrinsic viscosity can be considered a ”lumped parameter”, giving information on the polymer’s conformation in solution, which is an important characteristic, in particular if the intention is to compare the impact of polyelectrolytes of different molar mass, charge density, chemistry and/or chain architecture on technological processes. The intrinsic viscosity of three copolymers was determined by two different techniques: capillary viscometry and rolling ball viscometry. In this presentation, we show the comparative analysis of the intrinsic viscosity measurements obtained through these two alternative methods. Huggins correlation was used to extract intrinsic viscosity values from the raw experimental data.

KEYWORDS: intrinsic viscosity; polyelectrolytes; capillary viscometry; rolling ball viscometry

INTRODUCTION

Water-soluble synthetic polyelectrolytes are key compounds in a number of fields, including drinking water treatment, papermaking and personal care products manufacturing.[1] As charged, high molar mass molecules, these compounds often pose characterization difficulties.

Polyelectrolyte intrinsic viscosity is amongst the parameters whose determination may turn into a challenge.[2] The intrinsic viscosity can be seen as a “holistic” parameter, giving information on the conformation, and hence the hydrodynamic volume, of the polymer chains in the solution. This information is particularly relevant to compare the impact of multiple variables (e.g.

molecular weight, charge density, chemistry, chain architecture) on technological processes where the polymer coil dimensions are important, providing a basis to envisage the relative performance of different polyelectrolytes.

Polymer intrinsic viscosity is determined by dilution viscometry. The gravimetric capillary principle is widely applied through Ubbelohde viscometers. The main advantage of this technique is that gravity is employed as a reliable, not artificially generated driving force, which reduces potential experimental errors. Alternatively, intrinsic viscosity values may be obtained by implementing the rolling/falling ball principle, where gravity is also used as driving force, but the inclination angle of the capillary where a ball rolls has to be defined within the measurement procedure.

As part of an ongoing project aimed at describing the toxic potential and biological activity of cationic acrylamide/dimethylaminoethylacrylate methyl chloride copolymers (AM-co-DMAEA), the intrinsic viscosity has been determined for a variety of polyacrylamides with varying AM/DMAEA ratio.[3]

Here, intrinsic viscosity values obtained by the gravimetric capillary and rolling ball principles are reported and compared for three linear AM-co-DMAEA polyelectrolytes with different molecular weight and charge density (Table 1). The polyelectrolytes' molecular weights have been determined experimentally by static light scattering (SLS).

MATERIALS AND METHODS

Molecular weight determination

The molecular weights of the three polyelectrolytes under study were estimated based on SLS measurements in a Zetasizer Nano ZS, model number ZEN3600. Stock solutions (1.5 mg/mL) of each polymer were prepared by stirring purified samples in previously filtered (0.45 μm) 0.05M NaCl aqueous solution for at least 6h. The stock solutions were left to rest overnight prior use. Dilution series of 5 solutions in the concentration range 0.1-1.5 mg/mL were employed in the molecular weight measurements.

Intrinsic viscosity determination

The intrinsic viscosities of the polyelectrolytes were determined in both an automatic capillary viscometer Viscologic TI1 (Sematech, France) with a 0.58-mm capillary and a rolling ball Lovis 2000 M/ME microviscosimeter (Anton Paar, Austria). For the rolling ball technique, the angle of

inclination of the capillary was selected to 48° and several replicate measurements were taken by alternating the angle from +48° to -48° until the variation coefficient of the readings was below 0.05 %. The measurements had to be carried out at 20º C and 25 ºC for the gravimetric capillary and rolling ball techniques, respectively.

The dilution viscometry principle was applied. Intrinsic viscosity values [η] were obtained by determining the specific viscosities (η_{sp}) of polymer solutions of different concentrations and then extrapolating to zero concentration conditions. η_{sp} values were calculated either from the capillary running times or ball rolling times. From the η_{sp}, reduced viscosities could be calculated as the ratio η_{sp}/c (c being the polymer concentration). The limit of the reduced viscosity for infinitely diluted polymer solutions defined the intrinsic polymer viscosity. The Huggins fit (equation 1) was employed for the extrapolation to zero concentration:[4]

$$\eta_{red} = \frac{\eta_{sp}}{c} = [\eta] + K_H [\eta]^2 c \qquad (1)$$

The Huggins coefficient, K_H, is a constant for a given polymer-solvent system; the intercept (at the origin) for the plot reduced viscosity versus concentration gives the intended intrinsic viscosity.

Experimental polymer stock solutions were prepared by dissolving isolated (purified) polyelectrolyte samples in 0.05M NaCl aqueous solution. The stock solutions were stirred at least for 6 hours until complete dissolution. At least 4 concentrations in the range 10^{-5} to 10^{-4} g/mL per polyelectrolyte sample were prepared from the stock solutions. The dilution series used were selected so that the range of relative viscosities varied between 1.2 and 2.5 (values lower than 1.2 would lead to high uncertainty). Pure solvent running and rolling ball times were also measured.

Capillary cleanness was an essential aspect in both measurement techniques, and hence the solutions were injected in increasing concentration order and the capillaries were thoroughly washed between each measurement. Furthermore, in the non-automatic rolling ball viscometer, special care was taken when injecting the test solutions to avoid the formation of air bubbles that could disturb the regular movement of the ball through the viscous fluid.

RESULTS AND DISCUSSION

Table 1 summarizes the experimental data obtained. In all cases the Huggins correlation lead to a correlation coefficient above 90%. Consistent intrinsic viscosity trends were obtained by the two measuring techniques, with the 2 lower charge polyelectrolytes having lower intrinsic viscosities than the 50% charged E1. Since E1 and FHMW possess similar molar mass, charge density must be the main effect affecting the intrinsic viscosity. In absolute terms, however, the two alternative methods provided fairly different values, those obtained by rolling ball capillary viscometry being around 30% for all polymers. This "offset" may be reduced by selecting a lower angle of inclination of the capillary in the rolling ball viscometer. In fact the running time values in the rolling ball viscometer are much dependent on the angle of inclination and it is necessary to tune it considering the viscosity of the solution and the accuracy of the measurement of the running time. Also, the fact that this technique forced measurements to be carried at room temperature must have influenced the results.

TABLE 1 Chain characteristics and intrinsic viscosity values for the three polyacrylamides

Polyelectrolyte	Chain characteristics		Intrinsic viscosity values (ml/g)	
	Molecular weight (kDa)	Charge density (%)	Gravimetric capillary viscometry	Rolling ball viscometry
F1	Not determined	40	2547±13	1847
FHMW	644±165	40	2311±70	1630
E1	830±92	50	2982±66	2084

CONCLUSIONS

Both capillary viscometry and rolling ball viscometry allowed us to identify trends in the intrinsic viscosity of polyelectrolytes which could be correlated with the chain architecture, namely polymer charge density. An offset between both methods was systematically detected. This may be the result of the selection of the inclination angle in the case of the rolling ball technique, this parameter requiring a criterious tuning.

ACKNOWLEDGEMENTS

Financial support from the Portuguese Foundation for Science (Pest/C/EQB/UI0102/2013) and Marie-Curie Actions (PEOPLE-2013-ITN/EID 604825) is acknowledged.

REFERENCES

1. Harford, A.J.; Hogan, A.C.; van Dam, R.A., Ecotoxicological Assessment of a Polyelectrolyte Flocculant. Internal Report 575. Australian Government, Department of Environment, Water, Heritage and the Arts, Supervising Scientist Division: Darwin, **2010**
2. Bourdillon, L.; Hunkeler, D.; Wandrey,C., *Progress in Colloid Polymer Science*, **2006**, *131*, 141-149.
3. Barajas, J. H.; Wandrey, C.; Hunkeler, D., *Polymer News*, **2004**, *29*, 239-246.
4. Huggins, M. L., *Journal of the American Chemical Society*, **1942**, 64, 2716–2718.

P34

Adjusting the low critical solution temperature of poly(N-isopropylacrylamide) solutions by salts: A rheological study

Maria Carolina Morando Costa, Sérgio Manuel Campos da Silva, Filipe João Cotovio Eufrásio Antunes

Department of Chemistry, University of Coimbra, Rua Larga, 3004-535 Coimbra, Portugal

Correspondence to: Filipe Antunes (E-mail: *fcea@ci.uc.pt*)

ABSTRACT

The control over the Low Critical Solution Temperature (LCST) and the rheological properties of thermosensitive polymers is of crucial interest for various applications including drug delivery systems and temperature sensors. In this study we follow the LCST by rheology and show how the onset of LCST can be adjusted by chemical species that are able to change polymer solubility, such as salts. For this purpose a thermo-responsive polymer, poly(N-isopropyl acrylamide) or PNIPAM, and different salts like KCl, KBr and KSCN, were used. The LCST was investigated by means of rotational rheology, as it has been shown a good correlation between the LCST and the onset of the thickening-induced temperature. It was observed that salts can both increase and decrease the temperature at which the LCST occurs. This is attributed to the affinity of the different salts to the polymer. Hydrophobic salts such as KSCN shift the LCST of PNIPAM to higher temperature values while the opposite scenario is observed when hydrophilic salts such as KCl are added.

KEYWORDS

PNIPAM; LCST; Phase transition; Rheology; Viscosity; Salts.

INTRODUCTION

Thermo-responsive polymers comprise a class of stimuli-responsive polymers which have the ability to respond to thermal changes in solution and therefore can be used as temperature sensors. These polymers undergo a coil-to-globule transition at the LCST, the threshold of the change in the solubility in the solvent. Below the LCST, the polymer chains are hydrated and the polymer solution is clear. Above the

LCST, the polymer chains collapse and adopt a compact conformation. The hydrophobic effect is the main driving force for the polymer-polymer associations. This leads to the formation of polymer aggregates which are able to scatter light and dramatically decrease the transparency of the solutions. Previous studies report that the polymer solubility can be influenced by the presence of chemical species added to the system[1]. Above the LCST it happens the formation of a three dimensional network composed by the segments of the polymers which became more hydrophobic. This investigation aims to understand how to control the change of the LCST of a thermo-responsive polymer, in particular how to shift the LCST to a desired temperature. Rheological measurements has shown to be valuable to identify the LCST of the polymeric systems[2]. PNIPAM is a non-ionic homopolymer comprising both hydrophilic (amide) and hydrophobic (isopropyl) groups with great potential in biomedical applications since it shows a LCST close to the human body temperature. In literature, the LCST of PNIPAM is generally reported to be close to 33°C[3]. There are still many uncertainties about the mechanisms under the solubility/insolubility of PNIPAM and of other thermosensitive polymers. The LCST of thermoresponsive polymers is known to be dependent on the solubility of the macromolecules. Salts can increase or decrease the solubility of nonionic macromolecules such as PNIPAM, depending on the hydrophilic/hydrophobic character of the salts and their ability to change the organization of neighboring water molecules. Consequently, the type of salts added is expected to have a strong influence in the process of adjusting the LCST of PNIPAM. Phase transition phenomena were assessed by means of rheological studies carried out for various PNIPAM-salt-water systems. Salting-in and salting-out effects vary with the type of anion, according to the Hofmeister series[4]. In this work, a series of three different potassium salts (KCl, KBr and KSCN) in aqueous solutions of PNIPAM(20k) were used.

EXPERIMENTAL

PNIPAM was synthesized at the Department of Chemical Engineering of the University of Coimbra(Coimbra, Portugal). Molecular weight (M_n= 20 262 Da) was determined by gel permeation chromatography and size exclusion chromatography. KCl (≥99%), KBr (≥99%) and KSCN (≥99%) were purchased from Sigma-Aldrich. Polymer aqueous solutions were prepared by adding dry polymer and additives to Millipore water. The solutions were kept stirring until complete dissolution and were allowed to rest for a period of an hour, prior use. Rotational tests were performed using a Thermo Scientific HAAKE MARS III rheometer, with automatic gap setting and with a cone and plate geometry (35 mm, 1º), equipped with a solvent trap to prevent evaporation. Newtonian viscosity was investigated within 20-

50°C at a heating rate of 0.5°C/ min. The temperature control was achieved using a circulating water bath system. Dynamic or shear viscosity was analyzed by rotational shear experiments. Prior to this, a viscometry test was carried out in order to determine both Newtonian and non-Newtonian regimes. The stress applied to the samples was 10Pa.

RESULTS AND DISCUSSION

Effect of salts on PNIPAM aqueous solutions

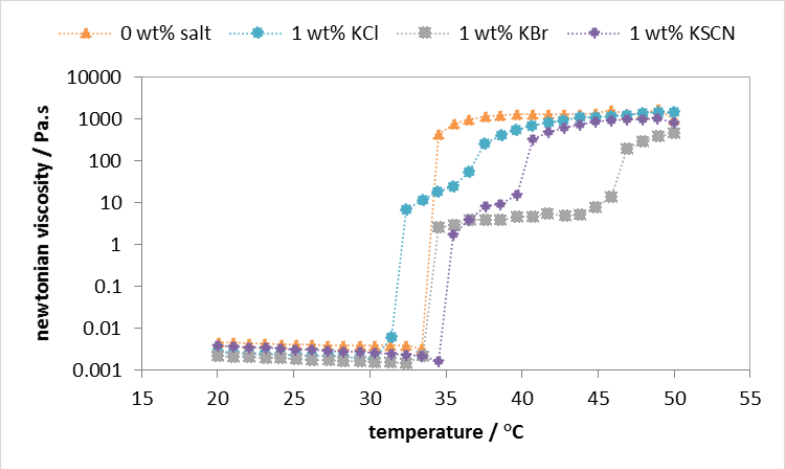

FIGURE 1 Dependence of Newtonian viscosity on temperature (heating system). Effect of anions in 5wt% PNIPAM(20k) solutions. The depicted lines are a guide to the eyes.

FIGURE 1 illustrates the role played by individual salts in PNIPAM systems. Below the LCST, the viscosity of the solutions slightly decreases with temperature in the presence of any salt due to increased dynamic effects. By heating, the polymer becomes more hydrophobic and LCST is attained. The direction to which LCST is shifted depends on the nature of the salt used.

solutions	PNIPAM 5%	+	KCl 1%	KBr 1%	KSCN 1%
LCST / (°C)	33.5 ± 0.5		30.5 ± 0.5	33.5 ± 0.5	34.5 ± 0.5

TABLE 1 LCST values for the three salt systems. Control refers to 5% PNIPAM aqueous solution.

TABLE 1 shows the LCST for the different salt systems. The presence of KCl promotes a decrease in the LCST, KBr has a negligible effect, while KSCN increases the LCST. Chaotrope anions such as SCN^- show a weak interaction with water molecules and a substantial affinity to the polymer. This causes the adsorption of salt onto the polymer and the formation of a charged complex. The formed polyanion complex possesses higher water solubility than the salt-free polymer, mainly due to the entropy of the counterions, and thus exhibits a higher LCST. Kosmotrope anions such as Cl^- are more hydrophilic and do not adsorb onto the polymer chains. Instead, these species compete with the polymer for the water and cause polymer dehydration and promote the decrease in the LCST. The ion Br^- is in the middle of the Hofmeister series and therefore shows an intermediate effect, comparatively to Cl^- and SCN^-. Interestingly, it can be observed a second plateau above the LCST, suggesting the existence of a second transition temperature. At rest, i.e., without being under a constant stress, the samples are turbid before the first plateau and phase separate near the second plateau. These results are in agreement with the two-step transition reported elsewhere[5].

CONCLUSIONS

It was concluded that the hydrophobicity of the salt added is crucial for the shift of the LCST. More hydrophobic salts bind to the polymer chains and shift the LCST to higher temperatures. More hydrophilic salts do not bind to the polymer and promote water competition with the polymer, which causes a decrease in LCST. The presented sets of results provide additional input to understand how to control the LCST and the rheological properties of PNIPAM solutions.

ACKNOWLEDGEMENTS

M.Sc. Luis Alves, M.Sc. Rose Cordeiro and Prof. Jorge Coelho are acknowledge for scientific assistance.

REFERENCES AND NOTES

1. Hofmann, C.; Schönhoff, M. Colloid and Polymer Science, 2009, 1369-1376.

2. Aubry, T.; Bossard, F.; Staikos, G.; Bokias, G., Journal of Rheology, 2003, 47, 577-587.

3. Okano, M.N.T.; Winnik, F.M., Material Matters, 2010.

4. Zhang, Y.; Furyk, S.; Bergbreiter, D.; Cremer, P.S., JACS, 2005, 127, 14505-14510.

5. Cho, Y.; Zhang, Y.; Christensen, T.; Sagle, L.B.; Chilkoti, A.; Cremer, P.S., The Journal of Physical Chemistry, 2008, B112, 13765.

Thermo-rheological properties of polyvinyl acetate based adhesives films

Miguel Hermida[1], Francisco López-Suevos[1], Beatriz Lagares[1], Ramón Moreira[2], Francisco Chenlo[2], Santiago Arufe[2]

[1]Centro de I + D + i, FORESA, Avda. De Doña Urraca 91, 36650 Caldas de Reis (Spain)

[2]Departamento de Enxeñaría Química, Universidade de Santiago de Compostela, Rúa Lope Gómez de Marzoa, s/n, 15782 Santiago de Compostela (Spain)

Correspondence to: Santiago Arufe (E-mail: *santiago.arufe@gmail.com*)

ABSTRACT

The influence of a plasticizer and an adhesive promoter on the viscoelastic properties of a polyvinyl acetate based adhesive was evaluated by parallel-plate rheometry. The resulting analyzed films showed clearly that the plasticizer reduced the polymer's T_g around 3-4ºC making the films more flexible and with enhanced damping capabilities at room temperature. Also, the adhesion promoter did not alter the polymer's T_g but caused a significant reinforcing effect, especially at higher temperatures (60-150ºC). The presence of the plasticizer and the adhesion promoter resulted in a film with combined properties, i.e. flexibility and mechanical strength.

KEYWORDS DMTA, PVAc, adhesive, promoter, plasticizer

INTRODUCTION

The main application of polyvinyl acetate (PVAc) resins is bonding of high porosity materials such as wood (veneered, furniture assembly, etc), cork and paper. Among the advantages in a PVAc resin are a high pot-life (higher than 6 months), the capability to bond multiple porous materials, very low toxicity (organic solvent free), ease of cleaning with a brush or water, and it develops an outstanding shear strength in dry conditions. On the other hand, it shows a thermo-plastic behavior, which means that above its glass transition, T_g, (e.g. typically T>35ºC) the formed PVAc film dramatically reduces its adhesive strength (i.e. a major softening occurs). Therefore, bonded materials with a PVAc resin cannot hold a heavy load for a long period of

time at $T>T_g$, and consequently, PVAc are not suitable for structural use applications. Also, PVAc generally cannot be used outdoor since they present poor water durability.

PVAc adhesives form a stiff film below the T_g which can break easily by applying a small strength. When a higher flexibility of the film is required, a plasticizer in the range between 1-7% wt. (on total PVAc composition) is commonly added. Low porosity materials might be also bonded with PVAc resins but the addition of adhesion promoters (1-5% wt.) is required to enhance the adhesion strength. Usually, these promoters are added to the PVAc prior to the intended application to avoid a dramatic decrease in the adhesive's pot life.

The objective of this study is to evaluate the influence of an adhesion promoter and a plasticizer in a PVAc based resin on the viscoelastic properties of the resulting films.

EXPERIMENTAL METHODS

Four commercial PVAc liquid based adhesives were formulated: 1) AB Plus (copolymer of vinyl acetate and other monomers with surfactants and a protective colloid), 2) ABF Plus, the same copolymer as AB PLUS with the addition of a plasticizer, 3) AB Plus + 4% (wt.) of a silane-based adhesion promoter and 4) ABF Plus + 4% (wt.) of a silane-based adhesion promoter.

To prepare the samples an adhesive film was extended with an applicator with a thickness of 350 μm on a Teflon sheet and after drying the film was removed and placed in a desiccator filled with silica gel for 5 days. Obtained films (thickness ≈ 100 μm) were studied by DMTA employing the same method reported in literature[1]. Rheological assays were carried out in a controlled stress rheometer (MCR 301, Anton Paar, Physica). Analyses were conducted in parallel-plate mode using plates with 8 mm of diameter from 10ºC to 150ºC (±0.1ºC). Five films were placed between the plates for each experiment. A normal force of 3 ± 0.2 N was applied through the whole experiment to ensure a perfect contact between the films and the plates. All samples were initially conditioned at 150ºC for 15 min in the rheometer before the experiments.

A strain sweep (γ, 0.01 - 10%) at standard frequency of 6.28 rad/s (1 Hz) and different temperatures (10, 30, 70, 110, 150ºC) were conducted to identify the LVER of every sample. DMTA were carried out within the LVER (0.1%) from 150ºC to 10ºC with a constant cooling/heating rate of 4ºC/min. Experiments were carried out at least in triplicate.

RESULTS AND DISCUSSION

Figure 1 shows the evolution of the storage modulus (G´) and tanδ with temperature for the four PVAc-based formulations prepared in this study. As it can be observed, three regions can be identified (from low to high temperature): 1) the glassy region, 2) the glass transition and 3) the rubbery plateau. In general, the typical viscoelastic behavior for a PVAc film is a constant value of G´ in the glassy region where the film shows maximum elasticity and, thus, a very low tanδ (<0.1) since the elastic component clearly dominates the viscoelastic behavior. In this low temperature range, the film is very fragile and, depending on the intended industrial application, it might be problematic. At higher temperature, a dramatic decrease in the G´ modulus of up to 3-4 decades indicates the presence of a major softening transition (glass transition), where the polymer film losses its mechanical strength. This is also observed in the tanδ peak where the viscous component (G´´) becomes increasingly dominant over the elastic component up to the T_g and, above the T_g, gradually less dominant. Tanδ is useful to evaluate the damping behavior of a material. The higher the intensity or the broader the peak, the higher the capability to dissipate energy (e.g. from an impact). Finally, in the high temperature range (aprox. T>80ºC, depending on the PVAc system) and above the polymer's T_g, the film behaves as a rubber (solid-liquid like behavior). This region provides insights on the polymer's crosslinking and reinforcement degree.

The addition of a plasticizer to the base copolymer of this study (AB Plus) has shifted the T_g to a lower temperature (from the tanδ peak: 46.7 vs. 42.3ºC). As a result, a film more flexible/less elastic was obtained at lower temperature. For instance, if the G' moduli of both curves are compared at 35ºC, the film that lacks the plasticizer is still very stiff whereas the plasticized one has nearly lost one decade of modulus. This is very interesting for post forming processes where the adhesive cannot be very rigid at the working temperature.

The presence of the adhesion promoter in the AB Plus polymer film has caused a significant increase in the G' modulus in the entire temperature range, i.e. the promoter is acting as a reinforcing agent. Interestingly, it has not significantly altered the T_g (from the tanδ peak: 46.7 vs. 45.9ºC) but it considerably reduced the intensity of tanδ and, therefore, its damping capability. Consequently, the AB plus + 4% Promoter has effectively increased the mechanical strength of the base film but it might be still too brittle at room temperature.

The plasticized film (ABF Plus) and the plasticized + reinforced film (ABF Plus + 4% Promoter) behaved similarly up to the T_g (aprox. 42-43 ºC) but differed at higher temperatures, thus confirming the reinforcing effect caused by the adhesive promoter.

Finally, a combined action of both the plasticizer and the adhesion promoter led to a reinforced effect above 60ºC (see the G' modulus) and a less fragile film at the low temperature range (from the tanδ peak T_g=42.9ºC). This type of behavior is desirable for applications that need high mechanical strength at high temperatures and high flexibility of the film at room temperature such as ballast stabilization.

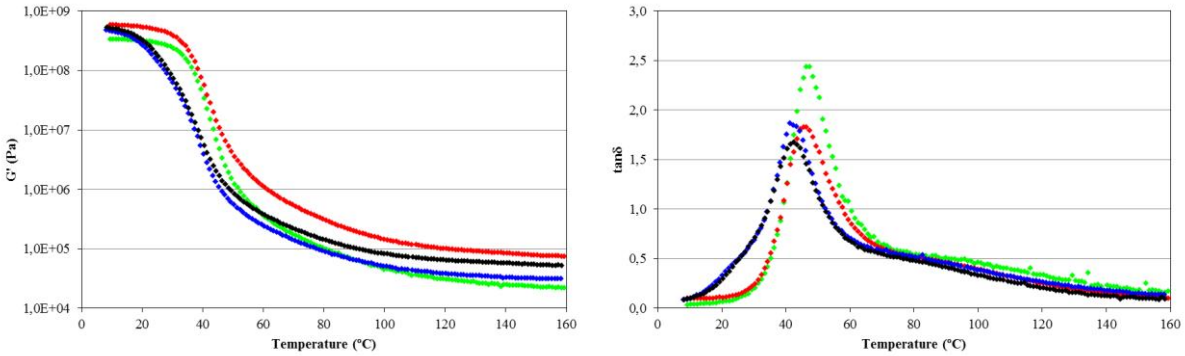

FIGURE 1. G' (left) and tanδ (right) experimental curves. AB PLUS (♦), AB PLUS + 4% Promotor (♦), ABF PLUS (♦), ABF PLUS + 4% Promotor (♦).

CONCLUSIONS

Mechanical properties of PVAc films can be modified depending on final application. In this sense, the addition of the plasticizer is advisable when adhesives with damping capabilities at lower temperatures (25-40ºC) are required. The addition of adhesion promoter is useful to increase mechanical strength but it makes the adhesive more brittle. The combined action of the adhesion promoter and the plasticizer results in more flexible films with higher damping capabilities at low temperatures (20-40ºC) and higher mechanical resistance at high temperatures (80-150ºC).

ACKNOWLEDGEMENTS

Authors acknowledge the financial support to FEDER and Ministerio de Economía y Competitividad (AEROVIAV-Interconnecta).

REFERENCES AND NOTES

1. López-Suevos, F.; and Frazier, C. E., Holzforschung, **2006**, 60, 561-566.

Influence of EVA concentration and vegetable oil on the rheology, tribology and microstructure of oleogels for lubricant purposes

J.E. Martín-Alfonso[1,2], C. Valencia[1,2] and J.M. Franco[1,2]

Departamento de Ingeniería Química, Química Física y Química Orgánica. Campus de "El Carmen". Universidad de Huelva. 21071 Huelva. Spain.

Correspondence to: J.E. Martín-Alfonso1 (E-mail: *jose.martin@diq.uhu.es*)

ABSTRACT

This work has been focused on the development of oleogels based on conventional (SO) and high-oleic sunflower (HOSO) vegetable oils and ethylene-vinyl acetate copolymer (EVA) for lubricant applications. The influence of EVA concentration was analyzed. Linear viscoelasticity functions with frequency for these oleogels were very similar to that obtained with a commercial lithium lubricating grease. EVA-HOSO oleogels present friction coefficient values slightly lower than EVA-SO oleogels but similar to the ones obtained with the commercial greases.

KEYWORDS (Vegetable oils; Ethylene-vinyl acetate copolymer; Oleogels; Rheology, Tribology)

INTRODUCTION

Oleogels are soft material systems comprising of oil as continuous phase that is physically entrapped in a threedimensional network of dispersed gelling agent. In previous work[1], rheological, thermal, and tribological studies of oleogels based on mineral oils and blends such as amorphous/recycled PP and organo-bentonite/recycled PP for lubricant purposes were reported. Nonetheless, due to the interest on development of new "green" products, in a recent work, we have studied the influence of vinyl acetate (VAc) content on the rheological properties and microstructure of oleogels based on conventional and high-oleic sunflower vegetable oils and EVA copolymer[2]. As this research goes on, this work explores the possibility of using EVA copolymer with 28% VAc content in different concentrations as thickener agent to formulate oleogels with high-oleic sunflower (HOSO) and sunflower (SO) oils, potentially applicable as lubricating greases. With this aim, rheological, tribological and microstructural characterization has been performed on oleogels.

EXPERIMENTAL

Materials

Two vegetable oils were used as base stocks, a refined high-oleic (85 wt.% oleic acid) sunflower (HOSO) oil, kindly supplied by the Instituto de la Grasa, CSIC (Seville, Spain), and sunflower (SO) oil, purchased in a local supermarket. Poly (ethylene-co-vinyl acetate), EVA, with 28% vinyl acetate content was kindly supplied by Repsol S.A. (Spain).

Preparation of oleogel formulations

The processing of oleogels was performed in an open vessel using an IKA RW-20 mixer (Germany) with a four-blade propeller to disperse the polymer and vegetable oil. Batches of 150 g were processed for 60 min in the molten state at 160ºC and rotation speed of 400 rpm. Polymer concentrations in the blends were 14, 19, 24, and 29 (% w/w).

Tests and measurements

Rheological measurements were carried out in controlled-strain (ARES, Rheometric Scientific, U.K.) rheometer, using a serrated plate and plate geometry (25 mm diameter, 1 mm gap) to avoid possible wall-slip phenomena. Small-amplitude oscillatory shear (SAOS) measurements, inside the linear viscoelasticity regime, were performed in a frequency range between 10^{-2} and 10^{2} rad/s, at 25ºC. Strain sweep tests, at a frequency of 6.23 rad/s, were previously performed to determine the linear viscoelastic regime. Viscous flow measurements were performed at 25 °C, in a shear rate range of 10^{-2}-10^{2} s^{-1}. At least two replications were performed on fresh samples.

Tribological tests were performed using a tribological cell coupled with a Physica MCR-501-Rheostress rheometer (Anton Paar, Austria). The tribology cell deals with a 1/2 in. diameter steel ball (1.4401 Grade 100, roughness = 0.10 μm) rotating on three 45º inclined steel plates (1.4301, roughness = 0.21 μm).

RESULTS AND DISCUSSION

Figure 1 shows the mechanical spectra of oleogels as a function of EVA concentration and type of vegetable oil, as well as a commercial grease. As can be observed, the linear viscoelastic response is qualitatively similar for all the oleogels studied and the commercial grease and to that found with other similar systems[3]. As can be observed in Figure 1a-b, the values of G’ and G’’ increase with EVA concentration, which is indicative of a stronger microstructural network.

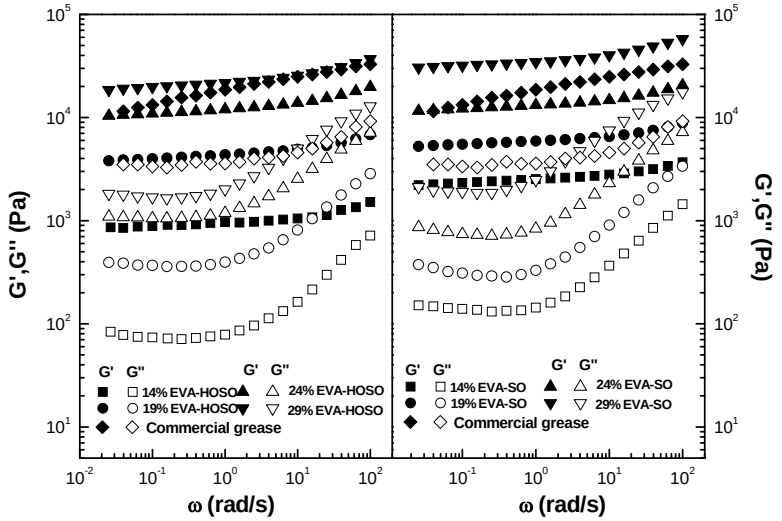

FIGURE 1. Frequency dependence of the storage and loss moduli for oleogels containing different EVA concentrations as function of type vegetable oil and commercial grease.

Figure 2 depicts the viscous flow behaviour of oleogels, as a function of EVA concentration. Shear fracture for oleogels with higher EVA concentration was observed. However, the Sisko model describes fairly well the flow behaviour observed within the shear rate range tested for oleogels with 14% and 19% of EVA copolymer. Viscosity clearly increases with EVA concentration, yielding higher values of the consistency index. The lubrication properties of oleogels were tested by tribological experiments. Table 1 shows the friction coefficient values obtained for all the oleogels studied. As can be observed, in both oleogels formulated with HOSO and SO the friction coefficient values became slightly lower when EVA content was decreased.

TABLE 1 Friction coefficient for all samples

Oleogels	Friction coefficient	Oleogels	Friction coefficient
14% EVA-HOSO	0.076	14% EVA-SO	0.101
19% EVA-HOSO	0.082	19% EVA-SO	0.113
24% EVA-HOSO	0.084	24% EVA-SO	0.107
29% EVA-HOSO	0.094	29% EVA-SO	0.115
Commercial grease	0.106		

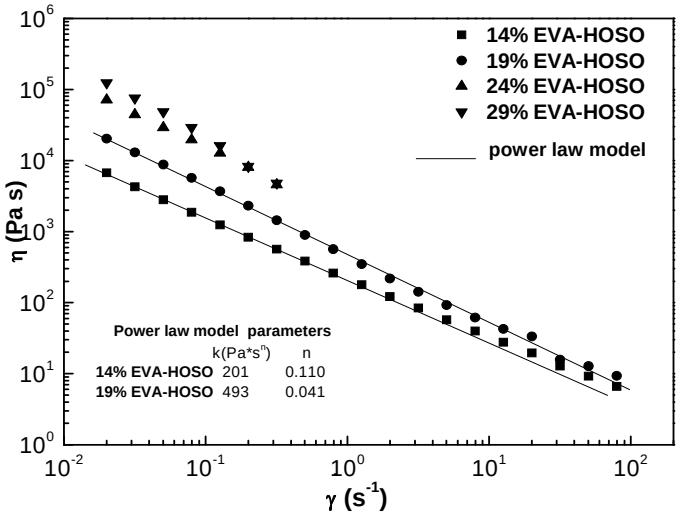

FIGURE 2. Viscous flow curves for EVA-HOSO based oleogels containing different EVA concentrations.

CONCLUSIONS

From the result obtained, it can be deduced that EVA copolymer can be potentially used as an effective thickener agent for lubricating greases. The evolution of the linear viscoelasticity functions with frequency for these oleogels was very similar to that obtained with a commercial lithium lubricating grease. Linear viscoelasticity functions increase with EVA concentration, which is an indicative of a stronger microstructural. On the contrary, the relative elasticity of the oleogel is not affected by EVA concentration. The oleogels studied exhibited shear-thinning behaviour which fitted the power law model at concentrations of 19% and 14%. Conversely, above this value all the oleogels showed fracture and expelling of sample in viscous flow behaviour. All oleogels studied showed successfully tribological responses, with values of the friction coefficient lower for EVA-HOSO oleogels.

ACKNOWLEDGEMENTS

J.E. Martín-Alfonso received a Postdoctoral Research Grant from "Fortalecimiento de las Capacidades I+D+I" Programme of University of Huelva (Spain). The authors gratefully acknowledge their financial support.

REFERENCES AND NOTES

1. Martín-Alfonso, J.E.; Valencia, C.; Franco, J.M., *Applied Clay Science*, **2014**,*87*, 265-271.
2. Martín-Alfonso, J.E.; Franco, J.M., *Polymer Testing*, **2014**,*37*, 78-85.
3. Martín-Alfonso, Romero, A.; Valencia, C.; J.E.; Franco, J.M., *Journal of Industrial and Engineering Chemistry*, **2013**, 19, 580-588.

Shear and extensional rheology of xanthan and guar gum solutions

J.E. Martín-Alfonso[1], C. Valencia[1], M. Stading[2] and M. Berta[2]

[1]Departamento de Ingeniería Química, Química Física y Química Orgánica. Campus de "El Carmen". Universidad de Huelva. 21071 Huelva. Spain.

[2]SIK (The Swedish institute for Food and Biotechnology), PO Box 5401, SE-402 29 Gothenburg, Sweden.

Correspondence to: J.E. Martín-Alfonso (E-mail: *jose.martin@diq.uhu.es*)

ABSTRACT

Small-amplitude oscillatory shear and extensional rheology of aqueous guar and xanthan gum solutions were studied for concentrations, ranging from 1 wt.% to 2 wt.%. Extensional rheometry measurements were successfully performed using a hyperbolic contraction flow method. The extensional viscosity exhibited an extensional-thinning behaviour over the entire extensional strain range used. Furthermore, the extensional viscosity diminished with decreasing concentration of the solutions, similarly to the shear properties of the samples.

KEYWORDS (Guar gum; Xanthan gum; Viscoelasticity; Extensional viscosity)

INTRODUCTION

Solutions of polysaccharides in water such as xanthan and guar gums are widely used as thickeners, stabilisers or gelling agents for food applications as well as in pharmaceutical, biomedical, chemical and cosmetic products. The molecular interactions between the polymer and water as well as polymer chain length determine the rheology of these solutions; polysaccharide chemical structure can, therefore, be exploited to develop new products, control processing quality and optimise the design of process equipment[1]. The majority of rheological studies of xanthan and guar gums have considered shear rheology: relatively few studies have investigated the extensional rheology of these solutions despite its importance in many food processing operations, consumer perception studies and product quality evaluation. Extensional viscosity characterizes how a material (fluid) behaves when subjected to an extensional strain with dependency on the type of material. Different experimental methods have been employed for quantifying the extensional viscosity[2]. The objective of this study was to examine the effects

of gum concentration on the shear and extensional rheology of xanthan and guar gum solutions. The aim is to improve the understanding of the rheological behaviour of these solutions in extension to allow these materials to be used more efficiently.

EXPERIMENTAL

Materials

Food grade powders of xanthan (X, Danisco, Sweden) and guar (G, Sigma-Aldrich, India) were used as the gelling agent.

Preparation of solutions

Aqueous solutions of xanthan and guar gums at concentrations of 1, 1.5 and 2 wt.%. were prepared. The polymer was dispersed in water by stirring at 1400 rpm on a magnetic stirrer at room temperature, between 20 and 23ºC, overnight to ensure complete hydration of the gums.

Tests and measurements

Rheological measurements were carried out in controlled-strain (ARES-G2, TA Instruments, New Castle, USA) rheometer, using a plate and plate geometry (40 mm diameter, 1 mm gap). Small-amplitude oscillatory shear (SAOS) measurements, inside the linear viscoelastic regime, were performed in a frequency range between 10^{-2} and 10^{2} rad/s, at 23ºC. Strain sweep tests, at a frequency of 6.23 rad/s, were previously performed to determine the linear viscoelastic regime. At least two replications were performed on fresh samples. The extensional rheological properties were measured using a Hyperbolic Contraction Flow[2] mounted in an Instron 5542 Universal Testing Instrument (Instron Corporation, Canton, USA). The extensional viscosity was measured at 23ºC using different speeds of the piston.

RESULTS AND DISCUSSION

Figure 1 shows the mechanical spectra (G’ and G’’ vs. angular frequency) of guar and xanthan aqueous solutions. The mechanical behaviour of the guar gum solutions (Figure 1a) was dependent on frequency and followed the shape reported elsewhere for similar guar gum solutions[3]. In all cases, both moduli increased with frequency by roughly three orders of magnitude between 0.01 and 100 rad/s. There is a crossover in the moduli and the elastic response prevails at higher frequencies. The crossover frequency decreased from 6.3 rad/s to 1

rad/s as the concentration increased from 1 wt.% to 2 wt.%., as a consequence of longer relaxation time. On the other hand, the mechanical behaviour of xanthan gum solutions is reported in Figure 1b. As can be observed, xanthan solution exhibits the typical pattern of a xanthan solution at such concentrations[4] where G' remains larger than G'', on the frequency on the whole range of frequency investigated. This indicates that the xanthan solution behaves like a weak gel with a low frequency dependence for both moduli at low frequencies $G' \sim \omega^{0.3}$ and $G'' \sim \omega^{0.2}$. This viscoelastic behaviour and its effective increase with the concentration is a result of the rigid elongated nature and the entanglement of the xanthan molecules.

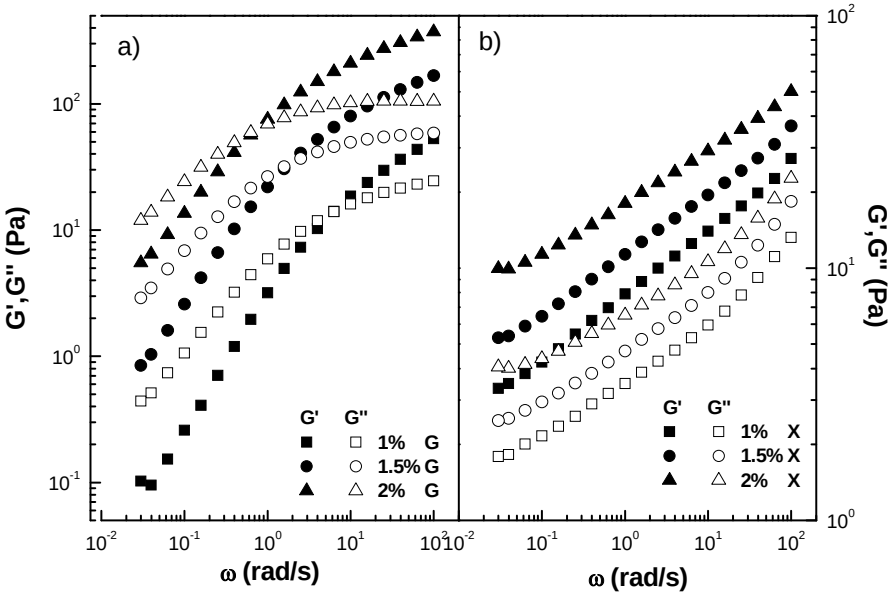

FIGURE 1 Frequency dependence of the storage and loss moduli for aqueous guar (a) and xanthan (b) solutions.

The extensional viscosity for aqueous guar and xanthan solutions is shown in Figure 2. The extensional viscosity decreased with increasing extensional strain rate, and it also diminished with lower gum concentration. As can be observed, guar solutions present higher viscosity than xanthan solutions on the whole range of extensional rate studied. It is worth noting that the extensional viscosity was much higher than the shear viscosity (result not shown) at all rates used here, i.e. the Trouton ratio was significantly higher than 3. The samples were allowed to recover for one minute upon applying every extensional strain rates in order to minimize memory effects. These memory effects were observed as a non-zero load at the beginning of the measurement, but after one minute of recovery the load was negligible. Such effects were more pronounced at higher rates as a result of the higher stresses.

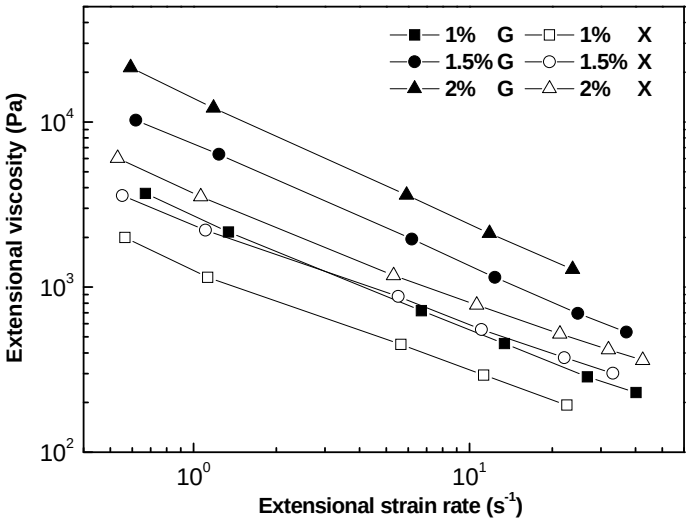

FIGURE 2 The extensional viscosity as a function of the extensional strain rate for aqueous guar and xanthan solutions.

CONCLUSIONS

SAOS tests within the linear viscoelastic region showed that xanthan gum solutions studied behaved as a weak gel, whereas guar gum solutions exhibit gel-like response and suggest the presence of physical entanglement. An increase in the viscoelastic moduli of the solutions can be explained by the increase of gum concentration. On the other hand, guar and xanthan gum solutions were successfully measured using a hyperbolic contraction flow method. It was demonstrated that the solutions exhibited a rather high extensional viscosity which is related to the concentration of the gum. Guar gum solutions showed higher viscosities than xanthan gum solutions.

ACKNOWLEDGEMENTS

J.E. Martín-Alfonso received a Postdoctoral Research Grant from "Ayudas para estancias de investigación postdoctorales" Programme of Campus de Excelencia Internacional Agroalimentario (ceiA3). The authors gratefully acknowledge their financial support.

REFERENCES AND NOTES

1. Torres, M.D., Hallmark, B., Wilson, D.I., Food Hydrocolloids, **2013**, 32: 331-340.
2. Moberg, T., Rigdahl, M., Stading, M., Bragd. E.L., Carbohydrate Polymers, **2014**, 102, 409-412.
3. Chenlo, F., Moreira, R., Silva, C., Journal of Texture Studies, **2010**, 41, 396-415.
4. Choppe, E.; Puaud, F.; Nicolai, T.; Benyahia, L., Carbohydrate Polymers, **2010**, 82, 1228-1235.

P22

Bioplastics from proteins: A comparison between different protein concentrates to obtain bioplastics by injection moulding

Manuel Félix, Víctor Pérez, Alberto Romero, Antonio Guerrero

[1]*Departamento de Ingeniería Química, Universidad de Sevilla, Facultad de Química, Profesor García González 1, 41012, Sevilla. Spain*

Correspondence to: Antonio Guerrero (E-mail: *aguerrero@us.es*)

ABSTRACT

Bioplastic materials from proteins, are becoming highly attractive for important industrial applications, in which thermo-mechanical techniques are increasingly being used. This study assesses injection moulding to produce bioplastic materials from blends previously mixed with glycerol and different protein systems. Results from dynamic mechanical thermal analysis, tensile tests and water uptake tests were compared for those protein-based specimens, indicating that protein content exerts a strong influence on the properties of the final plastic materials.

KEYWORDS Bioplastic, Injection moulding, Mechanical properties, Water-uptake capacity

INTRODUCTION

Nowadays, there is a growing interest in the use of bio-based packaging[1], such that bioplastics market has suffered an exponential increase since 2011. Proteins from different sources are among the most interesting raw materials used in the production of bioplastics. In fact, the need for cost-competitive[2] and biodegradable materials has led to products from agricultural sources as eco-friendly alternatives to oil-based polymers[3]. This interest for protein-based plastics is further increased when using surpluses and wastes (e.g. from the food industry). Protein systems are mixed with a plasticizer (e.g. glycerol) to reduce the glass transition temperature[4]. Injection moulding, which is one of the most useful polymer processing techniques, it is typically performed in two stages at lab-scale (a mixing process to form a blend, followed by an injection process with a plunger-type injection moulding machine). It is crucial to select suitable processing parameters to obtain specimens with suitable properties. The overall objective of this work is to evaluate the high potentials of different protein concentrates in order to produce

bioplastic materials, which may exhibit some comparable properties with regard to synthetic polymers. This study could be useful to validate the use of food industry surpluses, by-products and wastes in order to manufacture bioplastics.

EXPERIMENTAL SECTION

Materials

Albumen protein isolate (API, 83.2 wt%) was provided by OVOSEC S.A, soy protein isolate (SPI, 91.0 wt%) by Protein Technologies International (SUPRO 500E, Leper, Belgium), pea protein isolate (PPI, 91.0 wt%) by Roquette (Lestrem, France) and rice protein concentrate from rice husk (RPC, 78.2 wt%) by Remy Industries (Leuven-Wijgmaal, Belgium. Crayfish flour concentrate (CFC, 64.9 wt%) was supplied by ALFOCAN S.A. (Isla Mayor, Seville, Spain).

Samples preparation

Preparation of blends

Blends with constant protein/plasticiser ratio were manufactured by a two-stage thermo-mechanical procedure. Blends were mixed in a Haake Polylab QC two-blade counter-rotating batch mixer (Thermo Haake, Karlsruhe, Germany) at 25ºC and 50 rpm for 60 min. Two different protein/plasticiser ratios (wt%/wt%) were analysed in order to select a suitable proportion of each compound: 70/30, for concentrates (RPC, CFC), and 60/40 for isolates (API, SPI, PPI).

Preparation of biocomposites

Protein/GL blends were subsequently processed by injection moulding, using a MiniJet Piston Injection Moulding System II (Thermo Haake, Germany), to obtain bioplastic specimens. A temperature of 60°C and residence time of 100 s were selected for the pre-injection cylinder, in order to prevent thermally-induced protein crosslinking effects before the injection stage. The processing pressure and time selected were 50 MPa for 20 s for the injection stage and 20 MPa for 200 s over the packing stage. The temperature of the mould was 120ºC.

Characterization of biocomposites

Dynamic mechanical thermal analysis (DMTA)

DMTA was carried out by using rectangular specimens under dual cantilever bending with a RSA3 equipment (TA Instruments, New Castle, DE, USA). All the tests were carried out at constant frequency (6.28 rad s^{-1}) and strain within the linear viscoelastic region (0.01-0.30%). The selected heating rate was 3ºC min^{-1} and the temperature range covered was from -30 to 130ºC. All the samples were coated with Dow Corning high vacuum grease to avoid water loss.

Tensile strength measurements

Tensile tests were carried out with the 10-kN Insight Electromechanical Testing System (MTS, Eden Prairie, MN, USA), according to ISO 527-2[5] for tensile testing of plastics. Five duplicates of each product were tested using type IV specimens at 1 mm min^{-1} strain rate and 20ºC.

Water uptake capacity

Water uptake capacity was measured according to ASTM D570[6], as well as the loss of soluble matter. Both parameters are determined by the following equations:

$$\%\, Water\ uptake = \frac{Wet\ Weight - Initial\ Dry\ Weight}{Initial\ Dry\ Weight} \cdot 100 \qquad (1)$$

$$\%\, Loss\ of\ soluble\ material = \frac{Initial\ Dry\ weight - Final\ Dry\ weight}{Initial\ Dry\ weight} \cdot 100 \qquad (2)$$

RESULTS

Dynamic mechanical thermal analysis (DMTA)

Fig 1A shows how the values of *E'* change with temperature depending on the protein used for obtaining the bioplastics. Almost all the systems exhibit similar behaviour where E' modulus decreases with temperature until a minimum value (between 80 and 100ºC), remaining constant at higher temperatures. However, the profile for CFC protein differs in that *E'* decreases to markedly lower values and then increases again, reflecting a remnant thermosetting potential.

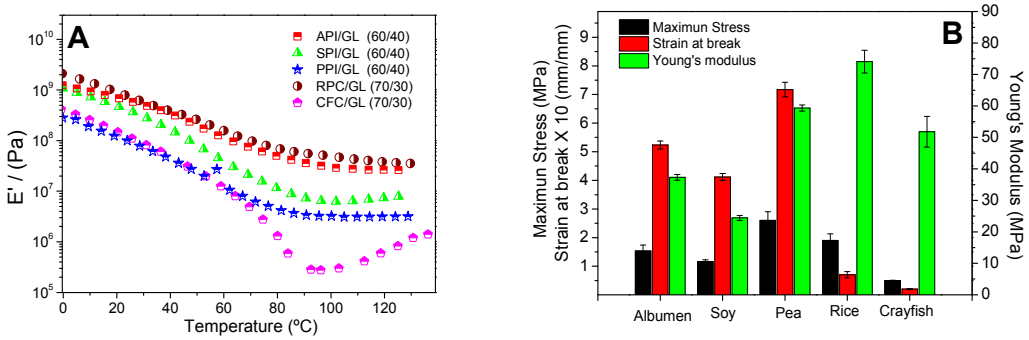

FIGURE 1. *Results from mechanical tests carried out for different protein/glycerol biobased specimens: (A) Storage modulus (E') from Dynamic Mechanical Analysis (DMA) measurements and (B) parameters from tensile strength measurements: Young's modulus, maximum stress and strain at break.*

Tensile strength measurements

Fig. 1B shows the values of the tensile parameters from tensile tests performed on these bioplastics. Systems with the 70/30 protein/plasticizer ratio show the highest values of Young's

Modulus and maximum stress, while systems based on the 60/40 protein/plasticiser ratio display the highest values for the strain at break

Water uptake capacity

As can be observed, PPI-based bioplastic shows the highest water uptake capacity, followed by SPI and API systems. It is worth noting the extremely low values found for CFC-based specimens compared to those shown by the plant protein-based specimens.

TABLE 1. *Water absorption capacity (%) after immersion for 2 h and 24 h and loss of soluble matter (%) for different protein/glycerol systems*

	% Water uptake (2h)	% Water uptake (24h)	% soluble matter Loss
API/GL (60/40)	30.4 ± 1.9	34.4 ± 1.1	40.2 ± 1.9
SPI/GL (60/40)	66.9 ± 3.6	67.4 ± 0.4	45.7 ± 3.6
PPI/GL (60/40)	105.7 ± 0.9	84.7 ± 0.2	38.1 ± 0.8
RFC/GL (70/30)	20.3 ±0.6	22.5 ± 0.6	28.9 ± 1.1
CFC/GL (70/30)	2.4 ± 0.5	0.7 ± 0.2	48,4 ± 2.1

CONCLUSIONS

Protein-based bioplastics processed by a two-stage thermo-mechanical process (mixing and injection moulding) are very promising materials for the substitution of conventional petroleum plastics in certain applications, since they have suitable mechanical properties, as well as processability and biodegradability.

ACKNOWLEDGEMENTS

This work is part of a research project sponsored by MINECO, "Ministerio de Economía y Competitividad", from the Spanish Government (Ref. MAT2011-29275-C02-02/01) and by the Andalousian Government, (Spain) (project TEP-6134).

REFERENCES AND NOTES

1. Kowalczyk, D., Baraniak, B., *Journal of Food Engineering*, **2011**, *105*, 295-305.
2. Zheng, H., Tan, Z., Zhan, Y.R., Huang J., *Journal of Applied Polymer Science*, **2003**,*90*, 3676-3682 (2003).
3. Gonzalez-Gutierrez J, Partal P, Garcia-Morales M., Gallegos C, *Bioresource Technology,* **2011**,*101*, 2007–2013.
4. Irissin-Mangata, J., Bauduin, G., Boutevin, B., Gontard, N., *European Polymer Journal*, **2011**,*37*, 1533-1541
5. ISO U-E. Plastics, International Organization for Standardization, In. Switzerland, **2012**.
6. ASTM D638-14, *ASTM International*, West Conshohocken, PA, **2014**.

P23

Rheological properties of kefiran compared to other neutral gums

Judith Piermaría, [2], Carlos Bengoechea[1], Analía Graciela Abraham[2], Antonio Guerrero[1]

[1]*Departamento de ingeniería química, Universidad de Sevilla, España*

[2]*Centro de Investigación y Desarrollo en Criotecnología de Alimentos – 47 y 116 (s/n) – La Plata (1900), Argentina*

Correspondence to: Carlos Bengoechea (E-mail: *cbengoechea@us.es*)

ABSTRACT

Kefiran is a water-soluble branched glucogalactan containing equal amounts of D-glucose and D-galactose produced by microorganisms present in kefir grains.

Aqueous dispersions of kefiran (K) were compared to three selected neutral gums used as reference: methylcellulose (MC), locust bean gum (LBG) and guar gum (GG). Their rheological behaviour is characteristic of low concentrated polysaccharide dispersions, in which a fluid-like behaviour is predominant at most frequencies studied. The neutral gums 2% solutions may be ranked, matching their molecular weights, according to their viscoelastic behaviour: GG > LBG > MC > K. Moreover, an increase in the gum concentration from 0.5 to 2% wt generally yields a strengthening of the structure.

Cross model is properly used to describe the shear-thinning behaviour of all the neutral gum solutions studied. Moreover, if log η_0 is represented versus log (polymer concentration) for the four gums, a linear fitting may be properly applied.

Kefiran solutions do not show important extensional properties at 2%, displaying a behaviour close to the Newtonian at low Hencky strains.

Thus, regarding the potential of kefiran as functional additive in food products, it may be necessary to consider the future addition of another ingredient into the formulation if higher viscoelastic properties are needed.

KEYWORDS Kefiran, rheology, apparent viscosity, extensional viscosity, Hencky strain

INTRODUCTION

Kefiran is a heteropolysaccharide synthetized by *Lactobacillus kefiranofaciens*, lactic acid bacteria present in kefir grains[1]. It improves the rheological properties of fermented milk[2], is able to form cryogels[3] and edible films with good mechanical and barrier properties[4]. Also, it has

been demonstrated that kefiran has the ability to protect epithelium against *Bacillus cereus in vitro* and has immunomodullatory effect[5].

Most of the rheological studies in the literature were conducted under a pure shear flow. Nevertheless, many industrial applications often involve a component of extensional mode of deformation and not always shear flow results can be extrapolated directly to the extensional behavior. The extensional properties of the fluid can be quantified by monitoring the kinetics of filament thinning[6].

The main objective of this research has been to study the shear and extensional rheological properties of kefiran suspensions in relation with other neutral polysaccharides used in food industry.

RESULTS

Shear Viscosity

When submitted to steady shear, all gums show a shear-thinning behaviour (Figure 1A), consequence of modifications in macromolecular organisation in the solution as the shear rate changes. First, a Newtonian plateau region, characterized by a zero-shear rate apparent viscosity, η_0, is found at low shear rates. This region is broader in the shear rate range studied when the molecular weight (MW) is lower (e.g. kefiran). When increasing shear rate, the disruption predominates over the formation of new entanglements, and then, molecules get aligned in the direction of flow and the viscosity decreases. As may be observed in Figure 1A, for all gums studied, the shear-thinning behaviour increases with concentration, since the critical shear rate ($\dot{\gamma}_c$) at which the flow behaviour becomes shear-thinning decreases as concentration increases.

A simplified Cross model has been used to describe the shear-thinning behaviour of all the neutral gum solutions studied

$$\eta = \frac{\eta_0}{[1 + (\tau\dot{\gamma})^m]} \qquad (1)$$

where $\dot{\gamma}$ is the shear rate (s^{-1}), η is the viscosity (Pa·s), η_0 is the zero-shear rate viscosity (Pa·s), τ(s) is a time constant, and m is a dimensionless constant.

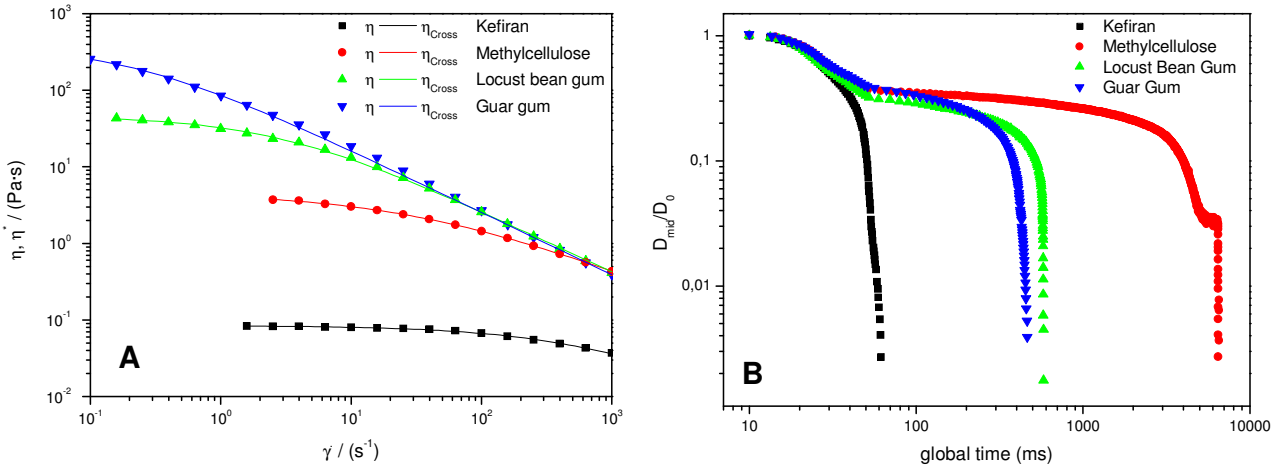

FIGURE 1 Shear flow curves (A) and dimensionless filament diameter versus time (B) for 2% neutral gums

Table 1 show how the simplified Cross model describe properly the experimental data of the kefiran solutions, as well as the rest of the neutral gums studied. As observed, kefiran, which shows the lowest MW (Table 1), also shows the lowest values for η_0 at all concentrations studied, as well as the lowest slope. Typical slopes for biopolymers range from 3 to 5, though some deviations have been found. The low values found for kefiran are in agreement with a system where the individual polysaccharide coils are free to move independently as they are well separated from each other. Anyway, the rate of formation of new entanglements seems to diminish as the molecular weight of the gum increases.

Extensional Viscosity

Figure 1B displays the normalized mid-filament diameter, D_{mid}, versus time profiles for the 2% solutions of the four neutral gums studied.

It may be observed how in all cases the polymer filament passes through four stages (rest-strecth-relaxation-breaking). Similar trends have been found previously. Very large differences exist between the different polysaccharides. The break-up time ranged between 61.67 ms (kefiran) and 6530.88 ms (methylcellulose) for the samples, being the relaxation phase less pronounced for Kefiran than for the rest. The reason of this may be in the possible mechanisms that oppose to the capillary forces after stretching. While for the 2% solutions of galactomannans

and methylcellulose the mid-filament evolution is basically controlled by the balance of surface tension and viscous/elastic forces, with viscous forces stabilizing the filament and surface tension destabilizing it, the 2% solution of kefiran, approach a nearly Newtonian fluid behaviour in comparison, with the diameter decaying almost linearly after the stretch stage.

TABLE 1 Molecular weights and Cross fitting parameters for 2% neutral gums

Gum	MW (kDa)	η_0 (Pa·s)	τ (s)	m	R^2
Kefiran	$6.0 \cdot 10^3 \pm 3.6 \cdot 10^3$	0.083 ± 0.00028	123.81 ± 11.93	0.36 ± 0.02	0.8962
Methylcellulose	$4.1 \cdot 10^3 \pm 3.4 \cdot 10^2$	4.01 ± 0.050	14.13 ± 1.47	0.50 ± 0.02	0.9985
Locust Bean Gum	$1.0 \cdot 10^4 \pm 5.7 \cdot 10^2$	43.54 ± 0.63	2.20 ± 0.13	0.75 ± 0.00	0.9884
Guar gum	$2.2 \cdot 10^4 \pm 3.0 \cdot 10^3$	374.011 ± 2.08	0.10 ± 0.002	0.77 ± 0.00	0.9996

CONCLUSIONS

This study has shown that kefiran solutions show a flow behaviour in shear qualitatively similar than other representative neutral gums. Nevertheless, it presents much lower viscosity values, which is explained on terms of its microstructure. This also would explain that kefiran solutions do not show important extensional properties at 2%, displaying a behaviour close the Newtonian.

ACKNOWLEDGEMENTS

The authors gratefully acknowledge the financial support provided by CONICET of Argentina, Universidad de La Plata (UNLP); Agencia Nacional de Promoción Científica y Tecnológica (Project PICT 0910).

REFERENCES

1. Micheli, L., Ucelletti, D., Palleschi, C., Crescenzi, V., *Applied Microbiology and Biotechnology*, **1999**, 53, 69-74

2. Rimada, P.S., Abraham, A.G., International Dairy Journal, **2006**,16 (1), 33–39.

3. Zavala, L., Roberti, P., Piermaria, J.A., Abraham, A.G., *Journal of Food Science and Technology*, **2014**, http://dx.doi.org/10.1007/s13197-014-1577-2

4. Piermaria, J., Bosch, A., Pinotti, A., Yantorno, O., Garcia, A. A., Abraham, A. G., *Food Hydrocolloids*, **2011**, 25, 1261- 1269.

5. Vinderola, C.G., Perdigón, G., Duarte, J., Farnworth, E., Matar, C., *Cytokines*, **2006**, 36(5-6):254-60

6. Rodd, L.E., Scott, T.P., Cooper-White, J.J. McKinley, G.H., *Appl. Rheol.*, 15 (1), **2005**, 12-27

IBER REO 15 Coimbra 2015

P39

Evaluation of rheological behavior of some polyethylene-polypropylene concentrated solutions

Ioana Stanciu

University of Bucharest, Faculty of Chemistry/Department of Physical Chemistry, 4-12 Elisabeta Blvd, 030018, Bucharest, Romania

istanciu75@yahoo.com

ABSTRACT

This paper presets the study of the rheological characteristics of the concentrated polyethylene-polypropylene copolymer solutions over the temperature range of 313-363 K and for shear rates between 3 and 1312 s^{-1}. The measurements were performed on a Haake VT 550 rotational rheometer with a HV_1 sensor. The rheology of the concentrated solutions is influenced by the shear rate, temperature and concentration of the tested copolymer. We have used a successful model that describes the rheological behaviour of the concentrated solutions in comparison to other models that do not consider the copolymer's concentration. The parameter A reaches a peak for the 10 g/dL solution and a minimum for the 3 g/dL solution. The parameter B displays close values for all of the studied solutions

KEYWORDS relationship, dynamic viscosity, concentrated solutions

INTRODUCTION

The base oils have a Newtonian behaviour in that the viscosity is independent of the temperature and the shear rate. The polymers that are added into the oil may change the solution's rheological parameters and influence the oil's viscosity according to the concentration and the shear rate. At high shear rates of 10^6 s^{-1}, in many industrial applications[1,2] we notice a temporary reduction in the viscosity due to the alignment of those polymer molecules with the shear rate and the temperature. High shear rates are important for the starting resistance and those shear rates are related to the oil pumping into the carter. In order to understand the performance of the viscous polymer solution over a wide range of shear rates, it is necessary to determine the efficacy of a certain additive.[3-5]The polyethylene-propylene polymer that is being used here is formed of some 45% units of ethylene concentrated in the middle of the chain (the polymer is produced inside a tubular reactor that provides for the control of the ethylene units positions along the chain). At low temperatures, the polymer's segments tend to connect

considerably and the solution's viscosity decreases. The rheological behaviour of the polyethylene-propylene copolymer has been studied by many researchers. The rheological behaviour depends on the shear rate at temperatures above 240°C and on the aggregation of various solvents. All those studies were performed at high temperatures and low shear rates. The equation models in the speciality literature showing the dependence of the dynamic viscosity natural logarithm on the absolute temperature are:[5]

Fulcher

$$ln\ \eta = A + B/(T + C) \quad (1)$$

Litovitz

$$ln\ \eta = A + a/RT^3 \quad (2)$$

Girifalco

$$ln\ \eta = C + (B/T) + (A/T^2) \quad (3)$$

Valzen

$$ln\ \eta = B[(1/T) - (1/T_0)] \quad (4)$$

The purpose of this study is to research the dependence of the dynamic viscosity natural logarithm on the inverse absolute temperature for the polyethylene-propylene copolymer in the SAE 10W oil. At concentrations of 3, 6, 10 and 12 g/dL of the polyethylene-propylene additive, we measured the viscosity for some shear rates from 10^5 to 10^6 s^{-1} using a rotational rheometer. The experimental results have been interpreted with other rheological models that are not available in the speciality literature. Using a linear fitting of the lines, we obtained the parameters A and B and the correlation coefficient R^2.

EXPERIMENTAL

The polyethylene-propylene copolymer is Paratone 8900 marketed by Exxon Chemical. The utilized SAE 10W oil is mostly paraffinic and contains 75% saturated hydrocarbons. The 3, 6, 10 and 12 g/dL solutions have been prepared at the room temperature for several weeks, using continuous mixing. To find the rheological characteristics of the concentrate polymer solutions, we made use of a Haake VT 550 rotational rheometer. This Haake VT 550 rheometer includes an HV_1 sensor that provides for the application of some shear rates from 3 to 1312 s^{-1} over the 313-363 K temperature range.

RESULTS AND DISCUTION

The figure 1 shows the dependence of the dynamic viscosity natural logarithm on the inverse absolute temperature for the 3 g/dL solution of the polyethylene-polypropylene copolymer over the 313-363K temperature range and the said shear rates.

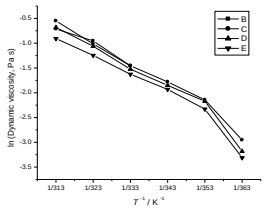

Figure 1. Dependence ln dynamic viscosity versus inverse absolute temperature for the 3 g/dL solution at shear rates: B – 243 s^{-1}, C – 437.9 s^{-1}, D – 729 s^{-1} and E – 1312 s^{-1}

The dependence of the dynamic viscosity natural logarithm on the inverse absolute temperature, we have used the experimental database to determine the equation (5) where the parameters A and B depend on the solution's concentration and the solvent's and the polymer's nature and type.

The equation that shows the dependence of the dynamic viscosity natural logarithm on the inverse absolute temperature is:

$$ln\eta = A + B/T \tag{5}$$

where A is $ln\eta_0$ and B is the slope.

The table 1 shows the shear rates range for which we represented the dependence of the dynamic viscosity natural logarithm on the inverse temperature for the 3 g/dL solution of polyethylene-polypropylene copolymer, the parameters A and B derived from the equation (5), the correlation coefficients derived from that equation and the statistical correlation coefficients.

The shear rates range for which the dependence of the dynamic viscosity natural logarithm on the inverse temperature for the 3, 6, 10 and 12 g/dL solutions of polyethylene-polypropylene copolymer, the parameters A and B derived from the equation (5), the correlation coefficients derived from that equation and the statistical correlation coefficients.

Table 1. The shear rate, the parameters A and B derived from the equation (5), the correlation coefficients obtained by polynomial fitting and the statistical correlation coefficients for the 3 g/dL copolymer polyethylene-polypropylene solution

Shear rate, s^{-1}	A	B	Correlation coefficient, R^2 (equation 5)	Correlation coefficient, R^2 statistical
243	-0.3426	-0.3710	-1.0000	-
437.9	-0.0286	-0.4874	-0.9976	0.9714
729	-0.0895	-0.5017	-0.9973	0.9430
1312	-0.3065	-0.4702	-0.9889	0.9303

CONCLUSIONS

The rheological characteristics of the polyethylene-polypropylene copolymer solution have been calculated over the temperature range of 313 - 363K shear rates from 3 to 1312 s^{-1}. The rheology of the concentrate solutions is influenced by the shear rate, the temperature and the concentration of the tested copolymer. The paper presents a model that describes the rheological behaviour of the concentrated solutions in comparison to other models that do not take into account the copolymer's concentration. The parameter A reaches a peak for the 10 g/dL solution and a minimum for the 3 g/dL solution. The parameter B has similar values for all of the solutions.

REFERENCES AND NOTES

1. McMillan, M.L.; Murphy, C.K.; Temporary viscosity loss and its relationship to journal bearing performance, SAE 780374. The relationship between engine oil viscosity and engine performances part III; SAE SP-429 (ASTM STP-621-52), **1978**.

2. Bartz, W.J.; Wiemann, W.; Determination of the cold flow behaviour of multigrade engine oils, SAE 770630. The relationship between engine oil viscosity and engine performances part II; SAE SP-419 (ASTM STP 621-51), **1977**.

3. Metznew, A.B., *Adv. Chem. Eng*., **1956**, *1*, 77-79.

4. Erickson, D.C.; Dongqing, L.; White, T.M.; Gao, J., *Ind. Eng. Chem. Res.*, **2001,** *40***,** 3523-3529.

5. Govindan, S.; Vasanthakumari, R.; Radja Sacravarthy, P., *International Journal of Emerging Technology and Advanced Engineering*, 2012, *2(7)*.

Comparison of the rheological properties of artists' oil-based mediums manufactured by *Natural Pigments* and *Winsor and Newton*

María del Pilar Aguilar[1], María Jesús Hernández[2], Margarita San Andrés[1]

[1] Departamento de Pintura y Restauración. Universidad Complutense de Madrid, 28040, Spain.
[2] Departament de Física de la Terra i Termodinàmica.Universitat de Valencia, 46100, Spain.

Correspondence to: M.J. Hernández (*M.Jesus.Hernandez@uv.es*)

ABSTRACT

Mediums are a combination of drying oils and other materials such as varnish, wax, gums and dryers, used to modify the texture of the oil paint. The aim of this work was to analyse the rheological properties of some artists' oil based mediums (labelled as thixotropic) created by two modern brands with different scale manufacturing: *Winsor and Newton* with *Liquin Original, Liquin Light Gel* and *Liquin Impasto,* based on alkyd resin and *Natural Pigments* that sells *Oleogel, Oleoresgel* and *Impasto Medium,* based on linseed oil and different thickening silica. Rheological characterization of the mediums was carried out at 20ºC with a RS1 Rheostress (TermoHaake, Germany). All mediums presented high shear thinning behaviour and important yield stresses, with different zero shear viscosities. They also showed a predominant elastic behaviour. Some differences were observed in time evolution of viscosity and the recovery of elastic modulus, which is related to the supposed thixotropy of these mediums.

KEYWORDS oil painting, oil based mediums, structure recovery, yield stress, thixotropy.

INTRODUCTION

Mediums are a combination of drying oils used in milling the colours (linseed oil, walnut oil, alkyd resin or modified oils) and other materials such as varnish, wax, gum, dryers...etc, that are mixed together to modify the way the paint handless straight from the tube.

At the XIX century some treatise writers and artists showed their interest in different oil painting mediums[1] that are supposed to be thixotropic. According to those texts some contemporary brands of fine arts materials have retaken these recipes to recreate old masters' brushstrokes.

Winsor & Newton is a big UK company founded in 1832 that sells a wide variety of artists' materials. *Liquin* family is one of the best-selling oil painting mediums: *"This Liquin formulation is a slight gel that breaks down on brushing (thixotropic) and flows out to give a non-drip effect when mixed with color [2]".*

Natural Pigments is a limited liability company founded in 2003 in California (USA) that supplies artists' materials used in historical painting: *"Oleogel and Oleoresgel are thixotropic painting. When a thixotropic gel is agitated, such as manipulated with a palette knife or brush, it begins to flow, but when the agitation is stopped it regains its former viscosity and stiffens[3]".*
As time factor is not clearly established, some confusion between shear thinning, thixotropic and viscoelastic behaviour could be present when describing them[4]. The aim of this work is to analyse these rheological properties in some mediums manufactured by the two brands[5].

EXPERIMENTAL METHODS

The oil based mediums studied are shown in Table 1 according to their visual appearance: from matte and thick to glossy and transparent mediums.

TABLE 1. Name of the tested mediums of each brand and composition indicated in labels.

Brand	Binder	Basic Composition
Winsor & Newton	*Liquin Impasto*	alkyd resin, drying oil and dryers
	Liquin Original	alkyd resin, drying oil and dryers
	Liquin Light Gel	alkyd resin, linseed oil and dryers
Natural Pigments	*Impasto Medium*	finely ground calcite, silica and bentonite in bodied linseed oil
	Oleoresgel	bodied linseed oil, alkyd resin, odorless mineral spirits, pyrogenic (fumed) silica
	Oleogel	linseed oil and pyrogenic silica

Rheological measurements were carried out with a controlled stress rheometer RS1 Rheostress (Haake), at 20ºC. Serrated plates (35mm, 60mm diameter) to avoid slippage were used. Before measurements, samples were kept at rest for 15 min. Step flow curves in controlled stress mode and frequency sweeps in linear viscoelastic region were performed. To analyse thixotropy, samples were sheared at 10 s^{-1} during 1 min, and storage modulus at 1 Hz and 10 Pa (within LVR) was recorded with time, before and after shearing, in order to evaluate their recovery.

RESULTS AND DISCUSSION

All the binders had a strong shear thinning behavior, similar in all binders. Flow curves were satisfactory fitted to Carreau model (1). The mean values for the parameters are shown in table 1.

$$\eta = \eta_0 \Big/ \left[1+\left(\dot{\gamma}/\dot{\gamma}_c\right)^2\right]^s \qquad (1)$$

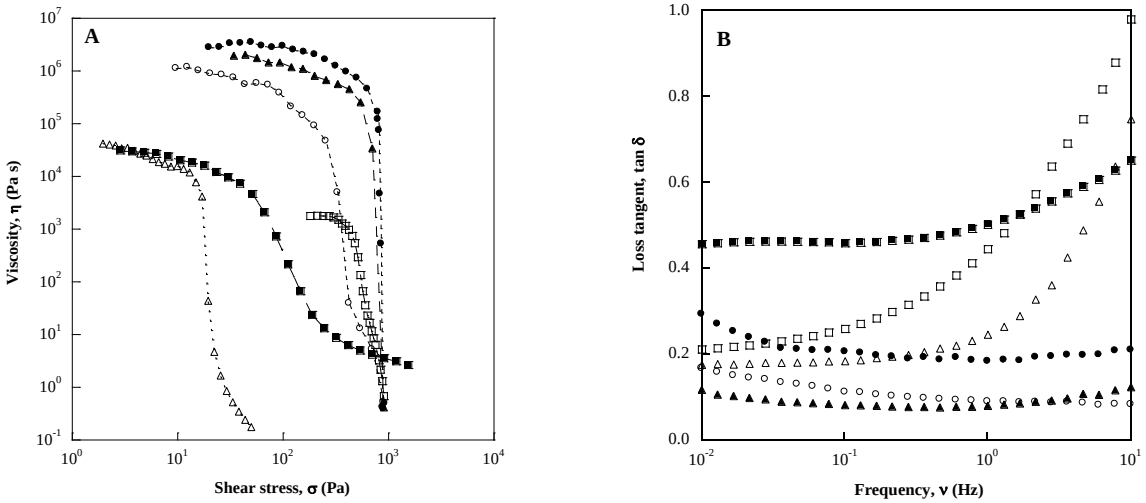

FIGURE 1 A) Flow curves obtained for the binders studied. B) Loss tangent (G"/G') as a function of frequency for the different mediums. *Winsor & Newton*: ○ Liquin Impasto, △ Liquin Original, □ Liquin Light Gel; *Natural Pigments:* ● Impasto medium; ■ Oleoresgel; ▲ Oleogel.

Important differences were observed in zero shear viscosity. The highest viscosity at rest corresponded to both *Impastos* and *Oleogel* (Figure 1A). These mediums were also the most structured systems, with lowest values of tan δ (Figure 1B) and high yield stresses (≅ 1000 Pa). On the other hand, consistency at rest was similar for *Oleoresgel* and *Liquin Original*, but the binder from *Natural Pigments* flowed more smoothly (lowest values of s). *Liquin Light Gel* was the less viscous medium, with a weaker structure (tan δ highest values and G' lowest values).

TABLE 2. Mean values ± standard deviation for: Carreau model (1) parameters for flow curves fits and storage modulus fits to a power law model ($G' = G'_1\ \nu^m$), and loss tangent (G"/G') at 1 Hz.

		Flow curves			Dynamic spectra		
Brand	Binder	$10^{-3} \times \eta_0$ (Pa s)	$10^3 \times \dot{\gamma}_c$ (s^{-1})	s ± 0.01	G'_1 (Pa)	m	tan δ (1 Hz)
Winsor & Newton	*Liquin Impasto*	3110±50	0.099±0.005	0.45	26000±2000	0.052±0.005	0.097±0.009
	Liquin Original	36±2	0.20±0.03	0.44	100±6	0.02±0.03	0.20±0.07
	Liquin Light Gel	1.6±0.3	1.5±0.2	0.40	13±10	0.21±0.05	0.56±0.17
Natural Pigments	*Impasto Medium*	1800±800	0.031±0.018	0.41	41000 ± 14000	0.130±0.013	0.21 ±0.02
	Oleoresgel	44±19	0.46±0.06	0.37	1100±200	0.282±0.018	0.505±0.004
	Oleogel	1400±600	0.11±0.02	0.45	10000±1600	0.049±0.007	0.09±0.01

Regarding shearing time dependence, viscosity (Fig 2 A) was fitted to Weltman model (2)

$$\eta = A - B \ln t \qquad (2)$$

and viscoelastic moduli were recorded as a function of time before and after agitation (Fig. 2B).

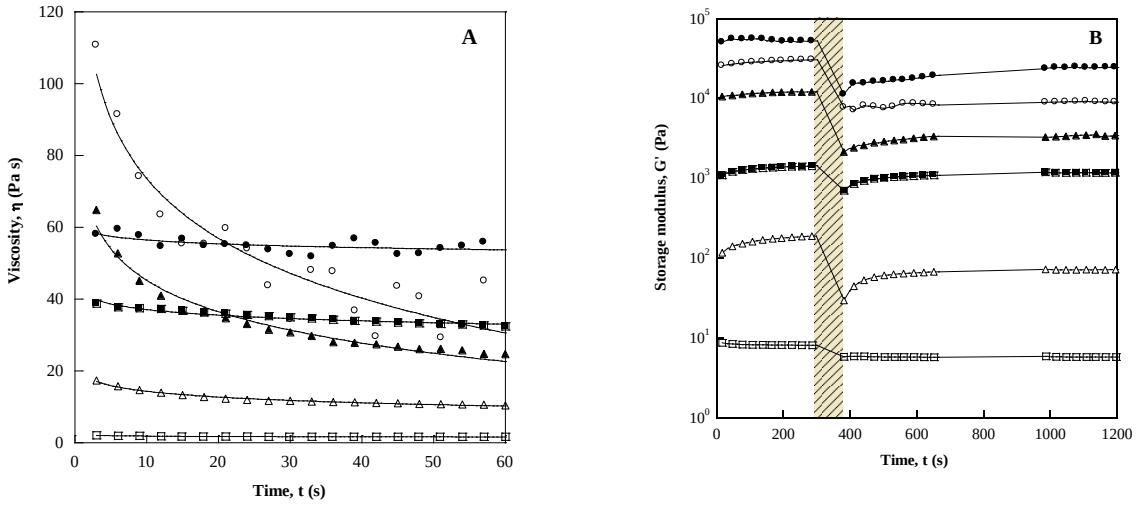

FIGURE 2. A) Evolution of viscosity with shear time at $\dot{\gamma}$=10 s^{-1}. Lines correspond to Weltmann model. B) Evolution of G' with time after shearing (dashed area) and rest. *Winsor & Newton*: ○ Liquin Impasto, △ Liquin Original, □Liquin Light Gel; *Natural Pigments:* ●Impasto medium; ■Oleoresgel; ▲ Oleogel.

Both *Impastos* had about 75 % of reduction of G' because of shear, but while *Winsor & Newton* presented a slow variation of h and about 30 % of recovery of G', *Natural Pigment* medium had an abrupt decay of η and almost no recovery (6%). The other intermediate viscosity mediums (*Oleoresgel* and *Liquin Original*) also presented a significant recovery (20-30%).

CONCLUSIONS

Both *Winsor & Newton* and *Natural Pigments* provide binders with not only different visual appearance, but also rheological properties: zero shear viscosity, stress necessary to flow and recovery of elastic modulus. In addition, *Natural Pigments* mediums measurements are less reproducible, maybe due to inhomogeneity induced by small-scale rolling machinery.

ACKNOWLEDGEMENTS

The authors would like to thank *Natural Pigments* for providing free samples of each medium.

REFERENCES AND NOTES

1. De Viguerie, L.; Cotte, M.; Lequeux, F.; Walter, P.; Moutard-Martin, T.: Historical evolution of oil painting media: A rheological study*; Comptes Rendus Physique*, **2009**, 10, 612-621.
2. Winsor and Newton website http://www.winsorandnewton.com
3. Natural Pigments website http://www.naturalpigments.com
4. Barnes, H.A: Thixotropy, a review, *Journal of Non-Newtonian Fluid Mechanics,* **1997**, 7, 1-33
5. Osterhold, M.M.; Rheological methods for characterising modern paint systems, *Progress in Organic Coatings, **2000***, 40, 131–137.

Understanding the role of EVA in the rheological properties of EVA modified bitumen for lower temperature application

Avido Yuliestyan, Antonio Abad Cuadri, Moises Garcia-Morales, Pedro Partal

Departamento de Ingenieria Quimica, Centro de Investigacion en Tecnologia de Productos y Procesos Quimicos (Pro2TecS), Campus de 'El Carmen', Univeridad de Huelva, 21071, Huelva (Spain)

Correspondence to: Avido Yuliestyan (E-mail: *avido.yuliestyan@diq.uhu.es*)

ABSTRACT

This research studies the influence of vinyl acetate (VA) content and Melt Flow Index (MFI) of ethylene vinyl acetate copolymer (EVA) in the rheological performance of bituminous binders. The results suggest that the combination of these two EVA properties could balance the in-service performance and the ease of processing required by bituminous binders for lower temperature application.

KEYWORDS Rheology, EVA, polymer modified bitumen, binder design, pavement material

INTRODUCTION

Bitumen, a petroleum derivative used as a binder for asphalt pavements, demands an enhanced in-service performance. In this sense, binder design through polymer modified bitumen (PMB) is an alternative to improve temperature susceptibility by means of higher stiffness at high service temperature[1]. The addition of polymer results in an increase in viscosity that leads to difficulties at coating the mineral aggregates during the road making. On top of that, hot mix asphalt (HMA) helps reduce the binder viscosity, but it is less favored concerning the health and environmental issues (ie. higher toxic compound emission and higher energy consumption). Development of reduced temperature technology, such as warm mix asphalt (WMA), is encouraged. The selection of a low melting point polymer, such as EVA copolymer, may provide an alternative which is not merely improving the in-service performance but also its process-ability in WMA temperature region. Previous comprehensive studies on the rheological behavior of EVA binders focused on the influence of neat bitumen type and EVA percentage[1]. In this work, two EVA parameters, VA content and MFI, are studied.

EXPERIMENTAL

Sample and Preparation

Binders were obtained by modifying bitumen 70/100 with EVAs, at VA contents of 18 and 28 wt.%, labeled as EVA-VA-18 and EVA-VA-28, respectively. MFI of 2 and 500 for VA18 and MFI of 7 and 400 for VA28 were selected to study MFI influence. Bitumen and EVA were supplied by Repsol SA (Spain). During process, 5 wt.% EVA was dispersed into 150 °C molten bitumen in two steps that consist of 1) melting at 3500 rpm for 15 mins and 2) mixing at 5000 rpm for 1 hr.

Tests and Measurements

Temperature sweep tests were conducted in CS HAAKE RS600 from 30 to 100 °C at 10 rad/s and 100 Pa by using PPR20 in oscillatory mode. Before that, stress sweeps were done to specify the LVE regime and the stress applied. Calorimetry scans (DSC), with Q100 TA instrument, were performed to witness any thermal event that affects the binder microstructural behavior. Additionally, binder microstructure at room temperature was seen from optical microscopy.

RESULTS AND DISCUSSIONS

Binder thermorheological properties at the medium-to-high temperature window were assessed by means of temperature sweeps.

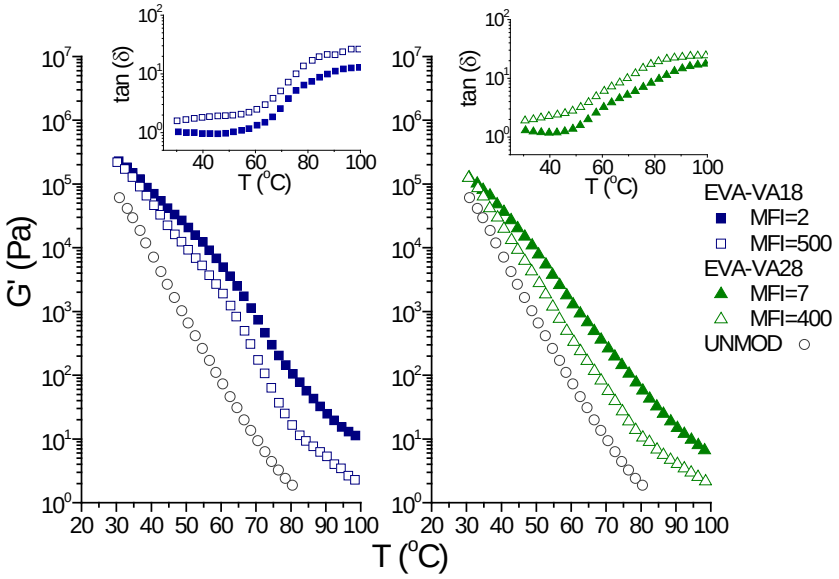

FIGURE 1 Dynamic shear temperature sweeps for the four EVA modified binders studied

Figure 1 presents the evolution of storage modulus (G´) and loss tangent (tanδ=G´´/G´) with temperature. EVA binders present higher G´ and lower tanδ values than neat bitumen, which suggests better elastic performance at in service temperature. Within EVA binders, each of them exhibits a decrease in G´ with increasing temperature which varies in behavior, depending on the VA content and MFI. Thus, VA content seems to control the LVE behavior at the low-to-medium temperatures studied, whilst MFI results to be the key parameter at the highest temperatures, when the polymer phase start to flow. On the other hand, an abrupt G' slope change, at 60 ºC approximately, can be clearly observed for the EVA-VA18 binder. However, EVA-VA28 binder does not show this event. The same response is observed in the evolution of tanδ with temperature.

TABLE 1 DSC data for EVA copolymers and their corresponding EVA modified binders

Type	MFI	Polymer		Binder	
		Tm (°C)	χc (%)	Tm (°C)	χc (%)
EVA-VA18	500	84.1	26.1	64.7	22.7
	2	84.5	25.9	65.0	23.7
EVA-VA28	400	68.8	17.6	--	--
	7	69.5	17.6	--	--

Moreover, Table 1 summarizes the melting temperatures (T_m) and crystallinity degrees (χ_c) of the EVA copolymers and their corresponding binders. In binders, EVA T_m is found lower than its pure polymer, that may be attributed to the smaller size crystallites due to the migration of the lightest compounds from the bitumen rich to the polymer rich phase. Hence, EVA melting event would be related to the sharp decrease in G´ observed for EVA-VA18 and the flattening in tan δ shown in Figure 1 for both EVA-VA18 and EVA-VA28 between 30 and 60ºC.

Interestingly, it was seen that the rheological behavior changes after the melting event, and depends more on MFI (in Figure 1). Similarly, binder viscous flow behavior at 135 °C (result not shown), above EVA melting point, is also affected by MFI variation. Knowing that EVA copolymer molecular weight and MFI values are inversely proportional, the chain entanglement and the friction affects the flow behavior[2], by means of high flowing effort as MFI values decrease and vice versa.

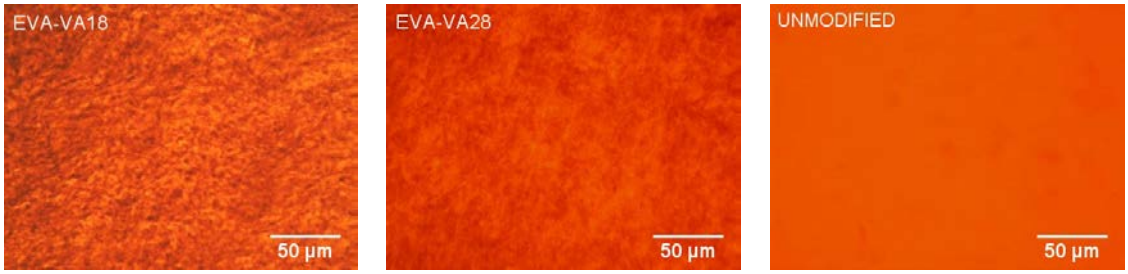

FIGURE 2 Optical microscopy observations, at 25°C, for selected EVA modified binders

Optical micrographs, in Figure 2, may deliver useful information on the binders microstructure at ambient temperature. EVA-VA18 modified bitumen appears having lightly toned region assigned to EVA rich region containing crystallites fraction, which is clearly different from neat bitumen (unmodified). The polymer three dimensional network, with a larger and more uniformly distributed crystals, is the responsible for the improvement in the rheological behavior of this binder, shown by previous dynamic shear temperature sweeps. On the other hand, EVA-VA28 binder presents a slightly different architecture, with a polymer network formed by highly dispersed polymer phase. This is in accordance to DSC data in Table 1, where χ_c could not be determined for this binder as a result of a high percentage of non-crystallizable fraction[3].

CONCLUSIONS

The experimental results suggest that considering the combination of these two EVA properties could balance the in-service performance and the ease of processing, that are assigned to the influence of VA content and MFI, respectively. In particular, the selection of low melting point polymer and the consideration of higher MFI may promote the reduction in binder application temperature.

ACKNOWLEDGEMENTS

The research is a part of the Marie Curie ITN (FP7-PEOPLE-2013-ITN) and financially supported by European Union's Seventh Framework Programme under grant agreement 607524.

REFERENCES AND NOTES

1. Airey, G.D., *Constr Build Mater* , **2002**, 16, 473–87.
2. Ravve, A., Principle of Polymer Chemistry; 3rd ed; Springer, **2012**.
3. Somrang N., Nithitanakul M., Grady B. P., Supaphol P., *European Polymer Journal*, **2004**, 40, 829–38.

P28

Starch-based innovative topical formulations: rheological and thermoanalytical preformulation studies

Joana Marto[1], Sérgio M. C. Silva[1,2], Filipe E. Antunes[2], Luís Filipe Gouveia[1], Alberto Canelas Pais [2], Eduardo Oliveira[3], António José Almeida[1], Helena Margarida Ribeiro[1]

[1] iMed.ULisboa, Faculty of Pharmacy, University Lisbon, 1649-003 Lisboa, Portugal
[2] Chemistry Department, University of Coimbra, Coimbra, Portugal
[3] Laboratórios Atral S.A., Rua da Estação 42, 2600 – 726 Castanheira do Ribatejo, Portugal
E-mail: *jmmarto@ff.ulisboa.pt*

ABSTRACT

Exploring novel applications for approved excipients with a history of safe use in medicine is a smart strategy to obtain improved medicinal products. Due to its unique properties, starch has been extensively used in various topical pharmaceutical applications as a sensorial enhancer, stabilizer and drug delivery polymer. The effects of the temperature on the physicochemical properties of five different native types of starch (rice, wheat, potato, corn and pre-gelatinized starch) were studied by means of DSC, hot-stage microscopy and rheological experiments, with both large strain (rotational) at different shear rates and small strain (oscillatory) tests. Native starches showed endothermic peaks between 60 and 80 °C and the transition temperatures and enthalpies of gelatinization were found dependent on the type of starch. The light microscopy images revealed that the morphology of all starches were affected by heat treatment. The viscoelasticity of heated starch dispersions was found to be strongly dependent on the type of starch. Thus, starch has an enormous potential for innovative applications in pharmaceutical formulation.

KEYWORDS Starch; DSC; Microscopy; Rheology; Pharmaceutical application

INTRODUCTION

Nowadays, scientists and technologists need to develop not only new delivery systems that are substantially better than the existing ones, but also to explore new ways of using well known excipients. For that reason, exploring novel applications for approved excipients with a history of safe use in medicine is a smart strategy to obtain improved medicinal products. Natural excipients still have an important role and application in the pharmaceutical industry, since they are, in most cases biodegradable, non-toxic and abundant compared to synthetic materials. Starch, unlike some synthetic compounds, ensures all these characteristics and has a low price. Due to its unique properties, starch has been extensively used in various topical pharmaceutical applications as a sensorial enhancer, a stabilizer and a drug delivery polymer[1].

METHODS

Sample preparation

Aqueous suspensions of different starches (rice, wheat, potato, corn and pre-gelatinized starch (Pre G)) were prepared by adding 2% of dry polymer to water. Due to the long hydration times, suspensions were kept stirring (200 rpm) for 24h before use.

Differential Scanning Calorimetry (DSC)

Thermoanalytical measurements were performed with a TA Instruments DSC Q200 system (TA Instruments, New Castle, USA). The sample and the reference (air) were placed in opened pans. A scan speed of 10 °C/ min and 10-20 mg of sample (aqueous solution of each starch) allowed an optimal response regarding resolution, temperature, accuracy and attenuation.

Hot stage microscopy

A light microscope (Olympus BX51, Japan) equipped with a THMS350V (Linkam, Surrey, England) hot stage was used to visualize the behavior of the emulsions under stress conditions. The system was equipped with a digital camera (Olympus XC30, Japan) and the software Olympus Stream Essentials®. Contact thermal microscopy was conducted by heating the samples from 25 °C to 80 °C using a 10 °C/min heating rate.

Dynamic and Oscillation measurements

Dynamic viscosity measurements were carried out between 1 and 1000 Pa on a logarithmic increment with a scan speed of 10°C/min. Oscillation frequency sweep tests were performed at frequencies ranging between 0.01 and 1 Hz with a scan speed of 10°C/min from 25 °C to 80 °C.

RESULTS AND DISCUSSION

DSC

The gelatinization of starch is an endothermic process, meaning that it can be measured with DSC. Native starches showed endothermic peaks between 60°C and 80°C and the transition temperatures and enthalpies of gelatinization were found dependent on the type of starch (Figure 1).

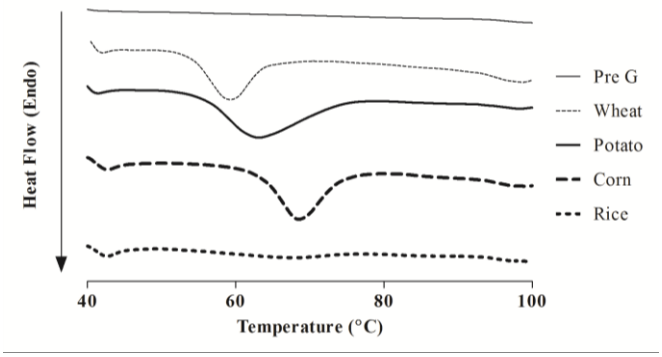

FIGURE 1 – DSC scanning thermograms of different starches.

Hot stage microscopy

As can be seen in Table 1, an increase in the temperature from 25 to 70ºC, caused the swelling and morphology alteration of the five types of granules of starch. It was observed that the granules gelatinized at different temperatures. Additionally the light microscopy images revealed that the morphology of all starches was affected by heat treatment.

TABLE 1 - Micrographs of different starches at different temperatures (25 and 70 °C) during the heating process.

Temperature (°C)	Pre-gelatinized starch	Wheat starch	Potato starch	Corn starch	Rice starch
25	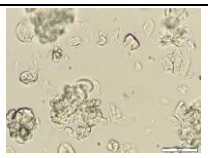	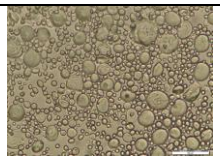	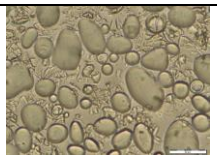	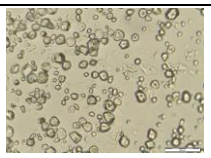	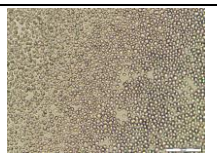
70	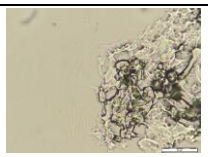	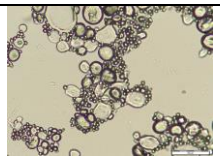	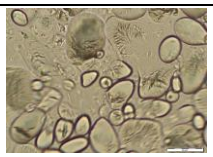	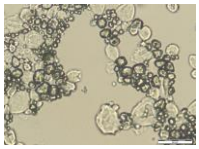	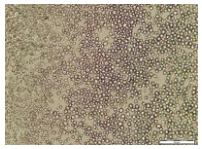

Dynamic and Oscillation measurements

It has been reported that concentration, volume fraction of the swollen granules, the deformability of the granules, and the degree of molecular entanglement influence the viscosity of starch gelatinization during heating[2]. For all starches suspensions, the viscosity started to increase at temperatures between 60 and 75°C (Figure 2 (a)). The increasing viscosity of starches

dispersions during heating was attributed to the swelling of the starch granules, supported by DSC and hot stage microscopy data.

The viscoelasticity of heated starch dispersions was found to be strongly dependent on the type of starch. For wheat, corn, potato and rice starch, G' is much higher than G", meaning a dominant elastic behavior (Figure 2 (b)). The G’ and G’’ increased upon heating, probably due to the onset gelatinization of the polymer. As expected, for pregelatinized starch, during the heating, the G’ decreased and the G’’ increased due to the previous treatment.

(a) (b)

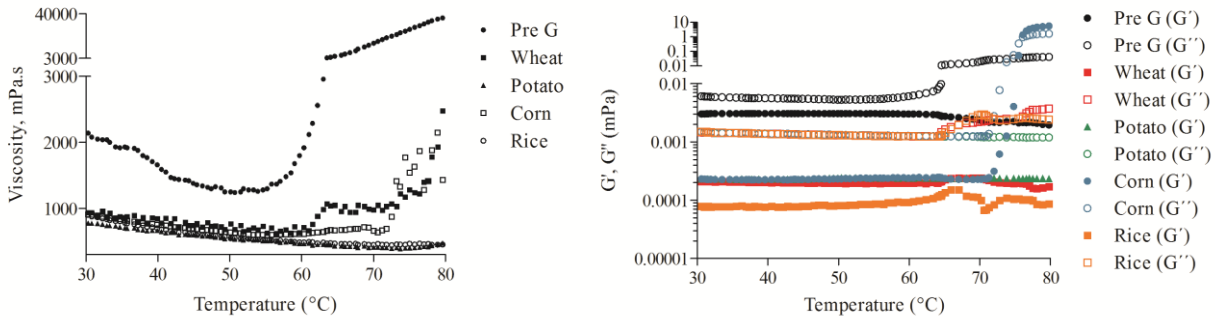

FIGURE 2 – (a) Viscosity of different starches at different temperatures. (b) Dependence of storage (G’) and loss (G’’) moduli for different starches at different temperatures.

CONCLUSIONS

Starch has an enormous potential for use in innovative applications in pharmaceutical formulations. The results confirmed a high variability related to its origin. Therefore, comprehensive preformulation studies are crucial to select the best starch type for the intended purpose.

ACKNOWLEDGEMENTS

This work was supported by FEDER, the Portuguese government (FCT; grant SFRH/BDE/51599/2011), strategic project Pest-OE/SAU/UI4013/2011 and Laboratórios Atral S.A., Portugal.

REFERENCES

1. Röper, H., Starch, 2015. 54(3-4): 89-99.
2. Yongfeng, A.i., Jay-lin Jane, Starch, 2015, 67, 213-224.

Assessment of the fatigue resistance of asphalt binders

Rui Micaelo[1], André Pereira[1], Luís Quaresma[1], Maria Teresa Cidade[2]

[1] Department of Civil Engineering, Universidade Nova de Lisboa, Caparica, PORTUGAL

[2] Department of Materials and CENIMAT/I3N, Universidade Nova de Lisboa, Caparica, PORTUGAL.

Correspondence to: Rui Micaelo (*ruilbm@fct.unl.pt*)

ABSTRACT

Asphalt fatigue cracking is a very important distress type in road pavements. Cracking occurs due to repeated traffic loading, within the bitumen or at the bitumen-aggregate interface. Over the last three decades many researchers investigated the fatigue properties of the bitumen, using different test apparatus and protocols.

This paper compares and discusses the application of several methods for the analysis of testing results and for quantifying fatigue resistance. A neat and a polymer modified bitumen (PMB) were tested with continuous and discontinuous loading and with incremental load amplitude.

The results showed that the test conditions and methods used to determine the fatigue resistance have a significant effect in the estimated bitumen fatigue life. The indexes obtained from dissipated energy methods show a very good correlation with $N_{f,50}$ obtained from the time sweep tests. The fatigue life law obtained from the linear amplitude sweep test is highly affected by the analysis method and the failure criterion. Healing during non-loading periods has a significant impact on the PMB fatigue life while no significant effect is observed in the neat bitumen fatigue life for small to intermediate rest periods.

KEYWORDS (asphalt binders; fatigue resistance; dynamic shear rheometer; failure criteria; damage mechanics)

INTRODUCTION

Asphalt mixtures have a complex microstructure comprising randomly oriented aggregate particles (large range-size variation), bitumen and air voids. The bitumen is a viscoelastic material at normal conditions (temperature, loading, etc) and, despite the low volume proportion in final mixture, defines the material's stress-strain response to loading.

Fatigue cracking results from repeated loading cycles which are below the ultimate stress of the material. Asphalt cracking occurs due to repeated traffic loading, within the bitumen or at the bitumen-aggregate interface. Hence, over the last three decades many researchers investigated the fatigue properties of the bitumen, using different test apparatus and protocols. Furthermore,

several methods were proposed for the analysis of the experimental results and for the estimation of the bitumen's fatigue life[1]. This paper compares and discusses the application of several methods proposed in literature to quantify the fatigue strength of two different bitumens, which were tested with two different test procedures.

MATERIALS AND TESTING PROGRAM

Two different bitumens were selected for this study: (i) paving grade 35/50; (ii) polymer modified bitumen PMB 45/80-65. The PMB is modified with 2-4% of SBS polymer using an undisclosed procedure by the supplier. The samples tested were not subject to any planned ageing effect. The binders were first characterized in terms of their behaviour under oscillatory shear and, afterwards, subjected to the fatigue tests. Measurements were performed with a Bohlin Gemini HR^{nano} rotational rheometer, which under dynamic tests is equivalent to a Dynamic Shear Rheometer. The samples were fabricated and prepared for testing in accordance with the EN 14770 standard. A minimum of three samples were used for each testing condition.
The tests were performed with the 8 mm (2 mm gap) and 25 mm (1 mm gap) parallel plate set-up. Two types of fatigue tests were performed: (i) time sweep tests (TST); (ii) linear amplitude sweep tests (LAS). The TST consisted in repeated cycles of oscillatory shear with constant amplitude (shear strain 1.2%, 1.6% and 2%), which were stopped when the complex shear modulus has fallen more than 50% of the initial value. The tests at the shear strain of 1.2% were repeated with the introduction of rest periods (4, 8 and 16s) after every 10 seconds of loading with the objective of studying the healing effect from periodic rest periods. The LAS [2,3] consists in a cyclic loading at systematically increasing loading amplitudes (shear strain 1 to 20%, with 1% step increments every 10 seconds). Both tests were performed at the temperature of 15 ºC and with a loading frequency of 10 Hz.
Pereira [1] gives the complete information about the materials and the testing program.

RESULTS

Fig. 1 shows the evolution of the complex shear modulus (|G*|) of the two bitumens in both tests. There is a significant decrease of |G*| with the loading cycles, which are significantly lower in LAS because the procedure was defined to cause damage rapidly. The same way as in TST test, the neat bitumen shows a quick decrease of the modulus with repeated loading. Table 1 lists the number of loading cycles (average and standard deviation) before failure in TST tests that is

defined as |G*| reducing 50% of the initial value. The PMB shows, as expected, to hold much more cycles before failure. Healing during rest periods has a significant impact on the PMB fatigue life while no significant effect was observed in the neat bitumen fatigue life for small to intermediate rest periods (4 and 8 s).

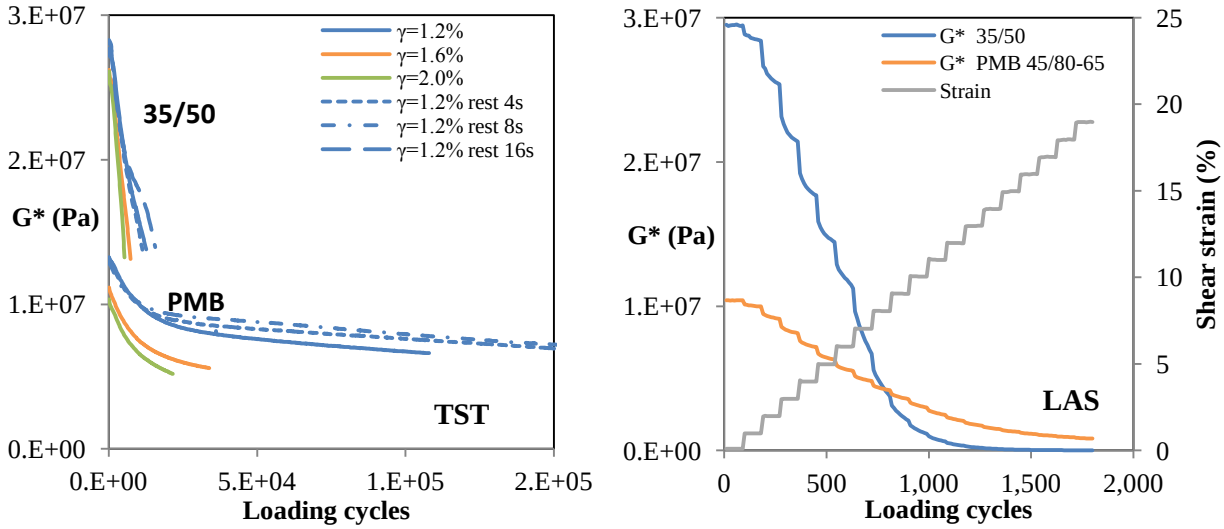

FIGURE 1 Evolution of the complex shear modulus in TST and LAS tests.

TABLE 1 Time sweet test results

Time-sweep		35/50		PMB 45/80-65	
		50% G^*_{ini}			
Strain (%)	Rest period (sec)	Average Nf,50	St.Dev Nf,50 (%)	Average Nf,50	St.Dev Nf,50 (%)
1.2	-	12,567	2.0%	103,033	5.5%
1.6	-	7,233	0.8%	34,100	7.2%
2	-	5,100	5.2%	21,600	2.3%
1.2	4	11,367	3.3%	172,000	5.8%
1.2	8	12,000	2.9%	228,267	10.1%
1.2	16	15,133	2.7%	-	-

Asphalt materials show a strong power law relationship between load stress or strain amplitude (X) and fatigue life (Nf),

(1)

where, *A* and *B* are constants. In case of the TST test, the values of the constants *A* and *B* were obtained from fitting the model to test results. The LAS test results were analysed using the method proposed by Johnson [2] based on the Viscoelastic Continuum Damage Mechanics

approach. The damage progression variable α is determined as 1/m or 1+(1/m), with *m* being the maximum slope of creep, *log J(t)*, or relaxation, *log G(t)*, curves. Due to the ambiguity in literature, both equations are used. Regarding fatigue failure, Jonhson [2] recommended defining failure when there is a 35% decrease in |G*|·sin (δ), where δ is the phase angle. Recently, Bahia[3] recommended using instead the point of the peak shear stress. Table 2 presents the fatigue laws obtained from the two tests. There are significant differences between models. The shear rate dependency (B) shows very similar values for the two bitumens, based on the LAS test results, while from the TST test it is concluded that the neat bitumen is less load amplitude dependent. The value of *A* is very sensitive to the value of α, being approximately 15 and 25 times higher with α=1+(1/m) for the 35/50 and the PMB, respectively. Regarding the failure criteria, for both binders the peak shear stress occurs when |G*|·sin δ has decreased more than 35%.

TABLE 2 Estimated fatigue laws

Bitumen	TST test: Failure criterion: 50% G* initial		m	α		LAS test: Failure criterion: C_f = 65%		LAS test: Failure criterion: τ_{max}	
	A	B		*(1/m)*	*1+1/m*	A	B	A	B
35/50	17,144	-1.774	0.435	1.297		6,657.7	-2.593	8,320.5	-2.593
					2.297	106,794.1	-4.593	145,770.2	-4.593
PMB 45/80-65	169,418	-3.094	0.410	1.437		26,345.1	-2.875	62,895.3	-2.875
					2.437	622,540.0	-4.875	2,273,468.9	-4.875

CONCLUSIONS

The fatigue life estimated from the time sweep tests, at constant amplitude, and from the linear amplitude sweep tests have substantial differences. Furthermore, the fatigue life is highly affected by the method used for the results analysis. Healing during non-loading periods has a large effect on the PMB fatigue life while no significant effect is observed in the neat bitumen fatigue life for small to intermediate rest periods.

REFERENCES

1. Pereira, A. Rheological characterization and evaluation of the fatigue resistance of bitumens with the Dynamic Shear Rehometer, MSc thesis, Universidade Nova de Lisboa, 2014.
2. Johnson, C.M. Estimating Asphalt Binder Fatigue Resistance Using an Accelerated Test Method. PhD Thesis, University of Wisconsin – Madison, 2010.
3. Bahia H., Tabatabaee H.A., Mandal T., Faheem A. Field Evaluation of Wisconsin Modified Binder Selection Guidelines - Phase II. University of Wisconsin Madison, Modified Asphalt Research Center, 2013.

Laminar blood flow in stenotic microchannels

Joana A. C. Calejo, Valdemar Garcia, Carla S. Fernandes

School of Technology and Management, Polytechnic Institute of Bragança, Campus de Santa Apolónia, 5301-857 Bragança, Portugal

Correspondence to: Carla S. Fernandes (E-mail: *cveiga@ipb.pt*)

ABSTRACT

In this work, Newtonian and non-Newtonian laminar blood flow in rectangular microchannels with symmetric and asymmetric atheroma were numerically studied. It was observed that the impact of symmetry of the atheroma is almost negligible and the non-Newtonian properties of blood leads to higher pressure drops and wall shear stresses than the ones obtained for Newtonian flows.

KEYWORDS : Microchannel; Atheroma; Computational Fluid Dynamics; Wall Shear Stress; Pressure Drop

INTRODUCTION

Over the past few decades, the interest in the atherosclerosis's studies has assumed a prominent place in medicine since this cardiovascular pathology has become one of the major causes of death. The dominant pattern is atherosclerosis, characterized by the formation of atheromas. Most of the times, the formation of an atheroma is accomplished by a thrombus formation. It is thought that the location of higher pressures and velocities promote the endothelium lesion and hence the formation of a thrombus, which normally conduce to a thromboembolism due to the high speeds and pressures[1]. Microfluidic devices are becoming one of the most promising new tools for diagnostic applications and treatment of several chronic diseases and the microchannels used in these devices usually have rectangular shape. Hence, it is essential to understand the blood flow behaviour involved in this kind of microchannels.

NUMERICAL SIMULATIONS

The simulations were carried out using the commercial finite-volume package FLUENT®(v 15.0.7). In the calculations, blood was considered both Newtonian and non-Newtonian fluid, its rheology being described, in the second case, by the Carreau model[2]. The simulations were

carried out in 3D rectangular geometries, Fig. 1. Six channels with distinct stenosis degrees - 15%, 30% and 50% - were studied, 3 of them with symmetric atheroma and the other 3 with asymmetric atheroma.

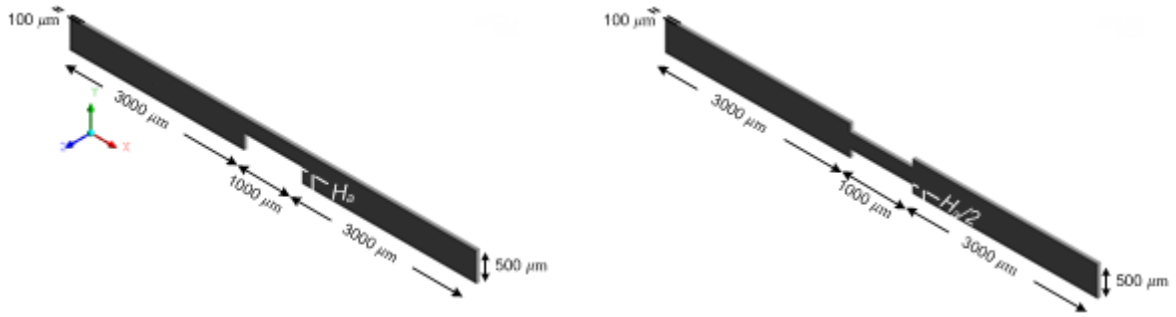

(a) (b)

FIGURE 1 Example of computational domains. (a) Asymmetric atheroma and (b) Symmetric atheroma.

Due to the symmetry of the studied microchannels, a symmetry plane was established leading to thinner computational domains. The discretization of these domains was made using meshes constituted by rectangular elements, the mesh being more refined close to the walls, where zero velocity was imposed. In addition to the referred boundary conditions, 6 distinct entry velocities, u, were imposed in the plane $x = 0$.

In order to validate the computational fluid dynamics calculations, two tests in the region before the atheroma were performed. First, velocity profiles were compared with the analytical solutions for the Newtonian fully developed flow in a rectangular microchannel[3] and it was observed a mean deviation lower than 0.8% for all the channels and operation conditions, Fig. 2.

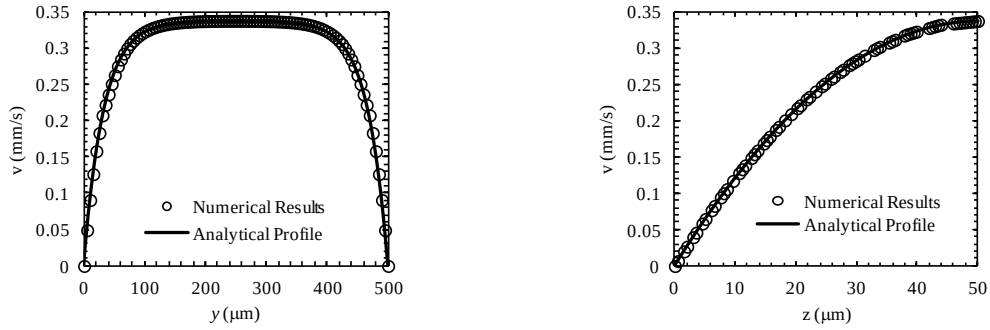

(a) (b)

FIGURE 2 Velocity profiles for fully developed flow in the region before the atheroma and u = 0.198 mm/s. (a) Symmetry plane (z = 50 μm); (b) Central plane (y = 250 μm).

The pressure drop, ΔP, was estimated resorting to the correlation $f = Po\,\mathrm{Re}^{-1}$, where f is the Fanning friction factor, Re the Reynolds number and Po the Poiseuille's number, which assumes the value 19.0 [4] for the studied region. The relative errors for ΔP ranged between 0.01 and 0.1%.

RESULTS

As expected, the influence of the symmetry of the atheroma in the pressure decrease with the decrease of the stenosis degree (Fig. 3(a)). In Fig. 3(a) it can be observed that pressure for Newtonian flow is higher than the one obtained for the non-Newtonian flow. Fig. 3(b) shows that pressure drops are higher for the non-Newtonian flows and the impact of non-Newtonian properties on this flow property decrease with the increase of mean velocity, u.

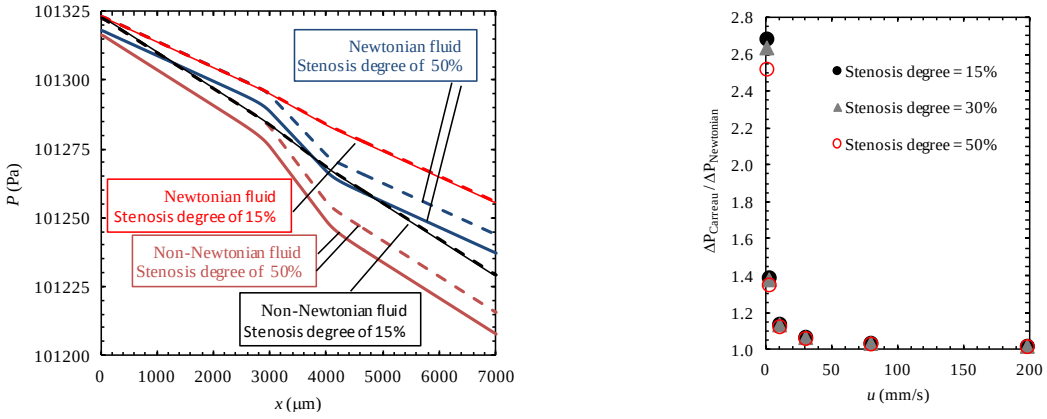

(a) (b)

FIGURE 3 (a) Pressure along channels for u = 1.98 mm/s: (---) symmetric atheroma; (–) asymmetric atheroma. (b) Ratio between pressure drop of non-Newtonian and Newtonian fluids.

The wall shear stress (WSS) along the channels for both Newtonian and non-Newtonian flows have been analyzed and it was verified that the maximum value was reached at the symmetry plane in the corner of the atheroma (Fig. 4).

The asymmetry of the WSS profile is more pronounced for the asymmetric atheroma, being this asymmetry less pronounced for lower velocities (Fig. 4). In the opposite side of the atheroma, Line 2 (Fig.4(b)), the presence of this obstruction is also felt, as can be observed in Fig.4(b).

The impact of non-Newtonian blood properties in the WSS was studied and it was concluded that WSS for Carreau fluid are higher than the ones developed for the Newtonian fluid and this impact increases with the decrease of mean velocity.

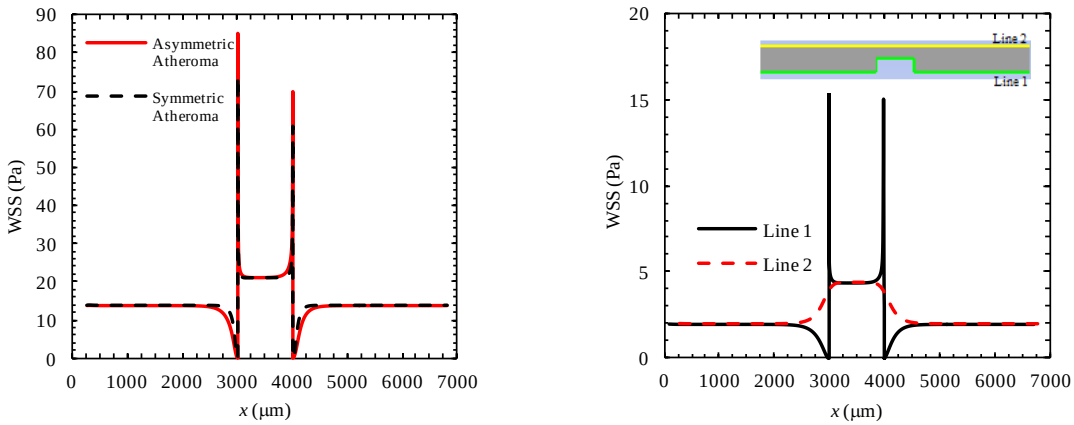

(a) (b)

FIGURE 4 (a) WSS along Line 1 for 30% of stenosis degree, Newtonian fluid for *u* = 79.2mm/s. (b) WSS in top and bottom of the channel with 50% of stenosis degree for the Carreau fluid for *u* = 9.9 mm/s.

CONCLUSIONS

With this study, the influence of blood's non-Newtonian properties, stenosis degree and symmetry of atheroma in laminar flow's properties in stenotic rectangular microchannels were analyzed. It was possible to conclude that in the range of studied mean velocities, local velocity is not affected by the used rheological model or symmetry of the atheroma. The non-Newtonian properties of blood leads to higher pressure drops and wall shear stress being this effect more pronounced for lower velocities.

ACKNOWLEDGEMENTS

The authors acknowledge the financial support provided by: EXPL/EMS-SIS/2215/2013 and PTDC/SAU-ENB/116929/2010 from FCT (Science and Technology Foundation), COMPETE, QREN and FEDER.

REFERENCES AND NOTES

1. Robbins, S.L.; R.S. Cotran; R.S., Kumar, V.; Collins, T., Fundamentos de Robbins – Patologia estrutural e funcional; Nova Guanabara: Rio de Janeiro, **2001**.
2. Johnston, B.M.; Johnston, P.R.; Corney, S.; Kilpatrick, D., *Journal of Biomechanics,* **2004**, *37*, 709-720.
3. Bruus H., Theoretical Microfluics; Henrik Bruus, Ed.; Oxford University Press: New York, Oxford, **2008**.
4. White M. F., Viscous Fluid Flow; Lyn Beamesderfer, John M. Morriss, Eds.; Mc Graw Hill: New York, **2005**.

Rheological characterisation of low denatured crayfish protein concentrates in a fluid interface

M. Felix[1], A. Romero[1], J. Vermant[2], A. Guerrero[1]

[1]Departamento de Ingeniería Química. Facultad de Química. Universidad de Sevilla. Profesor García González 1, 41012, Sevilla. Spain

[2] Department of Materials, ETH Zürich, Vladimir-Prelog-Weg 4, CH-8093 Zürich, Switzerland

Correspondence to: Antonio Guerrero (E-mail: aguerrero@*us.es*)

ABSTRACT

The interfacial behaviour of adsorbed crayfish protein (CFP) has been studied at the air/water and oil/water interfaces for two different crayfish protein derivatives: crayfish sarcoplasmic proteins (CFS) and crayfish hydrolysates (CFH) a function of time, concentration and pH. An analysis of the the adsorption kinetics determined by pendant drop tensiometry and shear measurements using a highly sensitive magnetic air bearing stress-controlled rheometer, have been carried out. A relationship between parameters from O/W and A/W interfaces, which depends on pH values and concentration below interfacial saturation, has been found. Crayfish proteins confer an elastic dominant behaviour to O/W interfaces showing low interfacial tension values. CFS fraction yields lower surface pressure but enhanced 2D gel-like behaviour, which should prevent droplet recoalescence and, as a result, would yield enhanced long-term stability.

KEYWORDS: Crayfish protein, interfacial pressure, interfacial shear rheology, double-wall ring.

INTRODUCTION

The key role of proteins in both the emulsification process and emulsion stability has been widely recognised over the last decades. The ability to emulsify is related to the reduction of interfacial tension as the protein molecules adsorb to the interface, which facilitates the breakup of droplets during emulsion formation. The interfacial ability and the ability of the protein to form an interface is mainly governed by the entropy (in terms of gain) which takes place due to the adsorption and denaturation of the protein at the interface[1]. Emulsion stability is rather associated to the formation of a viscoelastic film that helps to stabilize the newly formed droplets against coalescence, and possibly also Ostwald ripening[2]. Obtaining meaningful interfacial

rheological material functions is challenging. This is firstly due to the small magnitude of the forces and torques associated with the deformation of an interface, but secondly and more fundamentally to the intimate coupling between the flow and deformation in bulk and at the interface, which often makes the fluid mechanics analysis very complex to be accomplished[3].

This study has been conducted with the overall objective of analysing the ability of protein systems from crayfish by-products to display enhanced techno-functional properties (i.e. emulsification and foaming). The specific aim has been to study the interfacial behaviour of two protein derivatives obtained from CF surpluses, both showing little or no exposure to heat-induced protein denaturation at two different pH values (2 and 8), selected on the basis of their surface charges and protein solubility. The protein derivatives have been a globular protein fraction mainly consisting of sarcoplasmic proteins (CFS); and a protein hydrolysate, (CFH).

EXPERIMENTAL SECTION

Materials

Crayfish (CF) meat was separated from the shell by grinding and sieving and supplied as CF pulp by ALFOCAN (Isla Mayor, Sevilla, Spain). CF pulp was kept frozen until its use. First of all, the thawed CF pulp was subjected to alkaline solubilisation at pH 9 and then precipitated at pH 5. The supernatant was spray dried to obtain a fraction rich in globular sarcoplasmic proteins (CFS). The thawed CF pulp was also submitted to controlled enzymatic hydrolysis and then it was spray-dried to obtain a CF protein hydrolysate (CFH) with a hydrolysis degree of 50%. The protein content of both protein derivatives was determined in quadruplicate as % N x 6.25 using a LECO CHNS-932 nitrogen micro analyser (Leco Corporation, St. Joseph, MI, USA), being 52.6 ± 0.4 wt.% for CFS and 67.9 ± 0.9 wt.% for CFH.

Interfacial characterization

Determination of oil–water interface properties. Transient interfacial pressure (Π) was carried out using a pendant drop tensiometer from CAM200 (KSV, Finland). A single batch of commercial n-hexadecane oil was used to measure oil–water kinetic adsorption at 20ºC.

Determination of interfacial shear rheological properties. Measurements of interfacial shear rheology were performed using a double-wall-ring geometry (DWR) according to Vandebril et al[4]. Creep tests were performed at constant stress ranging from $6.5 \cdot 10^{-6}$ to $1.35 \cdot 10^{-5}$ Pa in water/n-hexadecane interface to evaluate interfacial behaviour.

RESULTS

Figure 1 shows the transient surface pressure response for the adsorption kinetics of CFS and CFH at the n-hexadecane/water interface at two different protein concentrations (1 and 2 mg flour/mL) and two pH values (figure 1A for pH 2 and figure 1B for pH 8). The adsorption is always characterized by a rapid increase in surface pressure followed by a slow evolution towards an equilibrium value (Π_{eq}). This evolution is likely due to the occurrence of different stages, starting with an initial stage where fast protein diffusion to the interface takes place, followed by a slower step, where penetration of protein molecules through the interfacial layer as well as some conformational rearrangements of proteins at the interface slow down the kinetics. The manner in which these stages contribute to the overall adsorption process depends on pH, protein concentration and molecular properties.

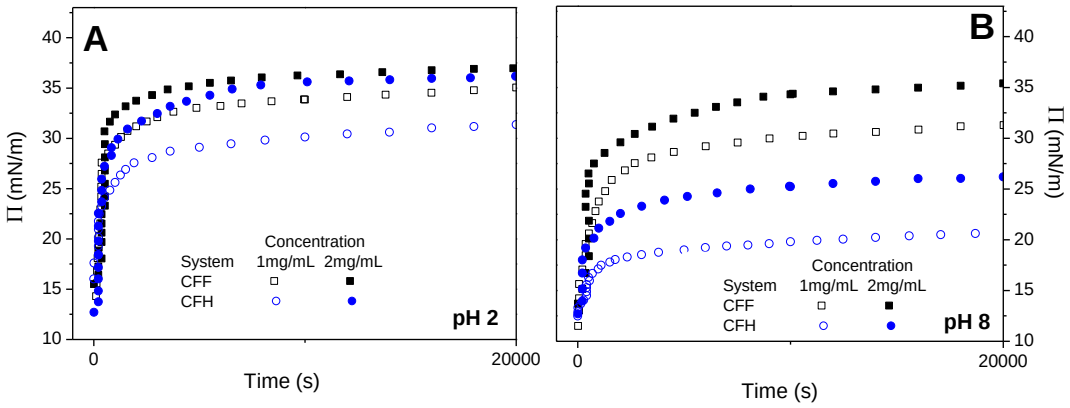

FIGURE 1: Adsorption of CFS and CFH at the n-hexadecane/water interface at two different protein concentrations (1 and 2 mg derivative/mL): (A) at pH 2; (B) at pH 8.

As may be observed, creep profiles (Figure 2), by means of interfacial creep compliance (J_i), for both CFS and CFH are highly sensitive to pH and the creep data really emphasize the differences between the underlying microstructures at pH 2, CFS and CFH both show significant viscoelastic response with both a nonlinear compliance and significant recoil. The slope J_i is initially decreasing showing a tendency towards constant slope. The values of J_i are independent on the stress applied to the interface, which confirms that the response is under the linear deformation regime. At this pH, a marked recovery response takes place, which is also consistent with the elastic-dominant behaviour. On the other hand, the response in creep at pH 8 exhibits an apparent Newtonian fluid response and no recovery is observed is shown for both CFS and CFH-adsorbed interfacial layers with practically nil recovery. This means that the maximum

deformation reached is also very different, being much higher at pH 8 (350 after 15 min) than at pH 2 (which is lower than 0.001), at the same interfacial shear stress.

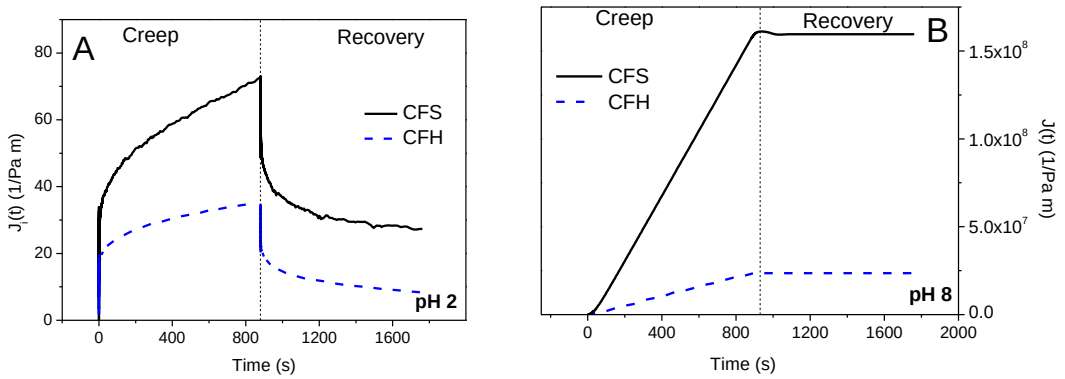

FIGURE 2. Results from creep tests performed at the oil/water interface by means of the DWR tool for protein derivatives CFS and CFH: (A) at pH 2; (B) at pH 8.

CONCLUSIONS

Two alternative procedures have been successfully used to obtain highly soluble protein systems, over a wide range of pH range studied, from crayfish pulp. A strong influence of the behaviour of protein at the complex fluid-fluid interfaces formed on pH and concentration has been found. The response to the application of an interfacial shear stress under creep and recovery measurements depend strongly on pH value. Hence, an elastic-dominant structure was found at pH 2, but at pH 8 the shear response for both protein derivatives shows a Newtonian response, indicating the absence of significant microstructure. This different behaviour must be related to electrostatic/hydrophobic association which are very pH-dependent. Finally, it should be pointed out that although crayfish proteins have shown a good potential for its use as food emulsifier, the complexity of the system makes difficult to carry out any prediction on emulsion stability.

ACKNOWLEDGEMENTS

Authors were sponsored by Andalousian Government, (Spain) (project TEP-6134). The authors gratefully acknowledge their financial support.

REFERENCES AND NOTES

1. Mezzenga, R. Fishcer, P, *Reports Progr. Phys*, **2013,** 76.

2. McClements, D. J. Food Emulsions: Principles, Practice and Techniques. CRC Press: Florida, Boca Raton, **2004**.

3. Sagis, L. M. C. *European Physical Journal-Special Topics*, **2013**,*222*, 39-46.

4. Vandebril, S., Franck, A., Fuller, G.G., Vermant, J, *Rheologica Acta*, **2010**,*49*, 131-144

P36

Emulsion-like and suspension-like interfaces in PP/PA blends and PP/PA/NS blend nanocomposites

Mercedes Fernández[1], Leire Sangroniz[1], Jordana Palacios[1], Antxon Santamaria[1], Alejandro Muller [1,2]

[1] Institute of Polymer Materials (POLYMAT) and Polymer Science and Technology Department, Faculty of Chemistry, University of the Basque Country (UPV/EHU), Paseo Manuel de Lardizabal 3, 20018 Donostia-San Sebastián, Spain

[2] IKERBASQUE, Basque Foundation for Science, E-48011 Bilbao, Spain

Correspondence to: mercedes.fernandez@ehu.es

ABSTRACT

Polypropylene (PP) mixtures with polyamide (PA) are investigated and compared with PP/PA blends that contain 5% of nanosilica (NS). The terminal viscoelastic zone is analysed using small amplitude oscillatory shear, SAOS, measurements in the linear regime. To investigate the non-linear viscoelastic behaviour, large amplitude oscillatory shear, LAOS, experiments are carried out. It is shown that alterations of the terminal zone and deviations observed in non-linearity, account for the interfacial effects of drops and drops surrounded by nanoparticles.

KEYWORDS BLENDS, EMULSIONS, INTERFACIAL TENSION, DYNAMIC VISCOELASTICITY, NON-LINEARITY

INTRODUCTION

Blending polymers constitutes an efficient strategy to obtain new materials which combine the best properties of each component. In most of the cases, the corresponding solubility parameters of the involved polymers differ considerably, which leads to immiscible mixtures. Processing conditions and mechanical properties depend on the morphology developed in these two phase/multiphase systems. In the case of an emulsion-like morphology, the effect is more remarkable as smaller is the size of the dispersed droplets. To achieve this goal, the interfacial tension should be reduced using compatibilizers. Recently[1], it has been proved that the addition of 5% nanosilica to polypropylene/polyamide and polypropylene/polycarbonate blends, respectively, produces a strong reduction of the droplet size, as a consequence of the NS emplacement at the interface.

In this paper, the rheological consequences of the morphological changes, associated to the size of the droplets and to the location of the nanosilica particles, are investigated. A careful analysis of dynamic viscoelastic data in the linear (SAOS), as well as in the non-linear (LAOS) regime, reveals the strong capacities of rheology to characterise polymer blends.

EXPERIMENTAL PART

Blends preparation

The materials were dried under vacuum at 80ºC overnight prior to extrusion and the polymer powders were mixed with silica. The blends and nanocomposites were prepared in a Collins co-rotating twin screw extruder with a profile temperature range from 200 to 240 °C in the extrusion zone was used at 40 rpm.

TABLE 1. Compositions (expressed in wt%) of the blends nanocomposites

	PP	PA	NS with respect to the total weight
PP/PA	80	20	
PP/PA/NS	80	20	5

Rheological measurements

The dynamic viscoelastic functions were evaluated using two TA Instruments rheometers: ARG2 and ARES with parallel plate geometries (25 mm diameter) under nitrogen atmosphere. Dynamic frequency sweeps, SAOS, were performed in ARG2 at 220ºC in the linear viscoelastic regime from 628.3 to 0.03 rad/s. Non linear viscoelastic properties were carried out in the ARES rheometer using large amplitude oscillatory shear, LAOS, flow from 5% to 1000% at 220ºC at a fixed frequency of 0.2 Hz.

RESULTS AND DISCUSSION

The so-called Han plots[2], i.e. the double logarithmic plot of the storage modulus *versus* the loss modulus, constitute an old but very interesting rheological technique to investigate polymer blends. In Figure 1a) such plots are shown, revealing the deviations at low frequencies (low values of G' and G'') observed in emulsion like PP/PA blends, as well as in PP/PA/NS blend

nanocomposites. For the latter, the deviation is a consequence of a suspension-like behavior. But in the case of the emulsion like PP/PA blends the deviation is due to the elastic contribution of the interfacial tension.

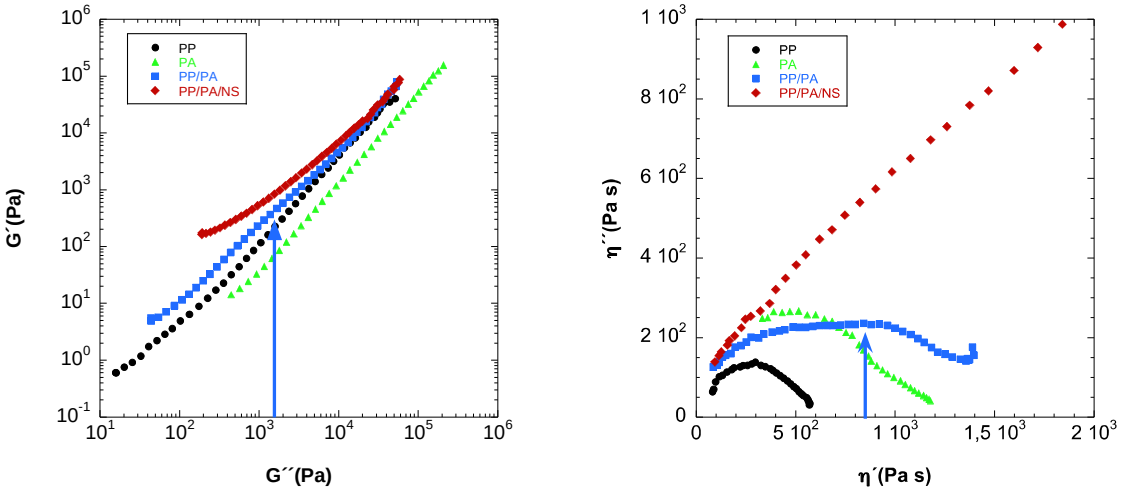

FIGURE 1. a) The so-called Han plots for PP/PA blend and PP/PA/NS blend nanocomposite, as well as neat PP and PA. The arrow indicates the frequency that corresponds to the inverse of the relaxation time obtained in Equation 1. b) The so-called Cole Cole plots for PP/PA blend and PP/PA/NS blend nanocomposite, as well as neat PP and PA. The arrow indicates the frequency that corresponds to the inverse of the relaxation time obtained in Equation 1.

Using the model proposed by Gramespacher and Meissner[3] (Equation 1) the relaxation time associated to the interfacial tension can be determined.

$$\alpha = \frac{\eta_m R}{\tau_0} \frac{(19k+16)(2k+3)}{40(k+1)} \left[1 + \phi \left(\frac{5(19k+16)}{4(k+1)(2k+3)} \right) \right] \quad (1) \qquad \text{where, } k = \frac{\eta_{dispersed-phase}}{\eta_{matrix}}$$

R is the radius of the dispersed phase, τ_0 is the shape relaxation time and the viscosities are the Newtonian viscosities.

According to literature results[4] the interfacial tension between PP and PA at T=220ºC is approximately α=9.2 mN/m. Applying Equation 1 this value leads to a relaxation time τ_0 =0.51s, which corresponds to a frequency of ω =1.98 rad/s. In Figure 1a) the arrow indicates the G' and G'' values that correspond to this frequency. It is observed that the position of the arrow comes

to coincide with the start of the deviation noticed for emulsion-like blends. Concomitant to the effect of the interfacial tension observed in the Han plots, the so-called Cole-Cole plots[5] (real part, η'', *versus* imaginary part, η' of the complex viscosity, η^*) also show a peculiarity associated to the interfacial tension. This can be observed in Figure 1b).

As a corollary of these results, a novel rheological method to evaluate the interfacial tension can be postulated. This consists in calculating the frequency at which deviation in the Han or Cole Cole plots takes place and subsequently use the equation of the Gramespacher and Meissner model to determine α.

Our current work indicates that LAOS experiments (not shown here) are not so conclusive as SAOS tests, so far, since only qualitative results about the interfacial tension can be obtained from their analysis.

CONCLUSIONS

The analysis of the dynamic viscoelastic results in the terminal zone reveals the effect of the interfacial tension in PP/PA blends. In particular, Han plots and Cole Cole plots show discontinuities that treated according to the Gramespacher and Meissner model can allow to evaluate the interfacial tension.

ACKNOWLEDGEMENTS

UPV/EHU (UFI 11/56), GIC IT-586-13 (Basque Government) and MAT 2014-53437-C2-2-P (Spanish Government).

REFERENCES AND NOTES

1.-Laoutid, F.; Estrada, M.; Michell, R.M.; Bonnaud, L.; Müller, A.J.; Dubois, P., *Polymer*, **2012**, *31*, 3982-3990.

2.-Han, J.H.; Feng, D.; Choi-Feng, C.; Han, C.D., *Polymer*, **1995**, *36*, *155-170.*

3.-Gramespacher, H.; Meissner, J., *Journal of Rheology*, **1992**, 36, 1127-1141.

4.-Shi, D.; Ke, Z.; Yang, J.; Gao, Y.; Wu, J.; Yin, J., *Macromolecules*, **2002**, 35, 8005-8012.

5.-Cole, K.S.; Cole, R.H., *The Journal of Chemical Physics*, **1941**, 9, 341-352.

P37

Interfacial rheology at the α-pinene/water interface and emulsifying properties of two eco-friendly surfactants

Luis Alfonso Trujillo-Cayado[1], Pablo Ramírez[1], María Carmen Alfaro[1], Manuela Ruiz[1], José Muñoz[1]

[1]Departamento de Ingeniería Química. Facultad de Química. Universidad de Sevilla c/ P. García González, 1, E41012, Sevilla, Spain.

Correspondence to: Pablo Ramírez (E-mail: *pramirez@us.es*)

ABSTRACT

In this work, an accurate study of two commercial non-ionic polyoxytheylene glycerol ester surfactants at the α-pinene/water interface was carried out, comprising a systematic analysis of dynamic adsorption properties, interfacial rheology and emulsifying properties. Polyoxyethylene glycerol esters were obtained from a renewable source (cocoa oil) and fulfil the environmental and toxicological requirements to be used as ecofriendly emulsifying agents[1]. α-Pinene is also a renewable biosolvent completely insoluble in water, which could find numerous applications. The dilatational rheology of these surfactants at the oil/water interface was studied by means of step area perturbations. The surfactant with the highest number of EO groups (Levenol C-201) turned out to be more surface active at the α-pinene/water interface. Furthermore, the surfactant with the lowest number of EO groups (Levenol H&B) was partly solubilized into the oil phase. Both surfactants allowed obtaining slightly concentrated α–pinene emulsions. Nevertheless, the results obtained demonstrated that the emulsions prepared using Levenol C-201 had smaller droplet sizes, lower polidispersity and showed higher physical stability than the emulsions prepared by using Levenol H&B.

KEYWORDS α-pinene; adsorption equilibrium; Levenol, surface rheology; emulsion

INTRODUCTION

In this work, emulsions were produced by using surfactants (polyoxyethylene glycerol esters derived from cocoa oil) and a solvent (α-pinene) obtained from renewable natural materials, which are more eco-friendly than traditional ones[2].

The main objective is to provide a systematic characterization of the interfacial rheological and emulsifying properties of two eco-friendly polyoxyethylene glycerol ester surfactants with different numbers of EO groups at the α-pinene/water interface.

MATERIALS AND METHODS

Two commercial polyoxyethylene glycerol ester surfactants derived from cocoa oil have been studied: Levenol® C201 (Glycereth-17 cocoate) and Levenol® H&B (Glycereth-2 cocoate). They were kindly provided by KAO and used as received. α-Pinene (0.84 g/mL at 25ºC) was purchased from Sigma–Aldrich® and purified with Florisil® resins (Fluka, 60–10 mesh).

Interfacial tension and dilatational rheology measurements were performed with a drop profile analysis tensiometer (CAM200, KSV, Finland).

Droplet size distribution measurements were performed using a static light scattering instrument (Malvern Mastersizer X). Multiple light scattering measurements carried out over 21 days at 20ºC with a Turbiscan Lab Expert were used in order to study the destabilization of the emulsions by creaming. To characterize the creaming process, the creaming index was used.

RESULTS AND DISCUSSION

Interfacial properties

Figure 1 shows the dynamic surface tension response of both surfactants at a bulk concentration of 1 gL^{-1}. Levenol C201 adsorbed faster and to a higher extent than Levenol H&B. Furthermore, the minimum value in surface tension obtained for Levenol H&B can be ascribed to the occurrence of a fast diffusion and adsorption of surfactant molecules at the interface followed by a slower solubilization of the previously adsorbed surfactants into the adjacent oil phase.

The interfacial behaviour of both surfactants at the α-pinene/water interface was studied by means of step area perturbations. The limiting elasticity E_0 was calculated using the following equation[3,4]:

$$E_0 = \Delta\gamma \frac{A_0}{\Delta A} \qquad \text{(Eq. 1)}$$

where $\Delta\gamma$ is the interface tension increase after the step, A_0 is the initial surface area and ΔA is the surface area step. Figure 2 show E_0 values as a function of Levenol C201 and Levenol H&B concentrations. It is worth noting that the presence of a minimum indicated the occurrence of conformational changes of the adsorbed layer, being more noticeable for the surfactant with higher number of ethoxylated units.

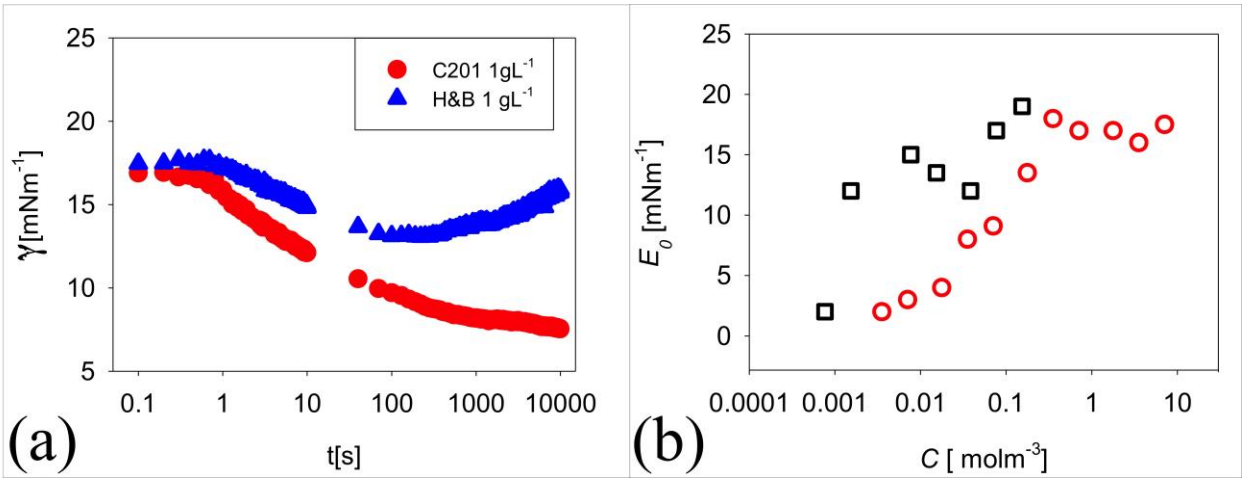

FIGURE 1. (a) Dynamic interfacial tension for Levenol C-201 (circles) and Levenol H&B (triangles) at the α-pinene/water interface for 1 g·L^{-1} concentration. (b) Interfacial limiting elasticity versus concentration for Levenol C-201 (open squares) and Levenol H&B (open circles) at the α-pinene/water interface. T=20°C.

Emulsifying properties

The emulsifying properties values for both surfactants are summarized in Table 1. Firstly, it should be stated that both emulsions showed a monomodal distributions pattern but the final size distribution of the emulsion is highly sensitive to the emulsifier used. Emulsion containing Levenol H&B aged for 1 day has a higher span value (span = 1.833) than those containing Levenol C201 (span = 1.491). These results may be interpreted taking into account the better surface properties of Levenol C201. This is in agreement with the results obtained from laser diffraction measurements because emulsions became more stable against creaming due to the combination of the reduction of the droplet size and the lower polidispersity. Results provided by laser diffraction and multiple light scattering demonstrated that both surfactants could be used as emulsifiers. However, Levenol C201 has better emulsifying properties, as smaller droplet sizes are more easily obtained and it has enhanced stability against creaming.

TABLE 1 Emulsifying properties of α-pinene/water emulsions of Levenol H&B and Levenol C201

	$D_{3,2}$ [μm]	Span	Creaming rate, ω [mm/day]
Levenol H&B	1.75	1.833	0.48
Levenol C201	1.85	1.491	0.08

CONCLUSIONS

We have carried out a detailed study of the interfacial properties at the biocompatible α-pinene/water interface and of the emulsion stabilizing properties of two polyoxyethylene glycerol ester surfactants derived from cocoa oil, which has recently become commercially available.

Dynamic surface tension measurements showed that Levenol H&B adsorbs more slowly and to a lesser extent than Levenol C201. Moreover, a minimum in the DST curve for Levenol H&B indicated a partly solubilization of Levenol H&B in the α-pinene oil phase.

Dilatational rheology measurements showed a conformational change of the adsorbed surfactants being more marked for the one with more EO units. (Levenol C201).

α-pinene-in-water emulsion produced by using Levenol C201 are more stable and with lower droplet size and span values than the ones obtained with Levenol H&B.

ACKNOWLEDGEMENTS

The financial support received (Project CTQ2011-27371) from the Spanish Ministerio de Economía y Competitividad (MINECO) and from the European Commission (FEDER Programme) is kindly acknowledged. The authors are also grateful to KAO for providing materials for this research.

REFERENCES

1. Trujillo-Cayado, L.A. ; Ramírez, P. ; Pérez-Mosqueda, L.M. ; Alfaro, M.C. ; Muñoz, J. Colloids and Surfaces A. **2014**, *458*, 195.
2. Santos, J. ; Trujillo-Cayado, L.A. ; Calero N. ; Muñoz, J. Aiche J. **2014**, *60*, 2644.
3. Calero, N. ; Muñoz, J. ; Ramírez P. ; Guerrero, A. Food Hydrocoll, **2010**, *24*, 659.
4. Pérez-Mosqueda, L.M. ; Ramírez, P. ; Alfaro, M.C. ; Rincón, F. ; Muñoz, J. Food Hydrocoll., **2013**, *32*, 440.

Author Index

Abraham, Analía Graciela – P23
Abreu, Danielly C. – P31
Aguilar, María del Pilar - P25
Alfaro, Mª Carmen - O9, O14, P37, P44, P49
Almeida, António José – O27, P28
Almeida, Pedro – O31
Alvarenga, Nuno – P13, P15
Alvarez, María Dolores – P45
Alves, Sara – P7
Andrés, Margarita San – P25
Antunes, Filipe E. – O27, P28, P34
Artiaga, R. – P32
Arufe, Santiago – O3, P5, P6, P17
Baltazar, Luis G. – P 41
Banobre, Manuel – P33
Bargiela, Verónica – P1, P2
Barreiro, S. Gómez – P32
Barrière, Thierry - O8
Batista, Vanessa – O22
Beceiro, J. López – P32
Bengoechea, Carlos – O21, P23
Berta, M. – P20
Boix, Miquel – P47
Borderías, .Javier – P1, P2
Branco, Fernando – O24
Burrica, Nuno – P13
Calafel, Itxaso – P47
Calejo, Joana A. C. – P38
Calero, Nuria – O7, P30, P50
Candeias, Bárbara – P13
Canet, Wenceslao – P45
Cardoso, Tiago – P41
Carmona, José Antonio – P30
Carrión-Maramoros, L.M. – P11
Carvalho, Maria João – P13, P15
Chenlo, Francisco – O3, P5, P6, P17
Cidade, Maria Teresa – O5, P29, P41
Conde, Jose Ignacio – P47
Cordobés, Felipe – O21
Costa, Ana C. – P31
Costa, Manuela – P15
Costa, Maria Carolina Morando – P34
Costa, Raquel – P33
Cuadri, Antonio Abad - O26, P26, P46, P48
Cuesta, Francisco – P45
Curado, Aurora Lucas - P30
Delgado-García, R. – P11
Diañez, Isabel – O34
Dias, João – P13
Duretek, Ivica - O25
Egas, Ana P. V. – P31
Faísca, Margarida – O22
Felix, Manuel – O17, P22, P35
Fernandes, Carla S. – P38
Fernández, C. Gracia – P32
Fernández, Mercedes – O4, O23, P36
Fernández-Espada, Lucia – O21
Ferreira, Abel G. M. – P31
Fradinho, Patrícia – O22, O33, P8
Franco, José M. – O31, P19
Fuentes, Raúl – P45
García, M. Carmen – O14, P44
Garcia, Valdemar - P38
García-Morales, Moisés – O6, O26, P26, P46, P48
Garrido, Rita – P33
Gelin, Jean-Claude – O8
Gomes, David Manuel Gama Simões - O20
Gómez-Merino, A.I. – O29
Gonçalves, Paulo – O5
Gonzalez-Gutierrez, Joamin – O25
Gooneie, Ali – O25
Goswami, Sumita – O5
Gouveia, Luís Filipe – O27, P28
Goyos-Pérez, L. – P11
Graça, Carla – P7
Guerrero, Antonio – O17, O21, P22, P23, P35
Haavisto, Sanna – O18
Henriques, Fernando M.A. – P41
Henriques, Marta Helena Fernandes - O20
Hernández, María Jesús - P9, P25
Herranz, Beatriz – P1, P2, P45
Holzer, Clemens – O25
Hunkeler, David – P33
Jäsberg, Ari – O18
Kasa, Seppo – O18
Koponen, Antti – O18
Kukla, Christian – O25
Landa, Maite – O4
Leal, Catarina R. – O31
Liashenko, Ievgenii – P48
Lille, Martina – O18
Loução, Neide – P13
Lourenço, Anita – P33
Martín-Alfonso, J.E. – P19, P20
Martínez, Inmaculada - O34, P48
Martínez-Boza, Francisco José - P46
Martín-Piñero, M. José - P44
Marto, Joana – O27, P28
Micaelo, Rui – P29

Moreira, Ramón – O3, P5, P6, P17
Moreno, Helena M. – P2
Muller, Antxon Santamaria – P36
Muñoz, José – O7, O9, O14, P30, P37, P44, P49, P50
Muñoz, Manuel – P9
Muñoz, María Eugenia – O4, O23, P47
Murillo-González, S. – O29
Narciso, Diana – P8
Navarro, F. Javier – O6, O26, P46
Nunes, Bruno - P13
Nunes, Sara - P15
Oliveira, Eduardo – O27, P28
Ortega, F.J. – O6
Páez-Flor, N.M. – O29, P11
Pais, Alberto Canelas – O27, P28
Palacios, Jordana – P36
Partal, Pedro – O6, O26, O34, P26, P46, P48
Pascual, Belén – P47
Patrício, Pedro – O31
Pazmiño-Renteria, A.J. – P11
Pereira, André – P29
Pereira, Carlos José Dias – O20
Pereira, Mara – P7
Pérez, María Dolores Torres – O1, P3
Pérez, Víctor - P22
Picó, Jose Antonio – P9
Piermaría, Judith - P23
Portela, Raquel – O31
Quaresma, Luís - P29
Raimundo, Luís – P7
Ramírez, Pablo – P30, P37
Rasteiro, Maria Graça G. – O24, P33
Raymundo, Anabela – O9, O22, O33, P7, P8
Ribeiro, Carlos – P15
Ribeiro, Helena Margarida – O27, P28
Rocha, Ana Filipa – O33
Rodriguez, Estibaliz – O23
Roman, Claudia – P46, P48
Romero, A. – P35
Romero, Alberto - O17, P22
Royer, Alexandre – O8
Rubio-Hernández, F.J. – O29, P11
Ruiz, Manuela – P37
Rustad, Turid – O17
Salvador, Ana – P4
Sánchez-Vicent, Alfonso – P9
Sangroniz, Leire – P36
Santamaría, Antxon – O4, O23, P47
Santos, Jenifer – O7, P50
Sanz, Teresa – P4
Schuschnigg, Stephan - O25
Silva, Sérgio M. C. – O27, P28, P34
Sobral, Rita G. – O31
Sousa, Isabel de – O9, O22, O33, P7, P8
Stading, M. – P20
Stanciu, Ioana – P39
Tovar, Clara. A – P1, P2
Trujill-Cayado, Luis A. – O9, P37, P44, P49
Valencia, C. – P19, P20
Vermant, J. – P35
Yuliestyan, Avido – P26